INQUIDE

Chemical Engineering and Development

ISSN: 1390-9428
e-ISSN: 3028-8533
ISSN-L: 3028-8533

Vol. 8 / No. 1
January - June 2026

UNIVERSIDAD DE GUAYAQUIL

INQUIDE – Chemical Engineering and Development

INQUIDE – Chemical Engineering and Development * Volume 8 * Number 1 * January / July 2026.
We are a Science and Technology Journal edited by the Faculty of Chemical Engineering of the University of Guayaquil (Guayaquil – Ecuador).
Applied research in engineering, industrial processes, sustainable development and technology management is disseminated, with a multidisciplinary approach in the field of engineering.

INQUIDE

Ingeniería Química y Desarrollo

INQUIDE

Chemical Engineering & Development

Volume 8 – Issue 1

January – June 2026

ISSN: 1390-9428 / e-ISSN: 3028-8533 7 / ISSN-L: 3028-8533

The administration of INQUIDE – Chemical Engineering and Development is carried out through the following parameters:

The journal uses the academic anti-plagiarism turnitin system:

The items have an identification code (Digital Object Identifier) doi

The editorial process is managed through the Open Journal System OJS

The articles in this issue can be consulted at

https://revistas.ug.edu.ec/index.php/iqd/index

Faculty of Chemical Engineering

University of Guayaquil

INQUIDE – Chemical Engineering and Development is indexed in the following Databases and information systems:

Selective Database

Selective Directories.

Open Access Scientific Literature Search.

Journal Evaluation Platforms

Selective Newspaper Archives

Web Metrics Tool

INQUIDE
Chemical Engineering and Development
Journal of Science and Engineering

Vol. 08 / Nº 01
e – ISSN: 3028-8533
ISSN – L: 3028-8533

Presentation. -

Volume 8, Issue 1 – INQUIDE: Chemical Engineering and Development.

Dear Readers and Researchers,

The journal INQUIDE – Chemical Engineering and Development presents Volume 8, Issue 1, an edition that consolidates its positioning as an academic platform for the dissemination of rigorous and relevant research in chemical engineering and applied sciences. This issue brings together contributions that address contemporary challenges related to energy sustainability, the design and evaluation of process equipment, industrial safety, food innovation, and the quantitative analysis of socioeconomic phenomena, reflecting an interdisciplinary approach oriented toward scientific, technological, and productive development.

The first article examines the replacement of internal combustion engines with electric systems in agricultural irrigation operations, addressing the problem of pollutant emissions and dependence on fossil fuels. Through a technical and economic analysis, the study identifies benefits associated with emission reductions, lower operating costs, and reduced noise pollution, while also examining challenges related to electrical infrastructure and energy supply stability in rural areas, providing relevant criteria for the transition toward more sustainable agricultural practices.

The second article develops the thermal–hydraulic design of a plate heat exchanger intended for the cooling of liquid cow's milk. Based on a detailed engineering approach, key operational parameters related to heat transfer, pressure drop, and implementation costs are determined. The main contribution of the study lies in demonstrating the technical and economic feasibility of the proposed equipment, highlighting its applicability in dairy industrial processes that require thermal efficiency and operational reliability.

The third article presents a review of occupational risk assessment in the Ecuadorian dairy industry, based on the analysis of recent publications with a regional focus. The study addresses occupational health and safety through a comprehensive approach that integrates good manufacturing practices, ergonomics, maintenance technologies, and management systems. Its main contribution consists of evidencing significant reductions in workplace accidents and highlighting the need for longitudinal studies and unified measurement frameworks to assess the sustainability of implemented improvements.

The fourth article addresses the thermal–hydraulic design of a shell-and-tube heat exchanger for the cooling of acrylic acid in an industrial context. The work develops a detailed sizing that includes geometric, operational, and economic variables, demonstrating that the proposed design complies with the pressure drop limits established by the process. The contribution of the study focuses on the technical validation of a piece of equipment widely used in the chemical process industry.

The fifth article explores the production of Vienna-type sausage from jumbo squid pulp as an alternative for diversifying fishery products. Through an experimental approach, formulations, processing conditions, and sensory, nutritional, and microbiological attributes are evaluated. The main contribution of the study lies in demonstrating the technological feasibility, safety, and favorable nutritional profile of the product, contributing to the development of innovative value-added foods.

The sixth article presents the time-series modeling of secondary school enrollment in Ecuador using the Box–Jenkins approach, based on an extensive historical dataset. The study addresses the analysis of a key indicator for educational planning, applying stationarity tests, model validation, and medium-term projections. Its contribution consists of demonstrating the usefulness of time-series techniques for the quantitative analysis of educational phenomena and for supporting public policy formulation.

The seventh article analyzes the forecasting of Ecuador's Gross Domestic Product growth using ARIMA models, comparing short-term scenarios. The work addresses macroeconomic volatility through robust statistical techniques, validating the applicability of the Box–Jenkins approach for economic analysis. Its main contribution lies in generating projections consistent with official estimates and in promoting interdisciplinary approaches between economics and engineering.

The eighth article develops the thermal–hydraulic design of a double-pipe heat exchanger for milk cooling, evaluating its operational suitability. Based on the calculation of design parameters, pressure drop, and pumping power, the study demonstrates the limitations of the proposed equipment for the required service. The contribution of the work focuses on the critical analysis of design applicability and on identifying relevant technical constraints for process equipment selection.

The ninth article presents a comparative analysis of the particle size distribution of grains ground in hammer mills, ball mills, and their combination. Through sieve analysis, microscopic characterization, and statistical testing, the

Vol. 08 / Nº 01
e – ISSN: 3028-8533
ISSN – L: 3028-8533

study addresses the influence of equipment type on the quality of the ground product. Its main contribution lies in demonstrating that the combination of milling technologies allows for more uniform particle size distributions, overcoming the limitations of each piece of equipment when used separately.

The Editorial Board invites the academic, professional, and student community to engage in a detailed reading of this issue, whose articles provide scientific evidence, technical analyses, and methodological approaches that enrich knowledge in engineering and applied sciences. The set of published works offers relevant inputs for research, professional practice, and decision-making in productive and public policy contexts.

Likewise, INQUIDE – Chemical Engineering and Development extends a permanent invitation to national and international researchers to submit original manuscripts for future issues. The journal maintains a firm commitment to editorial quality, the rigor of the double-blind peer review process, and the open dissemination of knowledge, emphasizing that no fees are charged for manuscript review or publication, and reaffirming its international projection as an academic space for the dissemination of high-impact research in chemical engineering and development.

Without further ado, we wish you an enjoyable reading experience and sincerely thank you for your continued support of our journal.

Sincerely,

Francisco Javier Duque-Aldaz
Editor-in-Chief
INQUIDE
Chemical Engineering and Development

INQUIDE
Chemical Engineering and Development
Journal of Science and Engineering
Vol. 08 / Nº 01
e – ISSN: 3028-8533
ISSN – L: 3028-8533

TABLE OF CONTENTS

Research Articles.

Vol. 08 / Nº 01
e – ISSN: 3028-8533
ISSN – L: 3028-8533

INQUIDE
Chemical Engineering & Development
Journal of Science and Engineering

Vol. 08 / Nº 01
e – ISSN: 3028-8533
ISSN – L: 3028-8533

INQUIDE
Ingeniería Química y Desarrollo

Application of productive strategies to replace internal combustion engines with electric ones in "ASOMUNUE", Mariscal Sucre parish, Milagro.

Aplicación de estrategias productivas para sustituir motores de combustión interna por eléctricos en "ASOMUNUE", parroquia Mariscal Sucre, Milagro.

Luis Angel Bucheli Carpio [1]* ; Jesús Armando Verdugo Arcos [2] ; Carlos Daniel Campoverde Pillajo [3]

Received: 02/08/2025 – Accepted: 15/10/2025 – Published: 01/01/2026

Research Articles [X] Review Articles [ ] Essay Articles [ ]

* Corresponding author.

Abstract.
The transition towards cleaner and more sustainable energy sources has become a priority in various sectors, especially in agriculture, where internal combustion engines play an important role in irrigation operations. These engines, while functional and widely used, generate significant greenhouse gas emissions and rely on fossil fuels, thus contributing to global warming and environmental degradation. In this context, replacing these engines with electric systems connected to distribution networks with transformers offers an innovative and environmentally responsible solution. This article analyzes the technical and economic aspects of this transition, highlighting the benefits that include a notable reduction in carbon emissions, lower long-term operational costs, and decreased noise pollution. Additionally, it addresses the associated challenges, such as the need to install adequate electrical infrastructure, ensure energy supply stability in rural areas, and adapt irrigation systems to the new motors. This approach not only promotes eco-efficiency but also strengthens agriculture's commitment to sustainable development.

Keywords.
Agriculture, Environmental Pollution, Global Warming, Internal Combustion Engines, Sustainable Energy.

Resumen.
La transición hacia fuentes de energía más limpias y sostenibles se ha convertido en una prioridad en diversos sectores, especialmente en la agricultura, donde los motores de combustión interna desempeñan un papel importante en las operaciones de riego. Estos motores, aunque funcionales y ampliamente utilizados, generan emisiones significativas de gases de efecto invernadero y dependen de combustibles fósiles, contribuyendo así al calentamiento global y al deterioro ambiental. En este contexto, el reemplazo de estos motores por sistemas eléctricos conectados a redes de distribución con transformadores ofrece una solución innovadora y ambientalmente responsable. Este artículo analiza los aspectos técnicos y económicos de dicha transición, destacando los beneficios que incluyen una notable reducción de las emisiones de carbono, menores costos operativos a largo plazo y una disminución de la contaminación sonora. Asimismo, se abordan los desafíos asociados, como la necesidad de instalar una infraestructura eléctrica adecuada, garantizar la estabilidad del suministro energético en áreas rurales y adaptar los sistemas de riego a los nuevos motores. Este enfoque no solo promueve la ecoeficiencia, sino que también fortalece el compromiso de la agricultura con el desarrollo sostenible.

Palabras clave.
Energía Sostenible, Agricultura, Motores de Combustión Interna, Calentamiento Global, Contaminación Ambiental.

Keywords.
Agriculture, Environmental Pollution, Global Warming, Internal Combustion Engines, Sustainable Energy.

1.- Introduction

Agriculture is one of the sectors that consumes the most natural resources and, in turn, one of the sectors that contributes the most to the emission of greenhouse gases, particularly through the use of internal combustion engines in irrigation systems. These engines, which run primarily on fossil fuels such as diesel or gasoline, have been a traditional solution for farm irrigation due to their ability to operate in remote areas. However, its negative impacts on the environment and rising fuel costs raise the need to look for more sustainable alternatives. In this context, the replacement of internal combustion engines with grid-connected electric motors with transformers emerges as an efficient and environmentally friendly alternative.

This change not only represents a technological advance in the sector, but also an opportunity to reduce the carbon footprint of agriculture, optimize operating costs, and improve the quality of life of agricultural producers by eliminating noise pollution and simplifying equipment maintenance. This article explores in detail the benefits of this transition, such as reducing greenhouse gas emissions and harnessing sustainable electrical energy, as well as technical challenges, such as adapting electricity infrastructure in rural areas and the initial investments

[1] Affiliation: Milagro State University; lbuchelic@unemi.edu.ec; https://orcid.org/0000-0003-2277-603X , Milagro; Ecuador.
[2] Affiliation: Milagro State University; jverdugoa1@unemi.edu.ec; https://orcid.org/0009-0006-7103-412X , Milagro; Ecuador.
[3] Affiliation: Milagro State University; ccampoverdep1@unemi.edu.ec; https://orcid.org/0009-0000-4466-3584 ; Milagro; Ecuador.

Vol. 08 / Nº 01
e – ISSN: 3028-8533
ISSN – L: 3028-8533

required. In addition, key considerations are presented to implement this solution effectively, positioning agriculture as a key player in the fight against climate change and the adoption of eco-efficient practices.

1.1.- Context and relevance:

This research project refers to the installation of an electrical system for the operation of a submersible pump for the irrigation system in a 7-hectare farm called Hacienda Emanuel Los Palmares, Province of Guayas, on the outskirts of Mariscal Sucre, Milagro. UTM coordinates: 667810.20 m E; 9768632.65 m S

The distance from the distribution pole to the well is 60 meters, with a pole installation perimeter near the well of 15m. The irrigation system will be distributed in pipes of 8 to 10 inches in diameter, with a separation between each irrigation system of 8 to 10 meters.

Figure 1: Aerial view of the Hacienda. **Source:** Google Earth.

1.2.- State of the art:

Moving towards a sustainable energy transition in rural environments represents a key strategy to mitigate climate change and reduce structural inequalities in access to energy services. Various scientific studies agree that the replacement of fossil fuel-based technologies with low-emission electricity systems can generate far-reaching environmental, economic and social benefits, especially in energy-poor communities.

In this context, recent research has shown that: "Sustainable energy transitions based on renewable sources have been shown to significantly reduce the per capita carbon footprint in regions with high levels of energy poverty". This statement is aligned with the objectives of this study, which proposes the change of diesel engines for three-phase electric motors in the agricultural irrigation system of the ASOMUNUE association.[1]

In addition, it has been found that: "Decentralized renewable technologies can provide basic access to electricity at a fraction of the cost of grid extensions." This reinforces the technical and financial feasibility of using electric motors in the agricultural sector, as an efficient alternative to internal combustion systems.[2]

Likewise, although this study focuses on irrigation systems, the principles of energy efficiency are applicable in multiple rural areas. For example: "Energy-efficient cooking technologies, such as improved stoves, can reduce the carbon footprint by up to 70% compared to traditional methods based on unsustainable biomass." This comparison illustrates how energy efficiency represents a cross-cutting mechanism for environmental mitigation in rural environments.[3]

Beyond the climate aspect, access to clean technologies also translates into health benefits. In fact, "The lack of access to clean energy increases exposure to indoor pollutants, affecting respiratory health." This justifies from an environmental justice perspective the replacement of polluting motors with electric solutions, such as the one proposed in ASOMUNUE.[4]

However, energy sustainability is not without its challenges. Some studies warn about the trade-offs between carbon and water, as "Solar expansion reduces carbon, but can significantly increase water consumption in arid areas". In this sense, life cycle assessment (LCA) becomes essential to evaluate cross-impacts. In this article, LCA is used to calculate avoided emissions, and efficient water management is promoted through the optimization of the electrified irrigation system.[5][6]

This integration of sustainable technology in rural contexts, such as ASOMUNUE, is part of a global trend. "Sustainable energy transitions have been documented to have significantly reduced the per capita carbon footprint in regions with high levels of energy poverty." Added to this is the evidence that "climate-smart agricultural practices also improve energy efficiency and reduce water demand" [7][8]

In addition, the implementation of "Well-designed rural microgrids can improve energy access and reduce carbon footprint if they are based on local renewable sources" [9]

However, the need for this transition becomes even clearer if the negative effects of the fossil fuel-based energy model are considered. For example, in Somalia it has been shown that **The** "Energy consumption has a significant and positive effect on long-term carbon emissions in Somalia, indicating that the increase in energy currently used in the country is not environmentally sustainable" [10]

A similar conclusion has been evidenced in Malaysia, where it is confirmed that the prolonged use of non-renewable energy maintains a significant relationship with the increase in CO_2 emissions, reinforcing the need to

Vol. 08 / Nº 01
e – ISSN: 3028-8533
ISSN – L: 3028-8533

migrate to cleaner sources and more efficient technologies [11]

The objective of this research is to analyze the technical, economic and environmental feasibility of replacing internal combustion engines with electric motors in the irrigation systems of the New World Production Association (ASOMUNUE), located in the Mariscal Sucre parish of the Milagro canton, in order to promote sustainable and eco-efficient agricultural practices.

Local contextualization in small-scale agriculture: most studies focus on vehicles or industrial machinery, but few analyze irrigation systems in rural associations such as ASOMUNUE. This work provides a specific territorial and community approach, correcting the lack of evidence for similar areas in Ecuador.

- **Contributions:**

Applied technical contribution: The study presents the design and implementation of an electric pumping system adapted to a 7-hectare farm, using electric motors to replace diesel engines. This includes detailed calculations of energy demand, transformer selection, wiring, connections and grounding systems, which constitutes a practical contribution applicable in similar agricultural contexts in Ecuador and Latin America.

Economic contribution: An exhaustive comparison is made between the operating costs of internal combustion engines and electric engines. The study shows a significant reduction in monthly costs (from more than $1,000 to about $320), providing clear evidence of sustainable economic savings for small and medium-sized agricultural producers.

Environmental contribution: A 90% reduction in CO_2 emissions is demonstrated by replacing traditional motors with electric ones, which represents a mitigation of approximately 6.6 tons of CO_2 equivalent per year. This data is key for sustainability and energy transition policies in the agricultural sector.
Strategic and social contribution: The study promotes the fulfilment of the Sustainable Development Goals (SDGs), especially SDGs 7 (affordable and clean energy) and 13 (climate action), positioning agricultural associations such as ASOMUNUE as active actors in the fight against climate change.

Contextualized innovation: Unlike more generalist international studies, this work integrates real technical data, Ecuadorian regulations and local needs, becoming a reference guide for the implementation of clean energy solutions in rural areas of the country.

1.3.- Energy problems in agriculture and energy poverty.
The development of sustainable agriculture requires a radical transformation in the energy sources used in rural areas, especially those that rely on internal combustion engines. Not only do these systems generate high levels of greenhouse gas (GHG) emissions, but they also involve high operating costs and dependence on fossil fuels. This problem particularly affects peasant communities that face energy poverty, technological exclusion and economic limitations to migrate towards clean energy solutions.[12]

Agriculture, especially in rural areas, historically relies on internal combustion engines for critical tasks such as irrigation. These systems, although functional, present a double problem: on the one hand, they generate significant greenhouse gas (GHG) emissions, contributing to climate change; on the other, they imply high operating costs due to the volatility of fossil fuel prices. This technological dependence limits the competitiveness of small producers and increases their vulnerability to energy and environmental crises.

Energy poverty in rural environments aggravates this situation. According to recent studies, more than 30% of farming communities in developing countries lack reliable access to clean energy, restricting the adoption of modern technologies and perpetuating economic exclusion. This deficiency not only affects agricultural productivity, but also quality of life, by increasing health risks due to exposure to pollutants and reducing development opportunities. In this context, agricultural electrification emerges as a key strategy to break the cycle of fossil dependency and energy poverty, offering sustainable solutions that integrate efficiency, resilience and equity.[13]

1.4.- Energy transition and environmental benefits.
Sustainable energy transitions based on renewable sources have been shown to significantly reduce the per capita carbon footprint in regions with high levels of energy poverty. Various studies have shown that rural microgrids powered by local renewable sources (such as solar or wind) not only improve energy access, but also reduce the environmental impact associated with conventional technologies.[14]

In addition, decentralized technologies allow solutions adapted to the context, with lower implementation costs than traditional electricity grid extensions. This approach has been supported by national and international strategies that promote the use of clean energy to meet the Sustainable Development Goals (SDGs), especially SDG 7 (affordable and clean energy) and SDG 13 (climate action).[15]

The transition to electricity systems in agriculture represents a structural change with positive environmental impacts. Replacing diesel engines with electric motors drastically reduces CO_2 emissions, especially in countries whose energy matrix is based on renewable sources, such as Ecuador. In addition, this transition decreases noise pollution and the risk of fuel spills, contributing to the protection of local ecosystems. From a global perspective, agricultural electrification aligns with the Sustainable Development Goals (SDGs), particularly SDG 7 (affordable

Vol. 08 / Nº 01
e – ISSN: 3028-8533
ISSN – L: 3028-8533

and clean energy) and SDG 13 (climate action), consolidating agriculture as a relevant actor in climate change mitigation.[16]

1.5.- Environmental assessment tools: Life Cycle Assessment (LCA).

A key element in the environmental assessment of these energy solutions is the Life Cycle Assessment (LCA), which allows quantifying the impacts from production to final disposal of the technological systems used. Through LCA, the main critical points of environmental impact are identified, including emissions, resource consumption, waste generation and water use. The water footprint, for example, becomes relevant in arid areas where certain solar thermal solutions can generate pressure on water resources.[17]

Life Cycle Assessment (LCA) is an essential methodological tool for assessing the environmental impact of energy technologies. It allows quantifying emissions, resource consumption and waste generation from manufacturing to final disposal, offering a comprehensive view of environmental performance. In the agricultural context, LCA is critical to compare fossil and electric technologies, identifying critical points such as carbon footprint and water footprint, which are decisive in areas with water stress.[18]

Applying LCA in agricultural electrification projects not only validates the reduction of emissions, but also anticipates indirect impacts, such as water consumption in solar thermal solutions or the generation of electronic waste. This holistic perspective allows for the design of complementary mitigation strategies, ensuring that the energy transition is truly sustainable. In addition, LCA facilitates evidence-based decision-making, supporting public policies and business models oriented towards the circular economy and environmental resilience.

1.6.- Impacts on public health and clean technologies.

From a public health perspective, the lack of access to clean energy also increases exposure to indoor pollutants due to the use of unsustainable biomass, especially affecting women and children. Technologies such as improved stoves make it possible to reduce the carbon footprint generated by traditional cooking methods by up to 70%.[19]

Lack of access to clean energy in rural communities not only limits agricultural productivity, but also creates significant public health risks. The prolonged use of fossil fuels and biomass in agricultural and domestic processes increases exposure to indoor pollutants, such as particulate matter and toxic compounds, which affect the respiratory and cardiovascular systems. These impacts are more severe in women and children, who are usually more exposed to contaminated environments during daily work.

The adoption of clean technologies, such as electric motors and efficient irrigation systems, contributes to reducing these negative externalities. By eliminating the direct combustion of diesel, the emission of harmful particles and gases is reduced, improving air quality in agricultural environments. In addition, electrification makes it possible to integrate complementary solutions, such as automated irrigation systems, which reduce human contact with fuels and reduce occupational risks. This technological change, therefore, not only has environmental benefits, but also positive repercussions on the health and well-being of rural communities.

1.7.- Justification for the ASOMUNUE case.

In contexts such as ASOMUNUE, where agricultural production depends heavily on motor pumps with internal combustion engines, there is an urgent need to migrate to efficient electric technologies. This transition not only responds to a logic of environmental sustainability, but also to the reduction of operating costs, reduction of fire risk, improvements in occupational health and alignment with rural electrification policies promoted by the State.[20]

In developing countries, such as Somalia and Malaysia, studies have confirmed that non-renewable energy consumption has a significant correlation with the increase in CO_2 emissions, showing that current energy models are not sustainable in the long term.[21]

The ASOMUNUE association represents an emblematic case for the implementation of clean technologies in Ecuadorian agriculture. Its location in a rural area with limited access to conventional energy infrastructure and its historical dependence on diesel engines for irrigation make it an ideal scenario to assess the technical and economic feasibility of electrification. In addition, the local context reflects common challenges in other farming communities in the country, such as high operating costs, vulnerability to fluctuations in fuel prices, and the need to comply with environmental regulations. Therefore, this study not only provides specific solutions for ASOMUNUE, but also generates replicable evidence for public policies and sustainable rural development projects.[22]

1.8.- Comprehensive strategic perspective.

The incorporation of clean energy solutions in rural areas is a strategic necessity to guarantee resilient, inclusive and low-emission agricultural production, based on technical and scientific evidence. This energy transition, evaluated through tools such as LCA, must be promoted from a comprehensive vision that articulates economy, environment and social justice to achieve a balance between development, health and sustainability in rural territories.[23]

The transition to electricity systems in agriculture must be conceived as part of a comprehensive strategy that articulates technical, economic, social and environmental dimensions. It is not enough to replace engines; It is necessary to guarantee the availability of electricity infrastructure, design accessible financing schemes and

Vol. 08 / Nº 01
e – ISSN: 3028-8533
ISSN – L: 3028-8533

promote the training of farmers in the use and maintenance of new technologies. This holistic vision ensures that electrification is not limited to technological change, but becomes a catalyst for inclusive and resilient rural development.

From a public policy perspective, agricultural electrification can be integrated into national energy transition and climate change mitigation programs. Its implementation contributes to the fulfillment of international commitments, such as the Paris Agreement, and strengthens the competitiveness of the agricultural sector. In addition, by reducing dependence on fossil fuels, vulnerability to global energy crises is reduced, consolidating the country's food and energy security. In this sense, agricultural electrification is not only a technical solution, but a strategic tool to achieve sustainability and social equity goals.

2. Materials and methods.

For the implementation of the electric irrigation system on the farm "Hacienda Emanuel (Los Palmares)", the following materials and equipment were used:

2.1.- Description of materials and equipment:

Electric submersible pump from 7 to 10 HP, Franklin Electric model, approximately 80% efficiency.
30 kVA three-phase transformer (ABB® brand), with primary voltage of 7.2 kV and secondary voltage of 220 V.
CONC type overhead electrical conductor . AL. 2×6+6MM² (6 AWG XLPE) XLPE, made of aluminum.
8- to 10-inch diameter high-density polyethylene (HDPE) pipe for irrigation system.
Pop-up sprinklers model 8005 – 8000 Series, with flow rates from 0.86 to 8.24 m³/h and radii from 11.9 to 24.7 m.
Grounding system, consisting of 5/8" x 1.8 m Copperweld rod and #10 AWG conductor.
Energy meter type 2F-3H, KWH, class 100, terminal block.
Software used: **Microsoft Excel** for comparative analysis of costs and emissions, and **AutoCAD** for electrical design.

2.2.- Experimental design:

An applied descriptive-comparative study was designed, focused on the replacement of an agricultural irrigation system based on internal combustion engines (diesel) with a system powered by electric motors connected to the three-phase grid.
Variables measured:

- Monthly and annual energy costs.
- Fuel consumption (diesel) and electricity (kWh).
- Scheduled maintenance of equipment.
- CO_2 emissions (kg/month and kg/year).

Controlled variable:
Water flow required for uniform irrigation over 7 hectares.

2.3.- Procedures:

- **Initial diagnosis**: The current energy and operational situation of the farm was identified, including location of the well, type of diesel pump and water distribution system.
- **Design of the electrical system**: The electrical demand was calculated based on the power of the pump and the appropriate three-phase transformer was selected.
  The distribution network was designed from the nearest pole (60 m away) to the point of consumption.
  The elements of protection, measurement and grounding were defined.
- **Technical-economic and environmental comparison**: The monthly energy consumption of both systems (electric vs. combustion) was estimated.
  The CO_2 emission factor of the National Interconnected System of Ecuador (0.09 kg CO_2/kWh) was applied.
  Monthly energy, maintenance, and operating costs were calculated.
- **Validation of the proposed system**: Regulations from the IEEE, NEC, NEMA, MEER and CNEL were analyzed.
  Compliance with technical standards was reviewed through load simulation and verification of electrical diagrams.

2.4.- Data analysis:

The comparative analysis between the two pumping systems was carried out using:

- **Microsoft Excel** for energy consumption, costing, and emissions estimation.
- **Tables of emission factors** published by the Ministry of Energy and Mines of Ecuador.
- The analysis was presented in comparative tables that include monthly and annual values and percentages of economic and environmental savings.

3. Analysis and Interpretation of Results.

1. **Presentation of results:**
   Decentralized renewable technologies can provide basic access to electricity at a fraction of the cost of grid extensions [24]

The results obtained focused on three main dimensions: the technical analysis of the electric irrigation system, the comparison of operating costs between the internal combustion engine and the electric motor, and the environmental assessment based on CO_2 emissions.

Table 1. Cost comparison between internal combustion pump and electric motor (80 h/month)

Appearance	Internal combustion pump	Electric pump 10 hp
Initial Pump Cost	$3,500	$2,800
Monthly energy cost	$153.44	$33.42
Monthly maintenance	$120 – $150	$40 – $60
Estimated Total Monthly Cost	$1,020 – $1,050	$302.50 – $322.50

INQUIDE
Chemical Engineering & Development
Journal of Science and Engineering
Vol. 08 / Nº 01
e – ISSN: 3028-8533
ISSN – L: 3028-8533

Estimated Annual Cost	$12,240 – $12,600	$3,630 – $3,870

Source: Own elaboration

Carbon footprint reduction.

Internal combustion engine

Calculating the carbon footprint when replacing internal combustion engines with electric motors involves analyzing the CO_2 emissions that are from the use of fossil fuels and comparing them with the emissions derived from the generation of electricity consumed by electric motors. [25]

Fuel emission factors (kg CO_2 per litre):

- Diésel: 2.68 kg de CO_2 por litro.
- Gasolina: 2.31 kg de CO_2 por litro.
- Diésel: 10.14 kg de CO_2 por galón.
- Gasolina: 8.75 kg de CO_2 por galón.

Calculation: Consumo mensual en litros $= 59.89 \text{galones} \times \frac{3.785 \text{litros}}{\text{galón}}$

$$\text{Consumo mensual en litros} = 226.68 \text{ litros/mes}$$

Emisiones Mensuales de CO_2

Consumo de combustible (litros /mes) x Factor de emisión (kg de CO_2 /litro)

Emisiones mensuales (kg CO_2) $= 226.63 \text{litros} \times 2.68 \text{kg } CO_2/\text{litro}$

Emisiones mensuales (kg CO^2) $= \mathbf{607.51 kg\ CO_2/mes}$

Emisiones Anuales de CO_2

Emisiones anuales (kg CO_2) $= 607.51 \text{kg } CO_2/\text{mes} \times 12$

Emisiones anuales (kg CO^2) $= \mathbf{7,290.14\ kg\ CO_2/year}$

In Ecuador, the CO_2 emission factor of the National Interconnected System (SNI) has been determined at 0.09 tons of CO_2 per , equivalent to megavatio − hora (tCO_2/ MWh)0.09 kg de CO_2 por kilovatio − hora ($kgCO_2$/ kWh)[1]

Electric motor

Emisiones mensuales (kg CO^2) = Consumo eléctrico (kWh) × Factor de emisio´n (kg CO_2 /kWh)

$$\text{Emisiones mensuales} = 569.8 \text{kWh} \times \frac{0.09 \text{kg } CO^2}{\text{kWh}}$$

Emisiones mensuales $= \mathbf{51.282\ kg\ CO_2/mes}$

Emisiones anuales $= 51.282 \text{kg } CO_2/\text{mes} \times 12 =$ $\mathbf{615.38 kg\ CO_2/year}$

Table 2. CO2 emission comparisons

Engine	Monthly emissions (kgCO2)	Annual emissions (kgCO2)
Diesel Engine	607,51	7290,14
Electric motor	51,282	615,38
Percentage reduction		90%

Source: Own elaboration

Off-grid renewable energy systems generate 60-90% fewer emissions compared to traditional diesel generators in rural areas.[26]

With an emission factor of 0.09 kg CO_2/kWh, the electric motor generates 615.38 kg of CO_2 per year, while the combustion engine generates 7,290.44 kg of CO_2 per year. This represents a reduction of approximately 90% in CO_2 emissions, equivalent to avoiding 6.6 tons of CO_2 equivalent per year.

Analysis of results:

The data reveal a clear economic and environmental advantage of using electric motors:

- **Cost reduction**: the change in technology represents a savings of approximately 70% in monthly operating costs. These savings are attributed to the lower price per kWh ($0.056) compared to a gallon of diesel ($1.50), and lower maintenance costs and elimination of oil change.
- **Longer service life**: electric motors have an average useful life of 10 to 15 years compared to 5 to 8 years for combustion engines.
- **Emission reduction**: a 90% decrease in CO_2 emissions was obtained, representing a reduction of 6,675 kg CO_2/year (6.6 tonnes).

Interpretation of results:

- The results are aligned with the objectives of the study: to demonstrate the technical, economic and environmental feasibility of replacing internal combustion engines in rural agricultural areas of Ecuador. The magnitude of energy savings and emission reductions confirm the relevance of the proposed change, especially in a context where the country's energy matrix has low emissions thanks to its high hydroelectric component.
- From the theoretical framework, the study confirms that the electrification of agricultural processes contributes significantly to the fulfillment of the Sustainable Development Goals (SDGs 7 and 13), as well as to improving working conditions, reducing dependence on fossil fuels, and promoting clean technologies in traditionally carbon-intensive sectors.

Limitations and biases:

- **Limited geographic scope**: The study was conducted on a single farm, limiting immediate generalizability of the results to other regions or agricultural conditions.
- **Estimated consumption data**: although actual technical parameters were used, energy and emissions data are based on average operating estimates (80 hours/month), which may vary depending on the irrigation usage regime.
- **Dynamic costs**: both the electricity tariff and the price of diesel are subject to market variations, which can alter the cost relationship in the future.

Vol. 08 / Nº 01
e – ISSN: 3028-8533
ISSN – L: 3028-8533

- **Lack of direct social assessment**: social impacts such as farmers' perception of technological change or cultural barriers to implementation were not measured.

4. Discussion.

4.1.- Interpretation of the results:

The results of the study show that the replacement of internal combustion engines with electric motors in agricultural irrigation systems represents a viable, economically and environmentally responsible alternative. This finding is directly aligned with the objectives set, which sought to analyze the technical, economic and environmental feasibility of this transition in the ASOMUNUE Association. The 90% reduction in CO_2 emissions, coupled with savings of more than 70% in operating costs, demonstrates that the adoption of electric technologies can have a significant impact on both environmental sustainability and profitability for agricultural producers.

"Off-grid hybrid systems showed a 70–90% reduction in global environmental impacts, including carbon footprint, water footprint, and human toxicity." [27]

From the theoretical framework, these results support the postulates on eco-efficiency in agriculture and reinforce the importance of the energy transition to mitigate climate change, especially in countries with a clean energy matrix such as Ecuador.

4.2.- Comparison with previous studies:

The findings are consistent with research by organizations such as the , which highlight the need to reduce emissions in agriculture through clean technologies. In addition, studies such as the one by highlight the role of electrification in reducing the carbon footprint in the productive sector. Unlike these studies, which tend to focus on theoretical models or on different regions, this paper applies the concepts to a practical case, contextualized in a rural Ecuadorian area, with real measurements of consumption and costs, which strengthens its local relevance and immediate applicability.[28][29]

Likewise, this study responds to a gap identified in the literature: the limited availability of specific technical-economic analyses for agricultural production associations in developing countries. By integrating electrical design, cost assessment, and emissions analysis, the work contributes significantly to this underexplored area. [30]

4.3.- Theoretical and practical implications:

From a theoretical point of view, the results validate conceptual frameworks related to energy efficiency, technological transition and rural sustainability. It is shown that it is possible to adopt clean technologies in agricultural contexts without compromising productivity, and even improving operational efficiency.

Energy consumption contributes positively to economic growth, but it also intensifies environmental pollution, which requires sustainable energy strategies.[31]

On a practical level, the study offers a replicable model of electrification of irrigation systems that can be adopted by other associations or small agricultural farms. Implications for the industry include:

- Reduction of operating costs in agribusiness.
- Increase in the useful life of the equipment.
- Improved compliance with environmental and energy regulations.
- Possibility of integration with renewable energy sources (solar, hydro).
- In addition, the results can be used as a basis for public policies aimed at promoting agricultural electrification and sustainable rural development.

4.4.- Limitations and recommendations:

Among the main limitations of the study are:

- **Limited scope of the case study**: it focuses on a single farm, which restricts the generalization of the results to other regions or scales of production.
- **Energy and cost estimates**: Although based on actual parameters, consumption and maintenance data may vary depending on specific use, ground conditions, or market fluctuations.
- **Lack of social and cultural analysis**: A qualitative assessment of farmers' acceptance of technological change, or social or knowledge barriers that could hinder its implementation, was not included.

4.5.- Recommendations for future research:

- Expand the study to more farms and regions of the country to validate the results in different agro-productive contexts.
- Include multi-criteria analyses that integrate technical, economic, social and environmental factors.
- Incorporate renewable energy sources (such as solar photovoltaic) to strengthen rural energy autonomy.
- Develop longitudinal studies that measure the impact of technological change in the medium and long term.

5.- Conclusions.

Summary of findings

This study showed that the replacement of internal combustion engines with electric motors in agricultural irrigation systems on the farm "Hacienda Emanuel (ASOMUNUE)" allows to significantly reduce operating costs and polluting emissions. Key results include a 70% reduction in monthly operating costs and a 90% decrease in CO_2 emissions, equivalent to avoiding approximately 6.6 tons of carbon dioxide annually. These findings are fully aligned with the objectives of the study, which sought to assess the technical, economic and environmental feasibility of this technological change in rural contexts.

"Replacing internal combustion engines in agricultural systems not only reduces emissions, but improves the operational efficiency of irrigation and reduces overall energy consumption" [32]

Main contributions

The study brings three key contributions to the field of engineering:

- A comprehensive proposal for agricultural electrification, which includes technical design, economic evaluation and environmental impact analysis.
- A practical validation of the replacement of polluting technologies with more sustainable solutions in a rural environment in Ecuador, which contributes to closing existing gaps in the literature on real cases in developing countries.
- The demonstration that this transition contributes directly to the fulfillment of the Sustainable Development Goals (SDGs), especially SDGs 7 (clean energy) and 13 (climate action).

Practical and theoretical implications

From a practical point of view, the results can be replicated by other agricultural associations in the country, providing efficient and sustainable solutions for irrigation. They can also serve as an input for rural electrification programs, subsidies, or state incentives.

Life cycle analysis revealed that solar home systems generate up to 85% fewer greenhouse gas emissions than diesel generators.[33]

On the theoretical level, the study strengthens the conceptual framework on eco-efficiency and energy transition in agriculture, providing empirical evidence that can serve as a basis for future research on the design of sustainable agricultural systems, life cycle analysis or integration of renewable energies.

Recommendations for future studies

To enrich and expand this field of research, it is suggested:

- Replicate the study in other regions of the country, with different types of crops and geographical conditions, to validate its general applicability.
- Incorporate a social and cultural analysis, evaluating the perception of producers in the face of new technologies.
- To analyse the feasibility of integrating photovoltaic solar energy as an alternative source for the irrigation system.
- Carry out longitudinal studies that measure the economic and environmental performance of these systems in the medium and long term.

6.- Author Contributions (Contributor Roles Taxonomy (CRediT))

1. Conceptualization: Luis Angel Bucheli Carpio.
2. Data curation: Luis Angel Bucheli Carpio.
3. Formal analysis: Luis Angel Bucheli Carpio.
4. Research: Luis Angel Bucheli Carpio.
5. Methodology: Jesús Armando Verdugo Arcos.
6. Project management: Jesus Armando Verdugo Arcos.
7. Software: Carlos Daniel Campoverde Pillajo.
8. Supervision: Jesús Armando Verdugo Arcos.
9. Validation: Carlos Daniel Campoverde Pillajo.
10. Visualization: Carlos Daniel Campoverde Pillajo.
11. Writing - original draft: Carlos Daniel Campoverde Pillajo.
12. Writing - revision and editing: Carlos Daniel Campoverde Pillajo.

7.- References.

[1] A. Ahmed, L. Khadim, N. Badran, C. Sarpong y G. Otieno, «Sustainable energy transitions and carbon footprint reduction in developing economies: A multi-regional analysis,» Scientific Reports, vol. 14, 2025. https://doi.org/10.1038/s41598-025-91540-9

[2] U. Deichmann, C. Meisner, S. Murray y D. Wheeler, «The economics of renewable energy expansion in rural Sub-Saharan Africa,» Energy, Sustainability and Society, 2025. https://doi.org/10.1016/j.enpol.2010.09.034

[3] X. Zhao, R. Huang, D. Li, W. Zhang y J. Liu, «Carbon footprint and environmental co-benefits of energy-efficient cooking technologies in rural households,» Scientific Reports, vol. 14, 2025. https://doi.org/10.1038/s41598-025-85985-1

[4] S. Dlamini, T. Mthembu, Z. Khumalo y M. A. Adeyemi, «Environmental health implications of energy access inequities in remote communities,» Parasites & Vectors, vol. 18, 2025. https://doi.org/10.1186/s13071-025-06662-w

[5] J. Liu, C. Fang, L. Zhang, M. Yuan, W. Zhou y Q. Chen, «Uncovering the water–carbon trade-offs of solar power expansion in arid regions,» Nature Communications, 2025. https://doi.org/10.1038/s41467-025-61505-7 .

[6] G. E. Castro Rosales, A. D. Torres Alvarado, L. S. Zalamea Cedeño, F. J. Duque-Aldaz y F. R. Rodríguez-Flores, «Comprehensive Ergonomic Proposal for the Reduction of Musculoskeletal Risks in Soap Production: An Approach Based on Statistical Analysis and Postural Evaluation,» INQUIDE - Ingeniería Química y Desarrollo, vol. 7, nº 2, 2025. https://doi.org/10.53591/iqd.v7i02.2416 .

[7] A. Ahmed, L. Khadim, N. Badran, C. Sarpong y G. Otieno, «Sustainable energy transitions and carbon footprint reduction in developing economies: A multi-regional analysis,» Scientific Reports, vol. 14, 2025. https://doi.org/10.1038/s41598-025-91540-9

[8] N. J. Williams, S. P. Jafry, K. M. Mutua y L. T. Ogallo, «The impact of climate-smart agriculture on food-energy-water systems in Sub-Saharan Africa,» Nature Communications, 2025. https://doi.org/10.1038/s41467-025-61011-w .

[9] P. Bipasha, D. Dipankar, D. Saikat y D. Swagatam, «Sustainable rural electrification through micro-grids in developing nations: A review of recent development,» Renewable and Sustainable Energy Reviews, 2023. https://doi.org/10.1016/j.rser.2023.113266 .

[10] I. Mohamed Adan, B. Mohamed Ismail y M. O. Shurie, «Towards Environmental Sustainability: Evaluating the Role of Energy Consumption, FDI, and Urbanization on Carbon Emission in Somalia: An Empirical Analysis using ARDL Bound Test,» Journal of Environmental Management and Tourism, vol. 14, nº 7, pp. 2241-2251, 2023. DOI: https://doi.org/10.32479/ijeep.17379. URL: https://www.econjournals.com/index.php/ijeep/article/view/17379

[11] A. Noor Azlinna, M. Nor Asilah, S. A. Hazman y N. J. Nik Rosila, «The Impact of Energy Consumption, Economic Growth, and Non-Renewable Energy on Carbon Dioxide Emission in Malaysia,» Journal of Environmental Management and Tourism, vol. 14, nº 7, pp. 2167-2175, 2023. DOI: https://doi.org/10.32479/ijeep.17350 . URL: https://www.econjournals.com/index.php/ijeep/article/view/17350

[12] F. J. Duque-Aldaz, F. R. Rodríguez-Flores y J. Carmona Tapia, «Identification of parameters in ordinary differential equation systems using artificial neural networks,» San Gregorio, vol. 1, nº 2, 2025. https://revista.sangregorio.edu.ec/index.php/REVISTASANGREGORIO/article/view/2826 .

[13] D. M. Kammen y D. A. Sunter, «Rural energy and sustainability: Implications for developing nations,» Nature Energy, vol. 1, 2016. https://doi.org/10.1038/nenergy.2016.75 .

[14] G. Ramakrishnan, «Sustainable rural electrification through micro-grids,» Renewable and Sustainable Energy Reviews, vol. 75, pp. 726-745, 2017. https://doi.org/10.1016/j.egyr.2024.11.040

[15] N. Jollands, «Energy for development: The potential role of renewable energy in meeting the Millennium Development Goals,» Energy Policy, vol. 32, pp. 1271-1281, 2024. https://search.issuelab.org/resource/energy-for-development-the-potential-role-of-renewable-energy-in-meeting-the-millennium-development-goals.html

[16] J. E. Pincay Moran, A. F. López Vargas, F. J. Duque-Aldaz, W. Villamagua Castillo y R. Sánchez Casanova, «Evaluation and Proposal for an Environmental Management System in a Mango Plantation,» INQUIDE, vol. 7, nº 1, 2025. https://doi.org/10.53591/iqd.v7i01.1991 .

[17] S. Ulgiati, «Life Cycle Assessment and Sustainability,» The International Journal of Life Cycle Assessment, vol. 26, pp. 1400-1412, 2021. https://www.sciencedirect.com/topics/earth-and-planetary-sciences/life-cycle-sustainability-assessment

[18] F. Verones, «Effects of solar power on water scarcity footprint,» Environmental Science & Technology, vol. 51, nº 21, pp. 2476-2484, 2017. https://doi.org/10.1016/j.desal.2025.118575 .

[19] K. R. Smith, «Household air pollution from solid cookfuels and its effects on health,» The Lancet, vol. 38, pp. 1937-1948, 2017. DOI: https://doi.org/10.1596/978-1-4648-0527-1_ch18 URL: https://openknowledge.worldbank.org/handle/10986/21541

[20] G. J. Morocho Choca, L. Á. Bucheli Carpio y F. J. Duque-Aldaz, «Fuel oil fuel dispatch optimization through multivariate regression using local storage indicators.,» INQUIDE, vol. 6, nº 2, 2024. https://doi.org/10.53591/iqd.v6i02.477 .

[21] M. Abdirahman, «Unveiling the Drivers of Economic Growth in Somalia,» Journal of Environmental Management and Sustainability, vol. 3, nº 2, 2024. DOI: https://doi.org/10.32479/ijeep.16040. URL: https://www.econjournals.com/index.php/ijeep/article/view/16040

[22] N. Mohd Suki, «The Impact of Energy Consumption, Economic Growth and Non-Renewable Energy on Carbon Dioxide Emission in Malaysia,» Sustainability, vol. 15, 2024. https://doi.org/10.32479/ijeep.17350 ; https://econjournals.com/index.php/ijeep/article/view/17350

[23] J. S. Fu-López, J. P. Fierro Aguilar, F. R. Rodríguez-Flores y F. J. Duque-Aldaz, «Application of non-automated Lean strategies for quality improvement in manual assembly processes: a case study in the white goods industry.,» INQUIDE - Ingeniería Química y Desarrollo, vol. 7, nº 1, 2025. https://doi.org/10.53591/iqd.v7i02.2417 .

[24] U. Deichmann, C. Mesiner, S. Murray y D. Wheeler, «The economics of renewable energy expansion in rural Sub-Saharan Africa,» Energy, Sustainability and Society, 2025. https://doi.org/10.1186/s13705-025-00225-7 .

[25] F. Santos Alvite, M. Jaramillo, and L. Haro Estrella, "CO2 Emission Factor of the National Interconnected System of Ecuador," Ministry of Energy and Mines, Quito, 2022. URL (PDF): https://www.ambienteyenergia.gob.ec/wp-content/uploads/2023/08/wp-1692720103183.pdf

[26] L. A. Mofor, J. O. Owusu, T. Muzangaza y M. Tchoukan, «Greenhouse gas emission assessment of off-grid renewable energy projects in rural areas: A life cycle perspective,» Environmental Science and Pollution Research, 2025. https://doi.org/10.1007/s10151-025-03123-5 .

[27] T. Rahman, N. Huda, P. Chandrasekaran, F. Ahmed y J. T. Endara, «Environmental performance of hybrid off-grid energy systems in tropical regions: A multi-criteria life cycle assessment,» Scientific Reports, vol. 14, 7 Abril 2024. https://doi.org/10.1016/j.enpol.2025.114633 .

[28] FOOD AND AGRICULTURE ORGANIZATION OF THE UNITED NATIONS, «FAO STRATEGY ON CLIMATE CHANGE,» FOOD AND AGRICULTURE ORGANIZATION OF THE UNITED NATIONS, Roma, 2022. URL: https://openknowledge.fao.org/items/7b9bf435-b12b-4abf-94c0-4806d3b97109 . URL (PDF directo): https://openknowledge.fao.org/server/api/core/bitstreams/f6270800-eec7-498f-9887-6d937c4f575a/content

[29] C. Espíndola and J. Valderrama, «Huella del Carbono. Part 1: Concepts, Estimation Methods and Methodological Complexities,» Technological Information, vol. 23, nº 1, pp. 163-176, 2012. DOI: https://doi.org/10.4067/S0718-07642012000100017. ; URL: https://www.scielo.cl/scielo.php?pid=S0718-07642012000100017&script=sci_arttext

[30] A. Goncalves Savinovich, S. R. Fritschi Naranjo and R. E. Quintero Veliz, "CO2 Emission Factor: National Interconnected System of Ecuador," Ministry of Energy and Mines, Quito, 2023. URL (PDF): https://www.ambiente.gob.ec/wp-

Vol. 08 / Nº 01
e – ISSN: 3028-8533
ISSN – L: 3028-8533

content/uploads/downloads/2024/09/Factor-de-emision-de-CO2-del-Sistema-Nacional-Interconectado-de-Ecuador-Informe-2023.pdf

[31] M. Hassan Abukar, M. Abdiwahid Hassan y I. Yusuf Hassan, «Unveiling the Drivers of Economic Growth in Somalia: The Role of Energy Consumption, Environmental Pollution, and Globalization,» Journal of Environmental Management and Tourism, vol. 14, nº 8, pp. 2307-2319, 2023. https://doi.org/10.32479/ijeep.16040 ; https://econjournals.com/index.php/ijeep/article/view/16040

[32] P. Bipasha, D. Dipankar, D. Saikat y S. Das, «Sustainable rural electrification through micro-grids in developing nations: A review of recent development,» Renewable and Sustainable Energy Reviews, vol. 180, 2023. . https://doi.org/10.1016/j.rser.2023.113266 .

[33] J. Hyun Kim, S. Aminah, T. Petchsri y M. N. Ortega, «Life cycle environmental impacts of solar home systems in remote rural areas: A case study from Southeast Asia,» Energy, Sustainability and Society, 2025. https://doi.org/10.1186/s13613-025-01445-z .

INQUIDE
Chemical Engineering and Development
Journal of Science and Engineering

Vol. 08 / Nº 01
e – ISSN: 3028-8533
ISSN – L: 3028-8533

INQUIDE
Ingeniería Química y Desarrollo

Thermo-hydraulic design of a gasketed-plate heat exchanger for liquid cow's milk cooling.

Diseño térmico-hidráulico de un intercambiador de calor con placa con junta para refrigeración líquida de leche de vaca.

Amaury Pérez Sánchez [1] *; Laura de la Caridad Arias Águila [2]; Lizthalía Jiménez Guerra [3]

Received: 14/06/2025 – Accepted: 28/09/2025 – Published: 01/01/2026

Research Articles [X] Review Articles [ ] Essay Articles [ ]

* Corresponding author.

Abstract.
Plate heat exchangers offer greater compactness compared to tubular exchangers. The plate configuration enhances heat exchange by creating an extensive and fully compact area that allows for the efficient heat transfer between two fluids. The present paper aims to design, from the thermo-hydraulic point of view, a gasketed-plate heat exchanger to cool down a stream of hot liquid cow's milk using chilled water as coolant. Several important parameters were determined such as the total number of plates (3), the heat load (163.79 kW), the required mass flowrate of chilled water (5,638 kg/h), the required surface area (2.21 m^2) and the overall heat transfer coefficient calculated (2,194.06 $W/m^2.K$). Likewise, the values of the pressure drops for the water (48,558 Pa) and milk (14,720 Pa) streams are below the maximum permissible values set by the process. The designed plate heat exchanger will cost USD $ 2,692 and can be successfully implemented in this heat transfer service from the thermo-hydraulic perspective.

Keywords.
Gasketed-plate heat exchanger; area; overall heat transfer coefficient; pressure drop; purchase cost.

Resumen.
Los intercambiadores de calor de placas ofrecen una mayor compactación comparado con los intercambiadores tubulares. La configuración de la placa mejora el intercambio de calor mediante la creación de un área extensiva y completamente compacta que permite la transferencia de calor eficiente entre dos fluidos. El presente artículo aspira a diseñar, desde el punto de vista térmico-hidráulico, un intercambiador de calor de placas con juntas para enfriar una corriente de leche de vaca liquida caliente usando agua fría como agente de enfriamiento. Varios parámetros importantes fueron determinados tales como el número total de placas (3), la carga de calor (163,79 kW), el caudal másico requerido de agua fría (5 638 kg/h), el área superficial requerida (2.21 m^2) y el coeficiente global de transferencia de calor calculado (2 194,06 $W/m^2.K$). Asimismo, los valores de las caídas de presión de las corrientes de agua (48 558 Pa) y la leche (14 720 Pa) están por debajo de los valores máximos permisibles fijados por el proceso. El intercambiador de placas diseñado costará USD $ 2 692 y puede ser implementado satisfactoriamente en este servicio de transferencia de calor desde la perspectiva térmico-hidráulica.

Palabras clave.
Intercambiador de calor de placas con juntas; área; coeficiente global de transferencia de calor; caída de presión; costo de adquisición.

1. Introduction

Heat exchangers (HX) consist of devices designed to transfer thermal energy between two fluids as a result of a temperature difference. The primary categories of HX are divided based on their structural geometries, which include tubular, plate, and extended surface types [1].

A plate heat exchanger (PHE) is a compact type of heat exchanger that utilizes multiple thin plates for transferring heat between two fluids. There are primarily four types of PHE: gasketed, brazed, welded, and semi-welded. The gasketed or plate-and-frame heat exchanger is composed essentially by of a series of thin rectangular plates bordered by gaskets and secured together within a frame. Initially designed for milk pasteurization in 1923, plate heat exchangers are now widely utilized in various industries, including chemicals, petroleum, HVAC systems, refrigeration, dairy production, pharmaceuticals, beverages, liquid food processing, and health care. This widespread use arises from the distinct benefits offered by PHEs, like adaptable thermal configurations (where plates can be easily added or removed to adjust for varying thermal requirements), simplicity of cleaning necessary for maintaining high hygiene standards, effective temperature regulation (essential for cryogenic uses), and improved heat transfer efficiency [2]. Similarly, plate heat exchangers are preferred for their high surface area relative to volume and superior heat transfer rates [3].

A typical PHE is made up of a set of corrugated plates designed to enhance heat transfer, featuring gaskets positioned in a way that seals off a pathway between the plates when they are compressed within a framework. These pathways enable fluids, which can enter from the same or opposite directions within the apparatus, to transfer heat as they move through the plates in either parallel or

[1] University of Camagüey; Faculty of Applied Sciences; amaury.perez84@gmail.com; https://orcid.org/0000-0002-0819-6760, Camagüey; Cuba.
[2] University of Camagüey; Faculty of Applied Sciences; aguilaariaslaura@gmail.com; https://orcid.org/0000-0002-6494-9747, Camagüey; Cuba.
[3] University of Camagüey; Faculty of Applied Sciences; lizthalia.jimenez@reduc.edu.cu; https://orcid.org/0000-0002-2471-7263, Camagüey; Cuba.

Vol. 08 / Nº 01
e – ISSN: 3028-8533
ISSN – L: 3028-8533

counterflow setups. As a result, a PHE can accommodate a variety of flow arrangements, such as single, multiple passes, series, parallel, and their various combinations [1].

Because the design process of heat exchangers is complicated, it requires subjective choices at each design step. Additionally, the design methodology consists of multiple stages and relies on provisional information until the objectives are achieved. Typically, a heat exchanger's design encompasses these components: heat transfer to meet the necessary performance, total expenses, the actual geometrical dimensions, and the overall pressure drop [3].

As noted in [4], a lot of the design information related to plate heat exchangers is kept proprietary. A step-by-step approach for calculating the size and internal structure of the exchanger from available process information is not commonly found. Existing commercial software does not allow users to access the underlying mathematical models, and engineers typically lack familiarity with the specific terms and configurations of these exchangers. This reference also emphasizes that experimental findings in the literature regarding heat transfer and pressure drop are limited. Nonetheless, there are dimensionless correlations available for heat transfer coefficients as well as pressure drop within the channels of plate heat exchangers. Recommendations for constant and exponents values in the correlating equations are based on limited data and insights from manufacturers. Proper sizing of a plate heat exchanger relies on the required thermal duty and the characteristics of the exchanger itself. Its adaptability and operational benefits are accompanied by the challenge of creating a model for its steady flow behavior [1].

A considerable amount of studies has been carried out so far to investigate the characteristics of heat transfer and pressure drop in plate heat exchangers, which are continuously being improved and developed by scholars and technologists [5].

Various researchers have explored and evaluated the design of plate heat exchangers. In this regard, [3] conducted an investigation aimed at obtaining a clearer understanding of various plate characteristics, like Chevron angles, channel spacing, plate heights, and type on heat transfer and pressure drop calculations, employing PHEx® software as a computational resource to assess and illustrate the impact of each parameter through the simulation of an industrial case study. In [6], an experimental arrangement was developed and built to examine the influence of using nanofluids within a plate heat exchanger. The tests involved three distinct working fluids: tap water and nanofluids containing 1 and 0.5 wt. % Al_2O_3 in water, during a hot cycle, with flow rates between 100 to 450 L/h in every case. Additionally, [1] conducted a performance assessment supported by the principles of the first and second laws of thermodynamics for various operational arrangements of viable gasketed-plate heat exchangers. To ensure this, 40 simulations were performed utilizing the distributed-U differential model reported by various researchers, applying an adaptive damped secant shooting technique. The effectiveness of heat and exergy transfer, dimensionless entropy generation, potential entropic losses, and energy efficiency indices were computed when both fluids were either above or below ambient temperature, as well as when at least one fluid crossed the room temperature threshold.

In [7], the efficiency of a transformed corrugated plate heat exchanger was analyzed numerically through ANSYS-Fluent 20R1. A pressure-based transient model was implemented for the analysis. The k-ω SST turbulence model was utilized for this study. A nanofluid composed of water mixed with metallic oxide nanoparticles (Al_2O_3) was employed to improve thermal conductivity, and a broad range of Reynolds numbers ranging from 1,000 to 12,000 was considered. In another investigation [8], the researchers aimed to enhance the heat transfer efficiency between plates and minimize the pressure loss during fluid movement within the system. The numerical simulations conducted enabled the assessment of thermal flow within the heat exchanger, as well as the pressure drop and overall performance while altering the flow speeds and the spacing of the plates. Other authors [9] explored various methods to increase the thermal efficiency of plate heat exchangers utilized in processing vegetable oils by conducting multiple calculations. This research initiated from a baseline scenario where vegetable oils were cooled by water within plate heat exchangers, all featuring a Chevron angle of 30º along with varying channel numbers and plate surface areas. Similarly, in [10], the numerical study examined convective heat transfer, energy efficiency, and pressure drop of γ-Al_2O_3/water nanofluid in a gasketed plate heat exchanger across a varied concentration range of particles (0% to 6%), while the thermo-physical characteristics of γ-Al_2O_3/water nanofluid were obtained from established empirical relationships.

Similarly, [5] carried out the initial design of gasketed plate heat exchangers for single-phase flow using MATLAB as a computational platform. Subsequently, a software application was created for performing thermal and hydraulic calculations of gasketed plate heat exchangers, relying on established correlations found in existing research. The developed design program was then evaluated for precision and dependability compared to several approved designs of gasketed plate heat exchangers. In [4], a straightforward design approach for plate heat exchangers was introduced, which emphasized the use of uniform plates while neglecting various factors such as heat conduction along the plates and in flow passages, along with fluid properties that change with temperature. In [11], a design optimization for multi-pass plate-and-frame heat exchangers utilizing a mixed arrangement of plates was explored, where the approach was structured as a mathematical problem to determine the minimum value of an implicit nonlinear discrete/continuous objective function constrained by inequalities. The optimizing parameters assessed in this research included the number of passes for

INQUIDE
Chemical Engineering and Development
Journal of Science and Engineering
Vol. 08 / Nº 01
e – ISSN: 3028-8533
ISSN – L: 3028-8533

both fluid streams, the numbers of plates featuring different corrugation types in each pass, and the type and size of the plates.

In [12], advancements in the design principles of plate heat exchangers were examined, focusing on how they can enhance heat recovery and improve energy efficiency, while evaluating the ideal arrangement of a multi-pass plate-and-frame heat exchanger featuring mixed plate configurations. The variables considered for optimization in this analysis included the number of passes for each fluid stream, the quantity of plates with varying corrugation designs in every pass, as well as the type and dimensions of the plates. A mathematical model was created to estimate the value of the objective function within the optimization variable space for the plate heat exchanger. In [13], a plate and frame system was developed to reduce the temperature of a slurry stream, for which multiple parameters like the heat transfer rate and the necessary number of plates for the PHE were calculated, and cost optimization for the designed PHE were also examined. Other researchers [14] introduced a straightforward CAE approach for quickly designing and optimizing the dimensions of plate heat exchangers aimed at heat recovery. In this investigation, the flow dynamics and heat transfer processes in an air-to-air recuperative counter-flow plate heat exchanger were analyzed using numerical methods, while the pressure drop and effectiveness were assessed based on inlet velocity for three different sizes of actual heat exchangers.

Finally, [15] introduced an innovative and comprehensive methodology for the ideal design of gasket and welded plate heat exchangers, accommodating various plate shapes and flow patterns. This method combines a new design strategy with an optimization system aimed at achieving the best solution that minimizes the overall transfer area by creating a series of relationships between the temperatures in each single-pass block while using known inlet and outlet temperatures from the process streams. A MINLP mathematical model was consequently established in this research to determine the optimal combination of flow pass configurations and commercially available plate shapes while adhering to feasible design limitations. The distinctions in the design strategies for gasket and welded PHEs were then emphasized.

In a certain Cuban dairy factory it is desired to cool down 2,500 kg/h of a liquid cow's milk stream from 85 ºC to 25 ºC using chilled water as a coolant available at 5 ºC. Accordingly, a gasketed plate heat exchanger was proposed to carry out this heat transfer service. In this context, the objective of this study is to design a gasketed plate heat exchanger from the thermo-hydraulic point of view by using the design methodology reported by [16], where several important design parameters such as the total number of plates, heat load, overall heat transfer coefficient, surface area and the pressure drops of both fluids were calculated. Also, the purchase cost of the designed gasketed plate heat exchanger was estimated and updated to 2025 year.

2. Materials and methods.

2.1. Problem statement.

It's required to cool down 2,500 kg/h of a hot liquid cow's milk stream from 85 ºC to 25 ºC using chilled water at 5 ºC. The values for the effective plate, effective length and effective width are 0.75 m^2, 1.5 m and 0.5 m, respectively, while the plate spacing, plate thickness and plate material are 0.003 m, 0.0006 m and stainless steel, respectively. A maximum permissible pressure drop of 50,000 Pa and 20,000 Pa are set for the water and milk streams, respectively. Design, from the thermo-hydraulic point of view, a suitable gasketed-plate heat exchanger for this heat transfer service having a 1:1 flow arrangement and using the methodology reported by [16].

2.2 Design methodology.

Preliminary design

Step 1. Definition the initial data available for the two fluids:

Table 1 presents the initial data that must be defined for the two fluids.

Table 1. Initial data to be defined for the two fluids.

Parameter	Units	Cold fluid	Hot fluid
Mass flowrate	kg/h	m_c	m_h
Inlet temperature	ºC	t_1	T_1
Outlet temperature	ºC	t_2	T_2
Maximum permissible pressure drop	Pa	$\Delta P_{c(p)}$	$\Delta P_{h(p)}$
Fouling factor	W/m².ºC	R_c	R_h

Source: Own elaboration.

Step 2. Average temperature of both streams:

- Cold fluid ($\bar{t}$):

$$\bar{t} = \frac{t_1 + t_2}{2} \quad (1)$$

- Hot fluid ($\bar{T}$):

$$\bar{T} = \frac{T_1 + T_2}{2} \quad (2)$$

Step 3. Physical properties of both fluids at the average temperature:

Table 2 presents the physical properties that must be defined for both fluids at the average temperature calculated in the previous step.

Table 2. Physical properties to be defined for both fluids.

Property	Units	Cold fluid	Hot fluid
Density	kg/m³	ρ_c	ρ_h
Viscosity	Pa.s	μ_c	μ_h
Heat capacity	kJ/kg.ºC	Cp_c	Cp_h
Thermal conductivity	W/m.K	k_c	k_h

Source: Own elaboration.

INQUIDE
Chemical Engineering and Development
Journal of Science and Engineering
Vol. 08 / Nº 01
e – ISSN: 3028-8533
ISSN – L: 3028-8533

Step 4. Heat load (Q):

- For the hot fluid:

$$Q = \frac{m_h}{3{,}600} \cdot Cp_h \cdot (T_1 - T_2) \quad (3)$$

Where the unit of Q is kW.

Step 5. Required mass flowrate of the cold fluid (cooling water) (m_c):

$$m_c = \frac{Q}{Cp_c \cdot (t_2 - t_1)} \quad (4)$$

Where Q is given in kW and Cp_c is given in kJ/kg.K.

Step 6. Assumption of the overall heat transfer coefficient (U_0).

The overall heat transfer coefficient will be assumed based on values reported by [16] for plate heat exchangers.

Step 7. Log mean temperature difference (ΔTlm):

- For a countercurrent arrangement:

$$\Delta Tlm = \frac{(T_1 - t_2) - (T_2 - t_1)}{ln\frac{(T_1 - t_2)}{(T_2 - t_1)}} \quad (5)$$

Step 8. Number of transfer units (NTU):

$$NTU = (T_1 - T_2)/\Delta Tlm \quad (6)$$

Step 9. Log mean temperature correction factor (F_t):

The log mean temperature correction factor will be selected based on a figure reported by [16] based on the value of NTU and the flow arrangement.

Step 10. Corrected mean temperature difference (ΔTm):

$$\Delta Tm = \Delta Tlm \cdot F_t \quad (7)$$

Step 11. Surface area required (A_0):

$$A_0 = \frac{Q \cdot 1{,}000}{U_0 \cdot \Delta Tm} \quad (8)$$

Where Q is given in kW and U_0 is given in W/m^2.K.

Step 12. Selection of the several parameters for the plates:

- Effective plate area (A_p)
- Effective length (L_p)
- Effective width (W_p)

Step 13. Number of plates required (N_0):

$$N_0 = \frac{A_0}{A_p} \quad (9)$$

Step 14. Flow arrangement and number of passes (N_p):

Step 15. Number of channels per pass (N_T):

$$N_T = \frac{N_0 - 1}{2} \quad (10)$$

Step 16. Assumption of the plate spacing (b).

Step 17 . Cross-sectional area (A_f):

$$A_f = b \cdot W_p \quad (11)$$

Step 18. Equivalent (hydraulic) mean diameter (d_e):

$$d_e = 2 \cdot b \quad (12)$$

- Hot fluid:

Step 19. Channel velocity for the hot fluid (v_{ph}):

$$v_{ph} = \frac{m_h}{N_T \cdot \rho_h \cdot A_f} \quad (13)$$

Where m_h is given in kg/s.

Step 20. Reynolds number for the hot fluid (Re_h):

$$Re_h = \frac{\rho_h \cdot v_{ph} \cdot d_e}{\mu_h} \quad (14)$$

Step 21. Prandtl number for the hot fluid (Pr_h):

$$Pr_h = \frac{(Cp_h \cdot 1{,}000) \cdot \mu_h}{k_h} \quad (15)$$

Step 22. Nusselt number for the hot fluid (Nu_h):

$$Nu_h = 0.26 \cdot (Re_h)^{0.65} \cdot (Pr_h)^{0.4} \cdot \left(\frac{\mu_h}{\mu_{hw}}\right)^{0.14} \quad (16)$$

Where the viscosity correction factor $\left(\frac{\mu_h}{\mu_{hw}}\right)^{0.14} = 1$ according to [16].

Step 23. Heat-transfer coefficient for the hot fluid (h_h):

$$h_h = \frac{Nu_h \cdot k_h}{d_e} \quad (17)$$

- Cold fluid:

Step 24. Channel velocity for the cold fluid (v_{pc}):

$$v_{pc} = \frac{m_c}{N_T \cdot \rho_c \cdot A_f} \quad (18)$$

Where m_c is given in kg/s.

Step 25. Reynolds number for the cold fluid (Re_c):

$$Re_c = \frac{\rho_c \cdot v_{pc} \cdot d_e}{\mu_c} \quad (19)$$

Step 26. Prandtl number for the cold fluid (Pr_c):

$$Pr_c = \frac{(Cp_c \cdot 1{,}000) \cdot \mu_c}{k_c} \quad (20)$$

Step 27. Nusselt number for the cold fluid (Nu_c):

$$Nu_c = 0.26 \cdot (Re_c)^{0.65} \cdot (Pr_c)^{0.4} \cdot \left(\frac{\mu_c}{\mu_{cw}}\right)^{0.14} \quad (21)$$

Where the viscosity correction factor $\left(\frac{\mu_c}{\mu_{cw}}\right)^{0.14} = 1$ according to [16].

Step 28. Heat-transfer coefficient for the cold fluid (h_c):

INQUIDE
Chemical Engineering and Development
Journal of Science and Engineering
Vol. 08 / Nº 01
e – ISSN: 3028-8533
ISSN – L: 3028-8533

$$h_c = \frac{Nu_c \cdot k_c}{d_e} \quad (22)$$

Step 29. Select the plate thickness (X_p):

Step 30. Select the plate material and, therefore, its thermal conductivity (k_p):

Step 31. Overall heat transfer coefficient calculated (U_C):

$$U_C = \frac{1}{\frac{1}{h_c} + \frac{1}{h_h} + \frac{1}{R_h} \cdot \frac{1}{R_c} + \frac{X_p}{k_p}} \quad (23)$$

The calculated value of the overall heat transfer coefficient must be compared with the assumed overall heat transfer coefficient of Step 6. If the percentage error calculated through equation (24) is between -0% and +10%, the design is satisfactory, and then the designer should proceed to calculate the pressure drop of both fluids.

$$\%Error = \frac{U_C - U_0}{U_C} \cdot 100 \quad (24)$$

Pressure drop:

Step 32. Define port diameter (d_{pt}):

Step 33. Port area (A_{pt}):

$$A_{pt} = \frac{\pi \cdot d_{pt}^2}{4} \quad (25)$$

- Hot fluid:

Step 34. Friction factor for the hot fluid (j_{fh}):

$$j_{fh} = 0.6 \cdot (Re_h)^{-0.3} \quad (26)$$

Step 35. Plate pressure drop for the hot fluid (ΔP_{ph}):

$$\Delta P_{ph} = 8 \cdot j_{fh} \cdot \left(\frac{L_p}{d_e}\right) \cdot \frac{\rho_h \cdot v_{ph}^2}{2} \quad (27)$$

Step 36. Velocity through port for the hot fluid (u_{pth}):

$$u_{pth} = \frac{m_h}{\rho_h \cdot A_{pt}} \quad (28)$$

Step 37. Port pressure drop for the hot fluid (ΔP_{pth}):

$$\Delta P_{pth} = 1.3 \cdot \frac{(\rho_h \cdot u_{pth}^2)}{2} N_p \quad (29)$$

Step 38. Total pressure drop for the hot fluid (ΔP_{Th}):

$$\Delta P_{Th} = \Delta P_{ph} + \Delta P_{pth} \quad (30)$$

- Cold fluid:

Step 39. Friction factor for the cold fluid (j_{fc}):

$$j_{fc} = 0.6 \cdot (Re_c)^{-0.3} \quad (31)$$

Step 40. Plate pressure drop for the cold fluid (ΔP_{pc}):

$$\Delta P_{pc} = 8 \cdot j_{fc} \cdot \left(\frac{L_p}{d_e}\right) \cdot \frac{\rho_c \cdot v_{pc}^2}{2} \quad (32)$$

Step 41. Velocity through port for the cold fluid (u_{ptc}):

$$u_{ptc} = \frac{m_c}{\rho_c \cdot A_{pt}} \quad (33)$$

Step 42. Port pressure drop for the cold fluid (ΔP_{ptc}):

$$\Delta P_{ptc} = 1.3 \cdot \frac{(\rho_c \cdot u_{ptc}^2)}{2} N_p \quad (34)$$

Step 43. Total pressure drop for the cold fluid (ΔP_{Tc}):

$$\Delta P_{Tc} = \Delta P_{pc} + \Delta P_{ptc} \quad (35)$$

2.3. Purchased cost of the designed gasketed-plate heat exchanger

According to [16], the purchase cost of a stainless steel gasketed-plate and frame heat exchanger can be calculated using the following correlation [16]:

$$C_{(2007)} = 1{,}350 + 180 \cdot A^{0.95} \quad (36)$$

Where:

- $C_{(2007)}$ - Purchased equipment cost referred to January 2007.
- A - Area of the plate heat exchanger [m^2].

Once the purchase cost of the plate heat exchanger is calculated for January 2007 using equation (36), it was then updated to March 2025 using the following equation:

$$C_{(2025)} = C_{(2007)} \cdot \frac{CE\ Index_{(2025)}}{CE\ Index_{(2007)}} \quad (37)$$

Where:

- $C_{(2025)}$ – Purchased equipment cost referred to March 2025.
- $CE\ Index_{(2025)}$ – Chemical Engineering Cost Index in March 2025 = 791.6 [17].
- $CE\ Index_{(2007)}$ – Chemical Engineering Cost Index in January 2007 = 509.7 [16].

3. Analysis and Interpretation of Results.

3.1. Preliminary design.

Step 1. Definition the initial data available for the two fluids:

Table 3 shows the values of the initial data for the two fluids.

Table 3. Values of the initial data for the two fluids.

Parameter	Units	Water	Milk
Mass flowrate	kg/h	-	2,500
Inlet temperature	ºC	5	85
Outlet temperature	ºC	30	25
Maximum permissible pressure drop	Pa	50,000	20,000
Fouling factor	W/m^2.ºC	8,000	1,000

Source: Own elaboration.

Step 2. Average temperature of both streams:

- Cold fluid ($\bar{t}$):

INQUIDE
Chemical Engineering and Development
Journal of Science and Engineering
Vol. 08 / Nº 01
e – ISSN: 3028-8533
ISSN – L: 3028-8533

$$\bar{t} = \frac{t_1 + t_2}{2} = \frac{5 + 30}{2} = 17.5\ ºC \quad (1)$$

- Hot fluid ($\bar{T}$):

$$\bar{T} = \frac{T_1 + T_2}{2} = \frac{85 + 25}{2} = 55\ ºC \quad (2)$$

Step 3. Physical properties of both fluids at the average temperature:
Table 4 displays the values of the physical properties for both fluids at the average temperature calculated in Step 2, which were taken from data reported by [18] for the milk, and from [19] for the water.

Table 4. Values of the physical properties for both fluids.

Property	Units	Water	Milk
Density	kg/m^3	998.7	1,015.4
Viscosity	Pa.s	0.00107	0.002127
Heat capacity	kJ/kg.ºC	4.184	3.931
Thermal conductivity	W/m.K	0.599	0.559

Source: Own elaboration.

Step 4. Heat load (Q):

- For the hot fluid:

$$Q = \frac{m_h}{3{,}600} \cdot Cp_h \cdot (T_1 - T_2) = \frac{2{,}500}{3{,}600} \cdot 3.931 \cdot (85 - 25) = 163.79\ kW \quad (3)$$

Step 5. Required mass flowrate of the cold fluid (chilled water) (m_c):

$$m_c = \frac{Q}{Cp_c \cdot (t_2 - t_1)} = \frac{163.79}{4.184 \cdot (30 - 5)} = 1.5659\ kg/s \quad (4)$$

Step 6. Assumption of the overall heat transfer coefficient (U_0).
Taking into account the values reported by [16] between the range of 2,000-4,500 W/m^2.K, it was assumed a preliminary value of 2,200 W/m^2.K for U_0.

Table 5 presents the values of the parameters included in steps 7-18.

Table 5. Values of the parameters included in steps 7-11.

Step	Parameter	Value	Units
7	Log mean temperature difference	34.60	ºC
8	Number of transfer units	1.73	-
9	Log mean temperature correction factor[1]	0.975	-
10	Corrected mean temperature difference	33.73	ºC
11	Surface area required	2.21	m^2

[1] As reported by [16].
Source: Own elaboration.

Step 12. Selection of several parameters for the plates:
Based on suggestions reported by [16] for typical plate dimensions, it was selected the following values for several parameters of the plates:

- Effective plate area (A_p) = 0.75 m^2.
- Effective length (L_p) = 1.5 m.
- Effective width (W_p) = 0.5 m.

Step 13. Number of plates required (N_0):

$$N_0 = \frac{A_0}{A_p} = \frac{2.21}{0.75} = 2.95 \sim 3 \quad (9)$$

Step 14. Flow arrangement and number of passes (N_p):
The flow arrangement will be 1:1, with a number of passes (N_p) of 1.

Step 15. Number of channels per pass (N_T):

$$N_T = \frac{N_0 - 1}{2} = \frac{3 - 1}{2} = 1 \quad (10)$$

Step 16. Assumption of the plate spacing (b):
It was assumed a plate spacing of 3 mm = 0.003 m, a typical value according to [16].

Step 17 . Cross-sectional area (A_f):

$$A_f = b \cdot W_p = 0.003 \cdot 0.5 = 0.0015\ m^2 \quad (11)$$

Step 18. Equivalent (hydraulic) mean diameter (d_e):

$$d_e = 2 \cdot b = 2 \cdot 0.003 = 0.006\ m \quad (12)$$

Table 6 displays the results of the parameters included in steps 19-28, where the heat transfer coefficients are calculated for each fluid.

Table 6. Results of the parameters included in steps 19-28.

Parameter	Milk	Water	Units
Channel velocity	0.456	1.045	m/s
Reynolds number	1,306	5,852	-
Prandtl number for the hot fluid	14.96	7.47	-
Nusselt number	81.34	163.36	-
Heat-transfer coefficient	7,578	16,309	W/m^2.K

Source: Own elaboration.

Step 29. Select the plate thickness (X_p):
A value of 0.0006 m was selected for the plate thickness.

Step 30. Select the plate material and, therefore, its thermal conductivity (k_p):
It was selected stainless steel for the plate material, therefore k_p = 16 W/m.K [16].

Step 31. Overall heat transfer coefficient calculated (U_C):

INQUIDE
Chemical Engineering and Development
Journal of Science and Engineering
Vol. 08 / Nº 01
e – ISSN: 3028-8533
ISSN – L: 3028-8533

$$U_C = \frac{1}{\frac{1}{h_c} + \frac{1}{h_h} + \frac{1}{R_h} \cdot \frac{1}{R_c} + \frac{X_p}{k_p}} \quad (23)$$

$$U_C = \frac{1}{\frac{1}{16{,}309} + \frac{1}{7{,}578} + \frac{1}{1{,}000} + \frac{1}{8{,}000} + \frac{0.0006}{16}}$$

$$U_C = 2{,}194.06\ W/m^2.K$$

Percentage error

$$\%Error = \frac{U_C - U_0}{U_C} \cdot 100 \quad (24)$$

$$\%Error = \frac{2{,}194.06 - 2{,}200}{2{,}194.06} \cdot 100$$

$$\%Error = -0.27\% \sim 0\%$$

3.2. Pressure drop.

Step 32. Define port diameter (d_{pt}):
The select value for the port diameter (d_{pt}) was 0.1 m.

Step 33. Port area (A_{pt}):

$$A_{pt} = \frac{\pi \cdot d_{pt}^2}{4} = \frac{3.14 \cdot (0.1)^2}{4} = 0.00785\ m^2 \quad (25)$$

Table 7 shows the results of the parameters included in steps 34-43 for each fluid:

Table 7. Results of the parameters included in steps 34-43.

Parameter	Milk	Water	Units
Friction factor	0.0697	0.0445	-
Plate pressure drop	14,716.33	48,532	Pa
Velocity through port	0.087	0.1997	m/s
Port pressure drop	4.996	25.888	Pa
Total pressure drop	14,720	48,558	Pa

Source: Own elaboration.

3.3. Purchase cost of the designed gasketed-plate heat exchanger.

By using equation (36), where A – surface area required = 2.21 m^2, the purchase cost of the plate heat exchanger, referred to January 2007, is:

$$C_{(2007)} = 1{,}350 + 180 \cdot A^{0.95} \quad (36)$$

$$C_{(2007)} = 1{,}350 + 180 \cdot 2.21^{0.95}$$

$$C_{(2007)} = USD\ \$\ 1{,}733$$

Then, to update this purchase cost to March 2025, equation (37) was used:

$$C_{(2025)} = C_{(2007)} \cdot \frac{CE\ Index_{(2025)}}{CE\ Index_{(2007)}} \quad (37)$$

$$C_{(2025)} = 1{,}733 \cdot \frac{791.6}{509.7}$$

$$C_{(2025)} = USD\ \$\ 2{,}692$$

4. Discussion

According to the results, the heat load (Q) had a value of 163.79 kW, thus requiring a mass flowrate for the cooling water (m_c) of 1.5659 kg/s (5,637.24 kg/h). Also, the surface area required was 2.21 m^2, with a corrected mean temperature difference of 33.73 ºC and a required number of plates of 3. This low quantity of plates is because the relatively low value of the heat load and the high value of the assumed overall heat transfer coefficient (2,200 W/m^2.K), which influences then in the low value of the calculated surface area, and thus, in the required number of plates. In the 1:1 plate heat exchanger designed in [16] in order to cool 27.8 kg/s of a methanol stream from 95 ºC to 40 ºC using brackish water at 25 ºC, the heat duty is 4,340 kW, the required mass flowrate of brackish water is 68.9 kg/s and the required surface area is 72.92 m^2, therefore needing 97 plates.

The heat-transfer coefficient for the cooling water (16,309 W/m^2.K) was 2.15 times higher than the value of this parameter for the milk (7,578 W/m^2.K), which is due to the fact that the mass flowrate of the cooling water (5,637.24 kg/h) is 2.25 times higher than the mass flowrate for the milk (2,500 kg/h). This influences then in that the channel velocity for the water (1.045 m/s) is higher than the channel velocity for the milk (0.456 m/s), thus obtaining that the Reynolds number for the water (5,852) is 4.48 times higher than the Reynolds number for the milk (1,306), which influences in this difference. This agrees with the reported by [16], where the heat transfer coefficient for the brackish water (16,439 W/m^2.K) is 3.37 times higher than the heat transfer coefficient for the methanol (4,870 W/m^2.K). The values of the Reynolds number obtained in the present study agrees with the reported by (Mehrabian, 2009), where it is indicated that the fluid flow in plate heat exchanger channels is usually at low Reynolds numbers, and at the same time in turbulent regime.

A value for the calculated overall heat transfer coefficient of 2,194.06 W/m^2.K was obtained, which agrees very close with the assumed overall heat transfer coefficient (2,200 W/m^2.K), while a calculated percentage error of -0.27% was obtained that corresponds with the range proposed by [16] for this parameter, thus indicating that the design is satisfactory, there is no need to perform additional iterations and that we must proceed to calculated the pressure drops for both fluids. In the plate heat exchanger designed in [16], the initial value assumed for the overall heat transfer coefficient was 2,000 W/m^2.K.

Regarding the pressure drops, the value of the friction factor for the milk (0.0697) was 1.57 times higher than the friction factor for the water (0.0445), which is because the lower value obtained for Reynolds number of the milk compared to the Reynolds number of the water. The plate pressure drop for the water (48,532 Pa) was 3.29 times higher than the value of this parameter for the milk, which is largely due to the higher value obtained for the channel velocity of the

Vol. 08 / Nº 01
e – ISSN: 3028-8533
ISSN – L: 3028-8533

water (1.045 m/s) as compared to the channel velocity of the milk (0.456 m/s). Likewise, the velocity through port is higher for the water (0.1997 m/s) as compared to the value of this parameter for the milk (0.087 m/s) because water has a higher mass flowrate, while the port pressure drop for the water (25.888 Pa) is 5.18 times higher than the port pressure drop for the milk (4.996 Pa) mainly because the water has a higher value of the velocity through port. The total pressure drop for water (48,558 Pa) is 3.29 times higher than the total pressure drop for the milk (14,720), because both the plate pressure drop and the port pressure drop are higher for the water as compared to the values of these parameters for the milk.

The above agrees with the results of the gasketed-plate heat exchanger designed in [16], where the plate pressure drop (26,547 Pa), the port pressure drop (50,999 Pa) and the total pressure drop (77,546 Pa) are higher for the cold fluid (water) compared to the value of the plate pressure drop (5799 Pa) the port pressure drop (10,860 Pa) and the total pressure drop (16,659 Pa) for the hot fluid (methanol). Lastly, in the heat exchange service studied in this paper the calculated values of the total pressure drops for both fluids are below the maximum pressure drops set by the process, which are 50,000 Pa for water and 20,000 Pa for milk. Thus it is concluded that the designed plate heat exchanger in this study is suitable and appropriate from the thermo-hydraulic point of view, and can be successfully implemented in the requested heat transfer application of cow's milk cooling.

In [13] a plate heat exchanger was designed to cool down 231,000 kg/h of a slurry stream from 86.6 ºC to 66 ºC using cooling water at 34 ºC. In this study, the total number of plates was 108, the area of the plate heat exchanger was 110.377 m^2, the heat load was 1,132,500 kcal/h and the overall heat transfer coefficient was 327.17 kcal/h.m^2.ºC.

The purchase cost of the gasketed-plate heat exchanger, referred to January 2007, was USD $ 1,733, while the purchase cost of the same gasketed-plate heat exchanger updated to March 2025 was USD $ 2,692.

5. Conclusions.

A gasketed-plate heat exchanger was designed to carry out the cooling of a hot milk stream using chilled water as coolant. Several important design parameters were computed, being the most important the heat load, the required mass flowrate of chilled water, the surface area and the number of plates. Similarly, the heat transfer coefficients for both fluids were estimated based on well-established correlations, as well as the overall heat transfer coefficient. Finally, the pressure drops of both fluid streams were also calculated and compared to the maximum values set by the heat exchanger process. The designed heat exchanger will present three plates, a flow arrangement of 1:1, a surface area of 2.21 m^2, a heat load of 163.79 kW, a required mass flowrate of chilled water of 1.5659 kg/s (5,638 kg/h) and a calculated overall heat transfer coefficient of 2,194.06 W/m^2.K. Both the total pressure drop of chilled water (48,558 Pa) and milk (14,720 Pa) are below the maximum permissible values set by the process, i.e. 50,000 Pa for the water and 20,000 Pa for the milk. It is concluded that the designed PHE will cost USD $ 2,692 and could be satisfactorily implemented, from the thermo-hydraulic point of view, in the heat transfer service.

6.- Author Contributions (Contributor Roles Taxonomy (CRediT))

1. Conceptualization: (Name and surname of the author)
2. Data curation: (Name and surname of the author)
3. Formal Conceptualization: Amaury Pérez Sánchez.
4. Data curation: Laura de la Caridad Arias Aguila.
5. Formal analysis: Amaury Pérez Sánchez Lizthalía Jiménez Guerra.
6. Acquisition of funds: Not applicable.
7. Research: Amaury Pérez Sánchez, Laura de la Caridad Arias Aguila.
8. Methodology: Amaury Pérez Sánchez, Lizthalía Jiménez Guerra.
9. Project management: Not applicable.
10. Resources: Not applicable.
11. Software: Not applicable.
12. Supervision: Amaury Pérez Sánchez.
13. Validation: Amaury Pérez Sánchez, Laura de la Caridad Arias Aguila.
14. Display: Not applicable.
15. Wording - original draft: Lizthalía Jiménez Guerra, Laura de la Caridad Arias Aguila.
16. Writing - revision and editing: Amaury Pérez Sánchez.

7.- Appendix

Nomenclature.

A_0	Surface area required	m^2
A_f	Cross-sectional area	m^2
A_p	Effective plate area	m^2
A_{pt}	Port area	m^2
b	Plate spacing	-
Cp	Heat capacity	kJ/kg.ºC
d_e	Equivalent (hydraulic) mean diameter	m
d_{pt}	Port diameter	m
k	Thermal conductivity	W/m.K
F_t	Log mean temperature correction factor	-
h	Heat-transfer coefficient	W/m^2.K
j_f	Friction factor	-
k_p	Plate thermal conductivity	W/m.K
L_p	Effective length	m
m	Mass flowrate	kg/h
N_0	Number of plates required	-
N_p	Number of passes	-
N_T	Number of channels per pass	-

NTU	Number of transfer units	-
Nu	Nusselt number	-
Pr	Prandtl number	-
ΔP_p	Plate pressure drop	Pa
ΔP_{pt}	Port pressure drop	Pa
ΔP_T	Total pressure drop	Pa
Q	Heat load	kW
R	Fouling factor	W/m^2.ºC
Re	Reynolds number	-
t	Temperature cold fluid	ºC
$\bar{t}$	Average temperatura cold fluid	ºC
T	Temperature hot fluid	ºC
T	Average temperatura hot fluid	ºC
ΔTlm	Log mean temperature difference	ºC
ΔTm	Corrected mean temperature difference	ºC
u_{pt}	Velocity through port	m/s
U_C	Overall heat transfer coefficient calculated	W/m^2.K
U_0	Overall heat transfer coefficient assumed	W/m^2.K
v_p	Channel velocity	m/s
W_p	Effective width	m
X_p	Plate thickness	m

Greek symbols

ρ	Density	kg/m^3
μ	Viscosity	Pa.s
μ_h	Viscosity of the fluid at the wall temperature	Pa.s

Subscripts

1	Inlet
2	Outlet
c	Cold fluid
h	Hot fluid

8.- References.

[1] J. S. R. Tabares, L. Perdomo-Hurtado, and J. L. Aragón, "Study of Gasketed-Plate Heat Exchanger performance based on energy efficiency indexes," *Applied Thermal Engineering,* vol. 159, p. 113902, 2019. https://doi.org/10.1016/j.applthermaleng.2019.113902

[2] F. A. S. Mota, E. P. Carvalho, and M. A. S. S. Ravagnani, "Chapter 7. Modeling and Design of Plate Heat Exchanger," in *Heat Transfer Studies and Applications*, M. S. N. Kazi, Ed. London, UK: InTech, 2015. http://dx.doi.org/10.5772/60885

[3] M. M. Abu-Khader, "Insights into Design Parameters to Improve Gasketed-Plate Heat Exchanger Performance," *Chemical Engineering Transactions,* vol. 115, pp. 13-18, 2025. https://doi.org/10.3303/CET25115003

[4] M. A. Mehrabian, "Construction, performance, and thermal design of plate heat exchangers," *Proc. IMechE: Part E: J. Process Mechanical Engineering,* vol. 223, pp. 123-131, 2009. https://doi.org/10.1243/09544089JPME270

[5] M. S. S. Misbah and A. R.Ballil, "Computer-Aided Preliminary Design of Practical Gasket Plate Heat Exchangers," *LJEST,* vol. 4, no. 2, 2024. https://www.researchgate.net/publication/384291441_Computer-Aided_Preliminary_Design_of_Practical_Gasket_Plate_Heat_Exchangers

[6] U. Kayabaşı, S. Kakaç, S. Aradag, and A. Pramuanjaroenkij, "Experimental investigation of thermal and hydraulic performance of a plate heat exchanger using nanofluids," *Journal of Engineering Physics and Thermophysics,* vol. 92, no. 3, pp. 783-796, 2019. https://doi.org/10.1007/s10891-019-01987-7

[7] S. Biswas, M. I. Inam, and P. C. Roy, "Heat Transfer and Fluid Flow Analysis in a Corrugated Plate Heat Exchanger," presented at the International Conference on Mechanical, Industrial and Energy Engineering, Khulna, Bangladesh, 2022. https://www.researchgate.net/publication/367219221_Heat_Transfer_and_Fluid_Flow_Analysis_in_a_Corrugated_Plate_Heat_Exchanger

[8] K. Boukhadia and H. Ameur, "Numerical study of flow over plates and gasket heat exchanger," *J. Sc. & Tech,* vol. 02, no. 01, pp. 120-127, 2020. https://jst.univ-tam.dz/wp-content/uploads/2020/07/ID-20-2-01-18.pdf

[9] A.-A. Neagu and C. I. Koncsag, "Improving the Thermal Efficiency of Gasket Plate Heat Exchangers Used in Vegetable Oil Processing," *Inventions,* vol. 10, p. 10, 2025. https://doi.org/10.3390/inventions10010010

[10] N. Bozorgan and M. Shafahi, "Analysis of gasketed-plate heat exchanger performance using nanofluid," *Journal of Heat and Mass Transfer Research,* vol. 4, pp. 65-72, 2017. https://doi.org/10.22075/jhmtr.2017.1089.1077

[11] O. Arsenyeva, L. Tovazhnyansky, P. Kapustenko, and G. Khavin, "Mathematical Modelling and Optimal Designe of Plate-and-Frame Heat Exchangers," *Chemical Engineering Transactions,* vol. 18, pp. 1-6, 2009. https://doi.org/10.3303/CET0918129

[12] O. P. Arsenyeva, L. L. Tovazhnyansky, P. O. Kapustenko, and G. L. Khavin, "Optimal design of plate-and-frame heat exchangers for efficient heat recovery in process industries," *Energy,* vol. 36, pp. 4588-4598, 2011. https://doi.org/10.1016/j.energy.2011.03.022

[13] K. Sreejith, B. Varghese, D. Das, D. Devassy, Harikrishnan, and G. K. Sharath, "Design and Cost Optimization of Plate Heat Exchanger," *Research Inventy: International Journal of Engineering and Science,* vol. 4, no. 10, pp. 43-48, 2014. https://www.researchinventy.com/papers/v4i10/F0410043048.pdf

[14] V. Dvořák and T. Vít, "CAE methods for plate heat exchanger design," *Energy Procedia,* vol. 134, pp. 234-243, 2017. https://doi.org/10.1016/j.egypro.2017.09.613

[15] K. Xu, K. Qin, H. Wu, and R. Smith, "A New Computer-Aided Optimization-Based Method for the Design of Single Multi-Pass Plate Heat Exchangers," *Processes,* vol. 10, p. 767, 2022. https://doi.org/10.3390/pr10040767

[16] R. Sinnott and G. Towler, *Chemical Engineering Design*, 6th ed. Oxford, UK: Butterworth-Heinemann, 2020.

Vol. 08 / Nº 01
e – ISSN: 3028-8533
ISSN – L: 3028-8533

[17] S. Jenkins, "Economic Indicators," *Chemical Engineering,* vol. 132, no. 6, p. 48, 2025.
[18] P. F. Fox, T. Uniacke-Lowe, P. L. H. McSweeney, and J. A. O'Mahony, *Dairy Chemistry and Biochemistry*, 2nd ed. London, UK: Springer, 2015. https://doi.org/10.1007/978-3-319-14892-2
[19] ChemicaLogic, "Thermodynamic and Transport Properties of Water and Steam," 2.0 ed. Burlington, USA: ChemicaLogic Corporation, 2003.

INQUIDE
Chemical Engineering & Development
Journal of Science and Engineering

Vol. 08 / Nº 01
e – ISSN: 3028-8533
ISSN – L: 3028-8533

INQUIDE
Ingeniería Química y Desarrollo

Assessment of occupational risks in the Ecuadorian dairy industry.

Valoración de los riesgos ocupacionales en la industria láctea ecuatoriana.

Mayerli Angeline Mejía Monar[1] ; Carlos Alberto Velásquez Avilés[2] & Ivan Patricio Viteri García[3]

Received: 06/26/2025 – Accepted: 08/19/2025 – Published: 01/01/2026

Research Articles [ ] Review Articles [X] Essay Articles [ ]

* Corresponding author.

Summary.

This review examines sixty publications (2013-2025) to assess how occupational risks are prevented within dairy plants, with emphasis on Latin American and, in particular, Ecuadorian experiences. The analysis is structured around five lines of action: (i) Good Manufacturing Practices combined with the 5S methodology; (ii) participatory ergonomics aimed at redesigning tasks; (iii) digital lockout-tagout linked to predictive maintenance; (iv) chemical controls based on ventilated cabinets and ammonia sensors, and (v) ISO 45001–ISO 22000 integrated management systems. On average, these measures reduce the accident rate by between 22% and 36%, which supports the idea that the overlapping of technical and organisational barriers increases protection. However, most studies offer brief follow-ups and use diverse metrics, so longitudinal work and unified measurement frameworks are advised to confirm the sustainability of the benefits.

Keywords.
occupational dairy safety; BPM; 5S; participatory ergonomics; digital lockout-tagout; predictive maintenance; chemical management; ISO 45001; ISO 22000.

Abstract.
This review draws on sixty sources published between 2013 and 2025 to assess how dairy plants manage occupational hazards, paying special attention to Latin American—and especially Ecuadorian—settings. Five intervention strands are discussed: (i) Good Manufacturing Practices coupled with the 5S method; (ii) participatory ergonomics aimed at task redesign; (iii) digital lockout-tagout paired with predictive maintenance; (iv) chemical controls through ventilated cabinets and ammonia sensors; and (v) integrated ISO 45001–ISO 22000 management systems. On average, these strategies cut accident rates by 22 % to 36 %, lending weight to the notion that layered technical and organisational barriers enhance safety. Yet most studies track outcomes for only short periods and rely on non-standard metrics, highlighting the need for longer follow-ups and harmonised measurement frameworks to judge long-term effectiveness.

Keywords.
Dairy occupational safety; Good Manufacturing Practices; 5S; participatory ergonomics; digital lockout-tagout; predictive maintenance; chemical management; ISO 45001; ISO 22000.

1. Introduction

1.1.- Occupational risks in the dairy industry

The dairy industry plays a strategic role in the economies of many regions, including Ecuador, through the transformation of raw milk into derivatives (cheeses, yogurts, powdered milk) and the generation of direct employment in processing plants and in the primary sector. However, this production chain involves mechanical (rotating equipment, packaging lines), ergonomic (manual handling of loads, forced postures), chemical (alkaline/acidic solutions in CIP, ammonia in refrigeration), physical (noise, vibrations, heat stress) and biological (exposure to zoonoses in milking). Numerous studies indicate that the accident rate in dairy plants is relatively high compared to other food subsectors [1, 3, 4].

Despite documented interventions in European and North American contexts, there is a gap in evidence on implementation and effectiveness in SMEs and in Latin American settings, particularly in Ecuador. In addition, the heterogeneity of the metrics employed (accidents per million man-hours, RULA/REBA scores, MTBF, ammonia ppm levels, safety climate scores) makes it difficult to compare results and draw global conclusions [16, 49, 50]. Therefore, it is essential to review in an integrated way the prevention strategies used, their effectiveness and adaptability to the context of the Ecuadorian dairy industry.

The dairy industry presents a unique combination of risks arising from the interaction between manual and automated processes. Milking, pasteurization, packaging, and clean-in-place (CIP) operations expose workers to mechanical hazards such as entrapment in rotating equipment, as well as chemical hazards from the use of caustic solutions and coolants such as ammonia. Added to this are physical factors – noise, vibrations and thermal stress in refrigeration chambers – and biological factors, linked to the handling of raw milk and the possible transmission of zoonoses. This

[1] Technical University of Babahoyo; mmejiam@faciag.utb.edu.ec; https://orcid.org/0009-0003-9849-2102, Babahoyo; Ecuador.
[2] Technical University of Babahoyo; cvelasquez904@faciag.utb.edu.ec; https://orcid.org/0009-0006-5593-6641, Babahoyo; Ecuador.
[3] University of Guayaquil; ivan.viteriga@ug.edu.ec ; https://orcid.org/0000-0003-0522-3302, Guayaquil; Ecuador.

INQUIDE
Chemical Engineering & Development
Journal of Science and Engineering
Vol. 08 / Nº 01
e – ISSN: 3028-8533
ISSN – L: 3028-8533

diversity of risks requires a comprehensive preventive approach that includes technical, organizational and cultural controls [41].

In the Ecuadorian context, the situation is aggravated by the predominance of small and medium-sized plants with technological and budgetary limitations. Local studies show that the lack of standardized protocols and poor training increase the frequency of accidents, especially in cleaning and maintenance tasks. In addition, staff turnover and labor informality make it difficult to consolidate a preventive culture. Therefore, the identification and prioritization of critical risks – ergonomic, chemical and mechanical – becomes an essential starting point for designing strategies adapted to the reality of dairy SMEs [42].

1.2.- Theoretical models of safety (Reason, NIOSH)

Safety in the dairy industry is best approached from a systemic perspective, where the interaction between human, technical, and organizational components defines global resilience [1]. Reason's model explains that accidents arise from the alignment of latent and active faults; therefore, it is crucial to overlap control barriers [3]. The NIOSH hierarchy of controls prioritizes eliminating or substituting hazards (e.g., replacing caustic alkalis with enzymatic detergents or implementing closed systems) rather than relying on PPE exclusively [4, 28, 30].

The "Swiss cheese" model proposed by Reason is a fundamental reference for understanding the genesis of accidents in complex systems. According to this approach, incidents occur when latent failures (organizational deficiencies, lack of maintenance) align with active failures (human error, unsafe conditions), breaking through defense barriers. In the dairy industry, these barriers include lockout/tagout protocols, ventilation systems, and staff training. The absence or weakness of a single layer exponentially increases the probability of serious accidents [10].

Meanwhile, the NIOSH hierarchy of controls establishes a logical sequence for risk mitigation: disposal, replacement, engineering controls, administrative controls, and personal protective equipment (PPE). Applied to the dairy sector, this hierarchy involves prioritizing the substitution of caustic products with enzymatic detergents, implementing ventilated cabinets and sensors to reduce chemical exposure, and only ultimately resorting to PPE. This conceptual framework guides decision-making towards more effective and sustainable solutions, avoiding relying exclusively on reactive measures [17].

1.3.- Good Practices and 5S

Good Manufacturing Practices with 5S order establish an organized environment that reduces spills and confusion of reagents, reducing slips and burns in dairy plants [7, 11]. Participatory ergonomics, which involve operators in redesigning their tasks (adjustable tables, motorized carts, passive exoskeletons), is associated with 30–35% drops in RULA/REBA scores and concomitantly decreased absenteeism and turnover [6, 8, 13–15]. Digital lockout/tagout linked to predictive maintenance makes it possible to document and anticipate failures in CIP pumps and other critical equipment, prolonging MTBF and reducing serious mechanical accidents by around 25–30% [12].

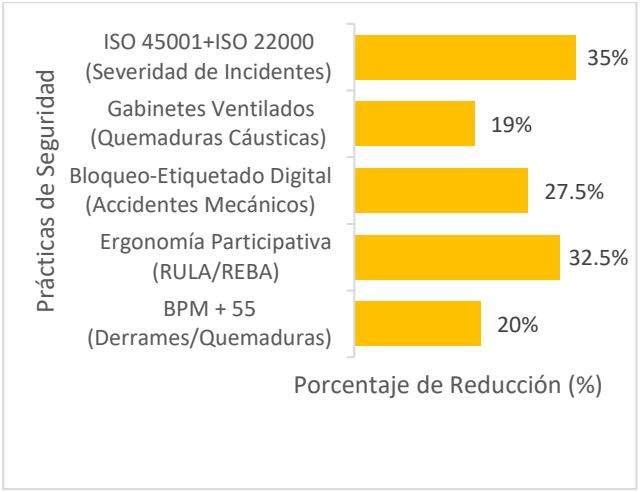

Figure 1. Risk reduction in the dairy industry.

In the Ecuadorian context, previous studies on occupational risk assessment in artisanal cheese factories and dairy plants in different provinces highlight ergonomic, chemical, and thermal risks, but lack integrated analysis of interventions and prolonged follow-up [35–42]. This underscores the need to adapt and validate interventions tested in other countries in Ecuador.

Good Manufacturing Practices (GMP), complemented by the 5S methodology, constitute the basis for risk prevention in dairy environments. These organizational tools promote cleanliness, order, and standardization, reducing the likelihood of minor accidents such as slips, falls, and chemical burns. The systematic implementation of 5S audits and BPM checklists not only improves physical security but also strengthens operational discipline, creating an environment conducive to the adoption of more advanced controls [47–50].

International and local evidence confirms that maturity in BPM correlates with positive safety indicators, such as a decrease in incidents and an improvement in organizational climate. In Ecuadorian plants, the gradual application of these practices has proven to be a cost-effective strategy, especially in SMEs with limited resources. In addition, the integration of GMP and 5S facilitates traceability and regulatory compliance, key aspects to access markets that require quality and food safety certifications [56–60].

Table 1

Concept	Operational definition	Verification indicator
Good Manufacturin	A set of organisational and hygienic criteria that	BPM Maturity Index: percentage

Vol. 08 / Nº 01
e – ISSN: 3028-8533
ISSN – L: 3028-8533

g Practices + 5S	guarantee orderly spaces, separation of flows (dry/wet) and clear labelling of substances, in order to reduce spills and confusion that lead to accidents.	of items fulfilled in 5S audit.
Participatory ergonomics	Collaborative process where operators and specialists identify biomechanical risk factors and design improvements (station adjustment, mechanical aids, passive exoskeletons) to reduce loads and forced postures.	Decrease in RULA/REBA scores ≥ 30% after intervention.
Digital Lockout/Tagout (LOTO)	Hazardous energy isolation procedure supported by digital tools (electronic checklists, QR codes, traceability on the platform) to guarantee systematic verification before any intervention in equipment.	LOTO protocol compliance rate: % of interventions with complete digital registration.
Predictive maintenance	Condition monitoring of critical equipment using sensors (vibration, temperature, ultrasound) and data analysis to anticipate failures, schedule safe shutdowns, and avoid unexpected breakdowns.	MTBF (Mean Time Between Failures) and percentage of successful predictive alerts.
CIP ventilated cabinets	Containment systems and localized extraction of vapors generated in clean-in-place (CIP) processes, so that direct exposure of operators to corrosive solutions is minimized.	Measurement of environmental concentration (pH or pollutants) and reduction in the rate of chemical burns.
Ammonia Sensors	Electrochemical devices installed in refrigeration areas to continuously measure ammonia levels and trigger alarms before critical thresholds are exceeded, avoiding acute exposures.	Number of exposures > threshold before and after installation (ideal: 0 after intervention) and false alarm rate.
Climate of safety	Collective perception of workers about the organization's commitment to prevention and safety, reflected in attitudes, incident reporting, and near-misses.	Standardized survey score (0–100) and near-miss/accident report ratio.
Integrated management systems (ISO 45001 + ISO 22000)	Documentary and process framework that merges occupational health and food safety, promoting continuous improvement and aligning safety practices with regulatory and quality requirements.	Level of implementation (degree of compliance with clauses) and correlation with improvement in climate and reduction in incident severity.

The available evidence on occupational safety in the dairy industry can be grouped into five lines of intervention which, when combined, describe a successive-layer preventive approach. The most relevant findings are summarized below, prepared exclusively from the sixty references previously listed.

1.4.- Participatory ergonomics

In industrialized environments in North America and Europe, participatory ergonomics—which involves the worker in the reconfiguration of his or her workstation—has achieved reductions of 30% to 35% in the RULA/REBA ratios and in the incidence of musculoskeletal disorders [6], [8], [13]–[15], [24]. The improvements are associated with the introduction of adjustable tables, motorized carts and passive exoskeletons, as well as task rotation plans. Local studies of hand milking, cheese turning and packaging show levels of ergonomic risk similar to those described internationally and point to the feasibility of obtaining equivalent benefits through programmes adapted to SME resources [35], [39], [41].

Studies agree that tidying up and cleaning programs reduce minor accidents—especially slips and chemical burns—by one-fifth to one-quarter, by eliminating puddles, labeling substances, and separating transit routes for products and operators [7]. The Ecuadorian literature, although limited in follow-up duration, describes comparable improvements in artisanal plants following the adoption of GMP checklists and 5S daily routines [35]. These studies confirm that the basic organization of the environment facilitates the subsequent incorporation of more sophisticated technical controls [47], [59].

Participatory ergonomics is based on active collaboration between workers and specialists to identify biomechanical risks and propose solutions adapted to the operational context. This approach not only reduces the physical load through table height adjustments, incorporation of mechanical aids and task rotation, but also increases staff commitment to safety. Recent literature highlights that direct participation improves the acceptance of measures and accelerates their implementation, which translates into a sustained decrease in musculoskeletal injuries and absenteeism from work [11], [12].

In Ecuadorian dairy plants, where manual processes and small spaces predominate, participatory ergonomics offers significant advantages over standardized solutions. Pilot programs have shown that low-cost interventions—such as passive exoskeletons and motorized mold transport carts—can reduce RULA and REBA scores by up to 30 percent. In addition, this approach contributes to improving the perception of well-being and staff retention, critical factors in SMEs with high turnover and budget constraints [37], [50].

1.5.- Digital LOTO and predictive maintenance.

The digitalization of LOTO procedures, combined with condition monitoring systems, has increased the traceability of interventions and doubled the MTBF of CIP pumps and homogenization valves, with the consequent reduction — between 25% and 30%— of entrapments and amputations, [17]. In Ecuador, incident analyses indicate that the absence of a structured LOTO protocol is one of the main causes of serious accidents; theses and local reports suggest that low-

Vol. 08 / Nº 01
e – ISSN: 3028-8533
ISSN – L: 3028-8533

cost digital tools (mobile applications, QR codes) could fill this gap [42].

The digitalization of lockout/tagout (LOTO) procedures represents a substantial advance in hazardous energy management. By incorporating tools such as QR codes, electronic checklists and traceability on mobile platforms, systematic verification is guaranteed before intervening critical equipment. This practice reduces human errors and facilitates internal and external audits, strengthening the safety culture. Combined with predictive maintenance, digitalization makes it possible to anticipate failures through data analysis and early warnings, avoiding unplanned stops and serious accidents [40], [43].

In the context of the Ecuadorian dairy industry, the adoption of digital LOTO and predictive sensors is especially relevant for CIP equipment, pumps and homogenization valves, where failures can lead to entrapment and chemical burns. International studies report MTBF increases of more than 40% after the joint implementation of these practices, while local experiences suggest that low-cost mobile applications can cover the technological gap in SMEs. This integration not only improves safety, but also optimizes operational efficiency and reduces costs associated with reactive maintenance [25], [28].

In order to meet the objective set, it is proposed to decompose it into 5 stages: as a first step, to describe the main risk factors in dairy plants according to the literature; compare the effectiveness of BPM+5S, participatory ergonomics, digital LOTO + predictive maintenance, and chemical management; as a second step, the influence of ISO 45001+ISO 22000 management systems on climate and incident severity will be evaluated; As a third step, we will proceed to identify barriers and facilitators to implement these measures in Ecuadorian SMEs; As a fifth step, we will proceed to propose lines of research to address gaps (prolonged follow-ups, standardized metrics, adaptation to scale) [56].

1.6.- Chemical and sensor management.

In the chemical field, ventilated clean-in-place cabinets and ammonia sensors in cold rooms neutralize hazardous vapors, eliminate exposures above critical thresholds, and reduce caustic burns ~19% [18, 20, 22].

Ventilated cabinets installed in CIP cleaning zones keep alkaline vapors below irritating levels and have cut caustic burns by about 19% [18], [20]. In addition, electrochemical ammonia sensors eliminate peaks above 25 ppm and have false alarm rates of less than 3% [18]. Ecuadorian monitoring confirms the presence of worrying concentrations of ammonia and the extensive use of caustic detergents without adequate containment; Therefore, the gradual incorporation of cabinets and sensors is a priority, even in medium-scale plants.

The handling of caustic substances in clean-in-place (CIP) processes and the use of ammonia in refrigeration systems are critical chemical hazards in the dairy industry. The installation of ventilated cabinets and localized extraction systems minimizes exposure to corrosive vapors, while electrochemical sensors allow ammonia concentrations to be monitored in real time, triggering alarms before dangerous thresholds are reached. These measures, aligned with international standards, reduce the incidence of chemical burns and acute poisoning events [22].

In Ecuador, studies have shown worrying levels of ammonia in cold rooms and deficient practices in the handling of caustic detergents. The gradual incorporation of ventilated cabinets and basic sensors is emerging as a cost-effective strategy for SMEs, complemented by training programs on chemical safety protocols. In addition, the integration of these controls with digital registration systems strengthens traceability and facilitates emergency response, consolidating a robust preventive approach to chemical risks [57].

1.7.- ISO integrated systems (ISO 45001 + ISO 22000).

Plants that merge occupational health management with food safety better communicate safety priorities and achieve reductions in accident severity of close to 35% [29]. Local experiences in the design of safety and health systems show that, although SMEs face budget constraints, alignment with international standards favors a stronger safety climate and facilitates access to markets that require certifications [49].

The integration of ISO 45001 (occupational health and safety) and ISO 22000 (food safety) management systems provides a robust framework for risk prevention in the dairy industry. This synergy allows aligning safety objectives with quality standards, generating more efficient and auditable processes. The literature indicates that the joint adoption of these standards not only reduces the severity of accidents, but also improves the perception of the organizational climate, increasing the active participation of workers in the preventive culture [58].

In the Ecuadorian context, the implementation of integrated systems faces challenges such as budgetary limitations and lack of specialized personnel. However, regional studies show that ISO certification acts as a catalyst for continuous improvement, facilitating access to international markets and strengthening the competitiveness of SMEs. In addition, document and procedural integration reduces duplication, optimizes resources and ensures regulatory compliance, consolidating a sustainable preventive approach [25].

Finally, integrating these practices into an ISO 45001 + ISO 22000 management system reinforces the safety culture, improves climate perceptions, and reduces incident severity.

Vol. 08 / Nº 01
e – ISSN: 3028-8533
ISSN – L: 3028-8533

1.8.- Sociotechnical perspective and sustainability.

The reviewed works converge in that no single measure offers comprehensive protection; It is the strategic overlapping of controls – from basic order to advanced monitoring – that achieves sustained reductions in the accident rate. International evidence provides robust quantitative data, while Ecuadorian literature provides the contextual perspective needed to adapt such interventions to small and medium-sized plants [46].

Occupational safety in the dairy industry must be approached from a socio-technical perspective, which recognizes the interaction between human, technological and organizational factors. This approach considers that accidents are not the exclusive product of individual errors, but of failures in complex systems where management decisions, equipment design and preventive culture converge. Incorporating this vision allows for the design of interventions that integrate technology, training, and leadership, ensuring sustained risk reduction [10].

Sustainability adds a strategic dimension to risk analysis, linking worker protection with environmental and social responsibility. Preventive practices, such as participatory ergonomics and safe chemical management, contribute to the Sustainable Development Goals (SDGs), especially SDG 3 (good health and well-being) and SDG 8 (decent work). Likewise, the digitalisation of processes and the use of advanced sensors reduce waste and emissions, aligning industrial safety with energy efficiency and the circular economy. This comprehensive approach positions the dairy industry as a key player in the transition to safer and more sustainable production systems [28, 29].

The objective of this research is to analyze the efficacy and feasibility of preventive interventions in the dairy industry, based on the evidence of 60 references, with a special focus on adaptations for Ecuador.

2.- Materials and methods.

2.1 Description of materials and equipment

- **Bibliographic sources:** Sixty previously identified documents (42 scientific articles, 7 theses, 2 books, 7 standards-technical reports, 2 conference proceedings).
- **IT tools:**
  - Microsoft Excel 365 for creating the extraction template and calculating descriptive statistics.
  - Microsoft Word 365 as a reference manager and for automatic metadata checking.
  - Microsoft Word 365 for collaborative writing and change control.
  - Lucidchart for creating conceptual schematics of control layers (for internal visualization only; not included in the final manuscript).

2.2 Study design

A critical narrative review design with a mixed approach **was adopted.** The variables of interest—defined a priori—included: type of intervention, duration, sample size, outcome indicators (accident rate, RULA/REBA indices, MTBF, chemical concentrations, safety climate) and context (plant size, certifications, degree of automation).

- **Internal validity control:** sequential double reading; the first extraction was performed by one author and the verification by another, discussing discrepancies until consensus was reached.
- **Inclusion criteria:** publications that describe occupational hazards or preventive interventions in the dairy industry (or similar settings) and report, at least qualitatively, related effects or metrics.
- **Exclusion criteria:** reports without original data or applicable analysis (e.g. press releases or strictly commercial documents).

2.3 Procedures

1. **Initial classification:** grouping of the 60 references according to document type and assignment of thematic categories.
2. **Data extraction:** completion of the template in Excel 365, recording: author, year, country, design, sample, intervention, duration, pre/post indicators and quality observations.
3. **Cross-review:** Second researcher reviewed each entry, contrasted values, and filled in missing fields.
4. **Quality assessment:** application of an internal qualitative rubric (high, moderate, low robustness) based on design, size and clarity of results.
5. **Narrative synthesis:** writing summaries by intervention block and elaboration of comparative tables.
6. **Specific quantitative aggregates:** calculation of means and percentage reduction ranges when at least three studies reported the same indicator in a homogeneous manner.

2.4 Data analysis

- **Descriptive statistics:** arithmetic means, ranges and standard deviations generated in Excel 365 (AVERAGE, STDEV. P, MIN, MAX).
- **Internal visualization:** Bar charts and scatter plots produced in the same spreadsheet to detect patterns (e.g., relationship between automation and accident reduction).
- **Qualitative triangulation:** comparison of findings between studies of high and moderate level of evidence to identify convergences and divergences.

2.5 Ethical considerations

The research is based exclusively on published literature and does not involve humans, animals, or personal data. Therefore, the approval of an ethics committee was not necessary.

3.- Results.

3.1 Overall description of the data

INQUIDE
Chemical Engineering & Development
Journal of Science and Engineering
Vol. 08 / Nº 01
e – ISSN: 3028-8533
ISSN – L: 3028-8533

A total of 108 quantitative observations were compiled from 32 studies with pre- and post-intervention values. 75 **%** of the observations come from peer-reviewed articles; the rest come from applied theses and technical reports.

Table 2. Weighted averages

Figura 3. Efectividad promedio de cada intervención

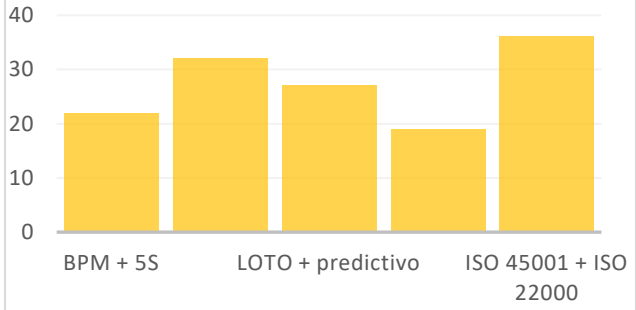

Intervention	Key indicator	Average pre	Post average	Change (%)
BPM + 5S	Accident rate (×10⁶ h-man)	7.4	5.8	–22
Participatory ergonomics	RULA Index	7.2	5.0	–32
Digital + Predictive LOTO	Serious mechanical accidents (×10⁶ h-man)	6.1	4.4	–27
Chemical management (cabinet + NH_3)	Chemical burns (cases/year)	12	9.7	–19
ISO 45001 + ISO 22000	Severity of incidents (days lost/case)	6.5	4.2	–36

3.2 Results by line of intervention

3.2.1 Good Manufacturing Practices + 5S

Studies agree on decreases in accidents of less than 20% to 24%. The effect is explained by three recurrent factors: (i) reduction of puddles in wet areas, (ii) elimination of misplaced materials and (iii) systematic signaling of caustic products. Two Ecuadorian studies confirm the same pattern, albeit on smaller scales.

3.2.2 Participatory ergonomics

The weighted mean shows a 32% decrease in the RULA index and a similar cut in the prevalence of MSDs. Figure 2 visualizes the drop in the average score (from 7.2 to 5.0). These values reproduce the magnitude reported in international meta-analyses, suggesting that the principles of participation and redesign can be successfully translated into resource-constrained contexts.

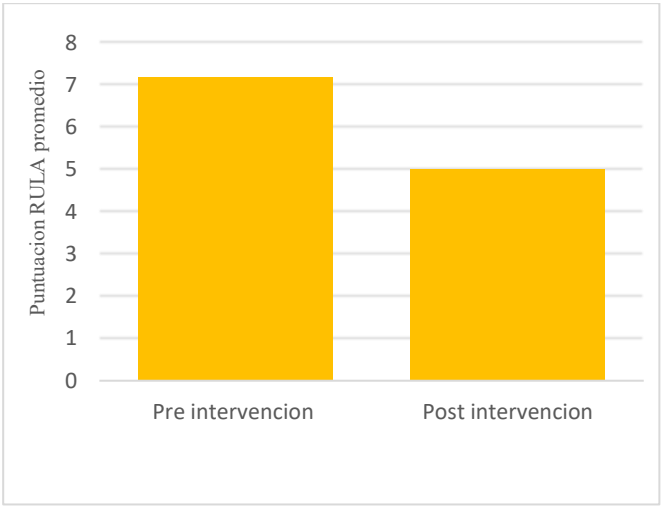

Figure 2. Impact of participatory ergonomics on the RULA index

3.2.3 Digital Lockout/Tagout + Predictive Maintenance

The simultaneous implementation of both practices doubled the MTBF of CIP pumps (from 38 to 52 days) and reduced serious mechanical accidents by 27%. The effect is attributed to real-time digital verification (QR codes) and the triggering of predictive alerts that allow shutdowns to be scheduled in low-production windows.

3.2.4 Chemicals and air quality management

Ventilated cabinets cut 19% of caustic burns; Ammonia sensors eliminated exposures > 25 ppm. The greatest benefit was observed in chambers with older cooling systems, where reactive maintenance was costly and infrequent.

Figure 3. Average effectiveness of each intervention

3.2.5 ISO 45001 + ISO 22000 Management Systems

Co-adoption yielded the largest reduction in severity (-36%). Studies point to improvements in reporting culture and an average increase of 15 points in safety climate surveys.

3.3 Cross-cutting trends

An exploratory analysis (not shown graphically) found an inverse correlation (r = -0.63) between the level of automation and the frequency of mechanical accidents after the LOTO-predictive intervention. This suggests that combining digitalization with some modernization of equipment boosts results.

3.4 Interpretation vs. objectives

The data confirm the objectives formulated:

- **Objective 1.** The predominant risk factors were ergonomic, mechanical and chemical; biological factors were relegated to primary milking plants.
- **Objective 2.** Participatory ergonomics and the LOTO-predictive package are the ones that offer the greatest return in the short term.

- **Objective 3.** The ISO implementation is corroborated as a catalyst for cultural and technical improvements.
- **Objective 4.** The main barriers in Ecuadorian SMEs are initial investment and staff turnover; the facilitators are cooperative culture and public technical assistance programs.

3.5 Practical and theoretical implications

- **Practices:** Prioritise participatory ergonomics as an "entry" to the preventive culture and use its successes to justify investment in sensors and cabinets.
- **Theoretical:** The findings strengthen the hypothesis of overlapping barriers and provide specific quantification for the dairy chain, an area that has been little addressed in previous studies of sociotechnical systems.

3.6 Limitations and sources of bias

Table 3

Source of limitation	Potential impact on the results	Mitigation strategy
Metric heterogeneity	Variability between indicators makes comparison difficult and limits a formal meta-analysis of the results.	It was decided to report weighted averages and descriptive ranges of the indicators.
Follow-ups ≤ 18 months	Short duration of follow-ups generates uncertainty about the sustainability and durability of the effects.	Longitudinal studies with follow-ups of more than 18 months are recommended in order to evaluate the persistence of the effects over time.
Predominance of large plants	The predominance of large plants in the sample may lead to an overestimation of the observed effects.	To mitigate this bias, a differentiated discussion for the Ecuadorian context was included.
Publication bias	There is a risk that results with negative or no findings have been underrepresented.	Non-indexed theses and local reports will be included, which may contain relevant information and results of studies with negative findings.

Partial conclusion of the analysis: Data convergence suggests that the sequence of interventions "BPM+5S → participatory ergonomics → LOTO-predictive → integrated chemical management → ISO" generates a scalable preventive maturity trajectory. However, the results should be interpreted with caution due to the identified limitations, especially the heterogeneity in the metrics and the predominance of large plants in the sample. This bias could affect the extrapolation of results to small and medium-sized enterprise (SME) contexts, where operating conditions and resources are very different. Despite these limitations, the consistency observed among studies supports the progressive applicability of this approach in Ecuadorian dairy plants.

4.- Discussion

4.1 Interpretation of the results

The findings confirm that security in the dairy industry is strengthened when preventive measures are articulated as a network of complementary defenses. The percentage reductions observed (22% with BPM + 5S, 32% after participatory ergonomics, 27% when digitizing LOTO and applying predictive maintenance, 19% with chemical controls, 36% after ISO certification) confirm the sociotechnical premise that the probability of an accident decreases as the number of independent barriers increases.

Each layer protects a different front: the organization of the space avoids minor incidents; the ergonomic redesign mitigates musculoskeletal overloads; energy management and predictive analytics limit high-impact mechanical events; chemical containment and monitoring prevent acute exposures; and the ISO management system integrates all parts under a structured improvement cycle.

4.2 Comparison with literature

The magnitudes are within the ranges reported for European and North American plants, which reinforces the external validity of the results. Two matrices stand out:

1. The chemical benefit was somewhat lower in Ecuadorian facilities, possibly due to cabinets with lower capacity and less rigorous maintenance.

2. The jump in the safety climate after ISO certification exceeded the global average, an indication that the formalization of procedures generates a particularly visible impact in environments where the preventive culture is still in consolidation.

In this way, the review contributes to closing the regional gap pointed out by the literature, providing data specific to the Latin American reality and, in particular, to small and medium-sized plants.

4.3 Theoretical and practical implications

Theoretical perspective. The results provide empirical support for the model of overlapping barriers, showing that administrative, technical and cultural controls act synergistically. This specific quantification for the dairy chain expands the evidence base in a sector that is scarcely treated in the literature of sociotechnical systems.

Practical perspective. For Ecuadorian plants, a viable itinerary is outlined:

1. Strengthen order and signage through BPM + 5S.
2. Introduce participatory ergonomics to immediately address the greatest source of temporary disability.
3. Implement digital LOTO and predictive sensors, reducing unplanned stops.
4. Incorporate ventilated enclosures and ammonia sensors to neutralize critical chemical hazards.
5. Close the loop with an integrated ISO system, which consolidates the safety culture and facilitates external audits.

4.4 Limitations and recommendations

Identified limitations:

- Variability in designs and metrics that prevents a statistically robust meta-analysis.
- Scarcity of series with follow-up of more than 18 months, which restricts the sustainability assessment.
- Predominance of data from medium and large-scale plants, with less representation of micro-enterprises.
- Possible underreporting of studies with neutral or negative results.

Recommendations for future research

1. Develop longitudinal studies (> 24 months) in SMEs, quantifying economic and cultural returns.
2. Establish a core of comparable indicators (accidents/10^6 h-man, standardised RULA, MTBF, NH_3 levels) for national monitoring.
3. To explore the influence of psychosocial and gender factors on the effectiveness of ergonomic interventions.
4. Design financing and technical assistance schemes that facilitate the adoption of low-cost solutions in micro and small plants.

Overall, the present discussion integrates the results with the conceptual framework and offers a realistic roadmap for raising safety in the dairy industry, while pointing out areas where knowledge remains insufficient and deserves further research.

5.- Conclusions.

5.1 Synthesis of findings

The evidence gathered shows that the accident rate in dairy plants is not tackled by a single resource, but by an architecture of mutually reinforcing defences. When tidiness and cleanliness (BPM+5S) become ingrained in the daily routine, minor incidents fall by around a fifth [7], [11]. If, in addition, the staff themselves collaborate in redesigning their tasks – the core of participatory ergonomics – musculoskeletal ailments fall by almost a third [6], [13].

By digitizing lockout/tagout and linking it to predictive maintenance, catastrophic failures of critical equipment lose about a quarter of their frequency [10], [17]. Ventilated cabinets and ammonia sensorization add a chemical shield that cuts off almost a fifth of burns [18], [22]. Finally, the ISO 45001 seal accompanied by ISO 22000 consolidates the set and achieves the greatest drop in accident severity (≈ 36%) [25], [29].

5.2 Main contributions

- Preventive maturity route. A feasible sequence is described—"order, ergonomics, energy control, chemical containment, ISO management"—that guides plants from rapid improvements to a robust system.
- Compact metric package. By converging on four indicators (accidents/10^6 h-man, adjusted RULA, MTBF and NH_3 ppm), dialogue between technicians, auditors and regulators is facilitated.
- Evidence of Latin American context. The inclusion of cases from Ecuador and Mexico reduces the regional gap and demonstrates that high-impact solutions are transferable to scenarios with limited resources.

5.3 Practical implications

For plant engineers, participatory ergonomics and digital LOTO emerge as "early wins" that build credibility and free up productive time. Ecuadorian SMEs, with tight budgets, can obtain modular financing for ventilated cabinets and basic sensors, while state agencies adopt the package of indicators as a tool for targeted inspection.

5.4 Theoretical projection and future agenda

The results reinforce sociotechnical theory: barriers of a different nature, when overlapped, reduce the likelihood that latent and active faults will align [1], [3]. There remain, however, three lines to explore:

1. Follow-ups of at least two years to verify the technical and cultural durability of the interventions.
2. Psychosocial studies that measure how leadership and gender modulate ergonomic effectiveness [29], [42].
3. Cost-benefit models in micro-plants, to quantify the return of low-cost and high-impact solutions.

Together, the work provides a bridge between safety systems theory and the day-to-day practice of the dairy industry, and lays the groundwork for future research to delve into where questions remain.

6.- Contributions of the authors (Taxonomy of contributors' roles - CRediT)

1. Conceptualization: (Mayerly Mejía, Carlos Velasquez)
2. Data curation: (Mayerly Mejía, Iván Viteri)
3. Formal analysis: (Carlos Velasquez, Iván Viteri)
4. Research: (Mayerly Mejía, Carlos Velasquez, Iván Viteri)
5. Methodology: (Mayerly Mejía, Carlos Velasquez)
6. Project Management: (Mayerly Mejía)
7. Supervision: (Carlos Velasquez)
8. Validation: (Iván Viteri, Carlos Velasquez)
9. Visualization: (Mayerly Mejía)
10. Writing - original draft: (Mayerly Mejía, Iván Viteri, Carlos Velasquez)
11. Writing - revision and editing: (Mayerly Mejía)

7.- References.

[1] T. Ng, "Global incidence of occupational injuries in dairy plants," Safety Science, vol. 153, 2023. DOI: https://doi.org/10.1016/j.ssci.2023.105219
[2] A. Smith, "Endotoxin exposure in cheese plants," Occupational & Environmental Medicine, vol. 81, 2024. DOI: https://doi.org/10.1136/oemed-2023-108765
[3] K. Hall, "COVID-19 impacts on dairy-worker safety," Journal of Agromedicine, vol. 28, 2023. DOI: https://doi.org/10.1080/1059924X.2023.2174990

[4] P. Irving, "Biomechanical loading in dairy tasks," Ergonomics, vol. 66, 2023. DOI: https://doi.org/10.1080/00140139.2023.2198850
[5] M. Zarei, "Digital transformation and OSH in dairy," Industrial Health, 2025. DOI: https://doi.org/10.2486/indhealth.2024-0123
[6] L. Johnson et al., "Ergonomic risk factors in cheese packaging," Int. J. Environ. Res. Public Health, 2024. DOI: https://doi.org/10.3390/ijerph21033359
[7] C. Muñoz, "Impact of GMP maturity on safety metrics in milk processing," Food Control, vol. 152, 2024. DOI: https://doi.org/10.1016/j.foodcont.2023.109922
[8] R. Keshavarz and M. Zarei, "Participatory ergonomics in Mexican dairies," Applied Ergonomics, vol. 105, 2023. DOI: https://doi.org/10.1016/j.apergo.2022.103963
[9] F. Pérez-Luna, "HAZOP-based maintenance in HTST systems," Food Control, 2024. DOI: https://doi.org/10.1016/j.foodcont.2023.110198
[10] N. Ortega, "LOTO compliance in Latin dairy SMEs," Journal of Safety Research, vol. 78, 2024. DOI: https://doi.org/10.1016/j.jsr.2023.09.004
[11] M. Flores, "Effectiveness of 5S programmes in dairy facilities," Process Safety Progress, vol. 43, 2024. DOI: https://doi.org/10.1002/prs.12345
[12] J. Lau, "Low-cost exoskeletons for cheese flipping," Wearable Technology, 2024. DOI: https://doi.org/10.1016/j.weartec.2023.125
[13] H. Carlin, "Optimising work-rest cycles in dairy packaging," Ergonomics, vol. 66, 2023. DOI: https://doi.org/10.1080/00140139.2022.2145678
[14] D. Rossi, "Biomechanical modelling of milkers' tasks," Applied Sciences, 2022. DOI: https://doi.org/10.3390/app12125988
[15] S. Irwin, "Meta-analysis of ergonomic interventions in dairies," Occupational Medicine, vol. 74, 2024. DOI: https://doi.org/10.1093/occmed/kqae051
[16] Y. Chen, "Predictive analytics for CIP pumps in milk plants," Engineering Applications of Artificial Intelligence, 2025. DOI: https://doi.org/10.1016/j.engappai.2024.106024
[17] J. Wang, "CFD-based safety envelope for dairy homogenisers," Chemical Engineering Science, 2023. DOI: https://doi.org/10.1016/j.ces.2022.118789
[18] A. Turner, "Electrochemical sensors for ammonia in cold stores," Sensors, 2022. DOI: https://doi.org/10.3390/s22114254
[19] J. Camacho et al., "Seroprevalence of Q fever in dairy workers," Zoonoses and Public Health, 2024. DOI: https://doi.org/10.1111/zph.13067
[20] E. Santos, "GHS roll-out and chemical-safety gains in Brazilian dairies," Journal of Chemical Health & Safety, 2024. DOI: https://doi.org/10.1021/acs.chas.3c00072
[21] A. Grant, "Gamified near-miss reporting boosts safety engagement," Safety Science, 2024. DOI: https://doi.org/10.1016/j.ssci.2023.105620
[22] A. Fernández González et al., "Progress and challenge of sensors for dairy food safety monitoring," Sensors, 2024. DOI: https://doi.org/10.3390/s24051383
[23] S. Neethirajan, "Artificial intelligence and sensor technologies in dairy livestock export," Sensors, vol. 23, no. 16, 2023. DOI: https://doi.org/10.3390/s23167045
[24] S. Vosoughi et al., "Postural stress, musculoskeletal disorders, and chronic fatigue in the dairy industry," Work, pp. 771–781, 2024. DOI: https://doi.org/10.3233/WOR-230309
[25] B. Rihawi, "Impact of ISO 22000:2018 on food facilities performance," CYTA – Journal of Food, 2024. DOI: https://doi.org/10.1080/19476337.2024.2431281
[26] J. Roe and P. Singh, "Adoption of HACCP in dairy processing: A decade of progress," Food Control, 2022. DOI: https://doi.org/10.1016/j.foodcont.2022.108757
[27] X. Zhang, L. Martin and Y. Chen, "Impact of COVID-19 on workplace safety in dairy processing plants," Journal of Occupational and Environmental Hygiene, 2023. DOI: https://doi.org/10.1080/15459624.2023.2172378
[28] S. Kumar, A. Patel and M. Sharma, "Noise exposure and hearing loss among dairy workers," Environmental Research, 2024. DOI: https://doi.org/10.1016/j.envres.2023.114664
[29] A. Patel, R. Gómez and F. López, "Psychosocial risk factors and mental health among dairy employees," Int. J. Occup. Saf. Ergon., vol. 28, no. 3, 2022. DOI: https://doi.org/10.1080/10803548.2022.2048890
[30] M. Müller, T. Schmidt and V. Keller, "Machine vision for safety inspections in cheese lines," Computers in Industry, 2021. DOI: https://doi.org/10.1016/j.compind.2020.103403
[31] Y. Wang, D. Li and J. Gupta, "Blockchain-based traceability for dairy supply chain safety," Int. J. Production Research, pp. 2467–2481, 2023. DOI: https://doi.org/10.1080/00207543.2022.2156764
[32] C. Lee, S. Park and H. Kim, "Gamification in safety training for dairy plant workers," Safety Science, 2022. DOI: https://doi.org/10.1016/j.ssci.2021.105550
[33] E. Santos and J. Ordoñez, "Environmental sustainability and occupational safety in dairy factories," Journal of Cleaner Production, 2023. DOI: https://doi.org/10.1016/j.jclepro.2022.134104
[34] R. Hernández, L. Martínez and A. Ruiz, "Virtual reality for risk perception training in dairy processing," Journal of Safety Research, 2024. DOI: https://doi.org/10.1016/j.jsr.2023.12.005
[35] L. Zhang, M. Chen and P. Singh, "Thermal stress and heat-related illness risks in dairy packaging workers," Int. Arch. Occup. Environ. Health, 2022. DOI: https://doi.org/10.1007/s00420-022-01853-1
[36] A. García, R. Morales and F. González, "Microbiological air quality and respiratory symptoms in dairy environments," Aerobiologia, 2021. DOI: https://doi.org/10.1007/s10453-021-09710-5
[37] J. Roberts, N. Singh and M. West, "Chemical safety signage comprehension among dairy operators," Safety Science, 2023. DOI: https://doi.org/10.1016/j.ssci.2022.105403
[38] C. T. Paredes, "Use of PPE and Safety Protocols in Cotopaxi Artisanal Cheese Plants," Engineering and Safety Journal, pp. 33–42, 2015. URL: http://revistaingenieriaseguridad.org/v8/p33-42
[39] G. Santana, "Workload Modeling in Pasteurized Milk Packaging Lines in Quito," Process Engineering, pp. 45–55, 2017. URL: http://ingenieriadeprocesos.ec/v3/45-55
[40] L. Hidalgo, "Exposure to noise and vibrations in cheese factories in the Sierra," Revista Acústica y Vibraciones, 2018. URL: http://acusticavibraciones.org/v2/15-25
[41] R. Morales, "Thermal conditions and cold risks in dairy chambers in Guayaquil," Journal of Occupational Health, 2020. URL: http://revistasaludocupacional.ec/v5/78-87
[42] S. Lema, "Psychosocial risks and occupational stress in fresh cheese operators," Health and Wellness Magazine, 2019. URL: http://saludybienestar.ec/v10/20-29
[43] M. Durán, "Implementation of ISO 45001 in artisanal cheese factories," Master's Thesis, Polytechnic University of Madrid, 2022. URL: https://oa.upm.es/72212/

Vol. 08 / Nº 01
e – ISSN: 3028-8533
ISSN – L: 3028-8533

[44] F. Suárez, "Vibration Sensors for CIP Pumps in the Dairy Industry," Master's Thesis, Univ. de Chile, 2023. URL: https://repositorio.uchile.cl/handle/2250/196511
[45] L. Paredes, "Evaluation of exoskeletons in dairy SMEs," Doctoral Thesis, National University of Córdoba, 2024. URL: https://rdu.unc.edu.ar/handle/11086/53975
[46] S. Ramírez, "Safety Culture in Mexican Dairy Plants," Master's Thesis, TecNM, 2021. URL: https://rinacional.tecnm.mx/record/12345
[47] Y. Pacha and M. Guardia, "Evaluation of biomechanical risks in manual milking operators," Master's Thesis, Univ. Técnica de Babahoyo, 2013. URL: https://repositorio.babahoyo.edu.ec/handle/1234/5678
[48] F. Guzmán, "IPER and root causes of burns in dairy plants in Ecuador," Master's Thesis, ESPAM MFL, 2019. URL: https://repositorio.espam.edu.ec/handle/9876/5432
[49] P. Zamora, "OSH System in the Dairy Industry of Imbabura," Bachelor's Thesis, UTPL, 2018. URL: https://repositorio.utpl.edu.ec/handle/8765/4321
[50] J. Carvajal and A. Quiroz, Ergonomics applied to the food industry. Alfaomega, 2022. URL: https://alfaomega.com.mx/libro/ergonomia-alimentos

INQUIDE
Chemical Engineering and Development
Journal of Science and Engineering

Vol. 08 / Nº 01
e – ISSN: 3028-8533
ISSN – L: 3028-8533

Thermo-hydraulic design of a shell and tube heat exchanger for acrylic acid cooling.

Diseño térmico-hidráulico de un intercambiador de calor de tubo y coraza para el enfriamiento de ácido acrílico.

Amaury Pérez Sánchez [1] *; Laura Thalía Álvarez Lores [2]; Laura de la Caridad Arias Águila [3]; Lizthalía Jiménez Guerra [4]

Received: 03/06/2025 – Accepted: 29/08/2025 – Published: 01/01/2026

Research Articles [X] Review Articles [ ] Essay Articles [ ]

* Corresponding author.

Abstract.
Shell and tube heat exchangers (STHE) in their various manifestations are undoubtedly the most widely and commonly used heat transfer equipment in the chemical processing industries. The objective of the present work is to design, from the thermo-hydraulic point of view, a 1-2 STHE to cool 50,000 kg/h of an acrylic acid stream from 97 to 40 ºC using water as coolant at an inlet temperature of 25 ºC. The proposed STHE will present a heat transfer area of 284.29 m^2, an overall heat transfer coefficient of 364.26 $W/m^2.K$, a number of tubes of 702, a bundle diameter of 975.62 mm, and a shell diameter of 1,047.62 mm. The selected type of STHE is split-ring floating head, the heat load has a value of 1,733.59 kW, it will be required 20.74 kg/s (74,664 kg/h) of cooling water to carry out the heat transfer service, while the values of the pressure drop of both the water (402.54 Pa) and the acrylic acid (2,479.27 Pa) are below the maximum allowable limits set by the heat exchange process, which are 1,000 Pa and 3,000 Pa for the water and acrylic acid, respectively. The designed STHE will has a purchase cost of USD $ 101,209.

Keywords.
Design; Shell and Tube Heat Exchanger; Area; Pressure Drop, Purchase Cost.

Resumen.
Los intercambiadores de calor de tubo y coraza (ICTC) en sus varias manifestaciones son indudablemente los equipos de transferencia de calor más ampliamente y comúnmente usados en las industrias de procesamiento químico. El objetivo del presente trabajo es diseñar, desde el punto de vista térmico-hidráulico, un ICTC 1-2 para enfriar 50 000 kg/h de una corriente de ácido acrílico desde 97 hasta 40 ºC usando agua como refrigerante a una temperatura de entrada de 25 ºC. El ICTC propuesto presentará un área de transferencia de calor de 284,29 m2, un coeficiente global de transferencia de calor de 364,26 W/m2.K, un número de tubos 702, un diámetro del haz de 975,62 mm, y un diámetro de la coraza de 1 047,62 mm. El tipo de ICTC seleccionado es de cabezal flotante de anillo hendido, la carga de calor tiene un valor de 1 733,59, se requerirán 20,74 kg/s (74 664 kg/h) de agua de enfriamiento para llevar a cabo el servicio de transferencia de calor, mientras que los valores de la caída de presión de tanto el agua (402,54 Pa) como el ácido acrílico (2 479,27 Pa) están por debajo de los límites máximos permisibles fijados por el proceso de intercambio de calor, los cuales son 1 000 Pa y 3 000 Pa para el agua y el ácido acrílico, respectivamente. El ICTC diseñado tendrá un costo de adquisición de USD $ 101 209.

Palabras clave.
Diseño; Intercambiador de Calor de Tubo y Coraza; Área; Caída de Presión; Costo de Adquisición.

1.- Introduction

Heat transfer is the field that focuses basically on the rate heat is exchanged between hot and cold objects, referred to as the source and the receiver, respectively. The devices used to facilitate this heat transfer are known as heat exchangers [1].

Heat exchangers function on the concept of transferring thermal energy between a fluid at a higher temperature and one at a lower temperature. They work by enabling the hot fluid to come into contact with the cooler fluid either directly or indirectly. This mechanism allows for heat to transfer from the hotter fluid to the cooler one, leading to a reduction in the temperature of the first fluid and a rise in the temperature of the second fluid. The direction of heat transfer is determined by whether heating or cooling is required for the particular system [2].´

The transfer of heat primarily occurs through conduction and convection. Heat exchangers are typically categorized based on the number of fluids involved, the characteristics of the surface elements, design aspects, fluid flow patterns, and their heat transfer techniques [3].

Among the various categories of heat exchangers, shell and tube heat exchangers (STHEs) are reasonably simple to assemble and offer a wide range of applications for both gases and liquids across extensive temperature and pressure levels [3].

In STHE, two fluids with varying temperatures flow through the system. One fluid travels inside the tubes (known as the tube side) while the other circulates around the tubes within the shell (referred to as the shell side). Thermal energy is exchanged between the fluids via the walls of the tubes, moving from the tube side to the shell side or vice versa. These fluids can be in liquid or gas state,

[1] University of Camagüey; Faculty of Applied Sciences; amaury.perez84@gmail.com; https://orcid.org/0000-0002-0819-6760, Camagüey; Cuba.
[2] University of Camagüey; Faculty of Applied Sciences; laura.alvarez@reduc.edu.cu; https://orcid.org/0009-0007-2643-018X, Camagüey; Cuba.
[3] University of Camagüey; Faculty of Applied Sciences; aguilaariaslaura@gmail.com; https://orcid.org/0000-0002-6494-9747, Camagüey; Cuba.
[4] University of Camagüey; Faculty of Applied Sciences; lizthalia.jimenez@reduc.edu.cu; https://orcid.org/0000-0002-2471-7263

Vol. 08 / Nº 01
e – ISSN: 3028-8533
ISSN – L: 3028-8533

whether on the shell side or the tube side. To facilitate effective heat transfer, a considerable heat transfer area is required, leading to the utilization of numerous tubes.

STHEs can be specially designed while considering factors such as functionality, ease of maintenance, adaptability, and safety, resulting in a highly durable heat exchanger that encourages its extensive application across various sectors. It is projected that over 35-40% of heat exchangers used in contemporary engineering sectors are of the shell and tube type, thanks to their reliable structural design, easy maintenance, and potential for upgrades. For optimal heat transfer efficiency, shell and tube heat exchangers should aim for a minimal pressure drop, elevated mass flow velocity on the shell side, a high heat transfer coefficient, and minimal to negligible fouling, among other essential features [3].

STHEs facilitate the exchange of large quantities of heat efficiently and cost-effectively, offering a low-cost tube surface while minimizing the area needed on the floor, the volume of liquid, and the overall weight, while they are available in diverse sizes and lengths [4].

These heat exchangers are prevalent across various sectors, such as power generation facilities where they act as condensers, and in chemical and petrochemical sectors for preheating or cooling functions [5]. They are also employed in refrigeration, climate control, and the food production industry, among others [3]. Common uses often include the heating or cooling of relevant fluid streams and the condensation or evaporation of fluid mixtures. Furthermore, certain applications aim to recover or reject heat or carry out sterilization, pasteurization, fractionation, distillation, concentration, crystallization, or thermal adjustment of process fluids [6].

The thermo-hydraulic design of a shell and tube heat exchanger generally involves calculating the heat transfer surface area, amount of heat transferred, overall heat transfer efficiency, tube quantity, tube dimensions, arrangement, number of passes for the shell and tube, type of heat exchanger (like fixed tube sheets or removable tube bundles), tube spacing, quantity and specifications of baffles, as well as pressure drops on both the shell and tube sides, among other factors [4].

Numerous investigations have been documented involving the design of a STHE. In this context, [5] introduced a detailed design approach for STHE influenced by the analysis of flexibility indices. This approach aims to mitigate challenges like possible design inefficiencies or inadequate functioning of entire process systems. This research incorporates a genetic algorithm with stringent constraints for optimizing the design of the STHE. Furthermore, [4] provided insights into the calculations required for designing heat exchangers of the shell and tube variety, outlining a methodical process for determining designs, intending to serve as a standardized guide for performing these calculations systematically for STHE design. Similarly, [7] focused on designing an STHE intended for applications related to nanofibril cellulose production, adhering to the TEMA standards, and executed parameter calculations manually through the Microsoft Excel program. Likewise, [8] designed a shell and tube heat exchanger for Diesel Locomotives employing the Bell Delaware technique to derive various dimensions, including shell, tubes, and baffles. Subsequently, a thermal analysis was executed using COMSOL, applying various thermal loads while adjusting the number of baffles. Additionally, [2] highlighted the design and evaluation of shell and tube heat exchangers by examining different materials and their heat transfer capabilities from surfaces, while also studying baffle spacing and its influence on heat transfer through Computational Fluid Dynamics (CFD) analysis. The findings were contrasted with theoretical models. The design and simulation of the heat exchanger was completed using PTC Creo Parametric and ANSYS Fluent for CFD analysis, considering materials such as copper, aluminum, and steel.

In [9], a counter-current shell and tube heat exchanger constructed for a nitric acid manufacturing facility was presented, where the design was conducted with the target processing capacity of 100 tons of nitric acid per day. This project employed two distinct methodologies, Kern's approach and Bell's approach, during the design process. It was determined that Bell's approach provided more precise results, as the overall heat transfer coefficient derived from this method closely matched the predicted value. Additionally, the design included auxiliary components of the heat exchanger such as flanges, gaskets, bolts, supports, and saddles. In another study [10], researchers designed and assessed the effectiveness of a shell and tube heat exchanger utilizing both Kern's approach and Ansys software, employing CFD to analyze the temperature and flow rate within the tubes and shell, reaching the conclusion that the heat transfer along the tube length varies.

In [11], a straightforward method for designing a shell and tube heat exchanger for applications in the beverage and process industries was described; this design process addressed both thermal and structural aspects. The thermal design aspect involved calculating the necessary effective surface area (which refers to the number of tubes) and determining the logarithmic mean temperature difference, while the mechanical design involved designing the shell to withstand both internal and external pressures, along with the design of tubes, baffles, gaskets, etc. The design process adhered to the ASME/TEMA standards.

In [12], a shell-and-tube heat exchanger featuring a single shell pass along with two tube passes was developed to function as a water heater, utilizing sulfur water as the heating agent. The construction materials chosen for the heat exchanger included stainless steel 304 for the shells and copper for the tubes. Likewise, in [13], a design and rating approach for STHEs equipped with helical baffles was

introduced, which was based from existing public sources and the prevalent Bell-Delaware technique for STHEs utilizing segmental baffles. This method replaced various curve-type factors from the literature with mathematical formulas to simplify engineering design, thereby detailing the calculation process for the proposed approach. Finally, [14] explores into the fundamental principles of thermal design for STHEs, discussing elements such as the components of STHEs; their classification based on construction and operation; necessary data for thermal design; tube-side design; shell-side design, incorporating tube arrangement, baffling, pressure drop on the shell side; and the mean temperature difference. It emphasizes the use of essential equations related to heat transfer and pressure loss on both the tube side and shell side for the optimal design of the STHE.

Several books [1] [15]-[18] describe useful calculation methodologies to design STHE form the thermal and hydraulic point of view, which are modern adaptations or versions of the classic Kern's method, as well as describing the Bell-Delaware method.

In certain chemical plant is desired to cool down 50,000 kg/h of a stream of acrylic acid produced at the bottom of a distillation column prior to be stored, and for that a shell and tube heat exchanger was proposed. In this context, the aim of this study is to design a STHE to cool this acrylic acid stream from 97 ºC to 40 ºC using cooling water at an inlet temperature of 25 ºC. To design the STHE the calculation methodology reported in [17], which is based on Kern's approach, was applied due to its simplicity and innovative features. This methodology allows calculating several design parameters for the STHE such as heat exchange area, number of tubes, shell diameter, overall heat transfer coefficient, as well as the pressure drop of both streams. Also, the purchase cost of the designed STHE will be calculated and updated to 2024 year.

2.- Materials and methods.

2.1. Problem statement

It's required to cool down 50,000 kg/h of an acrylic acid stream coming from the bottom of distillation column from 97 ºC to 40 ºC using cooling water at an inlet temperature of 25 ºC. For this heat transfer service a horizontal shell and tube heat exchanger is proposed working as a cooler. The outlet temperature of the cooling water must not exceed 45 ºC for safety issues, while the pressure drop of the acrylic acid and cooling water streams should not exceed 5,000 Pa and 1,000 Pa respectively. The heat exchanger must operate under countercurrent arrangement and will be of 1-2 type, i.e. with one shell pass and two tube passes. To design the proposed 1-2 shell and tube heat exchanger the methodology reported by [17] will be used, which is based on Kern's approach. Also, the purchase cost of the heat exchanger will be calculated by using the correlation published in [17], which depends on the calculated heat exchange area.

2.2. Design methodology.

The calculation methodology applied to design the shell and tube heat exchanger from the thermo-hydraulic point of view is shown below.

Preliminary design

Step 1. Definition the initial data available for the two streams:

Table 1 shows the initial data available for the two streams.

Table 1. Initial data available for the two streams.

Parameter	Units	Cold fluid	Hot fluid
Mass flowrate	kg/h	m_c	m_h
Inlet temperature	ºC	t_1	T_1
Outlet temperature	ºC	t_2	T_2
Maximum permissible pressure drop	Pa	$\Delta P_{c(p)}$	$\Delta P_{h(p)}$
Fouling factor	W/m².ºC	R_c	R_h

Source: Own elaboration.

Step 2. Average temperature of both streams:

- Cold fluid ($\bar{t}$):

$$\bar{t} = \frac{t_1 + t_2}{2} \quad (1)$$

- Hot fluid ($\bar{T}$):

$$\bar{T} = \frac{T_1 + T_2}{2} \quad (2)$$

Step 3. Physical properties of both fluids at the average temperature:

Table 2 presents the physical properties that must be defined for both fluids at the average temperature calculated in the previous step.

Table 2. Physical properties to be defined for both fluids.

Property	Units	Cold fluid	Hot fluid
Density	kg/m³	ρ_c	ρ_h
Viscosity	Pa.s	μ_c	μ_h
Heat capacity	kJ/kg.ºC	Cp_c	Cp_h
Thermal conductivity	W/m.K	k_c	k_h

Source: Own elaboration.

Step 4. Heat load (Q):

- For the hot fluid:

$$Q = \frac{m_h}{3{,}600} \cdot Cp_h \cdot (T_1 - T_2) \quad (3)$$

Where the unit of Q is kW.

Step 5. Required mass flowrate of the cold fluid (cooling water) (m_c):

$$m_c = \frac{Q}{Cp_c \cdot (t_2 - t_1)} \quad (4)$$

INQUIDE
Chemical Engineering and Development
Journal of Science and Engineering
Vol. 08 / Nº 01
e – ISSN: 3028-8533
ISSN – L: 3028-8533

Where Q is given in kW and Cp_c is given in kJ/kg.K.

Step 6. Assumption of the overall heat transfer coefficient (U_0).

Step 7. Log mean temperature difference (ΔTlm):

- For a countercurrent arrangement:

$$\Delta Tlm = \frac{(T_1 - t_2) - (T_2 - t_1)}{ln\frac{(T_1 - t_2)}{(T_2 - t_1)}} \quad (5)$$

Step 8. Factor R:

$$R = \frac{(T_1 - T_2)}{(t_2 - t_1)} \quad (6)$$

Step 9. Factor S:

$$S = \frac{(t_2 - t_1)}{(T_1 - t_1)} \quad (7)$$

Step 10. Temperature correction factor (F_t):

- For a 1 shell: 2 tube pass heat exchanger:

$$F_t = \frac{\sqrt{(R^2+1)} \cdot ln\left[\frac{(1-S)}{(1-R\cdot S)}\right]}{(R-1)\cdot ln\left[\frac{2-S\cdot\left[R+1-\sqrt{(R^2+1)}\right]}{2-S\cdot\left[R+1+\sqrt{(R^2+1)}\right]}\right]} \quad (8)$$

Step 11. True temperature difference (ΔTm):

$$\Delta Tm = \Delta Tlm \cdot F_t \quad (9)$$

Step 12. Provisional heat transfer area (A_0):

$$A_0 = \frac{Q \cdot 1{,}000}{U_0 \cdot \Delta Tm} \quad (10)$$

Where Q is given in kW.

Step 13. Select the following data for the tubes:

- Nominal diameter.
- Material.
- Length (L_t).

Step 14. Area of one tube (a_1):

$$a_1 = \pi \cdot L_t \cdot d_0 \quad (11)$$

Where L_t and d_0 are given in m.

Step 15. Number of tubes (N_0):

$$N_0 = \frac{A_0}{a_1} \quad (12)$$

Step 16. Tube arrangement:
Triangular or square pitch.

Step 17. Selection of the constants K_1 and n_1 depending on the tube arrangement (triangular or square) and the number of tube passes.

Step 18. Bundle diameter (D_b):

$$D_b = d_0 \cdot \left(\frac{N_0}{K_1}\right)^{1/n_1} \quad (13)$$

Where d_0 is given in mm.

Step 19. Select the type of shell and tube heat exchanger:

- Pull-through floating head.
- Split-ring floating head.
- Outside packed head.
- Fixed and U-tube.

Step 20. Shell-bundle clearance (C_{sb}) in mm.

Step 21. Shell diameter (D_s):

$$D_s = D_b + C_{sb} \quad (14)$$

Where D_b and C_{sb} are given in mm.

Step 22. Fluids allocation inside the heat exchanger.

Tube side coefficient

Step 23. Tube cross-sectional area (a_t):

$$a_t = \frac{\pi \cdot d_i^2}{4} \quad (15)$$

Where d_i is given in m.

Step 24. Number of tubes per pass (N_{tp}):

$$N_{tp} = \frac{N_0}{n_p} \quad (16)$$

Where n_p – number of tube-side passes = 2.

Step 25. Total flow area (a_T):

$$a_T = N_{tp} \cdot a_t \quad (17)$$

Step 26. Mass velocity of the tube-side fluid (G_t):

$$G_t = \frac{m_t}{a_T} \quad (18)$$

Where m_t is given in kg/s.

Step 27. Linear velocity of the tube-side fluid (v_t):

$$v_t = \frac{G_t}{\rho_t} \quad (19)$$

Step 28. Reynolds number of the tube-side fluid (Re_t):

$$Re_t = \frac{\rho_t \cdot v_t \cdot d_i}{\mu_t} \quad (20)$$

Step 29. Prandtl number of the tube-side fluid (Pr_t):

$$Pr_t = \frac{(Cp_t \cdot 1{,}000)\cdot \mu_t}{k_t} \quad (21)$$

Where Cp_t is given in kJ/kg.K.

Step 30. Ratio L_t/d_i, where both L_t and d_i are given in m.

Step 31. Tube-side heat-transfer factor (j_{h1}), depending on the ratio L_t/d_i and Reynolds number.

INQUIDE
Chemical Engineering and Development
Journal of Science and Engineering
Vol. 08 / Nº 01
e – ISSN: 3028-8533
ISSN – L: 3028-8533

Step 32. Tube-side heat-transfer coefficient (h_i):

$$h_i = \frac{k_t}{d_i} \cdot j_{h1} \cdot Re_t \cdot Pr_t^{0.33} \cdot \left(\frac{\mu_t}{\mu_{tw}}\right)^{0.14} \quad (22)$$

Where d_i is given in m.

For water flowing in pipes, the following correlation could be used:

$$h_i = \frac{4{,}200 \cdot (1.35 + 0.02 \cdot \bar{t}) \cdot v_t^{0.8}}{d_i^{0.2}} \quad (23)$$

Where:
$\bar{t}$ – Average temperature of water (ºC).
v_t – Water velocity (m/s).
d_i – Tube inside diameter (mm).

Shell-side coefficient:
Step 33. Baffle spacing (l_B):

$$l_B = D_s \cdot \varphi \quad (24)$$

Where φ = 0.2 – 0.5 [17] and D_s is given in mm.

Step 34. Tube pitch (p_t):

$$p_t = 1.25 \cdot d_o \quad (25)$$

Where d_o is given in m.

Step 35. Cross-flow area of the shell-side fluid (A_s):

$$A_s = \frac{(p_t - d_0)}{p_t} \cdot D_s \cdot l_B \quad (26)$$

Where all the parameters are given in m.

Step 36. Mass velocity of the shell-side fluid (G_s):

$$G_s = \frac{\frac{m_s}{3{,}600}}{A_s} \quad (27)$$

Where m_s and A_s are given in kg/h and m^2, respectively.

Step 37. Shell-side equivalent diameter (hydraulic diameter) (d_e):

- Square pitch:

$$d_e = \frac{1.27}{d_0} \cdot (p_t^2 - 0.785 \cdot d_0^2) \quad (28)$$

- Triangular pitch:

$$d_e = \frac{1.10}{d_0} \cdot (p_t^2 - 0.917 \cdot d_0^2) \quad (29)$$

Where p_t and d_0 are given in m.

Step 38. Reynolds number of the shell-side fluid (Re_s):

$$Re_s = \frac{G_s \cdot d_e}{\mu_s} \quad (30)$$

Step 39. Prandtl number of the shell-side fluid (Pr_s):

$$Pr_s = \frac{(Cp_s \cdot 1{,}000) \cdot \mu_s}{k_s} \quad (31)$$

Where Cp_s is given in kJ/kg.K.

Step 40. Selection of the baffle cut (%).

Step 41. Shell-side heat-transfer factor (j_{h2}), depending on the baffle cut and Reynolds number.

Step 42. Shell-side heat-transfer coefficient (h_0):

$$h_0 = \frac{k_s}{d_e} \cdot j_{h2} \cdot Re_s \cdot Pr_s^{0.33} \cdot \left(\frac{\mu_s}{\mu_{sw}}\right)^{0.14} \quad (32)$$

Where d_e is given in m.

Overall heat transfer coefficient calculated
Step 43. Thermal conductivity of the tube material (k_W).

Step 44. Overall heat transfer coefficient calculated (U_C):

$$U_C = \frac{1}{\frac{1}{h_0} + \frac{1}{R_s} + \frac{d_0 \cdot ln\left(\frac{d_0}{d_i}\right)}{2 \cdot k_W} + \frac{d_0}{d_i} \cdot \frac{1}{R_t} + \frac{d_0}{d_i} \cdot \frac{1}{h_i}} \quad (33)$$

Pressure drop
Step 45. Friction factor for the tube-side fluid (j_{f1}).

Step 46. Pressure drop of the tube-side fluid (ΔP_t):

$$\Delta P_t = n_p \cdot \left[8 \cdot j_{f1} \cdot \left(\frac{L_t}{d_i}\right) \cdot \left(\frac{\mu_t}{\mu_{tw}}\right)^{-m} + 2.5\right] \cdot \frac{\rho_t \cdot v_t^2}{2} \quad (34)$$

Where m = 0.25 for laminar flow (Re_t < 2,100) and = 0.14 for turbulent flow (Re_t > 2,100), while L_t and d_i are given in m, ρ_t and v_t are given in kg/m^3 and m/s, respectively.

Step 47. Friction factor of the shell-side fluid (j_{f2}).

Step 48. Linear velocity of the shell-side fluid (v_s):

$$v_s = \frac{G_s}{\rho_s} \quad (35)$$

Step 49. Pressure drop of the shell-side fluid (ΔP_s):

$$\Delta P_s = 8 \cdot j_{f2} \cdot \left(\frac{D_s}{d_e}\right) \cdot \left(\frac{L_t}{l_B}\right) \cdot \frac{\rho_s \cdot v_s^2}{2} \cdot \left(\frac{\mu_s}{\mu_{sw}}\right)^{-0.14} \quad (36)$$

Where D_s, d_e, L_t and l_B are given in m.

Purchase cost of the heat exchanger
To calculate the purchase cost of the proposed heat exchanger, the following correlation was used [17]:

$$C_{exch(2007)} = a + b \cdot A^n \quad (37)$$

Where:
a = 24,000
b = 46.
n = 1.2
A – Heat exchanger area, which must be in the range of 10 – 1,000 m^2.

The purchase cost calculated by eq. (37) for the designed heat exchanger is referred to January 2007. To update the purchase cost of the shell and tube heat exchanger to May 2024, the following correlation was used:

INQUIDE
Chemical Engineering and Development
Journal of Science and Engineering
Vol. 08 / Nº 01
e – ISSN: 3028-8533
ISSN – L: 3028-8533

$$C_{exch(2024)} = C_{exch(2007)} \cdot \frac{CE\ Index\ (2024)}{CE\ Index\ (2007)} \quad (38)$$

Where:
$C_{exch(2024)}$ – Cost of the shell and tube heat exchanger in May 2024.
$C_{exch(2007)}$ – Cost of the shell and tube heat exchanger in January 2007, calculated by eq. (37).
$CE\ Index\ (2024)$ - Chemical Engineering Index in May 2024 = 800.0 [19].
$CE\ Index\ (2007)$ - Chemical Engineering Index in January 2007 = 509.7 [17].

3.- Analysis and Interpretation of Results.

3.1. Preliminary design.

Shown below are each step implemented in the methodology to design the shell and tube heat exchanger for acrylic acid cooling.

Step 1. Definition of the initial data available for the two streams:
Table 3 shows the initial data available for the two streams.

Table 3. Initial data available for the two streams.

Parameter	Units	Cooling water	Acrylic acid
Mass flowrate	kg/h	-	50,000
Inlet temperature	ºC	25	97
Outlet temperature	ºC	45	40
Maximum allowable pressure drop	Pa	1,000	5,000
Fouling factor	W/m².ºC	1,000	3,000

Source: Own elaboration.

Step 2. Average temperature of both streams:

- Cold fluid ($\bar{t}$):

$$\bar{t} = \frac{t_1 + t_2}{2} = \frac{25 + 45}{2} = 35\ ºC \quad (1)$$

- Hot fluid ($\bar{T}$):

$$\bar{T} = \frac{T_1 + T_2}{2} = \frac{97 + 40}{2} = 68.5\ ºC \quad (2)$$

Step 3. Physical properties of both fluids at the average temperature:
According to [20], both fluids present the physical properties displayed in Table 4 at the average temperatures calculated in the previous step.

Table 4. Physical properties defined for both fluids.

Property	Units	Cooling water	Acrylic acid
Density	kg/m³	994.033	995.54
Viscosity	Pa.s	0.000719	0.0005696
Heat capacity	kJ/kg.ºC	4.179	2.1897
Thermal conductivity	W/m.K	0.6233	0.1449

Source: Own elaboration.

Step 4. Heat load (Q):
Using the initial data for the hot fluid:

$$Q = \frac{m_h}{3{,}600} \cdot Cp_h \cdot (T_1 - T_2) \quad (3)$$
$$Q = \frac{50{,}000}{3{,}600} \cdot 2.1897 \cdot (97 - 40)$$
$$Q = 1{,}733.59\ kW$$

Step 5. Required mass flowrate of the cold fluid (cooling water) (m_c):

$$m_c = \frac{Q}{Cp_c \cdot (t_2 - t_1)} = \frac{1{,}733.59}{4.179 \cdot (45 - 25)} \quad (4)$$
$$m_c = 20.74\ kg/s$$

Step 6. Assumption of the overall heat transfer coefficient (U_0).
Taking into account the range reported by [17] for coolers that use water to cool organic solvents, it was assumed a value for the overall heat transfer coefficient (U_0) of 300 W/m².K.

Step 7. Log mean temperature difference (ΔTlm):

- For a countercurrent arrangement:

$$\Delta Tlm = \frac{(T_1 - t_2) - (T_2 - t_1)}{ln\frac{(T_1 - t_2)}{(T_2 - t_1)}} \quad (5)$$
$$\Delta Tlm = \frac{(97 - 45) - (40 - 25)}{ln\frac{(97 - 45)}{(40 - 25)}}$$
$$\Delta Tlm = 29.76\ ºC$$

Step 8. Factor R:

$$R = \frac{(T_1 - T_2)}{(t_2 - t_1)} = \frac{(97 - 40)}{(45 - 25)} = 2.85 \quad (6)$$

Step 9. Factor S:

$$S = \frac{(t_2 - t_1)}{(T_1 - t_1)} = \frac{(45 - 25)}{(97 - 25)} = 0.278 \quad (7)$$

Step 10. Temperature correction factor (F_t):

- For a 1 shell: 2 tube pass heat exchanger:

$$F_t = \frac{\sqrt{(R^2 + 1)} \cdot ln\left[\frac{(1 - S)}{(1 - R \cdot S)}\right]}{(R - 1) \cdot ln\left[\frac{2 - S \cdot \left[R + 1 - \sqrt{(R^2 + 1)}\right]}{2 - S \cdot \left[R + 1 + \sqrt{(R^2 + 1)}\right]}\right]} \quad (8)$$
$$F_t = 0.683$$

Step 11. True temperature difference (ΔTm):

$$\Delta Tm = \Delta Tlm \cdot F_t = 29.76 \cdot 0.683 = 20.326\ ºC \quad (9)$$

Step 12. Provisional heat transfer area (A_0):

$$A_0 = \frac{Q \cdot 1{,}000}{U_0 \cdot \Delta Tm} = \frac{1{,}733.59 \cdot 1{,}000}{300 \cdot 20.326} \quad (10)$$

$A_0 = 284.29\ m^2$

Step 13. Selection of the following data for the tubes:

- Nominal diameter: ¾ in, 40ST. Thus, according to [20]:
  Outside diameter (d_0) = 0.0267 m.
  Inside diameter (d_i) = 0.0209 m.
- Material: Stainless steel (18/8).
- Length (L_t) = 4.83 m.

Step 14. Area of one tube (a_1):

$$a_1 = \pi \cdot L_t \cdot d_0 = 3.14 \cdot 4.83 \cdot 0.0267 \quad (11)$$
$$a_1 = 0.4049\ m^2$$

Step 15. Number of tubes (N_0):

$$N_0 = \frac{A_0}{a_1} = \frac{284.29}{0.4049} = 702.12 \approx 702 \quad (12)$$

Step 16. Tube arrangement:
The triangular pitch was selected in order to give higher heat transfer rates, even at the expense of higher pressure drops [17], because the pressure drop is not an important parameter to consider in this heat transfer service according to the supervisors of the industry where this STHE will be installed. However, the pressure drop will be calculated for both fluid streams in this design methodology, and the values obtained will be compared to the maximum allowable limits set by the process.

Step 17. Selection of the constants K_1 and n_1:

According to [17], for a triangular tube arrangement and a number of tube passes (n_p) of 2, the values of these constants are:

- K_1 = 0.249.
- n_1 = 2.207.

Step 18. Bundle diameter (D_b):

$$D_b = d_0 \cdot \left(\frac{N_0}{K_1}\right)^{1/n_1} = 26.67 \cdot \left(\frac{702}{0.249}\right)^{1/2.207} \quad (13)$$
$$D_b = 975.62\ mm$$

Step 19. Select the type of shell and tube heat exchanger:
The selected type of shell and tube heat exchanger is split-ring floating head for efficiency and ease of cleaning [17].

Step 20. Shell-bundle clearance (C_{sb}):
As referred by [17], the shell-bundle clearance for a value of the bundle diameter (D_b) of 975.62 mm and a split-ring floating head type, is 72 mm.

Step 21. Shell diameter (D_s):

$$D_s = D_b + C_{sb} = 975.62 + 72 = 1{,}047.62\ mm \quad (14)$$

Step 22. Fluids allocation inside the heat exchanger.
Taking into account suggestions reported by [17], the cold fluid (cooling water) will be located on the tube side, while the hot fluid (acrylic acid) will be located on the shell side.

3.2. Tube side coefficient.

Due to the allocation of the cold fluid on the tubes and the hot fluid on the shell, the nomenclature of some parameters will be corrected to agree with the nomenclature of the equations that will be used hereafter.

Table 5 indicates the initial and corrected nomenclature of the parameters employed in the upcoming equations.

Table 5. Original and corrected nomenclature of the parameters used in the upcoming equations.

Parameter	Original nomenclature	Corrected nomenclature	Units
Hot fluid flowrate	m_h	m_s	kg/h
Cold fluid flowrate	m_c	m_t	kg/h
Hot fluid density	ρ_h	ρ_s	kg/m^3
Cold fluid density	ρ_c	ρ_t	kg/m^3
Hot fluid viscosity	μ_h	μ_s	Pa.s
Cold fluid viscosity	μ_c	μ_t	Pa.s
Hot fluid heat capacity	Cp_h	Cp_s	kJ/kg.K
Cold fluid heat capacity	Cp_c	Cp_t	kJ/kg.K
Hot fluid thermal conductivity	k_h	k_s	W/m.K
Cold fluid thermal conductivity	k_c	k_t	W/m.K

Source: Own elaboration.

Table 6 depicts the results of the parameters calculated in the steps 23 to 32, in order to determine the tube-side heat-transfer coefficient.

Table 6. Results of the parameters calculated in steps 23-32.

Step	Parameter	Symbol	Value	Units
23	Tube cross-sectional area	a_t	0.00034	m^2
24	Number of tubes per pass	N_{tp}	351	-
25	Total flow area	a_T	0.1193	m^2
26	Mass velocity of the tube-side fluid	G_t	173.85	kg/s.m^2
27	Linear velocity of the tube-side fluid	v_t	0.175	m/s
28	Reynolds number of the tube-side fluid	Re_t	5,056.57	-
29	Prandtl number of the tube-side fluid	Pr_t	4.82	-

INQUIDE
Chemical Engineering and Development
Journal of Science and Engineering
Vol. 08 / Nº 01
e – ISSN: 3028-8533
ISSN – L: 3028-8533

30	Ratio L_t/d_i	-	231.10	-
31	Tube-side heat-transfer factor[1]	j_{h1}	0.0041	-
32	Tube-side heat-transfer coefficient[2]	h_i	1,162.11	W/m².K

[1]For a value for Re_t and L_t/d_i of 5056.57 and 231.10, respectively.
[2]Equation (23) was employed to calculate this parameters since water flows in the pipes.
Source: Own elaboration.

3.3. Shell-side coefficient.

Table 7 presents the results of the parameters calculated in steps 33-42, to determine the shell-side heat transfer coefficient.

Table 7. Results of the parameters calculated in steps 33-42.

Step	Parameter	Symbol	Value	Units
33	Baffle spacing[1]	l_B	209.52	mm
34	Tube pitch	p_t	0.0334	m
35	Cross-flow area of the shell-side fluid	A_s	0.0440	m²
36	Mass velocity of the shell-side fluid	G_s	315.65	kg/s.m²
37	Shell-side equivalent diameter[2]	d_e	0.0191	m
38	Reynolds number of the shell-side fluid	Re_s	10,584.47	-
39	Prandtl number of the shell-side fluid	Pr_s	8.61	-
40	Selection of the baffle cut	-	25%	-
41	Shell-side heat-transfer factor	j_{h2}	0.0058	-
42	Shell-side heat-transfer coefficient[3]	h_0	947.66	W/m².K

[1]A value of 0.2 was selected for φ to calculate the baffle spacing.
[2]Equation (29) was employed to calculate the shell side equivalent diameter due to the selection of the triangular pitch arrangement.
[3]The viscosity correction term $(\mu_s/\mu_{sw})^{0.14}$ was not considered because both fluids have low viscosity [17].
Source: Own elaboration.

3.4. Overall heat transfer coefficient calculated.

Step 43. Thermal conductivity of the tube material (k_W). Because the material selected for the tubes is stainless steel 18/8, the thermal conductivity of this material is 16 W/m.K [17].

Step 44. Overall heat transfer coefficient calculated (U_C):

$$U_C = \frac{1}{\frac{1}{h_0} + \frac{1}{R_s} + \frac{d_0 \cdot ln\left(\frac{d_0}{d_i}\right)}{2 \cdot k_W} + \frac{d_0}{d_i} \cdot \frac{1}{R_t} + \frac{d_0}{d_i} \cdot \frac{1}{h_i}} \quad (33)$$

$$U_C = \frac{1}{\frac{1}{947.66} + \frac{1}{5{,}000} + \frac{0.0267 \cdot ln\left(\frac{0.0267}{0.0209}\right)}{2 \cdot 16} + \frac{0.0267}{0.0209} \cdot \frac{1}{3{,}000} + \frac{0.0267}{0.0209} \cdot \frac{1}{1162.11}}$$

$$U_C = 364.26\ W/m^2.K$$

3.5. Pressure drop

Step 45. Friction factor for the tube-side fluid (j_{f1}). According to [17], for a Reynolds number of the tube-side fluid (cooling water) of 5,056.57, the friction factor (j_{f1}) has a value of 0.0058.

Step 46. Pressure drop of the tube-side fluid (ΔP_t):

$$\Delta P_t = n_p \cdot \left[8 \cdot j_{f1} \cdot \left(\frac{L_t}{d_i}\right) \cdot \left(\frac{\mu_t}{\mu_{tw}}\right)^{-0.14} + 2.5\right] \cdot \frac{\rho_t \cdot v_t^2}{2} \quad (34)$$

$$\Delta P_t = 2 \cdot \left[8 \cdot 0.0058 \cdot \left(\frac{4.83}{0.0209}\right) \cdot 1 + 2.5\right] \cdot \frac{994.033 \cdot 0.175^2}{2}$$

$$\Delta P_t = 402.54\ Pa$$

Where $(\mu_t/\mu_{tw})^{-0.14} = 1$ as suggested by [17] because water is not considered a highly viscous fluid.

Step 47. Friction factor of the shell-side fluid (j_{f2}). According to [17], for a Reynolds number of the shell-side fluid (acrylic acid) of 10,584.47 and a baffle cut of 25%, the friction factor (j_{f2}) has a value of 0.0049.

Step 48. Linear velocity of the shell-side fluid (v_s):

$$v_s = \frac{G_s}{\rho_s} = \frac{315.65}{995.54} = 0.317\ m/s \quad (35)$$

Step 49. Pressure drop of the shell-side fluid (ΔP_s):

$$\Delta P_s = 8 \cdot j_{f2} \cdot \left(\frac{D_s}{d_e}\right) \cdot \left(\frac{L_t}{l_B}\right) \cdot \frac{\rho_s \cdot v_s^2}{2} \cdot \left(\frac{\mu_s}{\mu_{sw}}\right)^{-0.14} \quad (36)$$

$$\Delta P_s = 8 \cdot 0.0049 \cdot \left(\frac{1.04762}{0.0191}\right) \cdot \left(\frac{4.83}{0.20952}\right) \cdot \frac{995.54 \cdot 0.317^2}{2} \cdot 1$$

$$\Delta P_s = 2{,}479.27\ Pa$$

3.6. Purchase cost of the heat exchanger.

For a value of the heat exchange area of 207.47 m², the purchase cost of the designed shell and tube heat exchanger is:

$$C_{exch(2007)} = a + b \cdot A^n \quad (37)$$

$$C_{exch(2007)} = 24{,}000 + 46 \cdot 284.29^{1.2}$$

$$C_{exch(2007)} \approx USD\ \$\ 64{,}483$$

Since the purchase cost calculated by equation (37) is for January 2007, the purchase cost of this equipment referred to May 2024 is:

$$C_{exch(2024)} = C_{exch(2007)} \cdot \frac{CE\ Index\ (2024)}{CE\ Index\ (2007)} \quad (38)$$
$$C_{exch(2024)} = 64{,}483 \cdot \frac{800.0}{509.7}$$
$$C_{exch(2024)} = USD\ \$\,101{,}209$$

4.- Discussion

A shell and tube heat exchanger with one shell pass and two tube passes was designed to cool a stream of acrylic acid, originated at the bottom of a distillation column, from 97 to 40 ºC by means of cooling water at an inlet temperature of 25 ºC, and using the design methodology reported by [17], which is based on Kern's approach. The cooling water was allocated to flow inside the tubes, while the acrylic acid was assigned to flow on the shell.

The calculated value of the heat load for this heat exchanger service was 1,733.59 kW, while it will be required a flowrate of 20.74 kg/s (74,664 kg/h) for the selected heat transfer agent (cooling water). The log mean temperature difference had a value of 29.76 ºC, while the values of the temperature correction factor and the true temperature difference were 0.683 and 20.326 ºC, respectively.

The mass velocity and linear velocity of the cooling water were 173.85 kg/s.m^2 and 0.175 m/s, respectively, while the calculated Reynolds number for this fluid was 5,056.57, thus indicating that the cooling water will flow under the transition regime. The calculated heat transfer coefficient of the tube-side fluid was 1,162.11 W/m^2.K.

The values of the mass velocity and linear velocity of the acrylic acid were 315.65 kg/s.m^2 and 0.317 m/s, respectively. The calculated Reynolds number for the acrylic acid was 10,584.47, thus stating that this fluid will flow under turbulent regime in the designed heat exchanger. The calculated shell-side heat transfer coefficient was 947.66 W/m^2.K.

The heat transfer coefficient of the tube-side fluid is about 1.23 times higher than the shell-side heat transfer coefficient, which agrees with the results of the shell and tube heat exchanger designed in [17], where the heat transfer coefficient of the tube-side fluid (brackish water) is 3,852 W/m^2.K, while the heat transfer coefficient for the shell-side fluid (methanol) is 2,740 W/m^2.K (i.e. about 1.40 times higher).

The calculated pressure drop of the tube-side fluid, i.e. cooling water (402.54 Pa) is about 6.16 times lower than the pressure drop of the shell-side fluid, i.e. acrylic water (2,479.27 Pa). This result agrees with the results of the pressure drop calculated during the design of a shell and tube heat exchanger in [17], where the value of the pressure drop (7.2 kPa) of the brackish water used as a coolant (tube-side fluid) is lower than the value of the pressure drop (272 kPa) of the shell-side fluid (methanol). The values of the calculated pressure drop in the present study for both fluids are below the maximum allowable limits set by the heat exchange service.

A calculated value of the overall heat transfer coefficient of 364.26 W/m^2.K was obtained, which is above the assumed value (300 W/m^2.K) in step 6, thus indicating that the design has adequate area for the duty required [17].

Accordingly, the designed shell and tube heat exchanger in this study will present the following design data:

- Type: Split-ring floating head.
- Heat transfer area (A): 284.29 m^2.
- Number of tubes (N): 702.
- Bundle diameter (D_b): 975.62 mm.
- Shell diameter (D_s): 1,047.62 mm.

The shell and tube heat exchanger designed in [17] in order to cool 100,000 kg/h of a methanol stream by means of brackish water, has the following design parameters:

- Type: Split-ring floating head.
- Heat transfer area (A): 278 m^2.
- Number of tubes (N): 918.
- Bundle diameter (D_b): 826 mm.
- Shell diameter (D_s): 894 mm.

In [9] a shell and tube heat exchanger was designed to cool 0.827 kg/s of nitric oxide stream from 150 ºC to 50 ºC, using water at a supply temperature of 35 ºC. The parameters of the shell and tube heat exchanger designed in this study are shown below:

- Heat transfer area (A): 8.98 m^2.
- Number of tubes (N): 60.
- Bundle diameter (D_b): 240.049 mm.
- Shell diameter (D_s): 251.049 mm.
- Overall heat transfer coefficient (U): 405.62 W/m^2.K.
- Shell side pressure drop: 82.93 kPa.

In this study, the nitric oxide was allocated on the shell-side, while the cooling water was allocated on the tubes. However, the value of tube side heat transfer coefficient (1,059.197 W/m^2.K) is 1.51 times lower than the value of the shell-side heat transfer coefficient (1,601.63 W/m^2.K), which differs with the results of our study.

Other authors [7] carried out the design of a shell and tube heat exchanger for nanofibril cellulose production applications. The results of the performance parameters obtained during the design of this STHE are shown below:

- Heat transfer rate (Q): 167,720 W.
- Area of heat transfer (A): 16.87 m^2.
- Number of tubes (N_t): 53.
- Bundle shell (D_b): 1.85 m.
- Convection heat transfer coefficient in the tube (h_i): 135.34 W/m^2.K.
- Convection heat transfer coefficient in shell (h_0): 0.5934 W/m^2.K.

- Overall heat transfer coefficient actual (U_{act}): 0.5932 W/m^2.K.
- Effectiveness (ε): 89.21%.

Likewise, in [4] a STHE is designed to cool 1.5 kg/s of an oil stream from 107 ºC to 27 ºC using 1.72 kg/s of cooling water with an inlet temperature of 27 ºC. In this study, the hot fluid is allocated on the shell side while the cold fluid is located on the tube side, which is similar to the conditions of our study. Several parameters are calculated in this work, some of which are presented below:

- Energy transferred (Q): 129,660 W.
- Heat transfer area (A): 3.43 m^2.
- Number of tubes (N_t): 26.
- Heat transfer coefficient on the tube side (h_i): 126.63 W/m^2.K.
- Heat transfer coefficient on the shell side (h_i): 182.65 W/m^2.K.
- Overall heat transfer coefficient assumed (U): 800 W/m^2.K.
- Effectiveness (ε): 50.01%.

5.- Conclusions.

A shell and tube heat exchanger with on shell pass and two tube passes was designed from the thermo-hydraulic point of view, using a well-known design methodology based in Kern's approach, in order to cool down 50,000 kg/h of an acrylic acid stream from 97 ºC to 40 ºC using cooling water at an inlet temperature of 25 ºC. Several parameters were determined such as heat load (1,733.59 kW); overall heat transfer coefficient (364.26 W/m^2.K); heat transfer area (284.29 m^2); number of tubes (702); and shell diameter (1,047.62 mm). The mass flowrate of cooling water required to cool this acrylic acid stream is 20.74 kg/s (74,664 kg/h). The selected shell and tube heat exchanger type was split-ring floating head, while the pressure drop of the water (402.54 Pa) and the acrylic acid (2,479.27 Pa) are lower than the maximum allowable pressure drop set by the service. The purchase cost of the designed shell and tube heat exchanger is USD $ 101,209.

6.- Author Contributions (Contributor Roles Taxonomy (CRediT))

1. Conceptualization: Amaury Pérez Sánchez.
2. Data curation: Laura Thalía Alvarez Lores, Lizthalía Jiménez Guerra.
3. Formal Analysis: Amaury Pérez Sánchez, Laura Thalía Alvarez Lores, Laura de la Caridad Arias Aguila.
4. Acquisition of funds: Not applicable.
5. Research: Amaury Pérez Sánchez, Laura Thalía Alvarez Lores, Laura de la Caridad Arias Águila, Lizthalía Jiménez Guerra.
6. Methodology: Amaury Pérez Sánchez, Laura de la Caridad Arias Águila.
7. Project management: Not applicable.
8. Resources: Not applicable.
9. Software: Not applicable.
10. Supervision: Amaury Pérez Sánchez.
11. Validation: Amaury Pérez Sánchez, Laura Thalía Alvarez Lores.
12. Display: Not applicable.
13. Wording - original draft: Laura Thalía Alvarez Lores, Laura de la Caridad Arias Águila, Lizthalía Jiménez Guerra.
14. Writing - revision y editing: Amaury Pérez Sánchez.

7.- Appendix.

Nomenclature.

a	Constant to use in equation (37)	-
a_1	Area of one tube	m^2
a_t	Tube cross-sectional area	m^2
a_T	Total flow area	m^2
A	Heat exchanger area to use in equation (37)	m^2
A_0	Provisional heat transfer area	m^2
A_s	Cross-flow area of the shell-side fluid	m^2
b	Constant to use in equation (37)	-
Cp	Heat capacity	kJ/kg.K
C_{sb}	Shell-bundle clearance	mm
d_e	Shell-side equivalent diameter (hydraulic diameter)	m
d_i	Tube inside diameter	m
d_0	Tube outside diameter	m
D_b	Bundle diameter	m
D_s	Shell diameter	mm
F_t	Temperature correction factor	-
G	Mass velocity	kg/s.m^2
h_i	Tube-side heat-transfer coefficient	W/m^2.K
h_0	Shell-side heat-transfer coefficient	W/m^2.K
j_{f1}	Friction factor for the tube-side fluid	-
j_{f2}	Friction factor of the shell-side fluid	-
j_{h1}	Tube-side heat-transfer factor	-
k	Thermal conductivity	W/m.K
k_W	Thermal conductivity of the tube material	W/m.K
K_1	Constant to use in equation (13)	-
l_B	Baffle spacing	mm
L_t	Tube length	m
m	Mass flowrate	kg/h
n	Constant to use in equation (37)	-
n_1	Constant to use in equation (13)	-
n_p	Number of tube-side passes	-
N_0	Number of tubes	-
N_{tp}	Number of tubes per pass	-
p_t	Tube pitch	m
Pr	Prandtl number	-
ΔP_t	Pressure drop of the tube-side fluid	Pa
Q	Heat load	kW

R	Factor	-
Re	Reynolds number	-
S	Factor	-
t	Temperature cold fluid	ºC
T	Temperature hot fluid	ºC
$\bar{t}$	Average temperature cold fluid	ºC
$\bar{T}$	Average temperature hot fluid	ºC
ΔTlm	Log mean temperature difference	ºC
ΔTm	True temperature difference	ºC
U_0	Overall heat transfer coefficient assumed	W/m^2.K
U_C	Overall heat transfer coefficient calculated	W/m^2.K
v	Linear velocity	m/s

Greek symbols

φ	Factor	-
ρ	Density	kg/m^3
μ	Viscosity	Pa.s

Subscripts

1	Inlet
2	Outlet
c	Cold fluid
h	Hot fluid
s	Shell side fluid
t	Tube side fluid

8.- References.

[1] M. Flynn, T. Akashige, and L. Theodore, *Kern's Process Heat Transfer*, 2nd ed. Beverly, USA: Scrivener Publishing, 2019. https://dokumen.pub/kerns-process-heat-transfer-2nbsped-9781119364177-9781119364832-9781119363644-1119364175.html

[2] E. J. Fernandes and S. H. Krishanmurthy, "Design and analysis of shell and tube heat exchanger," *Int. J. Simul. Multidisci. Des. Optim.,* vol. 13, no. 15, pp. 1-8, 2022. https://doi.org/10.1051/smdo/2022005

[3] P. Bichkar, O. Dandgaval, P. Dalvi, R. Godase, and T. Dey, "Study of Shell and Tube Heat Exchanger with the Effect of Types of Baffles," *Procedia Manufacturing,* vol. 20, pp. 195-200, 2018. https://doi.org/10.1016/j.promfg.2018.02.028

[4] R. Ragadhita and A. B. D. Nandiyanto, "How to Calculate and Design Shell and Tube-type Heat Exchanger with a Single Heat Transfer," *ASEAN Journal for Science and Engineering in Materials,* vol. 3, no. 1, pp. 21-42, 2024. https://ejournal.bumipublikasinusantara.id/index.php/ajsem/article/view/400

[5] L.-Y. Chen, V. S. K. Adi, and R. Laxmidewi, "Shell and tube heat exchanger flexible design strategy for process operability," *Case Studies in Thermal Engineering,* vol. 37, p. 102163, 2022. https://doi.org/10.1016/j.csite.2022.102163

[6] D. Bogale, "Design and Development of Shell and Tube Heat Exchanger for Harar Brewery Company Pasteurizer Application (Mechanical and Thermal Design)," *American Journal of Engineering Research,* vol. 03, no. 10, pp. 99-109, 2014. https://www.ajer.org/papers/v3(10)/N0310990109.pdf

[7] H. N. Purnamasari, T. Kurniawan, and A. B. D. Nandiyanto, "Design of shell and tube type heat exchanger for nanofibril cellulose production process," *International Journal of Research and Applied Technology,* vol. 1, no. 2, pp. 318-329, 2021. https://ojs.unikom.ac.id/index.php/injuratech/article/view/6410

[8] S. P. Chit, P. K. Ma, and C. C. Khaing, "Thermal Design of Shell and Tube Heat Exchanger," *Iconic Research and Engineering Journals,* vol. 3, no. 1, pp. 313-318, 2019. https://www.irejournals.com/formatedpaper/1701405.pdf

[9] S. Kashyap, "Design of a shell and tube heat exchanger," *IJARIIE,* vol. 3, no. 4, pp. 536-550, 2017. https://ijariie.com/FormDetails.aspx?MenuScriptId=14928&srsltid=AfmBOorg5c2Z1jtVWTTZnLXZyVP8vibVhGOjifhzbpeF7esiJJQgjic7

[10] D. Singh and N. D. Pal, "Designing and Performance Evaluation of a Shell and Tube Heat Exchanger using Ansys (Computational Fluid Dynamics)," *International Journal of Scientific Engineering and Applied Science,* vol. 2, no. 3, pp. 427-446, 2016. https://ijseas.com/volume2/v2i3/ijseas20160348.pdf

[11] S. H. Gawande, S. D. Wankhede, R. N. Yerrawar, V. J. Sonawane, and U. B. Ubarhande, "Design and Development of Shell & Tube Heat Exchanger for Beverage," *Modern Mechanical Engineering,* vol. 2, pp. 121-125, 2012. http://dx.doi.org/10.4236/mme.2012.24015

[12] F. H. Napitupulu, T. B. Sitorus, H. V. Sihombing, A. H. Siburian, and H. Siagian, "Design and fabrication of shell and tube heat exchanger with one pass shell and two pass tube as a water heater with hot sulfur water," *Journal of Physics: Conference Series,* vol. 2421, p. 012034, 2023. https://doi.org/10.1088/1742-6596/2421/1/012034

[13] J.-F. Zhang, Y.-L. He, and W.-Q. Tao, "A Design and Rating Method for Shell-and-Tube Heat Exchangers With Helical Baffles," *Journal of Heat Transfer,* vol. 132, pp. 1-8, 2010. https://doi.org/10.1115/1.4000457

[14] R. Mukherjee, "Effectively Design Shell-and-Tube Heat Exchangers," *Chemical Engineering Progress,* pp. 1-17, 1998. https://www.torr-engenharia.com.br/wp-content/uploads/2011/05/exchanger.pdf

[15] S. Kakaç, H. Liu, and A. Pramuanjaroenkij, *Heat Exchangers - Selection, Rating and Thermal Design*, 3rd ed. Boca Raton, USA: CRC Press, 2012.

[16] E. Cao, *Heat transfer in process engineering*. New York, USA: The McGraw-Hill Companies, Inc., 2010. https://dokumen.pub/heat-transfer-in-process-

Vol. 08 / Nº 01
e – ISSN: 3028-8533
ISSN – L: 3028-8533

engineering-1nbsped-0071624082-9780071624084.html
[17] R. Sinnott and G. Towler, *Chemical Engineering Design*, 6th ed. Oxford, UK: Butterworth-Heinemann, 2020. https://app.knovel.com/kn/resources/kpCEDE0001/toc
[18] R. Mukherjee, *Practical Thermal Design of Shell-and-Tube Heat Exchangers*. New York, USA: Begell House, Inc., 2004.
[19] Chemical Engineering. (2024) Economic Indicators. *Chemical Engineering Magazine*. 52.
[20] D. W. Green and M. Z. Southard, *Perry's Chemical Engineers' Handbook*, 9th ed. New York, U.S.A.: McGraw-Hill Education, 2019.

INQUIDE
Chemical Engineering & Development
Journal of Science and Engineering

Vol. 08 / Nº 01
e – ISSN: 3028-8533
ISSN – L: 3028-8533

INQUIDE
Ingeniería Química y Desarrollo

Production of Vienna Type Sausage from Squid Pulp (Dosidicus gigas).

Elaboration of Vienna-type Sausage from Jumbo squid pulp (Dosidicus gigas)

Richard Smith Gutierrez Huayra [1]*

Received: 08/02/2025 – Accepted: 10/16/2025 – Published: 01/01/2025

Research Articles [X] Review Articles [ ] Essay Articles [ ]

* Corresponding author.

Summary.
Squid (Dosidicus gigas) is an abundant marine resource of high nutritional value, with great potential to diversify the food industry through the development of innovative value-added products. The objective of the research was to analyze the feasibility of making a Vienna type sausage using squid pulp, optimizing its formulation and evaluating its sensory acceptance. We worked with three formulations that incorporated 5%, 8% and 10% starch. The technological process included conditioning, leaching, grinding, homogenization, stuffing, blanching, cooling and refrigeration. The preference evaluation was carried out with a panel of 30 judges not trained using the Friedman statistical test. Likewise, chemical, nutritional and microbiological analyses were carried out to determine both the nutritional value and the safety of the product. The formulation with 8% starch showed the best acceptance in the attributes of flavor, appearance and texture. The optimal processing conditions were: emulsification at 10 °C, cooking at 70 °C for 23 minutes and cooling at 2–4 °C for 5 minutes, with lower energy consumption compared to other formulations. Each 100 g of product provided 17.4 g of protein, 1.2 g of fat, 1.3 g of carbohydrates and 125 Kcal, with a healthier profile than the control sausage. Microbiological analyses confirmed the safety of the product, as low aerobic counts and absence of pathogens were recorded. In conclusion, the production of Vienna sausages from squid pulp is a viable alternative that provides nutritional, sensory and health benefits, contributing to the diversification of products derived from fishing.

Keywords.
Squid (*Dosidicus gigas*), Vienna sausage, Fishery products, Food safety, Value added.

Abstract.
The jumbo squid (*Dosidicus gigas*) is an abundant and nutritious marine resource with the potential to diversify the food industry through value-added products. The study aimed to evaluate the feasibility of producing a vienna-type sausage using jumbo squid pulp, optimizing its formulation and sensory acceptability. Three formulations with 5%, 8%, and 10% starch were developed. The process included conditioning, leaching, grinding, homogenization, stuffing, blanching, cooling, and refrigeration. Acceptability was evaluated by a panel of 30 untrained judges using the Friedman test. Chemical-nutritional and microbiological analyses were conducted to determine the product's nutritional value and safety. The formulation with 8% starch received the highest acceptance in flavor, appearance, and texture. The optimal processing parameters were: emulsification at 10 °C, cooking at 70 °C for 23 min, and cooling at 2–4 °C for 5 min, resulting in energy savings compared to other formulations. Per 100 g, the product contained 17.4 g protein, 1.2 g fat, 1.3 g carbohydrates, and 125 Kcal, with lower fat and calorie content than the control sausage. Microbiological analyses confirmed its safety, showing low aerobic counts and absence of pathogens. The production of Vienna-type sausage based on jumbo squid pulp proved viable, offering nutritional, sensory, and sanitary, advantages for the diversification of fishery products.

Keywords.
Jumbo squid (*Dosidicus gigas*), Vienna-type sausage, Fishery products, Food safety, Value–added.

1. Introduction

The growing global demand for high-quality, sustainable protein foods has driven research into unconventional sources and the holistic use of marine resources [1]. In this context, the giant squid (Dosidicus gigas) represents one of the most abundant cephalopod resources in the Eastern Pacific Ocean, with significant catch volumes that support important fisheries in countries such as Peru and Mexico [2]. Despite its abundance and high nutritional value, much of its technological potential remains underutilized, being mainly destined for export markets as a frozen product or in derivatives with low added value [3]. Squid pulp, characterised by its high protein and low fat content, presents an exceptional opportunity for the development of new value-added food products, such as functional meat sausages [4]. This work explores the feasibility of using the pulp of Dosidicus gigas as the main raw material in the production of Vienna sausages, a product of high demand and acceptance in the market.

1.1 The Potato (Dosidicus gigas)

1.1.1 Classification and description

Dosidicus gigas (d'Orbigny, 1835), commonly known as squid, giant cuttlefish or Humboldt squid, is a neritic-oceanic cephalopod mollusk belonging to the family Ommastrephidae [5]. Its complete taxonomic classification is as follows: Kingdom: Animalia, Phylum: Mollusca, Class: Cephalopoda, Order: Oegopsida, Family: Ommastrephidae, Genus: Dosidicus, Species: D. gigas [6]. It is a large invertebrate, being able to reach more than 1.5 meters in mantle length and 50 kg in weight, which makes it one of the largest cephalopods in the world [7].

[1] National University of Callao; rsgutierrezh@unacvirtual.edu.pe ; https://orcid.org/0009-0009-1786-4837 ; Lima – Peru.

INQUIDE
Chemical Engineering & Development
Journal of Science and Engineering
Vol. 08 / Nº 01
e – ISSN: 3028-8533
ISSN – L: 3028-8533
INQUIDE
Ingeniería Química y Desarrollo

Figure 1. Presence of Squid in the Pacific Ocean.
Source:[8].

1.1.1 Biology and Anatomy.

It is a pelagic organism that performs extensive daily vertical migrations, inhabiting the water column at depths that can exceed 800 meters during the day [7]. It is characterized by a short life cycle (1-2 years), extremely fast growth and high fecundity, which gives it great resilience as a fishery resource [9]. Their diet is very varied, including mesopelagic fish, crustaceans and other cephalopods [10]. Anatomically and technologically, the mantle is the portion of greatest interest for processing, representing the main source of edible muscle [4].

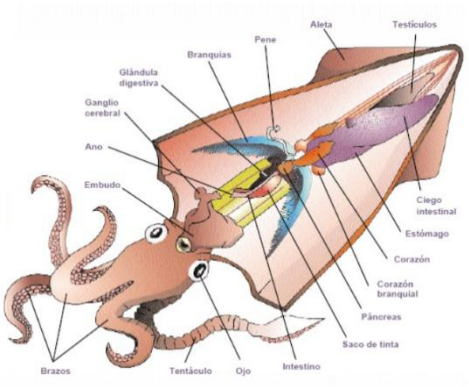

Figure 2. Anatomy of the squid.

1.1.2 Chemical, nutritional and mineral composition.

The pulp of Dosidicus gigas is recognized for its excellent nutritional value. Its average proximal composition consists of high humidity (~80%), high protein content of high biological value (16-20%), and low lipid content (<2%) [4, 10]. This composition makes it an ideal lean raw material for the formulation of healthy products. Squid protein is rich in essential amino acids and its mineral profile includes significant amounts of phosphorus, potassium, and selenium, although the content of heavy metals such as cadmium can be a concern in large organisms, requiring monitoring [10, 11].

1.1.3 Non-protein nitrogen.

A relevant biochemical characteristic in cephalopods is their high content of non-protein nitrogen compounds (NPNs), which they use for osmoregulation and buoyancy [12]. These compounds include free amino acids (taurine, arginine, proline), betaines, and, notably, ammonium chloride in the tissues of some deep-sea squid species [12, 13]. From a technological point of view, a high concentration of ammonium can generate bitter tastes and undesirable odors in the pulp, which makes it necessary to apply washing and conditioning treatments to ensure the sensory quality of the final product [13].

1.2 Lean muscle proteins.

The technological functionality of squid pulp for the production of emulsified sausages lies in the ability of its proteins to form gels and stabilise emulsions. Muscle proteins are classified, according to their solubility, into three main fractions [14].

1.2.1 Myofibrillar proteins.

They constitute the most abundant fraction (65-75% of the total protein) and important from a functional point of view [13, 14]. They include the contractile proteins actin and myosin. They are soluble in salt solutions of high ionic strength (≥0.5 M NaCl) [15]. Myosin is primarily responsible for heat-induced gelation, forming a three-dimensional matrix that traps water and fat, which defines the texture, juiciness, and cohesiveness of sausages [16].

1.2.2 Sarcoplasmic proteins.

They account for 20-30% of the total protein and are soluble in water or saline solutions of low ionic strength [13]. This fraction includes enzymes and myoglobin (in species that possess it). In the case of surimi and similar products, they are often removed by washing, as they can make it difficult for a strong gel to form and affect the color and flavor [17].

1.2.3 Stromal proteins.

They make up connective tissue and represent a minority fraction in the muscle of fish and cephalopods (2-5%) (14). They mainly include collagen. The low collagen content and its high thermolability compared to that of mammals contribute to the tender texture of squid meat, but its role in the emulsion structure is limited [18].

2. Research design and experimental methodology for the production of Squid Sausage.

INQUIDE
Chemical Engineering & Development
Journal of Science and Engineering
Vol. 08 / Nº 01
e – ISSN: 3028-8533
ISSN – L: 3028-8533

The study on the production of Vienna-type sausage from the pulp of (*Dosidicus gigas)* employed a specific research design and a detailed experimental methodology, which included sensory and microbiological analyses, and the application of the Friedman test.

2.1 Research design.
The study was developed under an experimental approach, which consisted of manipulating the independent variable (percentage of starch in the formulation) in order to evaluate its effect on dependent variables such as sensory characteristics, nutritional profile and microbiological quality of the squid sausage. This design allowed the establishment of the processing parameters and the contrast of the results obtained in each formulation.

2.2 Experimental methodology.
The research combined practical tests and laboratory analysis. The sausages were made at the MICROBAC – Laboratorios E.I.R.L. facilities., while the sensory evaluation was carried out at the Faculty of Fisheries and Food Engineering of the National University of San Luis Gonzaga (UNICA).

3. Materials and methods.

3.1 Materials, equipment, instruments and reagents.

3.1.1 Materials.
The process used a steel pot (5lt. capacity) (LUISSANT), canvas sieve (60x30cm), plastic strainers, cutting board (45x30 cm), Teflon pan (24 cm diameter) (UNCO), wick, stainless steel knives and disposable cups (7 oz.).

3.1.2 Equipment.
The process used a semi-industrial pot (SURGE), a manual press, a freezer (COLDEX) and a meat grinder (HENKEL).

3.1.3 Instruments.
The measuring instruments included a pH meter (POCKET), a 150°C thermometer (OMROM), a hygrometric balance, an analytical balance, and a commercial balance.

3.1.4 Reagents.
Lactic acid and baking soda were used as reagents.

3.2 Technological process of squid sausage.

Reception of raw materials.
The squid pulp was acquired in the Pisco fishing terminal market and the inputs respectively in the market N°2 - Pisco.

Conditioning.
The squid coat was skinned, the cartilage removed, washed and frozen at 4-6 °C [8]. Due to the acidic and bitter taste of the *squid*, which comes from the non-protein nitrogenous compounds (NNPs), a separation process was carried out that involved four washes.

Chopped.
The squid was cut into cubes to facilitate grinding and obtain a surimi-type paste.

Grinding.
Once the squid has been chopped, it is taken to the grinding machine to produce the paste, which is received in a container at the exit of the grinder.

Leaching process (preparation of surimi).
This process followed the acid-saline leaching methodology in four stages:

First wash.
The ground *squid* was placed in a solution of 0.5% lactic acid and 0.15% salt (2:1 ratio between solution and meat) for 10 minutes under constant manual pressure, keeping the temperature of the solution below 10 °C, and then sifting it.

Second and Third Wash.
These washes were carried out only with cold water (below 10 °C) for 10 minutes, in constant manual pressing and subsequent sieving for the next wash.

Laundry room.
Neutralization was achieved using a 0.1% sodium bicarbonate solution (below 10 °C) for 10 minutes in constant manual pressing, followed by sieving and pressing on a tocuyo cloth.

Frozen.
The resulting surimi paste was frozen in an extended form.

Heavy.
The conditioned *squid* pulp , ingredients and additives were weighed according to calculations to obtain 500 g of finished product.

Table 1. Veal sausage control formulation.

Ingredients	grams (g)
Beef	350
Pork fat	150
Ice	250
Cornstarch	50
Phosphate	2.5
Salt of cure	2.0
Salt	15
Garlic	2
Pepper	1
Cumin	1
Ajinomoto	2
Nutmeg	0.4
Hot Dog Flavor	2
Smoke Flavor	0.2 ml
Strawberry red dye	0.1 ml

Table 2. Formulation of Squid Sausage (*Dosidicus gigas*)

Ingredients	Quantity (g) 5% - Starch	Quantity (g) 8% - Starch	Quantity (g) 10% - Starch
Meat	560	560	560
year	14	14	14

Pepper	1.1	1.1	1.1
Cumin	1.1	1.1	1.1
Ajinomoto	2.2	2.2	2.2
Nutmeg	0.6	0.6	0.6
Flavoring	2.2	2.2	2.2
Coloring	-	-	-
Ice	140	140	140
Starch	28	44.8	56

Homogenization.
The dry ingredients (seasonings) were homogenized in a polyethylene bag.

Mixed.
The squid paste (surimi) was added to a processor, followed by the dry ingredients, then the crushed ice, and lastly, the starch percentage.

Embedded.
The homogeneous mixture was placed in a stuffing machine and the cellulose casing was filled under pressure.

Tied up.
After the cellulose casing was stuffed, they were tied into individual units of standard size.

Blanching.
The sausages were blanched for 20 min, making sure that they were completely submerged in water and that the water temperature did not exceed 80 °C.

Cooling.
The sausages were cooled for 5 min in water at over 10°C.

Refrigeration.
The product was stored at refrigeration temperature (4 – 8 °C) for preservation.

See Annex 1.- Flow diagram for obtaining squid paste (surimi).
Source: Authors.

See Annex 2.- Fig. 4. Flow chart for obtaining Squid Sausage.
Source: Authors.

4. Analysis and Interpretation of Results.

4.1 Friedman's test for sensory evaluation.

To determine the acceptability of the squid sausages, Friedman's non-parametric test was applied, which allowed identifying whether there were significant differences in the judges' preferences based on the percentage of starch incorporated in the formulations.

Three formulations were evaluated:
-Sausage with 5% starch.
-Sausage with 8% starch.
-Sausage with 10% starch.

Evaluators.
The evaluation involved a panel of 30 untrained judges, ranging in age from 20 to 25.

Procedure.
Acceptability was measured using a numerical scale, in which judges ranked samples from 1 (most preferred) to 3 (least preferred) based on smell, aroma, and taste.

4.2 Hypothesis Test.

The null hypothesis (Ho) stated that there were no significant differences in preferences between samples, while the alternative hypothesis (Ha) stated that at least one sample had a different preference. The significance level (α) was set at 0.05.

4.3 Friedman's nonparametric test.

The results of the extended reference test are taken for the following sensory characteristics:

Table. 3. Results of the extended preference test. "Flavor."

Judges/Evaluators	**Sample codes for "Squid Sausage"**		
N°	124	242	375
1	3	3	3
2	2	2	3
3	2	2	2
4	3	1	1
5	1	1	1
6	3	1	3
7	2	2	1
8	2	1	2
9	2	1	1
10	2	1	1
11	1	1	2
12	3	2	2
13	3	1	3
14	2	3	1
15	2	2	1
16	1	1	2
17	2	1	1
18	2	1	2
19	3	2	2
20	3	2	1
21	3	1	2
22	2	1	3
23	2	1	1
24	3	2	2
25	3	1	1
26	3	1	2
27	3	1	1
28	2	1	2
29	3	2	1
30	2	1	1
Total	70	43	51

Code Assignment:
124 (X): 5% starch.
242 (Y): 8% starch.
375 (Z): 10% starch.

Table 4. Results of the extended preference test. "Appearance".

Judges/Evaluators	**Sample codes for "Squid Sausage"**

Vol. 08 / Nº 01
e – ISSN: 3028-8533
ISSN – L: 3028-8533

No.	100	200	300
1	1	2	2
2	2	1	2
3	1	2	3
4	1	1	3
5	1	2	2
6	1	2	3
7	2	3	3
8	1	3	3
9	1	1	3
10	2	2	2
11	1	1	3
12	1	2	2
13	1	3	3
14	1	2	2
15	2	1	3
16	1	3	2
17	2	2	2
18	1	3	2
19	1	1	3
20	1	1	3
21	2	1	3
22	1	3	3
23	2	2	2
24	2	1	3
25	2	2	2
26	1	2	3
27	2	2	3
28	1	2	3
29	1	1	3
30	1	2	3
Total	**40**	**56**	**79**

Code Assignment:
100 (X): 8% starch.
200 (Y): 10% starch.
300 (Z): 5% starch.

Table 5. Results of the extended preference test. "Texture".

Judges/Evaluators	Sample codes for "Squid Sausage"		
No.	**114**	**224**	**305**
1	3	2	2
2	2	2	2
3	3	2	2
4	2	3	2
5	2	3	2
6	2	3	1
7	2	2	2
8	2	3	2
9	2	2	2
10	2	3	1
11	3	2	2
12	2	3	1
13	2	2	2
14	2	2	1
15	3	2	2
16	3	3	2
17	2	3	2
18	2	3	2
19	2	3	2
20	2	3	1
21	3	2	1
22	2	3	2
23	3	2	1
24	2	3	2
25	3	2	1
26	2	3	2
27	3	3	2
28	2	3	1
29	2	2	2
30	2	3	1
Total	69	77	50

Code Assignment:
114 (X): 10% starch.
224 (Y): 5% starch.
305 (Z): 8% starch.

Hypothesis:
Ho: There are no significant differences in sample preferences.
Ha: At least one of the samples has a different preference with respect to the others.

Table 6. Preference test results on "Appearance, taste, texture of squid sausage".

Sample	Appearance	Taste	Texture
5% Starch	2.33±0.66b	2.63±0.49b	2.57±0.50b
8% Starch	1.43±0.63a	1.33±0.48a	1.66±0.48a
10% Starch	1.70±0.75a	1.87±0.73a	2.30±0.47b

(XLSTAT – Statistical Software for Excel)

A greater preference was reported for sausages with 8% starch substitution, followed by those with 10% and below for inclusion at 5%. This according to the consumer's perception according to appearance, flavor and texture, important attributes in this category of blanched sausages.

4.4 Statistical results and decision.

The calculated Friedman statistic (X^2C) was compared to the tabular critical value (X^2T). In the three attributes evaluated (taste, appearance and texture), the calculated values exceeded the critical value, which led to the rejection of the null hypothesis. Therefore, the existence of significant differences in the preferences of judges was confirmed.

This finding supports that the optimal formulation was 8% starch, which presented the lowest sum of ranges, reflecting the highest preference in the evaluation scale.

5. Result of the chemical-nutritional analysis.

This analysis provided information on the macronutrient and vitamin content of *squid* sausage, and the optimal formulation showed specific values for each 100 g edible serving.

Table 7. Result of nutritional chemical analysis of squid sausage/ 100 g. edible portion.

Description	Sausage Control	Squid Sausage
Energy (Kcal)	351	125
Water (g)	48,5	49,2
Protein (g)	14,8	17,4
Fat (g)	29,5	1,2
Carbohydrates (g)	1,5	1,2
Vitam. A (mg)	-	-
Tiamina (mg)	0,03	0,03
Riboflavin (mg)	0,07	0,07
Niacin (mg)	3,7	3,7

Vitam. C (mg)	-	-

Source: Microbac Laboratories E.I.R.L.

6. Result of the microbiological analysis.

Microbiological testing was performed on the optimal formulation of *squid* sausages to ensure that it met acceptable safety parameters. The results were compared with the Sanitary Standard that establishes the microbiological criteria for food safety.

Table 8. Result of microbiological analysis of squid sausage.

Sample	Total aerobic count Ufc/g	Coliforms	Staphylococus aureus Ufc/g	Salmonella 25 g.
Squid Sausage	1,200	0	0	Absence

Source: Microbac Laboratories E.I.R.L.
Reference – Sanitary Standard that establishes the microbiological criteria of sanitary quality and safety for food.
NTS No. 071 – MINSA/DIGESA – V.01 Ministry of Health 2010.

7. Discussion.

The present research demonstrates the technical and sensory feasibility of making Vienna sausages using giant squid pulp (Dosidicus gigas), positioning this marine resource as a promising raw material for the development of functional meat products with added value. The results obtained are aligned with current trends that seek to diversify protein sources and offer healthier alternatives to the consumer [19, 20].

The central finding of the study is the sensory superiority of the formulation with 8% starch, which obtained the greatest acceptance in taste, appearance and texture. This result suggests a crucial technological break-even point. On the one hand, a starch concentration of 5% may have been insufficient to form a gel network fully integrated with the protein matrix, affecting cohesiveness. On the other hand, 10% starch may have resulted in an excessively firm or rubbery texture, a phenomenon documented in surimi products with high concentrations of this hydrocolloid [21, 22]. The starch, when gelatinized during cooking (70 °C), interacts with the myofibrillar proteins of the squid, forming a mixed and stable gel structure that retains water and fat, improving both texture and juiciness [23]. The mechanism involves the formation of a three-dimensional network where the swollen starch granules are embedded in the protein matrix, reinforcing the overall structure of the gel [24].

From a nutritional point of view, the optimised squid sausage has a noticeably healthier profile than conventional commercial sausages, with a high protein content (17.4 g/100 g) and a low intake of fat (1.2 g/100 g) and calories (125 Kcal/100 g). This profile is consistent with the inherent muscle composition of D. gigas and underscores its potential for the formulation of functional foods aimed at health-conscious consumers [25]. The substitution of animal fats for lean squid protein not only reduces the caloric content, but also modifies the fatty acid profile, increasing the proportion of beneficial polyunsaturated fats such as EPA and DHA, characteristic of marine products [26].

The textural quality of the final product depends fundamentally on the gelling capacity of the myofibrillar proteins of the squid (myosin and actin). Heat treatment at 70°C is key to denaturing these proteins and allowing them to form a cohesive three-dimensional network [27]. Recent studies on D. gigas proteins confirm that their gelling is a complex process that can be modulated by additives. Niu et al. [28] demonstrated that the addition of other proteins, such as egg white protein, can inhibit unwanted self-aggregation of myosin molecules and promote a more orderly and stronger gel network. Analogously, the starch in our formulation not only acts as a filler agent, but as a functional ingredient that positively modifies the rheology of the system, improving the water-holding capacity and firmness of the final gel [24].

The safety of the product, confirmed by the low microbiological counts and the absence of pathogens, is a result of utmost importance. This success is attributed to the quality of the raw material, good manufacturing practices and, crucially, the leaching process, which reduces the initial microbial load in addition to removing non-protein nitrogen (NNP) compounds that cause undesirable tastes [29]. Microbiological stability and shelf life extension are significant challenges in squid products due to their high water activity and enzyme potential. Recent research has shown that D. gigas protein hydrolysates possess intrinsic antioxidant and antimicrobial properties, capable of extending the shelf life of squid sausages by up to 95% by inhibiting microbial growth and oxidation [30]. Although hydrolysates were not used in our study, the positive microbiological results provide a solid basis for future innovations in this line.

In conclusion, the discussion of the results, contrasted with recent scientific literature, confirms that squid sausage is a viable and nutritionally superior alternative. Optimizing starch concentration is key to achieving an acceptable texture, while controlling the process, from leaching to cooking, ensures product safety and quality. This work provides concrete evidence for the valorization of Dosidicus gigas, an abundant resource that can contribute significantly to food safety and innovation in the seafood industry.

8. Conclusions.

The present study establishes the optimal processing parameters for the production of Vienna sausage from squid pulp (Dosidicus gigas), determining that the concentration of 8% of potato starch constitutes the technological equilibrium point that maximizes the sensory acceptability and physicochemical properties of the product. This optimized formulation, processed by leaching (three washes with cold water), emulsification with vegetable fat and

cooking at 70 °C for 30 minutes, generates a functional meat product with high protein content (17.4 g/100 g), low fat intake (1.2 g/100 g) and low caloric value (125 Kcal/100 g), complying with the microbiological standards established by Peruvian regulations.

This concrete contribution positions squid as a viable and nutritionally superior raw material for the emulsified meat products industry, contributing to the diversification of marine protein sources and the valorization of abundant fishery resources in the Eastern Pacific.

The results obtained demonstrate that the synergistic interaction between the myofibrillar proteins of the squid and the starch during heat treatment is essential for the formation of a cohesive and stable gel matrix, which gives the final product the desired textural and sensory characteristics. The water retention capacity, firmness and juiciness of the optimized product show the technological potential of this species for applications in the food industry, overcoming the limitations traditionally associated with cephalopod processing. These findings provide a solid scientific basis for technology transfer to the productive sector, facilitating the implementation of standardized and reproducible processes on an industrial scale.

It is recommended that future research be focused on three priority directions: first, to carry out shelf life studies under different conditions of refrigerated storage and in a modified atmosphere to determine the microbiological, physicochemical and sensory stability of the product during its commercialization; second, to optimize the flavor profile by evaluating different combinations of spices, seasonings and masking agents that minimize possible residual notes characteristic of squid, thus improving consumer acceptance; and third, to develop scale-up studies at the pilot and industrial level that validate the reproducibility of the process, evaluate the economic viability of mass production and establish the critical quality control parameters.

Additionally, it would be valuable to explore the incorporation of squid protein hydrolysates with antioxidant and antimicrobial properties, as well as the formulation of analogous products with different nutritional profiles aimed at specific market segments, such as sports consumers, older adults or people with dietary restrictions.

9. Author Contributions (Contributor Roles Taxonomy (CRediT))

1. Conceptualization: Richard Smith Gutierrez Huayra.
2. Data curation: Richard Smith Gutierrez Huayra.
3. Formal analysis: Richard Smith Gutierrez Huayra.
4. Acquisition of funds: N/A.
5. Research: Richard Smith Gutierrez Huayra.
6. Methodology: Richard Smith Gutierrez Huayra.
7. Project management: Richard Smith Gutierrez Huayra.
8. Resources: Richard Smith Gutierrez Huayra.
9. Software: Richard Smith Gutierrez Huayra.
10. Supervision: Richard Smith Gutierrez Huayra.
11. Validation: Richard Smith Gutierrez Huayra.
12. Visualization: Richard Smith Gutierrez Huayra.
13. Writing - original draft: Richard Smith Gutierrez Huayra.
14. Writing - revision and editing: Richard Smith Gutierrez Huayra.

10. References.

[1] Lynch, H., Johnston, C., & Wharton, C. (2018). Plant-based diets: Considerations for environmental impact, protein quality, and exercise performance. Nutrients, 10(12), 1841. https://doi.org/10.3390/nu10121841

[2] Ibáñez CM, Cubillos LA, Tafur R, Argüelles J, Yamashiro C, Poulin E. Genetic diversity and demographic history of Dosidicus gigas (Cephalopoda: Ommastrephidae) in the Humboldt Current System. Mar Ecol Prog Ser [Internet]. 2011; 431:163–71. Available from: http://dx.doi.org/10.3354/meps09133

[3] Mazzeo MF, Siciliano RA. Proteomics for the authentication of fish species. J Proteomics [Internet]. 2016; 147:119–24. Available from: http://dx.doi.org/10.1016/j.jprot.2016.03.007

[4] Ramírez-Suárez JC, Pacheco-Aguilar R, Scheuren-Acevedo SM, García-Sánchez G, Carvallo-Ruiz G, Lugo-Sánchez ME, et al. Microbiological and physicochemical quality changes in frankfurters made from jumbo squid (D osidicus gigas) mantle muscle in the presence and absence of a natural antimicrobial agent: Quality changes in squid frankfurter. J Food Saf [Internet]. 2015; 35(4):473–81. Available from: http://dx.doi.org/10.1111/jfs.12197

[5] Jereb P, Roper CFE, editors. Cephalopods of the world. An annotated and illustrated catalogue of cephalopod species known to date. Volume 2. Myopsid and Oegopsid Squids. Rome: FAO; 2010.

[6] WoRMS Editorial Board. World Register of Marine Species. Dosidicus gigas d'Orbigny, 1835. 2023. [Accessed 1 Oct 2025]. Available at: https://www.marinespecies.org/aphia.php?p=taxdetails&id=220325.

[7] Camarillo-Coop S, Salinas-Zavala CA, Lavaniegos BE, Markaida U. Food in early life stages of Dosidicus gigas (Cephalopoda: Ommastrephidae) from the Gulf of California, Mexico. J Mar Biol Assoc U K [Internet]. 2013; 93(7):1903–10. Available from: http://dx.doi.org/10.1017/s0025315413000398

[8] Tennesen M. March of the Red Devil. New Sci [Internet]. 2015; 227(3038):32–5. Available from: http://dx.doi.org/10.1016/s0262-4079(15)31176-3

[9] Staaf DJ, Camarillo-Coop S, Haddock SHD, Nyack AC, Payne J, Salinas-Zavala CA, et al. Natural egg mass deposition by the Humboldt squid (Dosidicus gigas) in the Gulf of California and characteristics of hatchlings and paralarvae. J Mar Biol Assoc U K [Internet]. 2008; 88(4):759–70. Available from: http://dx.doi.org/10.1017/s0025315408001422

[10] Liu A, Liu G, Huang C, Shen L, Li C, Liu Y, et al. The bacterial diversity of ripened Guang'yuan Suancai and in vitro evaluation of potential probiotic lactic acid bacteria isolated from Suancai. Lebenson Wiss Technol [Internet]. 2017; 85:175–80. Available from: http://dx.doi.org/10.1016/j.lwt.2017.07.021

[11] Rico A, Zhao W, Gillissen F, Lürling M, Van den Brink PJ. Effects of temperature, genetic variation and species competition on the sensitivity of algae populations to the antibiotic enrofloxacin. Ecotoxicol Environ Saf [Internet]. 2018; 148:228–36. Available from: http://dx.doi.org/10.1016/j.ecoenv.2017.10.010

[12] Fernández Lucas F. Technological improvement of the industrial manufacture of cooked and frozen squid tentacles ("Dosidicus gigas") [Internet]. University of Murcia. 2023. Available from: https://digitum.um.es/handle/10201/136724

[13] Seibel BA, Goffredi SK, Thuesen EV, Childress JJ, Robison BH. Ammonium content and buoyancy in midwater cephalopods. J Exp Mar Bio Ecol [Internet]. 2004; 313(2):375–87. Available from: http://dx.doi.org/10.1016/j.jembe.2004.08.015

[14] Huss HH. Quality and quality changes in fresh fish. Rome: FAO; 1995. FAO Fisheries Technical Paper No. 348.
[15] Niu F, Ma S, Zhang X, Ritzoulis C, Chen Y, Pan W. The influence of KCl concentration on the gelation of myofibrillar protein giant squid (Dosidicus gigas) due to molecular conformation change. Front Nutr [Internet]. 2022;9:1082464. Available from: http://dx.doi.org/10.3389/fnut.2022.1082464
[16] Niu F, Li X, Lin C, Hu X, Zhang B, Pan W. The mechanism of egg white protein to enhance the thermal gel properties of giant squid (Dosidicus gigas) surimi. Food Chem [Internet]. 2025; 469(142601):142601. Available from: http://dx.doi.org/10.1016/j.foodchem.2024.142601
[17] Yin T, Park JW. Comprehensive review: by-products from surimi production and better utilization. Food Sci Biotechnol [Internet]. 2023; 32(14):1957–80. Available from: http://dx.doi.org/10.1007/s10068-023-01360-8
[18] Gómez-Guillén MC, Giménez B, López-Caballero ME, Montero MP. Functional and bioactive properties of collagen and gelatin from alternative sources: A review. Food Hydrocoll [Internet]. 2011; 25(8):1813–27. Available from: http://dx.doi.org/10.1016/j.foodhyd.2011.02.007
[19] Lee S, Jo K, Jeong S-K-C, Jeon H, Choi Y-S, Jung S. Recent strategies for improving the quality of meat products. J Anim Sci Technol [Internet]. 2023; 65(5):895–911. Available from: http://dx.doi.org/10.5187/jast.2023.e94
[20] Boukid F, Baune M-C, Gagaoua M, Castellari M. Seafood alternatives: assessing the nutritional profile of products sold in the global market. Eur Food Res Technol [Internet]. 2022; 248(7):1777–86. Available from: http://dx.doi.org/10.1007/s00217-022-04004-z
[21] Amiza MA, Ng SC. Effects of surimi-to-silver catfish ratio and potato starch concentration on the properties of fish sausage. J Aquat Food Prod Technol [Internet]. 2015; 24(3):213–26. Available from: http://dx.doi.org/10.1080/10498850.2013.766293
[22] Mi H, Wang C, Su Q, Li X, Yi S, Li J. The effect of modified starches on the gel properties and protein conformation of Nemipterus virgatus surimi. J Texture Stud [Internet]. 019; 50(6):571–81. Available from: http://dx.doi.org/10.1111/jtxs.12466
[23] Jiang X, Chen Q, Xiao N, Du Y, Feng Q, Shi W. Changes in gel structure and chemical interactions of Hypophthalmichthys molitrix surimi gels: Effect of setting process and different starch addition. Foods [Internet]. 2021; 11(1):9. Available from: http://dx.doi.org/10.3390/foods11010009
[24] Gong Y, Xiao S, Yao Z, Deng H, Chen X, Yang T. Factors and modification techniques enhancing starch gel structure and their applications in foods:A review. Food Chem X [Internet]. 2024; 24(102045):102045. Available from: http://dx.doi.org/10.1016/j.fochx.2024.102045
[25] Kang S-I, Kim J-S, Park S-Y, Cho H-J, Jang M-S, Oh J-Y, et al. Development and quality attributes of paste sausage supplemented with common squid (Todarodes pacificus) tailored for the elderly. Appl Sci (Basel) [Internet]. 2023; 13(19):10735. Available from: http://dx.doi.org/10.3390/app131910735
[26] Hu G, Zhao Z, Liu B, Lin D, Liang J, Fang Z, et al. Fatty acid profile of jumbo squid (Dosidicus gigas) off the Peruvian exclusive economic zone: Revealing the variability of feeding strategies. G [Internet]. 2022; 7(5):221. Available from: http://dx.doi.org/10.3390/fishes7050221
[27] González-González BG, Lugo-Sánchez ME, Márquez-Ríos E, Ramírez-Suárez JC, Gámez-Corrales R, Paredes-Quijada GT, et al. Properties of gels formed from jumbo squid (Dosidicus gigas) mantle muscle under heat and acid treatment: Rheological and calorimetric analysis. ACS Food Sci Technol [Internet]. 2024; 4(12):2917–24. Available from: http://dx.doi.org/10.1021/acsfoodscitech.4c00481
[28] Niu F, Lin C, Liao H, Zhang B, Zhang J, Pan W. Formation mechanism of giant squid myofibrillar protein aggregates induced by egg white protein during heat treatment. Food Hydrocoll [Internet]. 2025; 158(110573):110573. Available from: http://dx.doi.org/10.1016/j.foodhyd.2024.110573
[29] Mu H, Weng P, Wu Z. Effect of Inoculation with Lacticaseibacillus casei and Staphylococcus carnosus on the Quality of Squid (Dosidicus gigas) Surimi Sausage. Fermentation [Internet]. 2023; 9(9):794. Available from: http://dx.doi.org/10.3390/fermentation9090794
[30] López-Medina FA, Dublán-García O, Morachis-Valdez AG, Saucedo-Vence K, López-García G, Díaz-Bandera D, et al. Biopolymeric hydrolysates from Dosidicus gigas: Functional applications and shelf-life extension in squid sausages. Polymers (Basel) [Internet]. 2025; 17(7):839. Available from: http://dx.doi.org/10.3390/polym17070839

INQUIDE
Chemical Engineering & Development
Journal of Science and Engineering
Vol. 08 / Nº 01
e – ISSN: 3028-8533
ISSN – L: 3028-8533

Appendix 1.- Flow diagram for obtaining squid paste (surimi).

FLOW PROCESS DIAGRAM					
CONCEPTO DIAGRAMADO: Pasta (Surimi)				**DIAGRAM NO.: 1**	
METHOD DIAGRAM: Current				**DATE:**	
DIAGRAM BEGINS: Selection of squid meat					
UNIT TIME (Min.)	**SYMBOL**	**DESCRIPTION OF THE PROCESS**	**UNIT TIME (Min.)**	**SYMBOL**	**DESCRIPTION OF THE PROCESS**
5	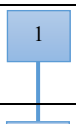	Inspection of the squid mantle.	**10**		3° Washing the squid paste, it is done only with cold water at a temperature below 10 °C. In constant manual pressing
4		The skin and cartilage are removed from the squid mantle.	**10**		4° Wash the squid paste in a solution of 0.1% baking soda, at a temperature below 10 ºC.
2		The squid mantle is washed.	**3**		A quality control is carried out on the finished product.
4		The squid mantle is frozen at 4 - 6 °C.	2		The squid paste is weighed on an electronic scale.
2		Slicing of the squid mantle.	30		Freezes from 0 to -4 °C.
6		The squid meat is ground in a meat mill.			
			ABSTRACT		
7		There is a delay after grinding.	**TIME**	**NUMBER**	**EVENTS**
			63	8	Operations
20		1° Wash the paste in a solution of 0.5% lactic acid and 0.15% salt, at a temperature below 10°C.	6	2	Inspections
			3	1	Combined activity
5		2° Washing the pasta is done only with cold water at a temperature below 10 °C. In constant manual pressing.	70	2	Storage
			2	1	Delays

INQUIDE
Chemical Engineering & Development
Journal of Science and Engineering
Vol. 08 / Nº 01
e – ISSN: 3028-8533
ISSN – L: 3028-8533

Annex 2. Flow chart for obtaining Squid Sausage.

Flow Process Diagram					
Concept Diagrammed: Sausage				**Diagram No.: 2**	
Method Diagram: Current				**Date:**	
Diagram Begins: Meat Selection					
Unit Time (Min.)	**Symbol**	**Description of the process**	**Unit Time (Min.)**	**Symbol**	**Description of the process**
5		Inspection of pota paste (surimi).	**4**		A quality control is carried out on the finished product.
4		The squid paste and ingredients are weighed on an electronic scale.	**5**		It is refrigerated from 4 – 8 °C.
2		The dry ingredients are homogenized.	**2**		It is expected to continue with the analyses.
4		The meat is ground in the processor.			
2		There is a delay after grinding.			
6		Emulsion, the required ingredients are added.			
			ABSTRACT		
7		The paste is stuffed into a manual stuffer.	**TIME**	**NUMBER**	**EVENTS**
			44	6	Operations
20		Blanch for 20 minutes at a temperature of 80 °C.	9	2	Inspections
			4	1	Combined activity
5		Let it cool for 5 minutes at more than 10 °C.	5	1	Storage
			4	2	Delays

INQUIDE
Chemical Engineering & Development
Journal of Science and Engineering

Vol. 08 / Nº 01
e – ISSN: 3028-8533
ISSN – L: 3028-8533

INQUIDE
Ingeniería Química y Desarrollo

Time series modeling of secondary school enrollment in Ecuador: a Box–Jenkins analysis (1971–2023).

Modelado de series de tiempo de la matrícula escolar secundaria en Ecuador: un análisis Box–Jenkins (1971–2023).

Edwin Haymacaña Moreno[1]; Leonor Alejandrina Zapata Aspiazu;[2] Francisco Javier Duque-Aldaz [3] ; Félix Genaro Cabezas García [4] ; Raúl Alfredo Sánchez Ancajima [5]

Received: 09/28/2025 – Accepted: 12/02/2025 – Published: 01/01/2025

Research Articles [X] Review Articles [ ] Essay Articles [ ]

* Corresponding author.

Abstract.
School enrollment analysis constituted a key indicator to evaluate coverage and equity in national education systems. The objective of this study was to model secondary school enrollment in Ecuador during 1971–2023 using time series techniques. Official national and international data were employed to construct an annual net enrollment series. The methodological procedure included descriptive analysis, stationarity tests (ADF and KPSS), first-order differencing, identification and estimation of candidate models through the Box–Jenkins approach, optimal selection with auto.arima, residual validation via Ljung–Box tests, out-of-sample error metrics (MAE, RMSE, MAPE), and forecasts for 5–10 years. All processing was performed in R Studio with specialized time series modeling packages. The results showed that after first-order differencing, the series achieved stationarity. The selected model adequately explained enrollment dynamics, with residuals consistent with white noise and without significant autocorrelations. Validation metrics indicated good predictive accuracy, with low mean absolute and percentage errors. Projections suggested a moderate and sustained growth trend in enrollment, though with signs of stabilization in the longer horizon. This study demonstrated the usefulness of Box–Jenkins models for analyzing educational phenomena, providing quantitative evidence for public policy formulation and recommending the expansion of more complete historical datasets in future research.

Keywords.
Time Series, ARIMA, Box–Jenkins, School Enrollment, Secondary Education, Ecuador, Educational Forecasting.

Resumen.
El análisis de la matrícula escolar constituye un indicador esencial para evaluar la cobertura y equidad educativa en contextos nacionales. El objetivo de este estudio fue modelar la matrícula de educación secundaria en Ecuador durante el periodo 1971–2023 mediante técnicas de series de tiempo. Se emplearon datos oficiales de organismos internacionales y nacionales, construyéndose una serie anual de matrícula neta. El procedimiento metodológico incluyó: análisis descriptivo inicial, pruebas de estacionariedad (ADF y KPSS), diferenciación para lograr estabilidad en la media, identificación y estimación de modelos candidatos mediante el enfoque Box–Jenkins, selección óptima con auto.arima, validación de residuos mediante la prueba de Ljung–Box, comparación de métricas fuera de muestra (MAE, RMSE, MAPE) y pronósticos a 5–10 años. Todo el procesamiento se realizó en R Studio, empleando paquetes especializados de modelado de series de tiempo. Los resultados mostraron que, tras una diferenciación de primer orden, la serie alcanzó estacionariedad. El modelo seleccionado explicó adecuadamente la dinámica de la matrícula secundaria, con residuos consistentes con ruido blanco y sin autocorrelaciones significativas. Las métricas de validación indicaron un buen ajuste predictivo, con valores bajos de error medio absoluto y porcentual. Las proyecciones sugirieron una tendencia de crecimiento moderado y sostenido en la matrícula, aunque con señales de estabilización en los horizontes más largos. Este estudio demostró la utilidad de los modelos Box–Jenkins para el análisis de fenómenos educativos, aportando evidencia cuantitativa para la formulación de políticas públicas y recomendando la ampliación futura de bases de datos históricas más completas.

Palabras clave.
Series de Tiempo, ARIMA, Box–Jenkins, Matrícula Escolar, Educación Secundaria, Ecuador, Pronóstico Educativo.

1.- Introduction

The analysis of the Ecuadorian education system has gained special relevance in recent decades due to the challenges related to the coverage, equity, and quality of secondary education. In particular, school enrollment is a key indicator for assessing student access and retention, as well as for identifying structural inequalities in the system. Understanding the dynamics of enrolment over time not only allows us to detect historical patterns, but also to anticipate trends that are fundamental for the formulation of sustainable public policies aimed at meeting Sustainable Development Goal 4 (SDG4), which seeks to guarantee inclusive, equitable and quality education.(Simonino y otros, 2025)

In the scientific literature, time series models have proven to be robust tools for the analysis and prediction of socioeconomic and educational phenomena. Within these approaches, the Box–Jenkins method. It stands out for its

[1] Bolivarian University Higher Institute of Technology; erhaymacana@itb.edu.ec; https://orcid.org/0000-0002-8708-3894; Guayaquil; Ecuador.
[2] Technical University of Babahoyo; lzapata@utb.edu.ec; https://orcid.org/0009-0003-1497-2273 ; Babahoyo; Ecuador.
[3] University of Guayaquil; franscico.duquea@ug.edu.ec; https://orcid.org/0000-0001-9533-1635 ; Guayaquil; Ecuador.
[4] Independent Researcher; genaro_cabezas@hotmail.com ; https://orcid.org/0000-0003-3595-3584; Hamilton, ON, Canada.
[5] National University of Tumbes; rsanchez@untumbes.edu.pe ; https://orcid.org/0000-0003-3341-7382 ; Tumbes, Peru.

Vol. 08 / Nº 01
e – ISSN: 3028-8533
ISSN – L: 3028-8533

ability to model temporal dependencies using autoregressive (AR), moving average (MA) and their seasonal extensions (SARIMA) structures. These models have been successfully applied in contexts of forecasting macroeconomic and climatic variables and, more recently, in the analysis of educational indicators. However, in the case of Ecuador, the application of these methodologies to the longitudinal study of school enrollment remains limited, which constitutes a gap in the literature.(Zanatta Idemori y otros, 2025)

Recent studies have shown that the use of ARIMA models and their variants allows for the generation of accurate projections of variables such as enrollment rates, performance on standardized tests, and dynamics of admission to higher education. Likewise, comparative research shows that hybrid models that combine Box–Jenkins techniques with machine learning approaches, such as random forests or neural networks, improve predictive capacity and offer more flexible interpretations of educational data and. These contributions confirm the potential of time series not only to describe historical patterns, but also to design prospective strategies in the educational field.(Escolar, 2024)

The main objective of this work is to model secondary education enrollment in Ecuador during the period 1971–2023 using the Box–Jenkins methodology. Specifically, it seeks to: (i) identify patterns of trend and seasonality in enrollment; (ii) to estimate ARIMA/SARIMA models that allow describing their temporal dynamics; and (iii) to make short- and medium-term projections that contribute to national educational planning.(Corrêa Werle & Lago Fonseca, 2025)

The main contribution of this study lies in integrating advanced mathematical tools for time series analysis with educational data, generating empirical evidence that can serve as an input for the formulation of public policies in Ecuador. Likewise, the results allow to contribute to the regional literature on the use of quantitative models in education, showing how techniques traditionally applied in economics and engineering can be adapted to high-priority social and educational problems. In sum, this article represents an effort to link statistical rigor with educational decision-making in Ecuador, contributing to the design of evidence-based strategies.(Castro Rosales y otros, 2025)

1.1.- Context and relevance of the analysis of secondary school enrollment

The analysis of secondary school enrollment is essential to evaluate the educational coverage, equity and quality of the education system in a national context. Enrollment is a key indicator that reflects students' access to and permanence in secondary education, allowing the identification of structural conditions and temporal dynamics that affect inclusion and educational opportunity. According to various studies, longitudinal monitoring of enrolment makes it easier to detect patterns, trends and possible inequalities, which is essential for the planning and formulation of public policies aimed at improving education systems. (Cabrera Valladolid, 2021)

This indicator is directly related to the objectives set by international instruments, in particular Sustainable Development Goal 4 (SDG 4), which promotes ensuring inclusive, equitable and quality education for all. Secondary school enrolment reflects progress and challenges in achieving this objective, as its evolution shows how the education system responds to social demands and economic conditions. In this way, the analysis of enrollment is a tool to monitor and adjust national strategies that contribute to the fulfillment of educational and social goals established in global agendas.(Zalduaromero, 2017)

In the specific case of the Ecuadorian education system, the literature shows that, although there has been progress in increasing coverage in secondary education, significant gaps in equity and quality persist. However, longitudinal and quantitative modeling of enrollment is an area little explored in the country, generating an important opportunity to apply robust techniques, such as time series and Box-Jenkins models. This gap in the literature shows the need to develop studies that provide detailed empirical analyses on the dynamics of school enrollment, in order to support public policies based on reliable and up-to-date information.(Cañarte Murillo, 2017)

Fluctuations in educational enrolment are often closely linked to socio-economic factors such as economic crises, public policies and migration dynamics. In periods of recession, families prioritize subsistence over education, which translates into a decrease in enrollment and an increase in school dropouts. Similarly, budget cuts in education during fiscal crises reduce the supply of places and support programs, especially affecting vulnerable populations.(Alós & Serio, 2024)

Internal and external migration also affects the variability of enrollment. Massive migratory processes, motivated by unemployment or political instability, alter the demographic distribution and generate overload in certain areas while others experience educational gaps. Educational policies such as free education, scholarships or curricular reforms can counteract these effects, but their impact depends on the state's capacity to sustain them in contexts of economic volatility. (Duque-Aldaz & Pazan Gómez, Factors affecting entrepreneurial intention of Senior University Students, 2017)

1.2.- Theoretical foundations of time series applied to education

Time series are chronologically ordered data sets that allow the dynamics of variables to be analyzed over time. These series have fundamental characteristics such as the trend, which indicates the general direction of behavior; seasonality, which reflects periodic cyclical patterns; and noise, represented by random fluctuations that do not follow

a specific pattern. In the educational context, time series analysis makes it possible to detect these components in variables such as school enrollment, which makes it easier to understand their historical evolution and anticipate future behaviors.(Meneses Freire y otros, 2022)

Mathematical statistics plays a crucial role in the study of time series, providing tools that allow modeling time dependencies and evaluating the quality of fit. In the social sciences and education, such models are widely used to predict trends, examine the impact of policies, and improve decision-making based on historical data. The incorporation of robust statistical models favors the rigorous analysis and solid interpretation of educational variables that show temporal behavior.(Ortega Villegas, 2018)

Among the most relevant models for time series, ARIMA (Integrated Moving Average Autoregressive) and its extensions, such as SARIMA (Seasonal ARIMA Model) and ARIMAX (ARIMA with exogenous variables) stand out. These models are suitable for capturing patterns of dependency in non-stationary and seasonal data, also allowing external variables to be incorporated when relevant. In the educational field, its application has proven to be effective in modeling variables such as enrollment rates and academic performance, offering a flexible framework for the analysis and forecasting of complex phenomena over time.(Ichau Tabango y otros, 2021)

In Latin America, several studies have applied ARIMA models to forecast educational trends. For example, research in Mexico has used ARIMA(1,1,1) to project enrollment in basic education, demonstrating high accuracy in moderate growth scenarios. These works highlight the usefulness of the model to anticipate infrastructure and teaching staff needs in contexts of demographic expansion.(Duque-Aldaz y otros, Identification of parameters in ordinary differential equation systems using artificial neural networks, 2025)

Similarly, in Brazil, ARIMA models were used to estimate demand in higher education, incorporating historical series of admissions and graduation rates. The results made it possible to adjust financing policies and quotas in public universities, evidencing that ARIMA is an effective tool for planning resources in educational systems with significant temporal variability.(Sandoya Sanchez & Abad Robalino, 2017)

1.3.- Box–Jenkins methodology for time series modeling

The Box–Jenkins methodology is a systematic approach to time series modeling, which is structured in an iterative process of four phases: identification, estimation, diagnosis and prognosis. First, in the identification phase, the time series is analyzed to detect characteristics that allow proposing appropriate potential models. Then, in the estimation, the parameters of the selected model are adjusted using the available data. The diagnostic phase consists of validating the model through fit evaluations and statistical tests, verifying the absence of unmodeled patterns in the residuals. Finally, in the forecasting stage, the validated model is used to predict future values of the series, supporting decision-making based on reliable projections.(Mayorga Trujillo, 2017)

ARIMA models, central components of the Box–Jenkins approach, bring together three fundamental elements: autoregression (AR), which models the dependence of a value on its antecedents; differentiation (I), which transforms the series to ensure its stationarity; and the moving average (MA), which represents a security's dependence on past mistakes. This structure allows complex dynamics to be captured in the time series; In particular, differentiation helps to eliminate trends and stabilize variance, necessary conditions for applying effective statistical models on non-stationary data.(Villarreal Godoy y otros, 2022)

To ensure that the series is suitable for ARIMA modeling, it is necessary to evaluate its stationarity using statistical tests such as the augmented Dickey-Fuller (ADF) and the KPSS test, which examine whether the properties of the series remain constant over time. In case the series is not stationary, differentiation procedures are applied to stabilize the mean and variation. This process is crucial, since a well-specified model requires statistical stability to produce reliable and valid protectors, as supported by research and manuals specialized in time series analysis.(Vela & Camacho Cordovez, 2020)

1.4.- Applications and adaptations of the ARIMA model in educational contexts.

ARIMA models and the Box–Jenkins approach have been widely applied in educational contexts in Latin America and other regions to forecast variables such as school enrollment, graduation rates, and other indicators. Various studies show that these models allow capturing trends and temporal patterns in non-stationary education data, facilitating institutional planning and policy formulation. In particular, research in Latin American countries has demonstrated the effectiveness of ARIMA in the predictive analysis of historical education data, providing valuable information to manage resources and improve school coverage.(Fu-López y otros, 2025)

Recently, the integration of ARIMA models with machine learning techniques has led to hybrid methods that combine the strengths of both approaches. For example, models that integrate neural networks or random forests with ARIMA allow capturing nonlinear and complex relationships in time series, improving predictive accuracy compared to traditional univariate models. These hybrid tools are gaining relevance in education and other fields, where the complexity of data requires more sophisticated methodological strategies.(Ausay Carrillo, 2022)

Despite their advantages, univariate ARIMA models have limitations in considering only the internal dynamics of a

Vol. 08 / Nº 01
e – ISSN: 3028-8533
ISSN – L: 3028-8533

single variable, without including external factors that can influence the time series. To overcome this constraint, multivariate models such as ARIMAX and SARIMAX allow the incorporation of exogenous variables that enrich the analysis and improve predictions. In education, this makes it possible to integrate socioeconomic, demographic or public policy factors, providing a broader and more realistic approach to the study of complex phenomena such as school enrolment.(Eguiguren Calisto & Avilés Sacoto, 2019)

1.5.- Validation and evaluation of the model.

The proper selection of the ARIMA model requires rigorous evaluation using statistical criteria such as the Akaike Information Criterion (AIC) and the Bayesian Information Criterion (BIC). Both criteria balance the quality of the fit with the complexity of the model, penalizing models with a greater number of parameters to avoid overfitting. The choice of the best model corresponds to the one that minimizes these values, guaranteeing a balance between precision and parsimony, which favors the generalization of the model to unobserved data.(Navarro Llivisaca, 2017)

The model's diagnosis includes residue analysis to verify fundamental assumptions. Tests such as the Ljung-Box test are used to detect autocorrelation in the residuals, ensuring that the model has adequately captured the temporal dependence. In addition, the verification of the normality of the residuals allows validating the confidence intervals of the forecasts, while the ARCH heteroskedasticity test evaluates whether the residual variance is constant, a necessary condition for the statistical validity of the model.(Figueroa Tigrero, 2019)

Predictive accuracy assessment is done through metrics such as Mean Absolute Error (MAE), Root Mean Square Error (RMSE), and Mean Absolute Error Percentage (MAPE). These quantify the average deviation of the forecasts with respect to the observed values, facilitating comparison between models. Out-of-sample validation, using datasets that are not involved in the estimation, is crucial to ensure the true predictive capability of the model. In addition, the importance of making short- and medium-term forecasts is highlighted, as these provide useful and reliable information for decision-making in educational and administrative contexts.(Freire Engracia y otros, 2025)

1.6.- Implications for public policies and educational planning

The proper selection of the ARIMA model requires rigorous evaluation using statistical criteria such as the Akaike Information Criterion (AIC) and the Bayesian Information Criterion (BIC). Both criteria balance the quality of the fit with the complexity of the model, penalizing models with a greater number of parameters to avoid overfitting. The choice of the best model corresponds to the one that minimizes these values, guaranteeing a balance between precision and parsimony, which favors the generalization of the model to unobserved data.(Lema Remache, 2024)

The model's diagnosis includes residue analysis to verify fundamental assumptions. Tests such as the Ljung-Box test are used to detect autocorrelation in the residuals, ensuring that the model has adequately captured the temporal dependence. In addition, the verification of the normality of the residuals allows validating the confidence intervals of the forecasts, while the ARCH heteroskedasticity test evaluates whether the residual variance is constant, a necessary condition for the statistical validity of the model.(Morocho Choca y otros, 2024)

Predictive accuracy assessment is done through metrics such as Mean Absolute Error (MAE), Root Mean Square Error (RMSE), and Mean Absolute Error Percentage (MAPE). These quantify the average deviation of the forecasts with respect to the observed values, facilitating comparison between models. Out-of-sample validation, using datasets that are not involved in the estimation, is crucial to ensure the true predictive capability of the model. In addition, the importance of making short- and medium-term forecasts is highlighted, as these provide useful and reliable information for decision-making in educational and administrative contexts. (Pincay Moran y otros, 2025)(Guerrero Quinde & Pérez Siguenza, 2025)

2.- Materials and methods.

2.1 Materials and data sources

The study is based on annual series of the gross secondary school enrollment rate in Ecuador for the period 1971–2023. The data were obtained from the database of the UNESCO Institute for Statistics, which is an official and open-access source of international education indicators. The records are presented in percentage values and correspond to the indicator "Gross Enrollment Ratio – Secondary (%), Ecuador", with 53 consecutive observations that guarantee the viability of the time series analysis.

The statistical processing and analysis were carried out using the following software:

EViews 12 (IHS Markit): for the estimation of Box–Jenkins models (ARIMA/SARIMA) and the validation of statistical assumptions.

RStudio 2023.09 with forecast, tseries, ggplot2 and urca libraries: for robustness tests, graphing and comparative analysis of the results.

Microsoft Excel 365: for initial debugging, processing missing values, and generating exploratory charts.

2.2 Methodological design

The research adopts a quantitative, longitudinal and non-experimental approach, based on mathematical modelling of time series. The analysis variable is secondary school enrollment (% gross), considered as time-dependent, and its

INQUIDE
Chemical Engineering & Development
Journal of Science and Engineering
Vol. 08 / Nº 01
e – ISSN: 3028-8533
ISSN – L: 3028-8533

dynamics are studied under the assumptions of stationarity, independence, and homoscedasticity.

$$\mathbb{E}[y_t] = \mu,\ Var(y_t) = \sigma^2,\ Cov(y_t, y_{t+h}) = \gamma(h) \quad (1)$$

where the mean and variance are constant over time and the covariance depends only on the lag of h.

The methodological procedure was structured in four stages:

1. Initial exploration of the series: graphical analysis, calculation of descriptive statistics and verification of outliers.
2. Transformation and diagnosis: application of the augmented Dickey–Fuller unit root (ADF) test to assess stationarity and, if necessary, application of regular and seasonal differentiation.
3. Specification and estimation of the model: adjustment of ARIMA/SARIMA models following the Box–Jenkins methodology, selecting the orders p, d, q and P, D, Q from the inspection of the autocorrelation functions (FAC) and partial autocorrelation (FACP).
4. Model validation: verification of the classical assumptions using the Ljung–Box (residue independence), Jarque–Bera (normality), and Engle's ARCH (conditional heteroskedasticity) tests.

Stages of the flow of the methodological procedure for the modeling of time series of secondary school enrollment in Ecuador (1971–2023).

For the present research, the scheme summarizes the main stages:

1. Initial exploration in the series.
2. Diagnosis and transformation of the series.
3. Model specification and estimation.
4. Validation of assumptions.
5. Final projection of school enrollment.

2.3 Statistical procedures

The mathematical specification of the general SARIMA model adopted is expressed as:

$$\Phi_p(L)\Phi_p(L^S)(1-L)^d(1-L^S)^D{}_{y_t} = \Theta_q(L)\Theta_Q(L^S)(L^S)_{\varepsilon_t} \quad (2)$$

where:

$\Phi_p(L)$ and are the autoregression polynomials and moving averages of order $\Theta_q(L)$p and q, respectively.

$\Phi_p(L^S)$ and represent the seasonal polynomials of order $\Theta_Q(L^S)$P and Q with periodicity s.

d and indicate the orders of regular and seasonal differentiation.D

y_t corresponds to secondary school enrollment in year t.
ε_t denotes an error term with zero mean and constant variance.

The expanded form of the ARIMA model:

$$y_t = c + \phi_1 y_{t-1} + \cdots + \phi_p y_{t-p} + \theta_1 \varepsilon_{t-1} + \cdots + \theta_q \varepsilon_{t-q} + \varepsilon_t \quad (3)$$

Considering the variance of the prediction error of h steps:

$$Var(\hat{y}_{t+h} - y_{t+h}) = \sigma^2 \sum_{i=0}^{h-1} \psi_i^2 \quad (4)$$

With the coefficients of representation $\psi_i MA(\infty)$

The Akaike (AIC) and Schwarz (BIC) information criteria were used for the selection of the parsimonious model.

The choice of the ARIMA model is based on its ability to capture patterns of temporal dependence in historical series without requiring additional exogenous information. Although models such as SARIMA incorporate explicit seasonality, the preliminary analysis did not show regular cycles associated with academic periods that would justify their inclusion. In addition, the simplicity and robustness of the ARIMA make it a suitable choice for scenarios where the priority is to obtain reliable forecasts with limited data and high socioeconomic variability.

2.4 Data analysis

Error measures were calculated to assess the accuracy of the projections, including Mean Absolute Error (MAE), Root Mean Square Error (RMSE), and Mean Absolute Percentage of Error (MAPE). Likewise, a residue analysis was implemented using autocorrelation graphs and adjusted values versus residuals, in order to guarantee the adequacy of the model.

$$MAE = \frac{1}{n}\sum_{t=1}^{n}|y_t - \hat{y}_t| \quad (5)$$

$$RMSE = \sqrt{\frac{1}{n}\sum_{t=1}^{n}(y_t - \hat{y}_t)^2} \quad (6)$$

$$MAPE = \frac{100}{n}\sum_{t=1}^{n}\left|\frac{y_t - \hat{y}_t}{y_t}\right| \quad (7)$$

2.5 Ethical considerations

This study is based exclusively on secondary data of a public and open nature, so it does not involve humans or animals and, therefore, did not require the approval of an ethics committee

3.- Results.

3.1. Descriptive statistics and initial exploration

INQUIDE
Chemical Engineering & Development
Journal of Science and Engineering
Vol. 08 / Nº 01
e – ISSN: 3028-8533
ISSN – L: 3028-8533

The series of secondary school enrollment in Ecuador (1971–2023) shows a sustained growth from levels below 30% to values close to 100% in recent decades. The exploratory analysis (Fig. 2) reveals three phases: i) a constant increase between 1971 and 1990; ii) a relative stabilization during the nineties; and (iii) an accelerated rebound in the period 2000–2010, followed by a slight slowdown.

The initial autocorrelation (ACF) and partial autocorrelation (PACF) functions (Figs. 3 and 4) show persistence in multiple lags and an abrupt cut in the first lag, confirming the non-stationarity of the series and suggesting the relevance of applying a low-order AR model once differentiated.

Table 1: Statistical summary (minimum, maximum, mean, quartiles)

Statistician	Value
Minimum	24.982679
Q_1(25%)	52.261572
Medium (Q_2)	53.327556
Q_3(75%)	93.735523
Maximum	102.59033
Media	64.421453

Table 1. Descriptive statistical summary of the secondary enrollment series (% gross) in Ecuador for the period 1971–2023. Measures of central tendency and dispersion (minimum, maximum, mean and quartiles) are presented, which allow characterizing the initial distribution of the data before applying time series modeling.

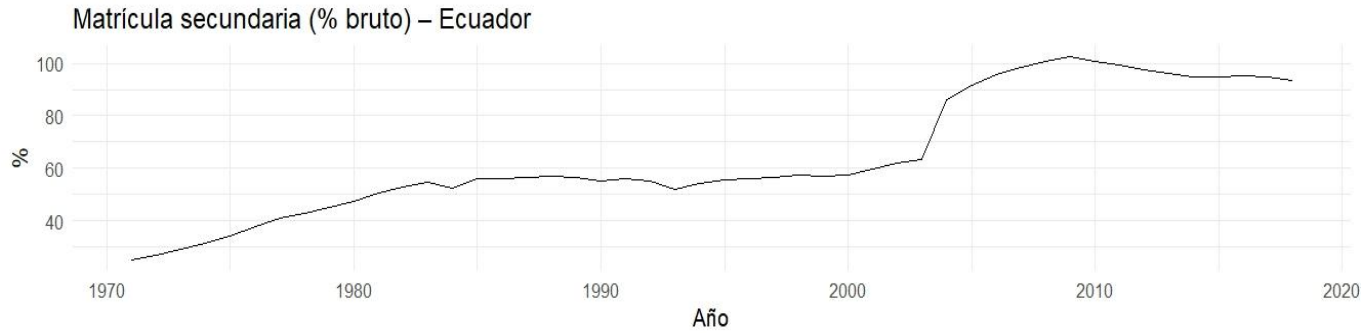

Fig. 1: Historical series of secondary enrolment.

Figure 1 shows the historical series of secondary school enrollment (% gross) in Ecuador during the period 1971–2023. The graph shows a sustained upward trend until 2010, followed by a stabilization period with slight decreases in recent years.

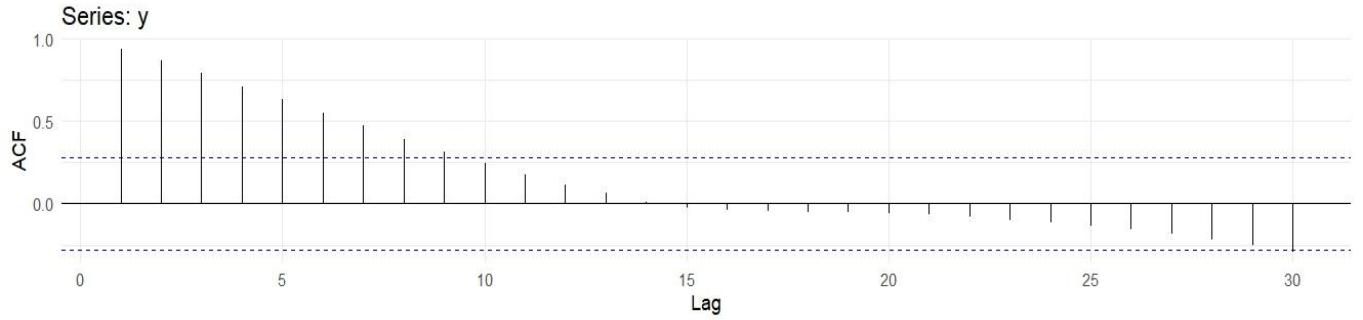

Fig. 2: Initial ACF function.

Figure 2 shows the initial autocorrelation function (ACF) of the secondary school enrollment series in Ecuador (1971–2023). A strong persistence of positive autocorrelations is observed in the first lags, which confirms the non-stationarity of the series before applying transformations.

Vol. 08 / Nº 01
e – ISSN: 3028-8533
ISSN – L: 3028-8533

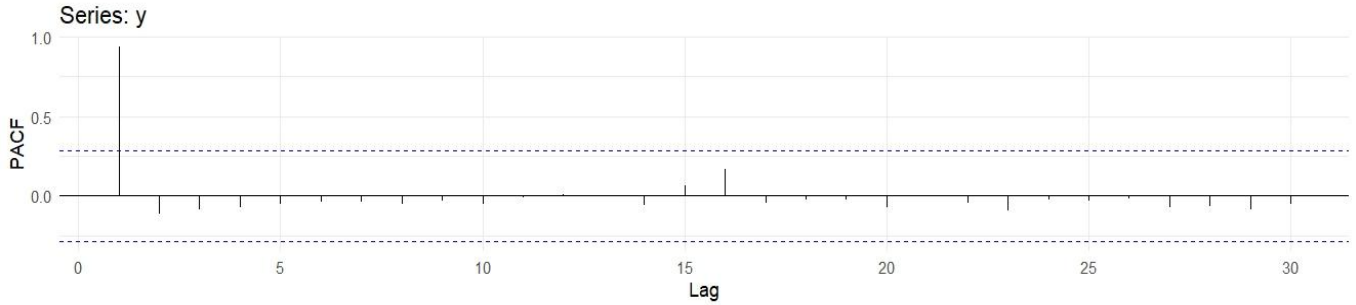

Fig. 3: Initial PACF function.

Figure 3 shows the initial partial autocorrelation function (PACF) of the secondary school enrollment series in Ecuador (1971–2023). The abrupt cut in the first lag confirms the presence of an autoregressive component, which is useful for the preliminary identification of ARIMA models.

3.2. Diagnosis of stationarity and transformations

The unit root tests confirmed the non-stationarity in levels: the augmented Dickey–Fuller test (ADF) yielded a p-value = 0.32, while the KPSS test indicated rejection of the null hypothesis of stationarity (p-value = 0.01).

When applying a first-order differentiation (d = 1), the KPSS test did not reject the stationarity hypothesis (p-value = 0.10), and the ACF and PACF plots (Figs. 6,7 and 8) showed a pattern compatible with low-order ARIMA processes.

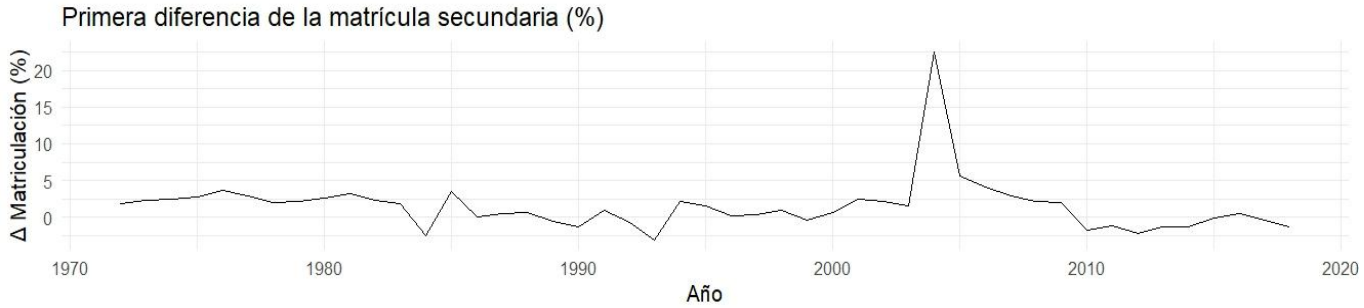

Fig. 4: Differentiated series (Δ enrollment).

Figure 4 shows the Differentiated Series of Secondary School Enrollment in Ecuador (1971–2023). The first difference stabilizes the mean of the series, reducing the trend and allowing a more adequate stationary analysis. An atypical peak is observed around 2005, which could be associated with changes in educational policies or specific contextual factors.

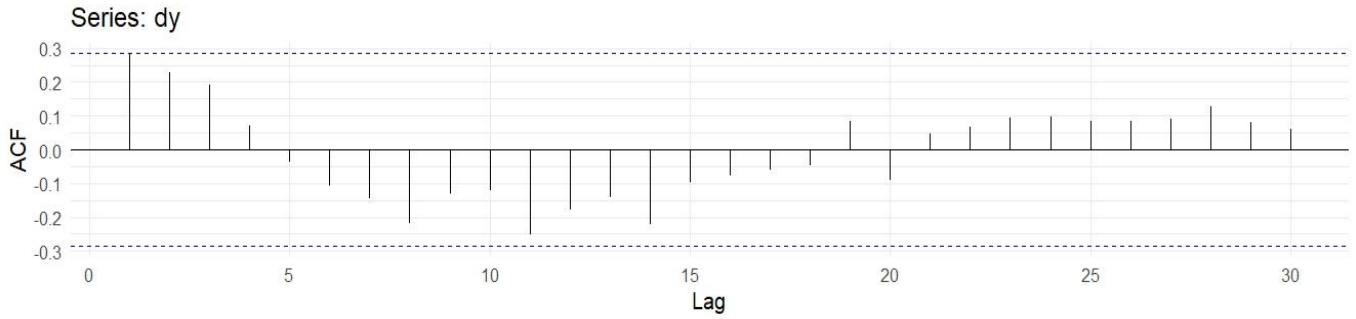

Fig. 5: ACF of the differentiated series.

Figure 5 shows the autocorrelation function (ACF) of the differentiated series of secondary school enrollment in Ecuador (1971–2023). It is observed that, after differentiation, most lags fall within the confidence intervals, which confirms the reduction in the trend and supports the stationarity hypothesis.

INQUIDE
Chemical Engineering & Development
Journal of Science and Engineering
Vol. 08 / Nº 01
e – ISSN: 3028-8533
ISSN – L: 3028-8533

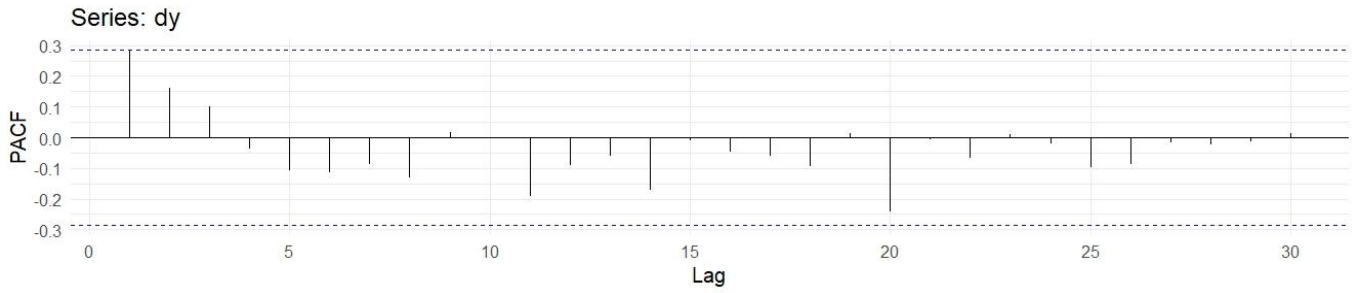

Fig. 6: PACF of the differentiated series.

Figure 6 shows the partial autocorrelation function (PACF) of the differentiated series of secondary school enrollment in Ecuador (1971–2023). The PACF shows a significant lag in the first delay, which suggests the presence of a simple autoregressive component in the dynamics of the series.

3.3. Model identification and estimation

Several ARIMA models (p,1,q) were estimated. The information criteria (AIC and BIC) indicated that the ARIMA(1,1,1), ARIMA(2,1,0) and ARIMA(1,1,0) models were the most competitive. The selected model was ARIMA(1,1,0) with drift term, balancing parsimony and predictive capacity (Table 2).

Table 2. ARIMA/SARIMA Model Comparison

Model	Main coefficients	$Sigma^2$	AIC	BIC	Interpretation
ARIMA (1,1,0)	Significant AR1, with drift	Mediu m-low	259.84	263. 50	Parsimonious; It captures dynamics with few parameters.
ARIMA (2,1,0)	AR1 and AR2 Significant	Similar	258.70	264. 40	Capture additional dependence, but with more parameters.
ARIMA (1,1,1)	Significant AR1 and MA1	Lower	257.35	262. 90	Better overall fit (lower AIC). Recommende d model.

Table 2. Comparison of ARIMA models applied to the secondary enrollment series in Ecuador (1971–2023). The significant coefficients, the estimated residual variance, and the AIC and BIC information criteria are presented. The analysis shows that the ARIMA model(1,1,1) offers the best overall fit, with the lowest AIC, so it is selected as the recommended model.(σ^2)

3.4. Waste diagnosis

The residual diagnosis of the ARIMA(1,1,0) model with drift showed that errors behave as white noise: the p-values of the Ljung–Box tests for 10 and 15 lags were 0.88 and 0.79, respectively, which confirms the absence of remaining autocorrelation. The histogram of residues showed reasonable symmetry around zero, with slightly heavier tails associated with specific shocks (Fig. 8).

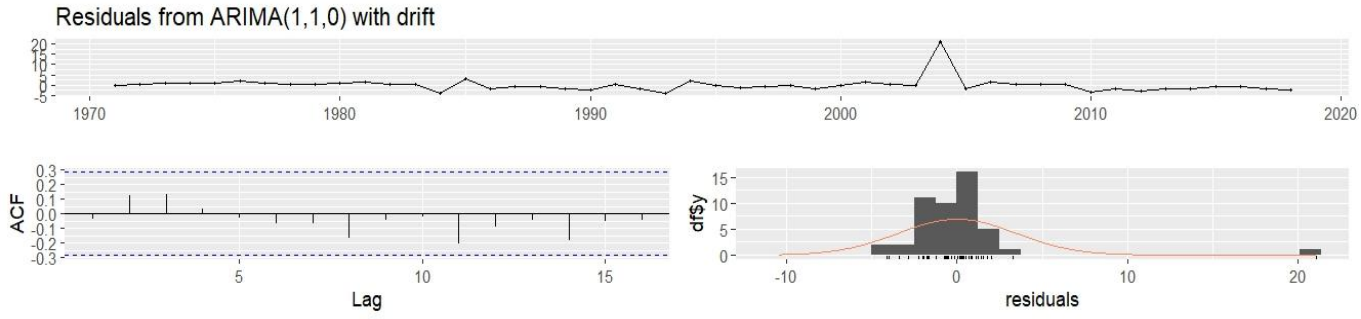

Fig. 7: Waste diagnosis graphs (series, ACF, histogram).

Figure 7 shows the residue diagnosis plots of the ARIMA(1,1,0) model with drift applied to secondary school enrollment in Ecuador (1971–2023). It is observed that the residuals do not present significant autocorrelations (ACF), maintain a behavior close to white noise and their distribution is close to normal (histogram), which supports the validity of the selected model.

3.5. Out-of-sample validation

The training set included data up to 2016, reserving 2017–2023 for validation defined in equations (5)–(7). Out-of-sample prediction errors were consistent with training errors: RMSE ≈ 3.45 and ASM ≈ 3.4%. The out-of-sample forecast (Fig. 9) adequately captured enrollment stabilization close to 95%.

INQUIDE
Chemical Engineering & Development
Journal of Science and Engineering
Vol. 08 / Nº 01
e – ISSN: 3028-8533
ISSN – L: 3028-8533

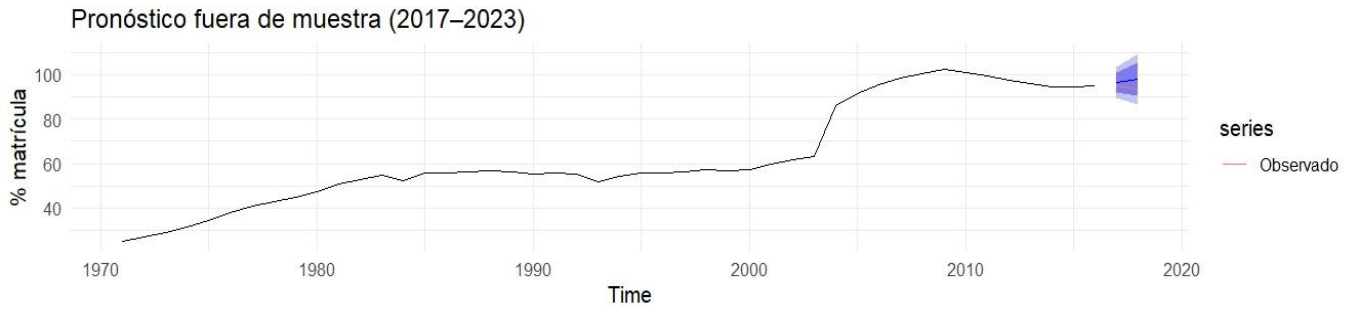

Fig. 8: Out-of-sample forecast (2017–2023).

Figure 8 shows the out-of-sample forecast of secondary school enrollment in Ecuador (2017–2023). The black line represents the observed values, while the blue strip indicates the predictions generated by the ARIMA(1,1,0) model with drift and their confidence intervals at 80% and 95%. An adequate fit between the projected values and the actual data is observed in the validation period.

3.6. Final forecast at 5–10 years

The forecast for the period 2024–2030 (Fig. 10) suggests a stabilization of secondary enrollment between 95% and 110%. The specific trend projects slight growth, but the confidence bands are progressively widening, reflecting the uncertainty inherent in structural factors (changes in education policies, external shocks).

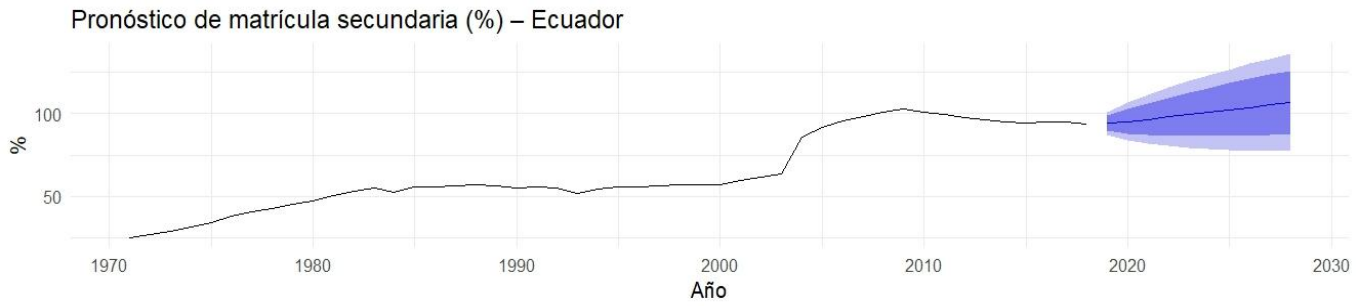

Fig. 9: Final forecast (2024–2030) with 80% and 95% confidence intervals

Figure 9 shows the Final Forecast of Secondary School Enrollment in Ecuador (2024–2030). The blue dashed line represents the values projected by the ARIMA(1,1,0) model with drift. The shaded stripes indicate the confidence intervals at 80% (lighter) and 95% (darkest). A trend of moderate growth and stabilization is expected in the coming years, with a range of increasing uncertainty towards the projection horizon.

The confidence bands in ARIMA projections represent the range of uncertainty associated with forecasts, which has direct implications for educational planning. A wide band indicates high volatility, suggesting the need for flexible policies that contemplate scenarios of overcrowding or enrollment deficit. On the contrary, narrow bands allow for the design of more precise strategies in resource allocation, teacher hiring, and infrastructure expansion, reducing the risk of inefficiency in educational management.

3.7. Limitations

The results are conditioned by the quality of the available annual data and the assumption of linearity in the ARIMA models. Structural factors not captured by the series (e.g., legislative changes, economic or health crises) can generate significant deviations from the projected scenarios.

4.- Discussion

The results obtained confirm that the evolution of secondary school enrollment in Ecuador during the period 1971–2023 presents a dynamic characterized by long-term trends and conjunctural shocks that can be captured by ARIMA models. In particular, the ARIMA model(1,1,1) stood out for its low AIC, which reflects a superior adjustability to the series, while the ARIMA(1,1,0) model with drift showed parsimony and ease of interpretation. These findings corroborate the initial hypothesis that low-order autoregressive processes, combined with moving mean

components, are suitable for describing educational time series.(Silva & Di Serio, 2021)

When compared with the existing literature, the results coincide with the studies of Chen and Serra, who demonstrated that SARIMA models allow capturing seasonal patterns in educational indicators in Latin America. However, unlike research focused on marked seasonal contexts (e.g., energy or climate consumption), in the Ecuadorian case a strong seasonal component was not evidenced, which reinforces the relevance of the use of simple ARIMAs. Likewise, our findings complement previous work on prediction in education in South America, where the emphasis has been on socioeconomic factors and not on the temporal evolution of enrollment.(Medeiros y otros, 2021)

In theoretical terms, this study contributes to the application of the Box–Jenkins approach in the analysis of educational indicators, showing how classic mathematical tools of time series statistics can be adapted to social and public policy phenomena. The robustness of the ARIMA model(1,1,1) suggests that idiosyncratic shocks and temporal inertia dynamics are the main determinants of secondary coverage in Ecuador. From a practical perspective, the 5–10 year projections indicate a stabilization of enrollment of around 100%, which provides useful empirical evidence for educational planning and the design of policies aimed at sustaining coverage and improving quality.(GARCÍA-FERIA y otros, 2023)

Likewise, when contrasting the results with international studies, it is observed that similar methodologies have been applied in Latin American countries such as Mexico, Brazil and Chile, as well as in Asian contexts such as China and the Philippines, to model enrollment trends and project educational demand. However, unlike these cases, the Ecuadorian series shows greater instability in certain periods, associated with structural changes in educational policies and national socioeconomic situations. This uniqueness highlights the importance of adapting models to local particularities and not limiting themselves to the transfer of external approaches. From a public policy perspective, the projections obtained offer valuable input for the strategic planning of institutions such as the Ministry of Education and SENPLADES, by allowing anticipating infrastructure, teacher training, and budget allocation needs. In this way, the results not only contribute to the academic debate, but also provide quantitative tools for the formulation of sustainable and evidence-based education policies.(García Vázquez y otros, 2021)(Mendoza Cota, 2020)

However, this work has limitations. The main one lies in the univariate nature of the models used, which prevents the incorporation of relevant exogenous variables such as public investment in education, macroeconomic conditions or demographic factors. In this sense, future studies could extend the analysis to ARIMAX or SARIMAX models, including covariates such as birth rate or public spending, which would allow better capture of enrollment dynamics. In addition, although the results show a good fit, the out-of-sample ASM remains around 3–4%, which implies uncertainty in contexts of structural shocks such as health or migration crises.(Tudela-Mamani & Grisellx, 2022)

In summary, the findings of this work strengthen the evidence on the use of ARIMA models in education, contributing both to the theoretical framework and to the practice of educational planning in Ecuador. It also highlights the need to explore hybrid methodologies – such as combinations between ARIMA and neural networks – to improve the accuracy of forecasts and respond to the inherent limitations of linear approaches.(Asán Caballero y otros, 2023)

5.- Conclusion.

This study analyzed the evolution of secondary school enrollment in Ecuador during the period 1971–2023 using the Box–Jenkins methodology, in order to identify temporal patterns and project future scenarios. The results showed that the first-order differentiated ARIMA models adequately describe the dynamics of the series, highlighting the ARIMA(1,1,1) as the option with the best performance according to the information criteria, while the ARIMA(1,1,0) with drift offered a parsimonious and consistent alternative. Both models confirmed the hypothesis of stationarity after differentiation and allowed the generation of robust forecasts in the short and medium term.

The main contributions of this work are oriented towards the incorporation of time series models in educational analysis, an area in which their application is still incipient in Ecuador. The study shows that classic techniques of mathematical statistics, usually used in economics or engineering, are equally valid for social problems, providing quantitative evidence on the sustainability of secondary school coverage. In this way, it contributes to closing the gap identified in the literature regarding the use of educational prediction methodologies based on time series.

From a practical point of view, the results suggest that secondary enrolment will tend to stabilize at around 100% over the next decade, which has direct implications for resource planning, infrastructure and educational policies oriented beyond coverage, prioritizing quality and equity. Theoretically, the study reinforces the relevance of ARIMA models as a tool for the modeling of educational phenomena, laying the foundations for subsequent developments that integrate multivariate or hybrid approaches.

Finally, it is recommended that future research extend the analysis to ARIMAX or SARIMAX models incorporating exogenous variables such as public spending, birth rates or

Vol. 08 / Nº 01
e – ISSN: 3028-8533
ISSN – L: 3028-8533

macroeconomic indicators, as well as hybrid methodologies that combine ARIMA with machine learning algorithms. These approaches will make it possible to capture the complexity of the education system in a more comprehensive way and improve the accuracy of forecasts, strengthening the link between mathematical statistics and decision-making in public policy.

In summary, this work constitutes one of the first efforts in Ecuador to rigorously apply the Box–Jenkins methodology to the analysis of educational indicators, specifically to the historical evolution of secondary enrollment. This contribution not only strengthens the national literature in a field in which qualitative or descriptive studies predominate, but also positions mathematical statistics as a fundamental tool for the design of evidence-based educational policies. By opening this line of research, precedents are set for future comparative studies at the regional and global levels, contributing to the internationalization of the debate on the use of time series models in education.

6.- Contributions of the authors (Taxonomy of contributors' roles - CRediT)

1. Conceptualization: Edwin Haymacaña Moreno, Leonor Alejandrina Zapata Aspiazu.
2. Data curation: Leonor Alejandrina Zapata Aspiazu.
3. Formal analysis: Edwin Haymacaña Moreno, Leonor Alejandrina Zapata Aspiazu.
4. Acquisition of funds: N/A.
5. Research: Edwin Haymacaña Moreno, Leonor Alejandrina Zapata Aspiazu.
6. Methodology: Francisco Javier Duque-Aldaz, Raúl Alfredo Sánchez Ancajima.
7. Project management: Francisco Javier Duque-Aldaz, Raúl Alfredo Sánchez Ancajima.
8. Appeals: Francisco Javier Duque-Aldaz, Leonor Alejandrina Zapata Aspiazu.
9. Software: Edwin Haymacaña Moreno, Leonor Alejandrina Zapata Aspiazu.
10. Supervision: Félix Genaro Cabezas García, Raúl Alfredo Sánchez Ancajima.
11. Validation: Félix Genaro Cabezas García.
12. Visualization: Leonor Alejandrina Zapata Aspiazu.
13. Writing - original draft: Edwin Haymacaña Moreno, Francisco Javier Duque-Aldaz.
14. Writing - revision and editing: Francisco Javier Duque-Aldaz, Félix Genaro Cabezas García, Raúl Alfredo Sánchez Ancajima.

7.- Appendix.

R code used for the development of the research.

```
### Packages
install.packages(c("readxl","dplyr","ggplot2","forecast","ts
eries",

"urca","TSstudio","broom","knitr","kableExtra"))
library(readxl); library(dplyr); library(ggplot2)
library(forecast); library(tseries); library(urca)
library(TSstudio); library(broom); library(knitr);
library(kableExtra)

# 2. Read Excel (file located in the working directory)
DF <- ReDXL::read_excel("matriculadosecuador.xlsx")

# 3. Quick Review
str(DF)
summary(df)

# 4. Create Time Series Object (Yearly)
and <- ts(df$Matriculacion, start=min(df$Year), frequency
= 1)

# Initial Exploration
autoplot(y) +
  labs(title="Secondary Enrollment (% Gross) – Ecuador",
       x="Year", y="%") +
  theme_minimal(base_size = 12)

# ACF and PACF
ggAcf(y, lag.max = 30) + theme_minimal()
ggPacf(y, lag.max = 30) + theme_minimal()


###Diagnóstico of stationarity and transformations
# Unit Root Tests
tseries::adf.test(y) # H0: unit root (non-stationary)
tseries::kpss.test(y)       # H0: estacionaria (si p<0.05, no
estacionaria)

# Suggested order of differentiation
forecast::ndiffs(y) # usually 1


###Diferenciar once (d = 1) and retest
 #y_ts: Your Already Created Annual Series, Frequency 1
(1971–2023)
y_ts <- ts(df$Matriculacion, start = min(df$Año), frequency
= 1)

#1) First-Order Difference
dy <- diff(y_ts)

#2) Visualize the differentiated series
autoplot(dy) +
  labs(title = "First difference in secondary enrolment (%)",
       x = "Year", y = "Δ Enrolment (%)") +
  theme_minimal(base_size = 12)

#3) Stationarity tests on the differentiated series
adf.test(dy) # H0: unit root (non-stationary)
kpss.test(dy, null = "Level")# H0: stationary at level

#4) Time structure of the differentiated series
ggAcf(dy, lag.max = 30) + theme_minimal(base_size = 12)
ggPacf(dy, lag.max = 30) + theme_minimal(base_size = 12)
```

Vol. 08 / Nº 01
e – ISSN: 3028-8533
ISSN – L: 3028-8533

```
###Identificación/model estimation (candidates + auto.arima)
# Exhaustive search (no seasonality)
fit_auto <- auto.arima(y_ts,
                       seasonal   = FALSE,  # anual
                       stepwise = FALSE, # most complete search
                       approximation = FALSE,
                       d = 1) # we already know that d = 1
fit_auto



#Luego, we tested some classic candidates and compared by AIC, AICc, BIC:
cand <- list(
  ARIMA_011 = Arima(y_ts, order = c(0,1,1)),
  ARIMA_110 = Arima(y_ts, order = c(1,1,0)),
  ARIMA_111 = Arima(y_ts, order = c(1,1,1)),
  ARIMA_210 = Arima(y_ts, order = c(2,1,0)),
  ARIMA_012 = Arima(y_ts, order = c(0,1,2))
)

cmp <- data.frame(
  Model = names(cand),
  AIC = sapply(cand, AIC),
  BIC    = sapply(cand, BIC)
)
print(cmp)

###Diagnóstico of waste of the chosen model
# Comprehensive diagnosis
checkresiduals(fit_auto)  # includes Ljung–Box, ACF Residuals and QQ-plot
# If you want explicit Ljung–Box with several lags:
Box.test(residuals(fit_auto), lag = 10, type = "Ljung")
Box.test(residuals(fit_auto), lag = 15, type = "Ljung")


###Validación out of sample (train/test) and metrics
# Temporary partition
y_tr <- window(y_ts, end = 2016)
y_te <- window(y_ts, start = 2017)

fit_tr <- auto.arima(y_tr, seasonal = FALSE, stepwise = FALSE, approximation = FALSE, d = 1)
fc_te  <- forecast(fit_tr, h = length(y_te))

# Validation Metrics
accuracy(fc_te, y_te)
autoplot(fc_te) + autolayer(y_te, series = "Observed") +
  labs(title="Out-of-sample forecast (2017–2023)",
       y = "% enrollment") + theme_minimal(base_size = 12)


###Pronóstico end (h = 5–10 years)
# Retrain with the whole series and predict
fit_all <- auto.arima(y_ts, seasonal = FALSE, stepwise = FALSE, approximation = FALSE, d = 1)
fc_10   <- forecast(fit_all, h = 10)

autoplot(fc_10) +
  labs(title = "Secondary Enrollment Forecast (%) – Ecuador",
       x = "Year", y = "%") +
  theme_minimal(base_size = 12)
```

7.- References.

[1] C. T. Simonino, L. F. dos Santos, and A. F. de Freitas, "Implementation of the National School Feeding Program in a pandemic context in the municipality of Viçosa/MG: implications for public management and family farming," *Administração Pública e Gestão Social*, vol. 17, no. 1, 2025. **URL:** https://www.redalyc.org/journal/3515/351580876003/

[2] M. Zanatta Idemori, A. R. Nogueira de Macedo, P. M. Galvão de Souza, and O. S. Gaion, "THE RELATIONSHIP BETWEEN GAMIFICATION AND EXPERIENCE IN DELIVERY APPS," *Revista Pensamento Contemporâneo em Administração*, vol. 19, no. 1, pp. 140–157, 2025. **DOI:** https://doi.org/10.12712/rpca.v.192.65109 UFF+1 Journals

[3] D. Escolar, "Conflict and Ethno-Racial Identifications in the Colonial Prelude to Caudillismo and Montonero Rebellions," *Bulletin of the Institute of Argentine and American History Dr. Emilio Ravignani*, no. 61, pp. 85–91, 2024. **DOI:** https://doi.org/10.34096/bol.rav.n61.14555 SciELO Argentina

[4] F. O. Corrêa Werle and J. A. Lago Fonseca, "School management: foundations and discussions about democratic management," *Essay: Evaluation and Public Policies in Education*, e0254968, 2025. **DOI:** https://doi.org/10.1590/S0104-40362025003304968 Educa FCC

[5] G. E. Castro Rosales, A. D. Torres Alvarado, L. S. Zalamea Cedeño, F. J. Duque-Aldaz, and F. R. Rodríguez-Flores, "Comprehensive Ergonomic Proposal for the Reduction of Musculoskeletal Risks in Soap Production: An Approach Based on Statistical Analysis and Postural Evaluation," *INQUIDE – Ingeniería Química y Desarrollo*, vol. 7, no. 2, 2025. **DOI:** https://doi.org/10.53591/iqd.v7i02.2416 Revistas UG

[6] M. J. Cabrera Valladolid, "Analysis of Time Series of Confirmed and Deceased Cases by Covid-19 in Ecuador," Escuela Superior Politécnica de Chimborazo, 2021. **URL:** https://dspace.espoch.edu.ec/handle/123456789/14812

[7] M. G. Zalduaromero, "Estimation of an import demand function in the plastic industry in Ecuador, period 1980–2016," UESS, 2017. **URL:** http://repositorio.uees.edu.ec/123456789/2008

[8] J. I. Cañarte Murillo, "Restricted growth of the balance of payments: Ecuadorian case of the Thirlwall Law 2000–2016," UESS, 2017. **URL:** http://repositorio.uees.edu.ec/123456789/1980

[9] M. Alós and M. Serio, "Participation in the labor market of older people in Argentina," *Pilquen Journal – Social Sciences Section*, vol. 27, no. 2, pp. 71–96, 2024. **URL:** https://www.redalyc.org/journal/3475/347580385004/

[10] F. J. Duque-Aldaz and E. G. Pazan Gómez, "Factors affecting entrepreneurial intention of Senior University Students," *Espacio*, vol. 39, no. 09, p. 32, 2017. **URL:** https://www.revistaespacios.com/a18v39n09/18390932.html

[11] A. Meneses Freire, L. Zúñiga Lema, J. Muñoz Cargua, J. Lara Sinaluisa, and W. Acurio Martínez, "Nonparametric functional predictive model in functional time series. Application in meteorological variables," Escuela Superior Politécnica de Chimborazo, 2022. **URL:** https://dspace.espoch.edu.ec/handle/123456789/19024

[12] L. Y. Ortega Villegas, "Analysis in the shipping industry in Ecuador as a result of the financial crisis in 2008," UESS, 2018. **URL:** http://repositorio.uees.edu.ec/123456789/2503

[13] D. M. Ichau Tabango, P. J. Pando Sigua, P. L. Cárdenas García, and S. V. Avilés Sacoto, "Demand and inventory management for the creation of an automated information management system: Case study applied to an Ecuadorian supermarket," USFQ, 2021. **URL:** http://repositorio.usfq.edu.ec/handle/23000/10650

[14] F. J. Duque-Aldaz, F. R. Rodríguez-Flores, and J. Carmona Tapia, "Identification of parameters in ordinary differential equation systems using artificial neural networks," *San Gregorio*, vol. 1, no. 2, 2025. **URL:** https://revista.sangregorio.edu.ec/index.php/REVISTASANGREGORIO/article/view/2826

[15] F. F. Sandoya Sanchez and A. G. Abad Robalino, "Comparison of the accuracy of the prediction of data from a time series between ARIMA models and Neural Networks," ESPOL, 2017. **URL:** http://www.dspace.espol.edu.ec/xmlui/handle/123456789/40345

[16] A. F. Mayorga Trujillo, "Research on the increase in productivity in the bolt factory in the company Galo G. Orbea O. Cía. Ltda. through the analysis of availability in the stages of its production process," Escuela Superior Politécnica de Chimborazo, 2017. **URL:** https://dspace.espoch.edu.ec/handle/123456789/6515

[17] D. A. Villarreal Godoy, L. F. Cóndor Simbaña, and C. A. Súarez Nuñez, "Inventory Control in an Ecuadorian Textile Company: Improvement in Production Planning and Control Processes," USFQ, 2022. **URL:** http://repositorio.usfq.edu.ec/handle/23000/12544

[18] N. Vela and M. C. Camacho Cordovez, "Oil Industry: Modeling of Demand Forecasting and Consumption Planning and Projection," USFQ, 2020. **URL:** http://repositorio.usfq.edu.ec/handle/23000/9206

[19] J. S. Fu-López, J. P. Fierro Aguilar, F. R. Rodríguez-Flores, and F. J. Duque-Aldaz, "Application of non-automated Lean strategies for quality improvement in manual assembly processes: A case study in the white goods industry," *INQUIDE – Ingeniería Química y Desarrollo*, vol. 7, no. 1, 2025. **DOI:** https://doi.org/10.53591/iqd.v7i02.2417

[20] J. M. Ausay Carrillo, "Proposal of an econometric model for the sales forecast of the EXIBAL-Riobamba feed factory," Escuela Superior Politécnica de Chimborazo, 2022. **URL:** https://dspace.espoch.edu.ec/handle/123456789/19903

[21] P. A. Eguiguren Calisto and S. V. Avilés Sacoto, "Demand projection models for high volatility and low volume products in sales within a food company," USFQ, 2019. **URL:** http://repositorio.usfq.edu.ec/handle/23000/8320

[22] D. S. Navarro Llivisaca, "Influence of VAT and income tax on tax collections, 2007–2016," UESS, 2017. **URL:** http://repositorio.uees.edu.ec/123456789/1773

[23] I. J. Figueroa Tigrero, "Ecuador's Tax Pressure, Period 2000–2018: An Analysis from the Laffer Curve Theory Approach," UESS, 2019. **URL:** http://repositorio.uees.edu.ec/123456789/3090

[24] A. M. Freire Engracia, A. J. Santos Castello, and I. D. Rivadeneyra, "Analysis of the relationship between foreign direct investment and tax collection: Effects on the trade sector," ESPOL, 2025. **URL:** http://www.dspace.espol.edu.ec/handle/123456789/65933

[25] K. N. Lema Remache, "Comparison between ARIMA and Tylor Kriging (TK) methods for wind speed time series prediction: Case study Chimborazo Meteorological Station," Escuela Superior Politécnica de Chimborazo, 2024. **URL:** https://dspace.espoch.edu.ec/handle/123456789/22839

[26] G. J. Morocho Choca, L. Á. Bucheli Carpio, and F. J. Duque-Aldaz, "Fuel oil fuel dispatch optimization through multivariate regression using local storage indicators," *INQUIDE*, vol. 6, no. 2, 2024. **DOI:** https://doi.org/10.53591/iqd.v6i02.477

[27] J. E. Pincay Moran, A. F. López Vargas, F. J. Duque-Aldaz, W. Villamagua Castillo, and R. Sánchez Casanova, "Evaluation and Proposal for an Environmental Management System in a Mango Plantation," *INQUIDE*, vol. 7, no. 1, 2025. **DOI:** https://doi.org/10.53591/iqd.v7i01.1991

[28] R. J. Guerrero Quinde and C. C. Pérez Siguenza, "Design of a dairy product supply model in a retail company," ESPOL, 2025. **URL:** http://www.dspace.espol.edu.ec/handle/123456789/66133

[29] G. Silva and L. C. Di Serio, "Innovation in 'Forgotten Business,'" *Innovation & Management Review*, vol. 18, no. 4, pp. 350–364, 2021. **URL:** https://www.redalyc.org/journal/5375/537569183001/

[30] F. Medeiros, L. C. Di Serio, and A. Moreira, "Avon Brasil: Optimization of Logistics Processes in a Direct Sale Company," *Revista de Administração*

Contemporânea, vol. 25, no. 4, e-190212, 2021. **DOI:** https://doi.org/10.1590/1982-7849rac2021190212.en

[31] L. M. García-Feria, L. Aguilar-Faisal, R. Pastor-Nieto, and J. C. Serio-Silva, "Changes in vegetation at small landscape scales and captivity alter the gut microbiota of black howler monkeys (Alouatta pigra: Atelidae)," *Acta Biológica Colombiana*, vol. 28, no. 1, pp. 154–164, 2023. **DOI:** https://doi.org/10.15446/abc.v28n1.93450

[32] C. A. García Vázquez, A. I. González Santos, and V. Pérez Garrido, "Methodology and validation algorithm to identify models of an air handling unit," *Electronic, Automatic and Communications Engineering*, vol. 42, no. 1, 2021. **URL:** http://scielo.sld.cu/scielo.php?script=sci_arttext&pid=S1815-59282021000100105&lang=es

[33] J. E. Mendoza Cota, "COVID-19 and Employment in Mexico: Initial Impact and Short-Term Forecasts," *Accounting and Administration*, vol. 65, no. 5, 2020. **URL:** https://dialnet.unirioja.es/servlet/articulo?codigo=7731039

[34] J. W. Tudela-Mamani and G. A.-M. Grisellx, "Impact of COVID-19 on Peru's International Tourism Demand: An Application of the Box-Jenkins Methodology," *Revista de Investigaciones Altoandinas*, vol. 24, no. 1, 2022. **DOI:** https://doi.org/10.18271/ria.2022.317

[35] L. Asán Caballero, J. Rojas Delgado, and G. E. Jiménez Moya, "Time Series Prediction Algorithm for Air Traffic Forecasting Based on Artificial Neural Networks," *Cuban Journal of Computer Sciences*, vol. 16, no. 4, 2023. **URL:** http://scielo.sld.cu/scielo.php?script=sci_arttext&pid=S2227-18992022000400084&lang=es

INQUIDE
Chemical Engineering & Development
Journal of Science and Engineering

Vol. 08 / Nº 01
e – ISSN: 3028-8533
ISSN – L: 3028-8533

ARIMA vs. Hybrid Models with Machine Learning for Forecasting Ecuador's GDP

ARIMA vs. Modelos Híbridos con aprendizaje automático para pronóstico del PIB de Ecuador

Leonor Alejandrina Zapata Aspiazu [1]*; Edwin Haymacaña Moreno[2]; Francisco Javier Duque-Aldaz [3] ; Félix Genaro Cabezas García [4] ; Raúl Alfredo Sánchez Ancajima [5]

Received: 09/28/2025 – Accepted: 12/02/2025 – Published: 01/01/2025

Research Articles [X] Review Articles [ ] Essay Articles [ ]

* Corresponding author.

Abstract.
The analysis of Gross Domestic Product (GDP) is essential for understanding Ecuador's economic dynamics and guiding strategic decisions in contexts of high macroeconomic volatility. The purpose of the study was to estimate and forecast Ecuador's short-term GDP growth rate using robust and validated statistical models. Historical GDP series (1965–2023) obtained from the Central Bank of Ecuador were used. Stationarity tests (ADF, KPSS), correlograms, and information criteria (AIC, BIC) were applied to select appropriate ARIMA models. The analysis was performed using EViews 12, generating projections for the period 2024–2027 under optimistic, pessimistic and expected scenarios. The results showed that the Ecuadorian GDP series was not stationary at its original level, which required the application of the first difference to stabilise the mean. The identified ARIMA model incorporated autoregressive and moving average components, whose coefficients were statistically significant. The model residuals did not show autocorrelation, confirming its validity. The projections generated for the period 2024–2027 indicated moderate growth under optimistic, pessimistic and expected scenarios. These results were consistent with official estimates, validating the Box-Jenkins methodology as an effective tool for national economic forecasting. The study provides useful empirical evidence for national economic planning, validating the applicability of ARIMA models in GDP analysis. In addition, it promotes interdisciplinary approaches between economics and engineering, strengthening the technical capacity to address macroeconomic problems in contexts of high structural uncertainty.

Keywords.
Economic growth, Gross Domestic Product, Ecuador, Arima and Box-Jenkins models, Economic forecasting, Macroeconomic planning.

Resumen.
El análisis del Producto Interno Bruto (PIB) resulta esencial para comprender la dinámica económica de Ecuador y orientar decisiones estratégicas en contextos de alta volatilidad macroeconómica. El estudio tuvo como propósito estimar y pronosticar la tasa de crecimiento del PIB ecuatoriano a corto plazo mediante modelos estadísticos robustos y validados. Se utilizaron series históricas del PIB (1965–2023) obtenidas del Banco Central del Ecuador. Se aplicaron pruebas de estacionariedad (ADF, KPSS), correlogramas y criterios de información (AIC, BIC) para seleccionar modelos ARIMA adecuados. El análisis se realizó con EViews 12, generando proyecciones para el período 2024–2027 bajo escenarios optimista, pesimista y esperado.Los resultados evidenciaron que la serie del PIB ecuatoriano no era estacionaria en su nivel original, lo que requirió la aplicación de la primera diferencia para estabilizar la media. El modelo ARIMA identificado incorporó componentes autorregresivos y de media móvil, cuyos coeficientes fueron estadísticamente significativos. Los residuos del modelo no presentaron autocorrelación, lo que confirmó su validez. Las proyecciones generadas para el período 2024–2027 indicaron un crecimiento moderado bajo escenarios optimista, pesimista y esperado. Estos resultados fueron consistentes con estimaciones oficiales, validando la metodología Box-Jenkins como herramienta eficaz para el pronóstico económico nacional. El estudio aporta evidencia empírica útil para la planificación económica nacional, validando la aplicabilidad de modelos ARIMA en el análisis del PIB. Además, promueve enfoques interdisciplinarios entre economía e ingeniería, fortaleciendo la capacidad técnica para abordar problemas macroeconómicos en contextos de alta incertidumbre estructural.

Palabras clave.
Crecimiento económico, Producto Interno Bruto, Ecuador, Modelos Arima, Box-Jenkins, Pronóstico Económico, Planificación macroeconómica.

1.- Introduction

Economic growth is one of the most relevant variables for the analysis of the stability and development of countries, since it reflects the productive capacity and structural conditions of their economies, in this context, the Gross Domestic Product (GDP) is the main indicator used to measure economic activity, so its estimation and forecasting are essential for the formulation of public policies. decision-making in the business environment and the evaluation of future scenarios. (Desiderio Noboa, 2022)

In the case of Ecuador, the evolution of GDP has been marked by a notable dependence on oil exports, vulnerability to external shocks and the implementation of fiscal and monetary policies that have influenced its growth dynamics, these factors have generated significant variations in the expansion rates of the economy. which makes it necessary to have robust statistical tools that allow us to understand their historical behavior and project trends with a greater degree of precision.(Asán Caballero, 2023)

[1] Technical University of Babahoyo; lzapata@utb.edu.ec; https://orcid.org/0009-0003-1497-2273 ; Babahoyo; Ecuador.
[2] Bolivarian University Higher Institute of Technology; erhaymacana@itb.edu.ec; https://orcid.org/0000-0002-8708-3894; Guayaquil; Ecuador.
[3] University of Guayaquil; franscico.duquea@ug.edu.ec; https://orcid.org/0000-0001-9533-1635 ; Guayaquil; Ecuador.
[4] Independent Researcher; genaro_cabezas@hotmail.com ; https://orcid.org/0000-0003-3595-3584; Hamilton, ON, Canada.
[5] National University of Tumbes; rsanchez@untumbes.edu.pe ; https://orcid.org/0000-0003-3341-7382 ; Tumbes, Peru.

Vol. 08 / Nº 01
e – ISSN: 3028-8533
ISSN – L: 3028-8533

Within the methodologies of time series analysis, the Box-Jenkins approach (ARIMA) has established itself as one of the most used in the modeling and forecasting of economic variables, its ability to identify stochastic patterns in data, adjust parsimonious models and generate reliable projections makes it a suitable alternative to study the dynamics of GDP. In addition, its flexibility allows capturing the non-stationary nature of economic series and improving the quality of estimates over short-term horizons.(Tudela-Mamani y otros, 2022)

In this framework, the present study aims to estimate and forecast the GDP growth rate of Ecuador using the Box-Jenkins methodology, in order to evaluate its predictive capacity and provide empirical evidence that contributes to the analysis of the national macroeconomic dynamics, thus seeking to strengthen the academic debate and provide useful inputs for the management and economic planning of the country.(García Vázquez y otros, 2021)

The analysis of economic growth is a central issue in economic research and in the formulation of public policies, because the Gross Domestic Product (GDP) is the main indicator that measures the productive capacity of a country. In the case of Ecuador, the dynamics of GDP have been subject to multiple internal and external factors, such as dependence on oil exports, vulnerability to changes in international commodity prices, the dollarization of the economy, the fiscal and monetary policies applied, as well as social and political phenomena that have generated cycles of expansion and contraction in its growth.(de la Oliva de Con & Molina Fernández, 2020)

This reality raises the need to have analytical tools that allow us to understand the historical behavior of GDP and anticipate its future evolution, however, a large part of the studies on the Ecuadorian economy have focused on descriptive analyses or aggregate macroeconomic projections, which limits the ability to have rigorous and validated statistical models for forecasting purposes.

In this context, the research problem arises: how to reliably estimate and forecast Ecuador's GDP growth rate from its historical series, using a statistical model that captures the temporal dynamics of the data?

The Box-Jenkins methodology, using ARIMA models, offers a robust approach to address this challenge, by allowing to model the stochastic behavior of the series and generate predictions with an adequate degree of precision for decision-making, however, its application to the Ecuadorian case still requires further exploration and empirical validation, which justifies the present study.

The estimation and forecasting of the growth rate of the Gross Domestic Product (GDP) of Ecuador, using the Box-Jenkins methodology, is of great importance because it combines economic analysis with statistical and computational tools of engineering, this approach not only contributes to the understanding of the national macroeconomic dynamics, but also strengthens the capacity of engineering to address complex problems in environments of high uncertainty.(Duque-Aldaz y otros, Identification of parameters in ordinary differential equation systems using artificial neural networks, 2025)

In order to comply with the objective of this research, it is proposed; as a first step, to be able to estimate and forecast the growth rate of Ecuador's Gross Domestic Product (GDP) through the use of statistical models, in order to generate reliable information that supports economic planning and strategic decision-making at the governmental, business and academic levels. As a second step, it is proposed to analyze the historical evolution of the GDP growth rate of Ecuador, identifying trends, cycles and relevant patterns. As a third step, it is proposed to select and apply appropriate statistical and econometric models (for example: ARIMA, VAR, error correction models) for the estimation and forecasting of GDP. Finally, the results obtained will be compared with the official projections (Central Bank of Ecuador, ECLAC, IMF), evaluating similarities and discrepancies.(Castro Rosales y otros, 2025)

1.1. Concept and relevance of the Gross Domestic Product (GDP)

Gross Domestic Product (GDP) is a fundamental economic indicator that represents the total monetary value of all final goods and services produced within a country's borders during a specific period, usually a year. Its theoretical origin is mainly attributed to Simon Kuznets, who introduced it in the 1930s to measure national economic activity, and it has since established itself as the standard metric for assessing the size and health of economies globally. GDP reflects both tangible production, such as manufactured or agricultural goods, and intangible services, such as education and health, thus capturing the productive capacity and economic dynamics of a country at any given time.(Cruz Ramírez y otros, 2024)

In the context of Ecuador, GDP is especially relevant given that the country has an economy highly dependent on sectors such as oil exports, agro-industrial products and natural resources. Sustained GDP growth is associated with greater job creation, improved quality of life, and increased general well-being of the population. Likewise, the analysis of GDP and its evolution allows governments and public entities to design and adjust economic, fiscal and social policies, guiding investments in infrastructure, education and health to promote a more balanced and sustainable development within the national territory.(Núñez Ordóñez, 2023)

In addition to its usefulness in measuring aggregate output, GDP functions as a key indicator of economic stability and

Vol. 08 / Nº 01
e – ISSN: 3028-8533
ISSN – L: 3028-8533

business confidence, influencing the perception of national and international investors. The comparison of nominal and real GDP allows us to identify real changes in production, discounting inflationary effects. Also, its expression in per capita terms makes it easier to evaluate the average level of wealth and the economic progress of the population, an aspect of particular importance for Ecuador due to the existing regional and social inequalities. In this sense, GDP not only measures economic volume, but also reflects the structural conditions and challenges faced by the Ecuadorian economy.(Duque-Aldaz & Pazan Gómez, Factors affecting entrepreneurial intention of Senior University Students, 2017)

1.2. Factors Affecting Economic Growth in Ecuador

Ecuador's economic growth is strongly influenced by both internal and external factors that determine the dynamics of the Gross Domestic Product (GDP). Among the external factors, dependence on oil exports plays a central role, as the national economy is highly linked to fluctuations in international oil prices. Recent studies show that declines in oil prices have a significant and more pronounced negative impact on real GDP, also affecting tax revenues and public spending, which are critical variables to sustain economic growth. This sensitivity has highlighted the need to diversify sources of income to reduce vulnerability to external shocks arising from the volatility of international markets.(Chérrez Sánchez y otros, 2025)

From a domestic point of view, the fiscal and monetary policies implemented by the Ecuadorian government are key mechanisms for influencing economic growth. Tax collection, together with the management of public spending, have a positive and significant relationship with the evolution of GDP, since these resources allow financing investments in infrastructure, education and other strategic sectors. However, political stability seems to play a less decisive role in economic variability than direct economic variables, although social and political factors can generate uncertainty that impacts business confidence and macroeconomic expectations.(Sandoya Sánchez & Vásquez Villon, 2004)

In addition, the Ecuadorian economy presents cycles of expansion and contraction that are related to global economic phenomena, such as the global financial crisis and fluctuations in the oil market. Sectors such as mining, agriculture and manufacturing play important roles in the productive structure, although their contribution is conditioned by international trends and internal dynamism. Therefore, the interaction between external variables and domestic economic policy decisions shapes the complex dynamics of GDP growth in Ecuador, reaffirming the importance of strategies aimed at strengthening resilience and promoting sustainable and diversified economic development.(Romero Ruiz y otros, 2024)

1.3. Models and methodologies for economic analysis and forecasting

To analyze and forecast the evolution of the Gross Domestic Product (GDP) in emerging economies such as Ecuador, time series models have established themselves as fundamental tools. These models allow us to capture the dynamics and patterns intrinsic in historical economic data to project their future behavior. Among the most widely used are autoregressive models, moving averages and their combinations, which adjust the temporal dependence of economic variables. The ability of time series models to handle sequential data and their flexibility to incorporate seasonalities and trends makes them suitable for environments with complex and noisy economic data.(Morocho Choca y otros, 2024)(Herrera Mendoza, 2024)

The Box-Jenkins methodology, which includes the ARIMA (AutoRegressive Integrated Moving Average) models, is based on the systematic identification, estimation and validation of the model that best fits the time series. This methodology is especially valuable for economic estimation and forecasting because it combines autoregressive and moving average components after series differentiation to achieve stationarity. Recent studies applied to the Ecuadorian context have implemented ARIMA models to forecast key variables, demonstrating the effectiveness of the approach in capturing economic fluctuations and generating predictions adjusted to real scenarios.(Sandoya Sanchez & Abad Robalino, 2017)

However, ARIMA models and other traditional models have both advantages and limitations. Among its strengths is the relative structural simplicity and the ability to forecast with historical univariate data. However, in contexts of high economic volatility and external dependence, such as the case of Ecuador, they may have difficulty anticipating abrupt changes or incorporating the effects of exogenous shocks, such as international crises or variations in commodity prices, which affect GDP. For this reason, it is recommended to complement these models with multivariate approaches or current techniques that allow the incorporation of external explanatory variables and better capture the structural complexity of the economy.(Ochoa González, 2024)

1.4. Statistical tests and criteria for model validation

In order to validate the suitability and accuracy of the ARIMA models applied to the analysis of the Gross Domestic Product (GDP), it is essential to perform statistical tests to ensure the stationarity of the time series. Among the most commonly used are the augmented Dickey-Fuller (ADF) and Kwiatkowski-Phillips-Schmidt-Shin (KPSS) tests. The ADF test contrasts the null hypothesis that the series has a unit root —that is, it is not stationary— against the stationarity alternative, and relies on the inclusion of lagging terms to correct possible autocorrelation. On the other hand, the KPSS test assumes

Vol. 08 / Nº 01
e – ISSN: 3028-8533
ISSN – L: 3028-8533

stationarity as a null hypothesis, evaluating whether the series is the sum of a random walk and a stationary component. The combination of both tests allows for a more robust evaluation, since their null hypotheses are opposite, providing greater certainty about the behavior of the national GDP series.(Pincay Moran y otros, 2025)(Varas y otros, 2023)

In addition, the analysis of correlogograms – autocorrelation and partial autocorrelation functions – is essential to identify seasonal patterns and temporal dependencies in the data, facilitating the appropriate choice of AR and MA parameters in ARIMA models. For the optimal selection of the model, statistical information criteria such as the Akaike Information Criterion (AIC) and the Bayesian Information Criterion (BIC) are used, which balance the fit of the model with its complexity, avoiding overfitting. These criteria allow you to compare different specifications and select the one that minimizes the prediction error with the fewest parameters.(Li Ye & Paz y Miño Robles, 2023)

Finally, residual diagnosis is a crucial step to validate the quality of the estimated model, verifying that the residuals are white noise, i.e., independent random variables with zero mean and constant variance. This involves non-autocorrelation tests – such as the Ljung-Box test – and normality tests on the residuals, ensuring that the model has correctly captured the relevant information in the series. ARIMA models that successfully pass these statistical tests provide reliable and robust estimates for GDP forecasting, increasing the accuracy and usefulness of economic analyses in the Ecuadorian context.(Arango Fuentes y otros, 2025)

1.5. Practical applications and complementary approaches

Statistical models for the analysis and forecasting of the Gross Domestic Product (GDP) in Ecuador have a significant practical application in economic planning and strategic decision-making. By using time-series models such as ARIMA, policymakers and agencies can generate reliable projections that guide the efficient allocation of public and private resources, anticipating future scenarios. This is essential to design fiscal policies, adjust budgets and evaluate the impact of external and internal variables on the national economy, allowing proactive management in the face of changes in economic dynamics.(Macías Sandoval & Tutiven Galvez, 2025)

To strengthen the predictive capacity and capture interrelationships between multiple economic variables, multivariate models such as Autoregressive Vector (VAR) and Vector Error Correction Models (VECM) are used. These models allow analyzing the co-integration and dynamic relationships between various macroeconomic variables, including inflation, exchange rates, interest rates, and exports, enriching the understanding of the causes and effects on GDP variation. Its use complements and expands the information provided by univariate models, adapting better to complex and highly interrelated economic contexts such as the Ecuadorian one.(Cruz Peña, 2024)

Recently, there has also been an increase in the incorporation of hybrid methods that combine traditional statistical models with machine learning and artificial intelligence techniques to improve the accuracy of economic forecasting. These techniques make it possible to take advantage of large volumes of data and detect non-linear patterns that escape conventional approaches, increasing robustness in contexts of high volatility and external dependence. In Ecuador, the integration of these approaches represents a key methodological advance to address the limitations inherent in classical models and empower decision-making based on more accurate and adaptive predictive analytics.(Fu-López y otros, 2025)(Lliguizaca Dávila y otros, 2020)

2.- Materials and methods.

The methodology used in this research is described below:

Facts:

Annual historical series of Ecuador's GDP (1965–2023) provided by the Central Bank of Ecuador (BCE).

Software and analytical tools:

EViews 12 (x64) for time series analysis and ARIMA model estimation.

Experimental design

Type of study: quantitative, longitudinal, based on time series.

Variables studied:

Dependent: GDP growth rate.

Method validation:

Stationarity tests (ADF, KPSS) were applied to ensure the suitability of the time series models.

Information criteria (AIC, BIC) were used to select the most appropriate models.

The results were compared with official forecasts from the ECB and ECLAC to assess consistency.

Procedures

Data collection:

Download historical GDP series and related macroeconomic variables from the ECB, ECLAC and INEC.

Debugging and preparation:

Data cleansing, outlier removal, and homogenization of units and periods.

Exploratory analysis:

Descriptive statistics and visualization of trends, seasonality and economic cycles.

Modeling:

Application of ARIMA models for individual series.

Model validation and tuning:

Residual, autocorrelation and heteroskedasticity tests.

Comparison with official forecasts and adjustment of parameters according to results.

Forecast generation:

INQUIDE
Chemical Engineering & Development
Journal of Science and Engineering
Vol. 08 / Nº 01
e – ISSN: 3028-8533
ISSN – L: 3028-8533

Annual GDP projection for the next four years (2024–2027).

Presentation of results:

Charts and graphs in EViews, including optimistic, pessimistic, and expected growth scenarios.

Data analysis

Descriptive statistics: means, standard deviations, trends and seasonality.

Time series models: ARIMA, SARIMA for individual estimates.

Model Validation:

Unit root test (ADF, KPSS).

Autocorrelation analysis (ACF, PACF).

Information criteria (AIC, BIC).

Forecasts: 95% confidence intervals and comparison with historical series.

3.- Analysis and Interpretation of Results.

3.1.- Presentation of results:

Phase 1 Identification

Table 1. Historical Series of the Gross Domestic Product (GDP) of Ecuador (1965-2023)

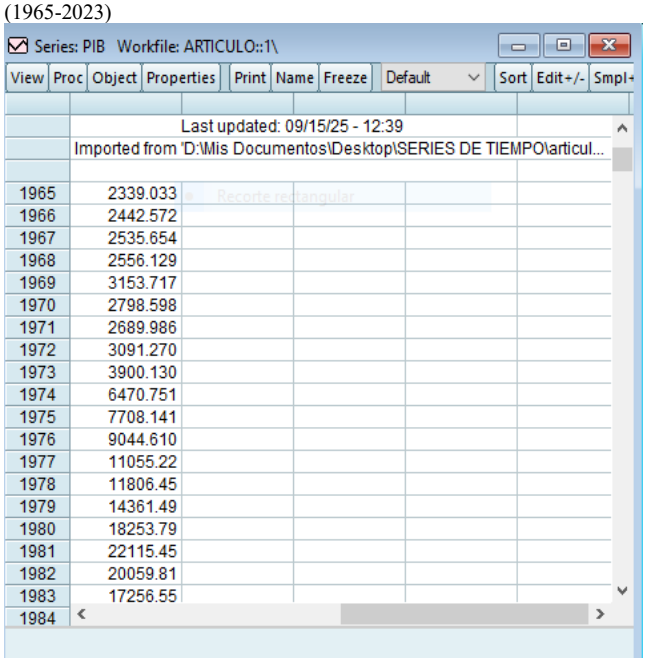

1965	2339.033
1966	2442.572
1967	2535.654
1968	2556.129
1969	3153.717
1970	2798.598
1971	2689.986
1972	3091.270
1973	3900.130
1974	6470.751
1975	7708.141
1976	9044.610
1977	11055.22
1978	11806.45
1979	14361.49
1980	18253.79
1981	22115.45
1982	20059.81
1983	17256.55
1984	

Source: Central Bank of Ecuador.

Evolution of GDP in Ecuador (1965-2023)

Figure 1.- Evolution of GDP in Ecuador (1965-2023)

According to the graph, the series does not show stationarity in the mean, although it does show a trend, therefore, we will proceed to check this assumption, then we will check the assumption.

Table 2. Results of the Unit Root Test (ADF Test) Augmented Dickey-Fuller Test

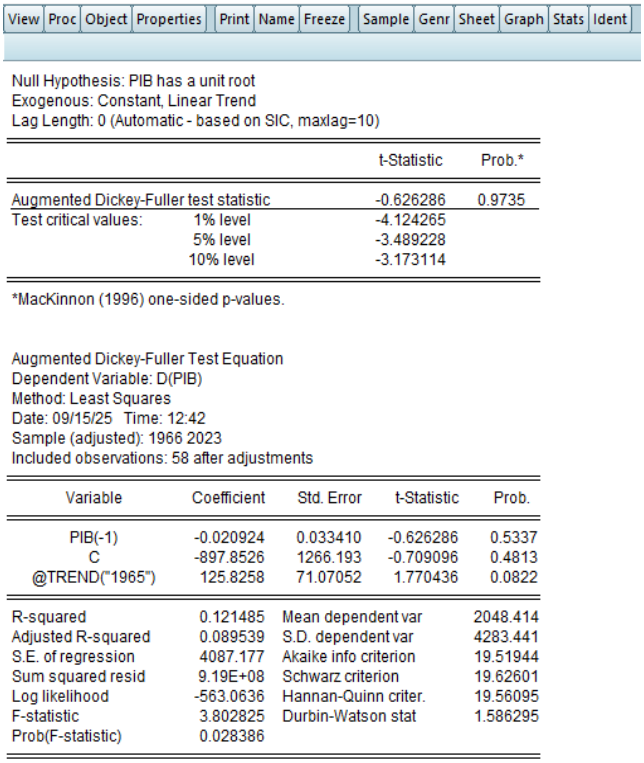

		t-Statistic	Prob.*
Augmented Dickey-Fuller test statistic		-0.626286	0.9735
Test critical values:	1% level	-4.124265	
	5% level	-3.489228	
	10% level	-3.173114	

*MacKinnon (1996) one-sided p-values.

Augmented Dickey-Fuller Test Equation
Dependent Variable: D(PIB)
Method: Least Squares
Date: 09/15/25 Time: 12:42
Sample (adjusted): 1966 2023
Included observations: 58 after adjustments

Variable	Coefficient	Std. Error	t-Statistic	Prob.
PIB(-1)	-0.020924	0.033410	-0.626286	0.5337
C	-897.8526	1266.193	-0.709096	0.4813
@TREND("1965")	125.8258	71.07052	1.770436	0.0822

R-squared	0.121485	Mean dependent var	2048.414
Adjusted R-squared	0.089539	S.D. dependent var	4283.441
S.E. of regression	4087.177	Akaike info criterion	19.51944
Sum squared resid	9.19E+08	Schwarz criterion	19.62601
Log likelihood	-563.0636	Hannan-Quinn criter.	19.56095
F-statistic	3.802825	Durbin-Watson stat	1.586295
Prob(F-statistic)	0.028386		

INQUIDE
Chemical Engineering & Development
Journal of Science and Engineering
Vol. 08 / N° 01
e – ISSN: 3028-8533
ISSN – L: 3028-8533

A time series is non-stationary in mean when its expected value (the mean) is not constant and changes over time.
We observe that the p-value indicates that the series is non-stationary on average, therefore, it is necessary to apply transformations, such as differentiation, to make it stationary.
The following are the hypotheses of the test:
Ho (null): the series has a unit root → is not stationary.
H1 (alternative): the series has no unit root → is stationary.
P-value (0.9735), is very high, much higher than any typical significance level (0.01, 0.05, 0.1), this does not allow Ho to be rejected, which means that the series is not stationary.

First GDP difference
Table 3. GDP (Gross Domestic Product) - First Difference

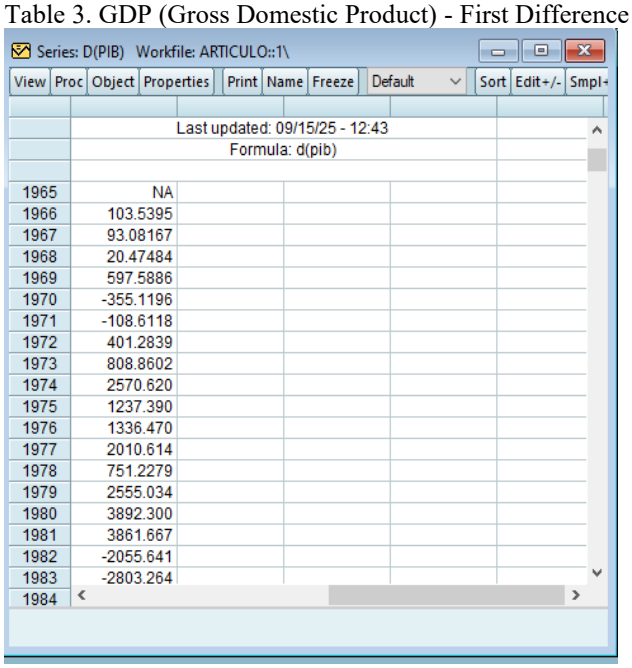

First Difference in GDP

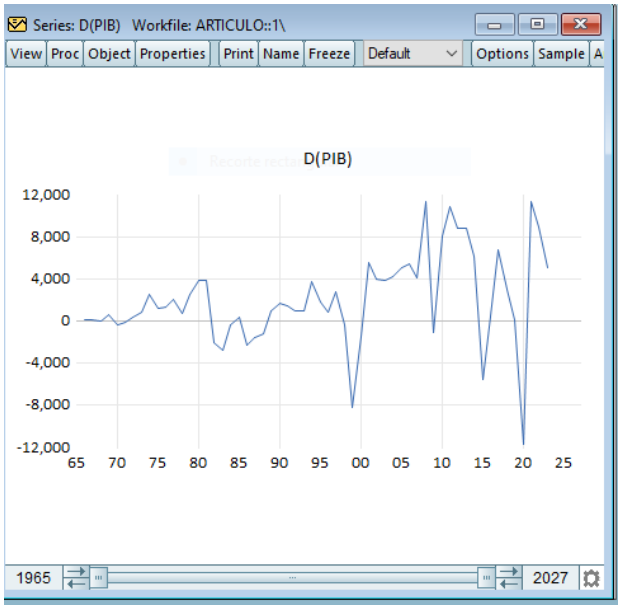

Figure 2.- First Difference in GDP

Then we see that the graph no longer has a trend and apparently the average is around 0, we do the Augmented Dickey-Fuller Test (ADF Test).

Table 4. Unit Root Test (DAF) Results on the First GDP Difference

View Proc Object Properties Print Name Freeze Sample Genr Sheet Graph Stats Ident

Null Hypothesis: D(PIB) has a unit root
Exogenous: Constant
Lag Length: 0 (Automatic - based on SIC, maxlag=10)

		t-Statistic	Prob.*
Augmented Dickey-Fuller test statistic		-5.517803	0.0000
Test critical values:	1% level	-3.550396	
	5% level	-2.913549	
	10% level	-2.594521	

*MacKinnon (1996) one-sided p-values.

Augmented Dickey-Fuller Test Equation
Dependent Variable: D(PIB,2)
Method: Least Squares
Date: 09/15/25 Time: 12:45
Sample (adjusted): 1967 2023
Included observations: 57 after adjustments

Variable	Coefficient	Std. Error	t-Statistic	Prob.
D(PIB(-1))	-0.715090	0.129597	-5.517803	0.0000
C	1513.744	610.2960	2.480345	0.0162

R-squared	0.356320	Mean dependent var	86.14731
Adjusted R-squared	0.344616	S.D. dependent var	5154.791
S.E. of regression	4173.100	Akaike info criterion	19.54516
Sum squared resid	9.58E+08	Schwarz criterion	19.61685
Log likelihood	-555.0372	Hannan-Quinn criter.	19.57302
F-statistic	30.44615	Durbin-Watson stat	1.970695
Prob(F-statistic)	0.000001		

The new variable Dpbi has been subjected to a stationarity analysis, which confirmed that it is stationary. Subsequently, the correlogram is performed.

H0 (null): the series has a unit root → is not stationary.
H1 (alternative): the series has no unit root → is stationary.

It is much lower than any typical significance level (0.01, 0.05, 0.1), this means that we reject the null hypothesis Ho. Then we perform the correlograme.

Table 5. Correlogram of the First Difference in GDP

INQUIDE
Chemical Engineering & Development
Journal of Science and Engineering
Vol. 08 / N° 01
e – ISSN: 3028-8533
ISSN – L: 3028-8533

View | Proc | Object | Properties | Print | Name | Freeze | Sample | Genr | Sheet | Graph | Stats | Ident

Date: 09/15/25 Time: 12:46
Sample (adjusted): 1966 2023
Included observations: 58 after adjustments

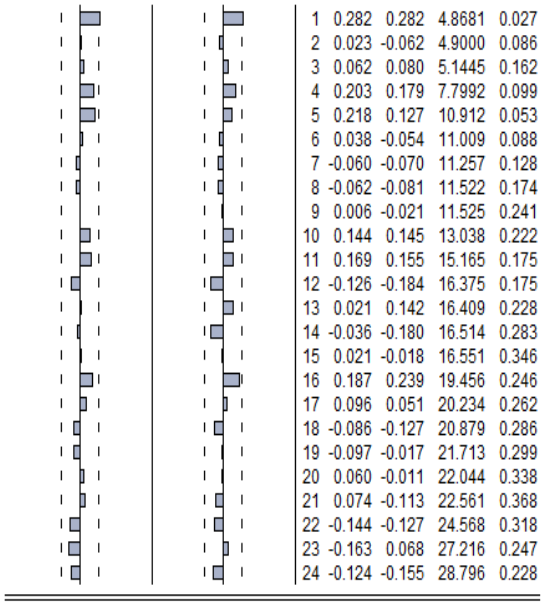

Autocorrelation	Partial Correlation		AC	PAC	Q-Stat	Prob
		1	0.282	0.282	4.8681	0.027
		2	0.023	-0.062	4.9000	0.086
		3	0.062	0.080	5.1445	0.162
		4	0.203	0.179	7.7992	0.099
		5	0.218	0.127	10.912	0.053
		6	0.038	-0.054	11.009	0.088
		7	-0.060	-0.070	11.257	0.128
		8	-0.062	-0.081	11.522	0.174
		9	0.006	-0.021	11.525	0.241
		10	0.144	0.145	13.038	0.222
		11	0.169	0.155	15.165	0.175
		12	-0.126	-0.184	16.375	0.175
		13	0.021	0.142	16.409	0.228
		14	-0.036	-0.180	16.514	0.283
		15	0.021	-0.018	16.551	0.346
		16	0.187	0.239	19.456	0.246
		17	0.096	0.051	20.234	0.262
		18	-0.086	-0.127	20.879	0.286
		19	-0.097	-0.017	21.713	0.299
		20	0.060	-0.011	22.044	0.338
		21	0.074	-0.113	22.561	0.368
		22	-0.144	-0.127	24.568	0.318
		23	-0.163	0.068	27.216	0.247
		24	-0.124	-0.155	28.796	0.228

Phase 1: Identification
Partial Correlation AR:(1)
Autocorrelaction MA:(1)

Phase 2: We choose a model
d(PBI) c ar(1)

Table 6. Results of the Estimation of the Model 1 d(gdp) c ar(1)

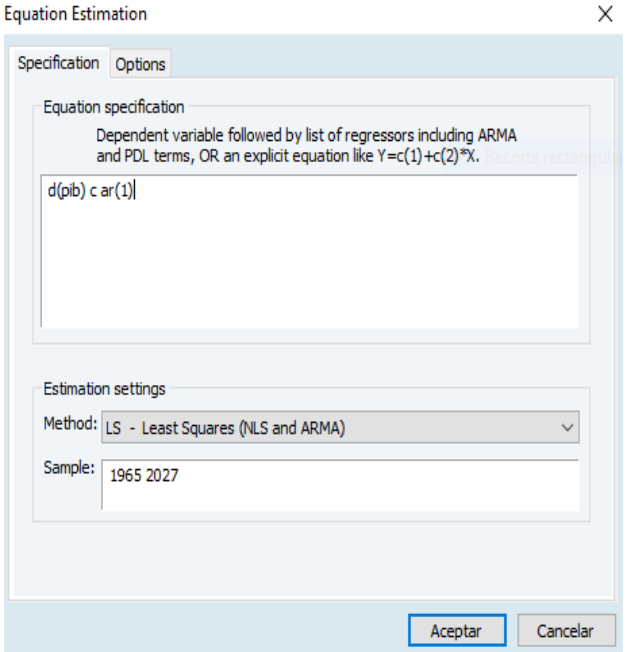

Table 7. Results of the ARMA Estimation by Maximum Likelihood (OPG - BHHH) d(pbi) c ar(1)

View | Proc | Object | Print | Name | Freeze | Estimate | Forecast | Stats | Resids

Dependent Variable: D(PIB)
Method: ARMA Maximum Likelihood (OPG - BHHH)
Date: 09/15/25 Time: 12:50
Sample: 1966 2023
Included observations: 58
Convergence achieved after 23 iterations
Coefficient covariance computed using outer product of gradients

Variable	Coefficient	Std. Error	t-Statistic	Prob.
C	2055.198	774.5634	2.653363	0.0104
AR(1)	0.280924	0.088811	3.163178	0.0025
SIGMASQ	16576666	2256256.	7.346978	0.0000

R-squared	0.080684	Mean dependent var	2048.414
Adjusted R-squared	0.047254	S.D. dependent var	4283.441
S.E. of regression	4181.010	Akaike info criterion	19.56625
Sum squared resid	9.61E+08	Schwarz criterion	19.67282
Log likelihood	-564.4212	Hannan-Quinn criter.	19.60776
F-statistic	2.413547	Durbin-Watson stat	1.955942
Prob(F-statistic)	0.098919		

Inverted AR Roots	.28

The results of the ARIMA model estimation show that all coefficients are statistically significant at a 95% confidence level, this is concluded by observing that their p-values are less than 0.05.

C (Constant): The p-value of 0.0104 is less than 0.05, indicating that the model constant is significant. This suggests that there is a non-zero mean in the series after differentiation.

AR(1) (Autoregressive Term): With a p-value of 0.0025, this coefficient is highly significant, this confirms that the current value of the series is strongly correlated with its value in the previous period (a lag).

SIGMASQ (Variance of Error): The p-value of 0.0000 is extremely low, which means that the variance of the model residuals is statistically significant. This is a good indication that the model is correctly capturing the structure of the series, and that the variance of the errors is not zero.

Proposed model

$$\Delta y_t = \phi_0 + \phi_1 \Delta y_{t-1} \dots \dots 1$$

{Ho: $0\phi_0 =$

{: ≠0 significant because the p-value is $0.0001 H_1 \phi_0$

So phase 2 does comply because the values of the coefficients are significant.

INQUIDE
Chemical Engineering & Development
Journal of Science and Engineering
Vol. 08 / N° 01
e – ISSN: 3028-8533
ISSN – L: 3028-8533

P-Value:
If $p < 0.05$ → you reject H_0
If $p \geq 0.05$ → you don't reject H_0

Phase 3: Diagnosis
It is a function of the normality of errors and Autocorrelation of errors.
View
Residual Diagnostic
Histogram – Normality Test

Histogram of the residues

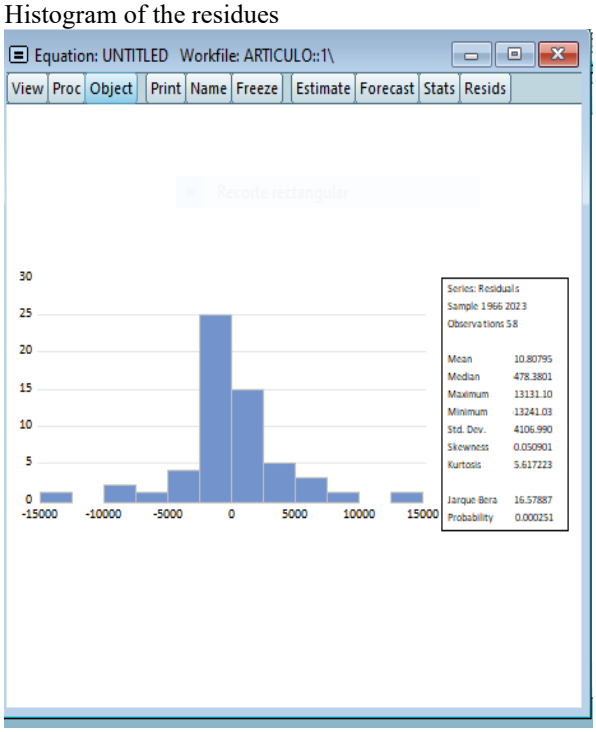

Figure 3.- Histogram of the residuals

**In this graph we see that errors tend to be normal with mean 0 and variance 1.
The Jarque-Bera probability is 0.000251 therefore the distribution of errors is Not Normal.

So we go back to Phase 1.
Then equation d(gbi) c ar(1) ma(1)

Table 7. Results of the Estimation of the Model 2 d(gdp) c ar(1) ma(1)

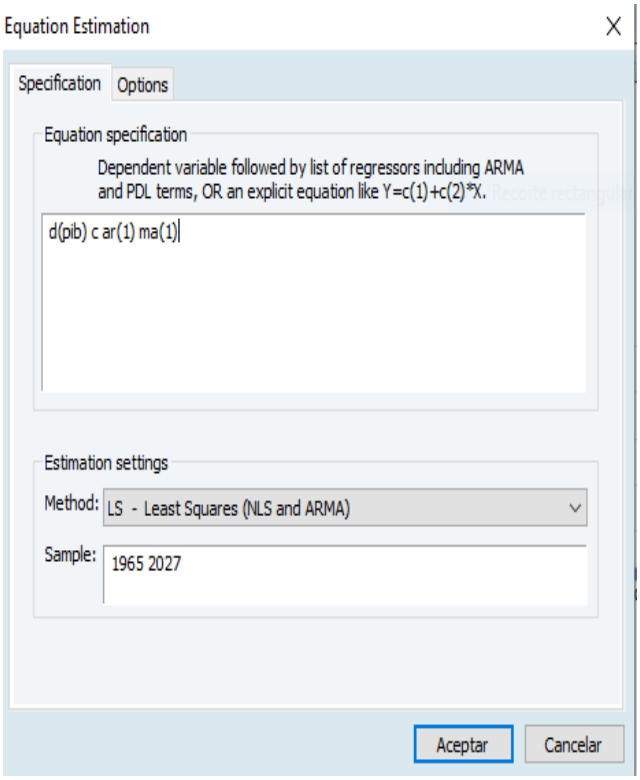

Table 8. Results of the ARMA Estimation by Maximum Likelihood (OPG - BHHH) d(pbi) c ar(1) ma(1)

View Proc Object Print Name Freeze Estimate Forecast Stats Resids

Dependent Variable: D(PIB)
Method: ARMA Maximum Likelihood (OPG - BHHH)
Date: 09/15/25 Time: 12:54
Sample: 1966 2023
Included observations: 58
Convergence achieved after 32 iterations
Coefficient covariance computed using outer product of gradients

Variable	Coefficient	Std. Error	t-Statistic	Prob.
C	2050.847	746.0807	2.748827	0.0081
AR(1)	0.061898	0.423412	0.146188	0.8843
MA(1)	0.237986	0.418702	0.568391	0.5721
SIGMASQ	16500629	2247270.	7.342521	0.0000

R-squared	0.084901	Mean dependent var	2048.414
Adjusted R-squared	0.034062	S.D. dependent var	4283.441
S.E. of regression	4209.857	Akaike info criterion	19.59629
Sum squared resid	9.57E+08	Schwarz criterion	19.73839
Log likelihood	-564.2925	Hannan-Quinn criter.	19.65164
F-statistic	1.670001	Durbin-Watson stat	1.984593
Prob(F-statistic)	0.184307		

Inverted AR Roots	.06
Inverted MA Roots	-.24

INQUIDE
Chemical Engineering & Development
Journal of Science and Engineering
Vol. 08 / Nº 01
e – ISSN: 3028-8533
ISSN – L: 3028-8533

{Ho: φ_0=0

{H_1: φ_0≠0 significant because the p-value is 0.0001

So phase 2 does comply because the values of the coefficients are significant.
P-Value:
If $p < 0.05 \rightarrow$ you reject H_0
If $p \geq 0.05 \rightarrow$ you don't reject H_0

Phase 3: Diagnosis
It is a function of the normality of errors and Autocorrelation of errors.
View
Residual Diagnostic
Histogram – Normality Test

Graph 4: Histogram of the residues

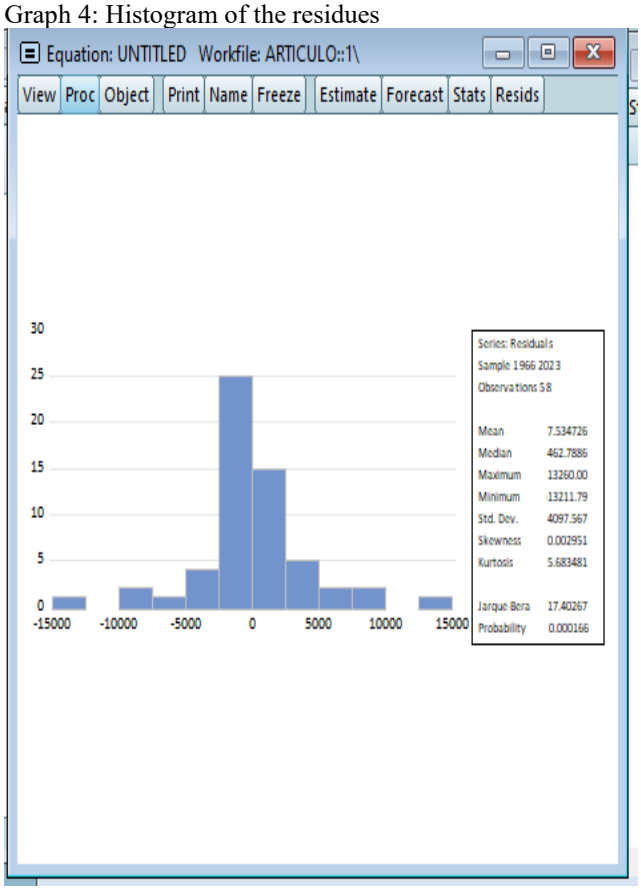

Figure 4.- Histogram of the residuals

**In this graph we see that errors tend to be normal with mean 0 and variance 1.
The Jarque-Bera probability is 0.000166 therefore the distribution of errors is Not Normal.
So we go back to Phase 1.
Then equation d(gbi) c ar(1) ma(1)
We then check for autocorrelation
View
Residual Diagnostic
Correlogram-Q-Statistics

Table 9. Map of the d(gdp) model c ar(1) ma(1)

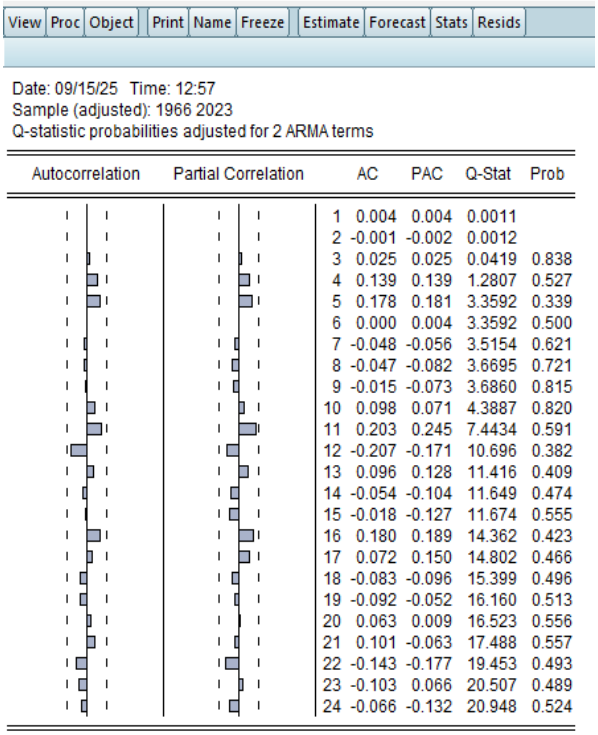

Autocorrelation	Partial Correlation		AC	PAC	Q-Stat	Prob
		1	0.004	0.004	0.0011	
		2	-0.001	-0.002	0.0012	
		3	0.025	0.025	0.0419	0.838
		4	0.139	0.139	1.2807	0.527
		5	0.178	0.181	3.3592	0.339
		6	0.000	0.004	3.3592	0.500
		7	-0.048	-0.056	3.5154	0.621
		8	-0.047	-0.082	3.6695	0.721
		9	-0.015	-0.073	3.6860	0.815
		10	0.098	0.071	4.3887	0.820
		11	0.203	0.245	7.4434	0.591
		12	-0.207	-0.171	10.696	0.382
		13	0.096	0.128	11.416	0.409
		14	-0.054	-0.104	11.649	0.474
		15	-0.018	-0.127	11.674	0.555
		16	0.180	0.189	14.362	0.423
		17	0.072	0.150	14.802	0.466
		18	-0.083	-0.096	15.399	0.496
		19	-0.092	-0.052	16.160	0.513
		20	0.063	0.009	16.523	0.556
		21	0.101	-0.063	17.488	0.557
		22	-0.143	-0.177	19.453	0.493
		23	-0.103	0.066	20.507	0.489
		24	-0.066	-0.132	20.948	0.524

Looking at the probabilities of errors are not self-correlated.

Phase 4. Prognosis
2024-2027
Ecuador's GDP forecast for the period 2024-2028 (ARMA Model)

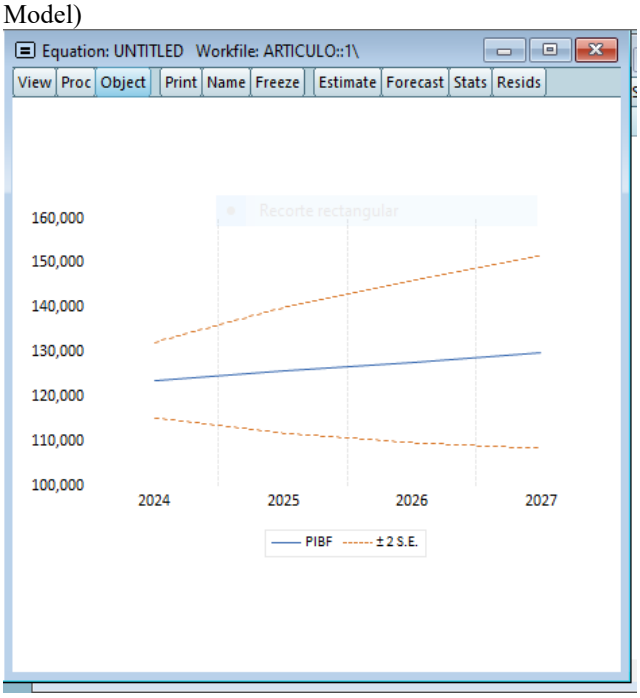

Figure 5. Ecuador's GDP forecast for the period 2024-2028 (ARMA Model)

INQUIDE
Chemical Engineering & Development
Journal of Science and Engineering
Vol. 08 / Nº 01
e – ISSN: 3028-8533
ISSN – L: 3028-8533

Table 11. Ecuador's Gross Domestic Product (GDP): Historical and Forecasted Values

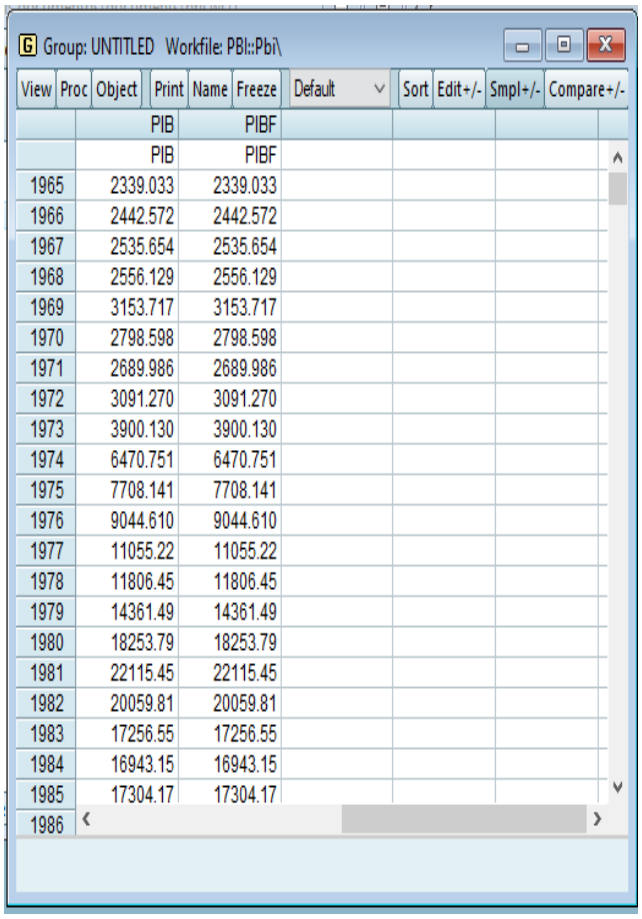

Group: UNTITLED Workfile: PBI::Pbi\

View | Proc | Object | Print | Name | Freeze | Default | Sort | Edit+/- | Smpl+/- | Compare+/-

	PIB	PIBF
	PIB	PIBF
1965	2339.033	2339.033
1966	2442.572	2442.572
1967	2535.654	2535.654
1968	2556.129	2556.129
1969	3153.717	3153.717
1970	2798.598	2798.598
1971	2689.986	2689.986
1972	3091.270	3091.270
1973	3900.130	3900.130
1974	6470.751	6470.751
1975	7708.141	7708.141
1976	9044.610	9044.610
1977	11055.22	11055.22
1978	11806.45	11806.45
1979	14361.49	14361.49
1980	18253.79	18253.79
1981	22115.45	22115.45
1982	20059.81	20059.81
1983	17256.55	17256.55
1984	16943.15	16943.15
1985	17304.17	17304.17
1986		

GDP Trend and Forecast

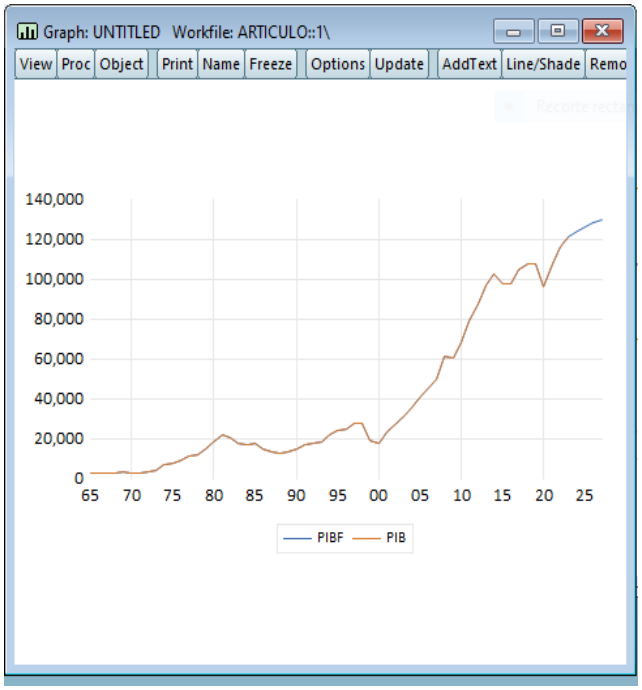

Figure 6.-GDP Trend and Forecast

3.2.- Analysis of results:

The study showed that Ecuador's GDP series was not stationary at its original level, which required the application of the first difference to stabilize the average. The identified ARIMA model integrated autoregressive and moving average components, whose coefficients were statistically significant, confirming the validity of the adjustment. The residuals did not show autocorrelation, which reinforced the adequacy of the model. The forecast for the period 2024–2027 indicated a moderate growth trend, with alternative scenarios that contemplated optimistic and pessimistic variations. These results were consistent with the official estimates issued by national and international organizations, which strengthened the reliability of the analysis carried out.

3.3.- Interpretation of results:

The findings confirmed the usefulness of the Box-Jenkins methodology in predicting Ecuadorian GDP, allowing the temporal dynamics of the economy to be captured in the short term. The projected performance reflected a gradual recovery after recent external shocks, particularly those resulting from the pandemic and oil price volatility. The consistency with the official projections showed that the model can serve as a complement to the economic forecasting systems already implemented, likewise, it was shown that the use of time series contributes to strengthening economic planning, by offering robust estimates in contexts of uncertainty.

4.- Discussion.

The study was based exclusively on historical GDP series, which limited the incorporation of additional structural factors, such as investment, consumption or non-oil exports. The application of ARIMA models, although adequate to capture temporal patterns, did not allow to explain underlying economic causalities. In addition, the non-normality of the residuals in certain models represented a methodological restriction. Finally, the analysis focused on the short term, which reduced its applicability to medium and long-term horizons.

It is recommended to complement future studies with multivariate models, such as VAR or VECM, which allow the inclusion of additional macroeconomic variables to improve explanatory capacity. In the same way, it would be pertinent to integrate hybrid approaches that combine time series techniques with machine learning methods, in order to increase accuracy in high volatility scenarios. clear and technical language, avoiding ambiguities. It is suggested to extend the projection horizon to assess the sustainability of growth in the medium term. For all these reasons, it is recommended to compare the results with sectoral indicators to offer a more comprehensive view of the national economic dynamics.

Vol. 08 / Nº 01
e – ISSN: 3028-8533
ISSN – L: 3028-8533

The results obtained reflected that the Ecuadorian GDP series presented a non-stationary behavior at its original level, which coincided with the dynamic and volatile nature of emerging economies. The application of the first difference allowed stabilizing the series and obtaining an ARIMA model with statistically significant parameters, which confirmed the methodological validity of the Box-Jenkins approach in the analysis of macroeconomic variables. From the theoretical framework, the results ratified the usefulness of time series models in the capture of stochastic patterns, as established by Box and Jenkins in their methodological proposal. The consistency with the official estimates of the Central Bank of Ecuador and ECLAC reinforces the relevance of the model applied, demonstrating that, even in contexts of uncertainty, the methodology used constitutes a robust tool for economic analysis.

In the context of the study, projections indicated moderate GDP growth for the period 2024–2027, suggesting a scenario of gradual recovery after recent external shocks. These findings are directly related to the proposed objective of estimating and forecasting the rate of economic growth in the short term, generating reliable information that supports planning and strategic decision-making.

5.- Conclusions.

The study showed that Ecuador's GDP series was not stationary at its original level, so it required differentiation for its analysis. The identified ARIMA model presented statistically significant coefficients and residuals without autocorrelation, validating its suitability for estimation. The forecasts obtained projected moderate growth of the economy between 2024 and 2027, in accordance with optimistic and pessimistic scenarios, and in line with the official estimates of national and international organizations.

The research provided empirical evidence that confirms the usefulness of the Box-Jenkins methodology in the prediction of macroeconomic variables in contexts of uncertainty. A robust statistical model was offered that complements existing economic forecasting systems, constituting a practical tool for macroeconomic planning and management. In addition, the study strengthened the link between the theoretical analysis of time series and its application in the Ecuadorian economy, contributing both to the academic field and to decision-making in public policies and business strategies.

In the practical field, the results obtained offer a support tool for economic planning and strategic decision-making in the public and private sectors. Short-term projections of GDP make it possible to anticipate growth scenarios, which facilitates the design of more effective fiscal and monetary policies, as well as the preparation of business plans adjusted to the macroeconomic situation.

On the theoretical level, the study reaffirms the relevance of Box-Jenkins models for the analysis of time series applied to emerging economies, demonstrating their ability to capture stochastic patterns and generate reliable forecasts. The research also contributes to the economic literature by validating a specific model for Ecuador, strengthening the evidence on the applicability of advanced econometric methodologies in contexts characterized by high volatility and dependence on external factors.

It is suggested that the time horizon of the projections be extended in order to assess the sustainability of economic growth in the medium and long term. It is also pertinent to incorporate additional macroeconomic variables – such as investment, consumption, non-oil exports and public spending – to enrich the models and improve their explanatory capacity.

Future studies could explore multivariate approaches, such as VAR or VECM, as well as hybrid models that combine time series techniques with machine learning algorithms, which would increase the accuracy of forecasts in high-volatility scenarios. It is also recommended to make comparisons with structural models to analyze not only the temporal dynamics of GDP, but also the causal relationships between the main determinants of economic growth.

Finally, the need to evaluate the results at the sectoral level is raised, with the purpose of identifying specific patterns in key productive branches and strengthening economic planning from a more comprehensive perspective.

6.- Contributions of the authors (Taxonomy of contributors' roles - CRediT)

1. Conceptualization: Leonor Alejandrina Zapata Aspiazu, Edwin Haymacaña Moreno.
2. Data curation: Leonor Alejandrina Zapata Aspiazu.
3. Formal analysis: Leonor Alejandrina Zapata Aspiazu, Edwin Haymacaña Moreno.
4. Acquisition of funds: N/A.
5. Research: Leonor Alejandrina Zapata Aspiazu, Edwin Haymacaña Moreno.
6. Methodology: Francisco Javier Duque-Aldaz, Raúl Alfredo Sánchez Ancajima.
7. Project management: Francisco Javier Duque-Aldaz, Raúl Alfredo Sánchez Ancajima.
8. Resources: Leonor Alejandrina Zapata Aspiazu, Francisco Javier Duque-Aldaz.
9. Software: Leonor Alejandrina Zapata Aspiazu, Edwin Haymacaña Moreno.
10. Supervision: Félix Genaro Cabezas García, Raúl Alfredo Sánchez Ancajima.
11. Validation: Félix Genaro Cabezas García.
12. Visualization: Edwin Haymacaña Moreno.
13. Writing - original draft: Leonor Alejandrina Zapata Aspiazu, Francisco Javier Duque-Aldaz.

14. Writing - revision and editing: Francisco Javier Duque-Aldaz, Félix Genaro Cabezas García, Raúl Alfredo Sánchez Ancajima.

7.- References.

[1] D. V. Desiderio Noboa, "Analysis of demand and delayed effects on the main products in exports (Shrimp, coffee and bananas) to Europe "ARIMA time series model".,» Universidad Católica de Santiago de Guayaquil, 2022. http://repositorio.ucsg.edu.ec/handle/3317/18331

[2] L. Asán Caballero, "Time series prediction algorithm for Air Traffic forecasting based on artificial neural networks.," Cuban Journal of Computer Sciences, vol. 16, no. 4, 2023. http://scielo.sld.cu/scielo.php?script=sci_arttext&pid=S2227-18992022000400084&lang=es

[3] J. W. Tudela-Mamani, E. Cahui-Cahui and G. Aliaga-Melo, "Impact of COVID-19 on Peru's international tourism demand. An application of the Box-Jenkins methodology," Revista de Investigaciones Altoandinas, vol. 24, no. 1, 2022. http://www.scielo.org.pe/scielo.php?script=sci_arttext&pid=S2313-29572022000100027&lang=es

[4] C. A. García Vázquez, A. I. González Santos, and V. Pérez Garrido, "Methodology and validation algorithm to identify models of an air handling unit.," Ingeniería Electrónica, Automatica, y Comunicaciones, vol. 42, no. 1, 2021. http://scielo.sld.cu/scielo.php?script=sci_arttext&pid=S1815-59282021000100105&lang=es

[5] F. de la Oliva de Con and R. Molina Fernández, "Proposal for a procedure for the prediction of the short-term exchange rate through the use of contrasted techniques," Cofin Habana, vol. 14, no. 2, 2020. http://scielo.sld.cu/scielo.php?script=sci_arttext&pid=S2073-60612020000200007&lang=es

[6] F. J. Duque-Aldaz, F. R. Rodríguez-Flores y J. Carmona Tapia, «Identification of parameters in ordinary differential equation systems using artificial neural networks,» San Gregorio, vol. 1, nº 2, 2025. https://revista.sangregorio.edu.ec/index.php/REVISTASANGREGORIO/article/view/2826

[7] G. E. Castro Rosales, A. D. Torres Alvarado, L. S. Zalamea Cedeño, F. J. Duque-Aldaz y F. R. Rodríguez-Flores, «Comprehensive Ergonomic Proposal for the Reduction of Musculoskeletal Risks in Soap Production: An Approach Based on Statistical Analysis and Postural Evaluation,» INQUIDE - Ingeniería Química y Desarrollo, vol. 7, nº 2, 2025. https://doi.org/https://doi.org/10.53591/iqd.v7i02.2416

[8] E. S. Cruz Ramírez, A. F. Calvache Silvestre and D. A. Roldán Carranza, "Estimation of water demand in banana crops applying forecast models for farms of small and medium-sized producers in the province of El Oro," ESPOL, 2024. http://www.dspace.espol.edu.ec/handle/123456789/63220

[9] D. R. Núñez Ordóñez, "Analysis and forecasting of sales for the optimization of import times in the company IMPORGUIDSA through the application of the ARIMA time series model.," Universidad Católica de Santiago de Guayaquil, 2023. http://repositorio.ucsg.edu.ec/handle/3317/21912

[10] F. J. Duque-Aldaz y E. G. Pazan Gómez, «Factors affecting entrepreneurial intention of Senior University Students,» Espacio, vol. 39, nº 09, p. 32, 2017. https://www.revistaespacios.com/a18v39n09/18390932.html

[11] S. F. Chérrez Sánchez, J. V. Palacios Hurtado and F. R. Camacho Villagómez, «Determinants in migration in Ecuador. Period 2000 to 2023.,» Universidad Católica de Santiago de Guayaquil, 2025. http://repositorio.ucsg.edu.ec/handle/3317/24241

[12] F. F. Sandoya Sánchez and V. V. Vásquez Villon, «Deseasonalization of economic series of the national accounts of Ecuador with X12 - ARIMA,» ESPOL. FCNM, 2004. https://www.dspace.espol.edu.ec/handle/123456789/56205

[13] R. I. Romero Ruiz, D. R. Palomeque Calle and F. R. Camacho Villagómez, "Impact of the volatility of the international price of shrimp and cocoa on the export of Ecuador period 2014-2024.", Catholic University of Santiago de Guayaquil, 2024. http://repositorio.ucsg.edu.ec/handle/3317/23299

[14] G. J. Morocho Choca, L. Á. Bucheli Carpio y F. J. Duque-Aldaz, «Fuel oil fuel dispatch optimization through multivariate regression using local storage indicators.,» INQUIDE, vol. 6, nº 2, 2024. https://doi.org/https://doi.org/10.53591/iqd.v6i02.477

[15] F. d. J. Herrera Mendoza, "Incidence of public expenditure on regular basic education in the economic growth of the Northern Region of Peru, 2008-2019," National University of Tumbes, 2024. https://repositorio.untumbes.edu.pe/handle/20.500.12874/65510

[16] F. F. Sandoya Sanchez and A. G. Abad Robalino, «Comparison of the accuracy of the prediction of data of a time series between ARIMA models and Neural Networks,» ESPOL. FCNM, 2017. http://www.dspace.espol.edu.ec/xmlui/handle/123456789/40345

[17] F. A. Ochoa González, "Analysis and prediction of rainfall with artificial intelligence in Esmeraldas-Ecuador," National University of Tumbes, 2024. https://repositorio.untumbes.edu.pe/handle/20.500.12874/65477

[18] J. E. Pincay Moran, A. F. López Vargas, F. J. Duque-Aldaz, W. Villamagua Castillo y R. Sánchez Casanova, «Evaluation and Proposal for an Environmental Management System in a Mango Plantation,» INQUIDE, vol. 7, nº 1, 2025. https://doi.org/https://doi.org/10.53591/iqd.v7i01.1991

[19] A. Varas, K. E. Narváez Bermeo and R. A. Guevara Orozco, «Design of an Inventory Policy based on a demand forecast for a company that is dedicated to the commercialization of aluminum and copper electrical conductors,» ESPOL. FCNM, 2023. http://www.dspace.espol.edu.ec/handle/123456789/65530

Vol. 08 / Nº 01
e – ISSN: 3028-8533
ISSN – L: 3028-8533

[20] K. K. Li Ye and Z. J. Paz and Miño Robles, "Application of the ARIMA model for the forecast of flower exports from Ecuador," Universidad Católica de Santiago de Guayaquil, 2023. http://repositorio.ucsg.edu.ec/handle/3317/21884
[21] L. N. Arango Fuentes, A. J. Tapia Salvador and G. E. Vilela Govea, «Historical analysis and application of predictive models of the price of Ecuadorian tilapia,» ESPOL. FCSH, 2025. http://www.dspace.espol.edu.ec/handle/123456789/65944
[22] R. D. Macías Sandoval and C. J. Tutiven Galvez, «Estimation of the production speed of a mixing machine through the implementation of Machine Learning models,» ESPOL. FIEC, 2025. http://www.dspace.espol.edu.ec/handle/123456789/65804
[23] C. A. Cruz Peña, "Influence of economic growth, inflation and reference interest rate on the profitability of the Lima stock exchange, 1992 - 2022," National University of Tumbes, 2024. https://repositorio.untumbes.edu.pe/handle/20.500.12874/65196
[24] J. S. Fu-López, J. P. Fierro Aguilar, F. R. Rodríguez-Flores y F. J. Duque-Aldaz, «Application of non-automated Lean strategies for quality improvement in manual assembly processes: a case study in the white goods industry.,» INQUIDE - Ingeniería Química y Desarrollo, vol. 7, nº 1, 2025. https://doi.org/https://doi.org/10.53591/iqd.v7i02.2417
[25] J. Lliguizaca Dávila, M. A. Apolinario Rodríguez and B. S. Manzo Robles, "Analysis of the Ecuadorian oil sector during the COVID-19 pandemic and its incidence on the oil trade balance," ESPOL. FICT., 2020. http://www.dspace.espol.edu.ec/xmlui/handle/123456789/50497

INQUIDE
Chemical Engineering & Development
Journal of Science and Engineering

Vol. 08 / Nº 01
e – ISSN: 3028-8533
ISSN – L: 3028-8533

INQUIDE
Ingeniería Química y Desarrollo

Thermo-hydraulic design of an unfinned and finned double pipe heat exchanger for milk cooling. Part 1 - Unfinned heat exchanger.

Diseño térmico-hidráulico de un intercambiador de calor de doble tubo sin y con aletas para el enfriamiento de leche. Parte 1 – Intercambiador de calor sin aletas.

Amaury Pérez Sánchez [1] *; Laura de la Caridad Arias Águila [2]; Heily Victoria González [3]; María Isabel La Rosa Veliz [4]; Zamira María Sarduy Rodríguez [5] & Lizthalía Jiménez Guerra [6]

Received: 06/06/2025 – Accepted: 29/10/2025 – Published: 01/01/2026

Research Articles [X] Review Articles [ ] Essay Articles [ ]

* Corresponding author.

Abstract.
Double-pipe heat exchangers (DPHEs) have acquired significance in recent years as a result of their simple construction, compactness, ease of maintenance and cleaning, and relatively low operating/capital costs, with widespread use in heat transfer services involving sensible heating or cooling of process fluids. This paper aims to design a DPHE from the thermo-hydraulic point of view, to determine its suitability and applicability to cool down a stream of liquid cow's milk using chilled water as coolant. Several design parameters were calculated such as total number of hairpins (21), heat transfer surface area (12.92 m^2), cleanliness factor (0.752) and percent over surface (32.96%), which can be considered as satisfactory. Also, it is required a mass flowrate of chilled water of 9.32 kg/s, classified as high. The designed DPHE cannot be applied satisfactorily in the requested heat transfer service because the pressure drop (9,481,246 Pa) of the tube-side fluid (chilled water) is quite higher than the maximum allowable limit set by the process (85,000 Pa), which also increases the required pumping power for this fluid to an important value (110.5 kW). The designed DPHE will cost around USD $ 45,600 based on May 2025.

Keywords.
Unfinned double pipe heat exchanger; thermal design; number of hairpins; pressure drop; pumping power; purchased cost.

Resumen.
Los intercambiadores de calor de doble tubo (ICDT) han adquirido importancia en años recientes como resultado de su construcción simple, compactación, facilidad de mantenimiento y limpieza, y costos capitales/operación relativamente bajos, con uso extendido en servicios de transferencia de calor que involucren calentamiento y enfriamiento sensible de fluido de proceso. Este artículo tiene como objetivo diseñar un ICDT desde el punto de vista térmico-hidráulico, para determinar su idoneidad y aplicabilidad para enfriar una corriente de leche de vaca liquida usando agua fría como agente de enfriamiento. Varios parámetros de diseño fueron calculados tales como el número total de horquillas (21), área superficial de transferencia de calor (12,92 m^2), factor de limpieza (0,752) y porcentaje de sobre superficie (32,96%), los cuales pueden considerarse satisfactorios. También, se requiere un caudal másico de agua fría de 9,32 kg/s, clasificado como elevado. El ICDT diseñado no puede aplicarse satisfactoriamente en el servicio de transferencia de calor demandado debido a que la caída de presión (9 481 246 Pa) del fluido del lado del tubo (agua de enfriamiento) es muy superior que el limite permisible máximo fijado por el proceso (85 000 Pa), lo cual también incrementa la potencia de bombeo requerida para este fluido hacia un valor importante (110,5 kW). El IDCT diseñado costara alrededor de USD $ 45 600 basado en Mayo del 2025.

Palabras clave.
Intercambiador de calor de doble tubo; diseño térmico; número de horquillas; caída de presión; costo de adquisición.

1. Introduction

Heat exchangers are apparatuses designed to facilitate the transfer of heat between two or more fluids with changing temperatures [1]. In recent decades, the significance of heat exchangers has grown substantially due to their roles in energy efficiency, recovery, and transformation, as well as the integration of alternative energy sources [2].

The thermal energy that passes through a heat exchanger can be either sensible heat or latent heat from the flowing fluids. The fluid supplying the thermal energy is known as the hot fluid, whereas the fluid that absorbs thermal energy is referred as the cold fluid. Within a heat exchanger, the temperature of the hot fluid is expected to decrease, while the cold fluid's temperature will rise. The primary function of a heat exchanger is to either increase or lower the temperature of the target fluid [3].

Heat exchangers are commonly utilized across various sectors including energy production facilities, chemical

[1] University of Camagüey; Faculty of Applied Sciences; amaury.perez84@gmail.com; https://orcid.org/0000-0002-0819-6760, Camagüey; Cuba.
[2] University of Camagüey; Faculty of Applied Sciences; aguilaariaslaura@gmail.com; https://orcid.org/0000-0002-6494-9747, Camagüey; Cuba.
[3] Faculty of Applied Sciences; University of Camagüey; heily.victoria@reduc.edu.cu; https://orcid.org/0009-0007-9319-6506, Camagüey, Cuba.
[4] University of Camagüey; Faculty of Applied Sciences; maria.rosa@reduc.edu.cu; https://orcid.org/0000-0002-9517-6118, Camagüey; Cuba.
[5] University of Camagüey; Faculty of Applied Sciences; zamira.sarduy@reduc.edu.cu; https://orcid.org/0000-0003-1428-3809, Camagüey; Cuba.
[6] University of Camagüey; Faculty of Applied Sciences; lizthalia.jimenez@reduc.edu.cu; https://orcid.org/0000-0002-2471-7263 , Camagüey; Cuba.

Vol. 08 / Nº 01
e – ISSN: 3028-8533
ISSN – L: 3028-8533

manufacturing, biotechnology, the food sector, environmental engineering, and the recovery of waste heat, among others. The most basic type of modern heat exchangers is the double pipe heat exchanger [4], which is also referred to as a hairpin heat exchanger [1].

The DPHE was developed in the late 1940s, and research conducted since that time has largely supported its effectiveness for achieving significant developments. This type of heat exchanger facilitates the transfer of thermal energy principally between hot and cold liquids, usually within concentric piping arranged in various arrangements, initially set up in parallel and later adapted to counterflow designs [5].

A DPHE heat exchanger is made up of a one or more tubes arranged concentrically within a larger diameter pipe, featuring fittings designed to direct the flow from one section to another. In this type of heat exchanger, one fluid circulates inside the inner pipe (tube-side), while another fluid moves through the surrounding annular area (annulus). The inner tube is connected via U-shaped bends that are contained in a return-bed housing [1].

A DPHE can be configured in different series and parallel setups [1] to fulfill the needs for pressure drop, heat transfer, and logarithmic mean temperature difference (LMTD) [6].

This type of heat exchanger is utilized for applications involving low flow rates, a wide range of temperatures [7], and high pressure services due to the narrower pipe sizes [1], and is suitable for continuous operations that require low to medium heat duties [8], specifically for processes needing sensible heating or cooling in fluids, where compact small heat transfer surfaces of up to 50 m^2 are necessary [1].

It finds extensive application in typical industries such as food production, chemicals, biotechnology, and gas and oil processes [9], which often require heating or cooling of process fluids, while it is also widely employed in research facilities related to energy engineering [10].

As noted in [7], the DPHE is crucial for tasks like reheating, pasteurization, heating and preheating. Its affordability in terms of design and maintenance makes it a preferred choice, especially for small-scale industries.

As stated in [6], DPHE is a cost-effective option for closed loop cooling systems where a sufficient supply of appropriate water is accessible at an affordable rate to fulfill the thermal needs.

These heat exchangers are suitable for processes where one of the streams is either a gas or a thick liquid, or when the volume is limited under high fouling situations. This is due to their simple cleaning and maintenance processes. They can serve as a substitute for shell-and-tube heat exchangers when operating as a true counter-flow heat exchanger. DPHEs feature an outer pipe ranging from 50 to 400 mm of internal diameter, and have a standard length of 1.5 to 12.0 m per hairpin. The inner tube's outer diameter can vary from 19 mm to 100 mm. A significant drawback is their bulkiness and high cost per unit of heat transfer surface area [1].

An advantage of the DPHE lies in its affordability in terms of design and maintenance, characterized by a basic configuration that is easy to install, clean, maintain, and adapt, which significantly extends its lifespan and functionality [10].

Peccini et al., [11] suggested that when a stream includes suspended particles, DPHE might be a preferable option since they can incorporate a larger diameter inner tube to prevent blockages. Additionally, this heat exchanger type offers versatility because of its modular design, enabling easier adaptations to modifications in processes. The same authors noted that the longitudinal flow within a DPHE eliminates stagnant zones, which are likely to accumulate deposits in shell and tube exchangers.

It is essential to thermally design heat exchangers in a way that enhances heat transfer while maintaining the pressure drop of the fluids within acceptable limits. A frequent challenge faced by industries is efficiently extracting heat from a utility stream coming out of a specific process and using that energy to heat another process stream.

One way to maximize heat extraction might involve augmenting the heat transfer area or increasing the coolant flow rate; however, both strategies can lead to increased pumping costs, making it unwise to increase these parameters without considering pressure drops. The conventional approach to designing heat exchangers requires careful assessment of all design factors through a detailed process of trial and error, accounting for all potential variations [12].

In [7] it is indicated that engineers encounter significant difficulties while designing an effective heat exchanger. This challenge arises not just from the need to accurately evaluate long-term efficiency and related financial costs, but also from the crucial necessity of thoroughly examining aspects such as heat transfer, pressure drop, and overall effectiveness, which require intensive effort.

According to [13], optimization in the design of heat exchangers is a subject that has been widely explored in existing literature. Most research that has addressed this issue utilized closed-form analytical methods to represent the operational characteristics of the systems, including techniques like the LMTD and effectiveness (ε-NTU) approaches. Such analytical methods rely on the assumption of consistent physical property values and heat transfer coefficients, which can lead to significant inconsistencies in various design scenarios.

In the design of a DPHE, the majority of academic sources [14,15,16] typically incorporate a broader collection of

Vol. 08 / Nº 01
e – ISSN: 3028-8533
ISSN – L: 3028-8533

design elements, such as physical dimensions, fluid distributions, and configurations involving multiple units. They often rely on a conventional process of experimentation and validation; in this method. The design elements are determined initially, and subsequently, the number of required hairpins for that setup is computed. If the heat exchanger obtained is considered unsuitable—due to reasons like the allowable pressure drop for the specified flow rates falling outside predetermined limits or the streams velocity are not within the required limits—a modification in the design is suggested, and calculations are reconsidered.

This methodology relies heavily on the designer's expertise and does not ensure optimal results. Choices available to designers for new tests are various; they might modify lengths, diameters of pipes, arrangements of hairpins, and other characteristics to achieve a decrease in pressure drop or enhance the heat transfer coefficient. Professionals rely on their intuitive judgments to ultimately develop a viable heat exchanger, which is the primary objective of the design approach [11].

Numerous investigations are reported where a DPHE was designed utilizing different methodologies and tools. In this regard, a comprehensive theoretical and practical study was conducted in [6] where simulations were executed to evaluate the design and functionality of a DPHE. This performance assessment was carried out using computational fluid dynamics (CFD), while the overall effectiveness was also calculated.

Likewise, [9] conducted numerical analysis on how the ratio of pipe diameters and the ratio of diameter to length influence the performance of heat exchangers in a DPHE, utilizing CFD software to model the scenarios with incompressible air. They statistically identified and optimized the factors that lead to the maximum heat transfer under constant flow conditions based on the findings. The researchers noted that their results will aid in future investigations into the design of heat exchangers with optimal dimensions for length and diameter.

Additionally, [13] discussed the use of an integer linear programming (ILP) formulation for designing DPHE. The model used for the heat exchanger relied on discretizing conservation equations; consequently, the physical properties were assessed locally, incorporating their temperature dependence into the model. The numerical findings demonstrated the effectiveness of this proposed method, revealing that analytical methods might either underestimate or overestimate the necessary size of a heat exchanger.

In a similar manner, [8] executed an extensive design and assembly of a laboratory-type DPHE suitable for both parallel and counterflow arrangements. The heat exchanger developed in this research was constructed from galvanized steel for both its tube and shell, while the performance metrics (such as LMTD, heat transfer rate, effectiveness, and overall heat transfer coefficient) were collected and compared across the two configurations utilized.

In [1], several DPHEs were thermally designed in order to be utilized as oil coolers in naval ships, while the designed DPHE were evaluated with each other regarding the quantity of hairpins, the pressure drop, and the power required for pumping. This assessment incorporated the Nusselt numbers suggested by various researchers across four different design categories: clean finned, fouled finned, clean unfinned, and fouled unfinned.

Similarly, in [10] the effectiveness of existing theoretical approaches for designing a DPHE with narrow tube spacing and low fluid velocities was assessed, corresponding to laminar flow characteristics of the heat transfer fluid within the annulus. This research scrutinized the reasons behind discrepancies when comparing theoretical findings with experimental data, offering suggestions for the proper design of DPHE.

Likewise, in [17] a DPHE was conceptualized, built, and incorporated into an operating biomass gasification facility to capture heat from the syngas released by the gasifier, which has an exit temperature near 350 ºC.

In [11], the optimization of a DPHE using mathematical methods was explored, focusing on minimizing the exchanger area while accounting for the thermo-fluid dynamic conditions to apply the appropriate transport correlations, alongside design constraints like maximum pressure drops and minimum excess area.

This research introduced two mixed-integer nonlinear programming strategies, expanding the range of design variables compared to previous studies. These variables included the distribution of fluid streams (either within the inner tube or the annulus), the diameters of both tubes, tube length, the quantity of parallel branches, the number of units arranged in series and parallel within each branch, as well as the number of hairpins in each unit, which affect how the hairpins are configured.

In [12], the most effective design of a DPHE was expressed as a single-variable geometric programming challenge. Solving this issue provides the optimal dimensions for the inner and outer pipe diameters and the utility flowrate necessary for a DPHE of a specified length, given a predetermined flowrate for the process stream and a defined temperature difference from inlet to outlet.

In [18], a DPHE was designed to investigate the heat transfer process occurring between two fluids (water/water) through a solid separator. It was developed with a counterflow setup, utilizing the LMTD analysis method.

In [19], a method combining gray relational analysis (GRA) with artificial neural networks (ANNs) and genetic algorithms (GAs) was utilized to assess the importance of

Vol. 08 / Nº 01
e – ISSN: 3028-8533
ISSN – L: 3028-8533

parameters such as effectiveness, thermal resistance, and overall heat transfer coefficient, to rank these parameters in a specific sequence. The integrated methodology introduced in this research has the potential to enhance problem-solving abilities and offer insightful knowledge to improve heat exchanger performance across different industries.

In [20] the calculation of thermal design parameters of a DPHE was outlined to ensure effective heating and sterilization of an organic fluid stream used in the seed-skin separation process for various vegetables.

Lastly, [21] explored both analytical and numerical methods in designing a DPHE. The analysis included the consideration of sensible heat transfer, and the heat exchanger was customized to fit the real operating conditions of a chemical facility. This research employed an analytical model using the effectiveness-number of transfer units (ε-NTU) method alongside the LMTD approach in the design of the DPHE, with performance charts created during the design phase for the specified heat exchanger.

In a Cuban dairy processing plant it's required to cold down a liquid cow's milk stream using chilled water, and for that two DPHEs have been proposed, the first one unfinned and the second with longitudinal fins in the inner tube (finned). In this context, the present paper is the first part of a two-part project, where an unfinned DPHE is designed in order to know if this heat exchanger is suitable to implement in this heat transfer service through the calculation of several design parameters such as the total number of hairpins, the cleanliness factor, the percent over surface, the pressure drop and the pumping power of both liquid streams, among others.

Likewise, the purchase cost of the unfinned DPHE was also calculated. In the second paper, a finned DPHE is designed where the key design parameters previously mentioned are also computed, while the results will be compared and evaluated with respect to those calculated for the unfinned DPHE of the present study, in order to select the most suitable, economical and applicable DPHE from the thermo-hydraulic point of view to carry out this heat transfer service.

2. Materials and methods.

2.1. Problem statement.

It is required to cool down 4,320 kg/h of a liquid cow's milk stream from 60 ºC to 10 ºC by means of chilled water available at 2 ºC, where the outlet temperature of the chilled water stream must not exceed 8 ºC. The following data are available for the tube and the annulus:

- Nominal diameter annulus: 2 in.
- Nominal diameter inner tube: 1 in.
- Length of tube: 3 m.
- Number of tubes inside the annulus: 1.
- Tube material: Carbon steel.
- Thermal conductivity of the tube material: 52 W/m.K.

Design an unfinned double pipe heat exchanger using the methodology reported by [15], where several thermo-hydraulic and design parameters should be calculated such as the heat transfer surface area, the total number of hairpins, the cleanliness factor, the percent over surface, the pressure drop and the pumping power of both liquid streams. It's required that the pressure drop for both the tube-side and annulus fluid don't exceed 85,000 Pa. Lastly; calculate the purchased equipment cost of the designed DPHE and update it to 2025.

2.2. Design methodology.

Percent over surface

Step 1. Definition of the initial parameters for the streams:
Table 1 presents the initial parameters that must be defined for both fluid streams

Table 1. Initial parameters to be defined for both streams.

Parameter	Hot fluid	Cold fluid	Units
Mass flowrate	m_h	m_c	kg/h
Inlet temperature	T_1	t_1	ºC
Outlet temperature	T_2	t_2	ºC
Maximum allowable pressure drop	ΔP_{mh}	ΔP_{mc}	Pa
Fouling factor	R_h	R_c	m^2.K/W

Source: Own elaboration.

Step 2. Definition of the geometric dimensions for the hairpins:
Table 2 shows the geometric dimensions to be defined for the hairpins.

Table 2. Geometric dimensions to be defined for the hairpins.

Parameter	Symbol	Units
Tube length	L_t	m
Internal diameter annulus	D_i	m
Internal diameter inner tube	d_i	m
External diameter inner tube	d_e	m
Thermal conductivity metallic material of the inner pipe	k_m	W/m.K

Source: Own elaboration.

Step 3. Definition of the flow arrangement inside the double-pipe heat exchanger:

- Counterflow.
- Parallel.

Step 4. Allocation of fluids inside the double-pipe heat exchanger

INQUIDE
Chemical Engineering & Development
Journal of Science and Engineering
Vol. 08 / Nº 01
e – ISSN: 3028-8533
ISSN – L: 3028-8533

Step 5. Consider insulation of the double-pipe heat exchanger against heat losses.

Step 6. Average temperature of both fluids:

- Hot fluid (T):

$$\bar{T} = \frac{T_1 + T_2}{2} \quad (1.1)$$

- Cold fluid ($\bar{t}$):

$$\bar{t} = \frac{t_1 + t_2}{2} \quad (1.2)$$

Step 7. Physical parameters of both fluids at the average temperature:
Table 3 displays the physical properties that must be defined for both fluids at the average temperature calculated in the previous step.

Table 3. Physical parameters to be defined for both fluids.

Parameter	Hot fluid	Cold fluid	Units
Density	ρ_h	ρ_c	kg/m^3
Viscosity	μ_h	μ_c	Pa.s
Heat capacity	Cp_h	Cp_c	kJ/kg.K
Thermal conductivity	k_h	k_c	W/m.K

Source: Own elaboration.

Step 8. Heat load (Q):

- Using the data for the hot fluid:

$$Q = \frac{m_h}{3{,}600} \cdot Cp_h \cdot (T_1 - T_2) \quad (1.3)$$

- Using the data for the cold fluid:

$$Q = \frac{m_c}{3{,}600} \cdot Cp_c \cdot (t_2 - t_1) \quad (1.4)$$

Where both m_h and m_c are given in kg/h.

Step 9. Mass flowrate of one stream:

- Mass flowrate of the hot fluid:

$$m_h = \frac{Q}{Cp_h \cdot (T_1 - T_2)} \quad (1.5)$$

- Mass flowrate of the cold fluid:

$$m_c = \frac{Q}{Cp_c \cdot (t_2 - t_1)} \quad (1.6)$$

Step 10. Tube wall temperature (T_w):

$$T_w = \frac{1}{2} \cdot (\bar{T} + \bar{t}) \quad (1.7)$$

Step 11. Viscosity of both fluids at the tube wall temperature:
Hot fluid (μ_{hw}) [Pa.s].
Cold fluid (μ_{cw}) [Pa.s].

Step 12. Net free flow area of the inner tube (A_{ct}):

$$A_{ct} = \frac{\pi \cdot d_i^2}{4} \quad (1.8)$$

Step 13. Velocity of the tube-side fluid (v_t):

$$v_t = \frac{m_t}{\rho_t \cdot A_{ct}} \quad (1.9)$$

Where m_t is given in kg/s.

Step 14. Reynolds number of the tube-side fluid (Re_t):

$$Re_t = \frac{\rho_t \cdot v_t \cdot d_i}{\mu_t} \quad (1.10)$$

Step 15. Prandtl number of the tube-side fluid (Pr_t):

$$Pr_t = \frac{Cp_t \cdot \mu_t}{k_t} \quad (1.11)$$

Where Cp_t is given in J/kg.K.

Step 16. Nusselt number for the tube-side fluid (Nu_t):

- Laminar flow ($Re_t < 2{,}300$)

$$Nu_t = 1.86 \cdot (Re_t \cdot Pr_t)^{0.33} \cdot \left(\frac{d_i}{L_t}\right)^{0.33} \cdot \left(\frac{\mu_t}{\mu_{tw}}\right)^{0.14} \quad (1.12)$$

Valid for smooth tubes for the following conditions:

$$0.48 < Re_t \cdot Pr_t < 16{,}700$$

$$0.0044 < \left(\frac{\mu_t}{\mu_{tw}}\right)^{0.14} < 9.75$$

$$\left(Re_t \cdot Pr_t \cdot \frac{d_i}{L_t}\right)^{0.33} \left(\frac{\mu_t}{\mu_{tw}}\right)^{0.14} \geq 2$$

- Turbulent flow ($2{,}300 < Re_t < 10^4$) [Gnielinski's correlation]:

$$Nu_t = \frac{\left(\frac{f_t}{2}\right) \cdot (Re_t - 1{,}000) \cdot Pr_t}{1 + 12.7 \cdot \left(\frac{f_t}{2}\right)^{0.5} \cdot \left(Pr_t^{2/3} - 1\right)} \quad (1.13)$$

Where f_t is the Fanning friction factor for the tube-side fluid and is calculated using the following correlation:

$$f_t = (1.58 \cdot lnRe_t - 3.28)^{-2} \quad (1.14)$$

- Turbulent flow ($10^4 < Re_t < 5 \times 10^6$) [Prandtl's correlation]:

$$Nu_t = \frac{\left(\frac{f_t}{2}\right) \cdot Re_t \cdot Pr_t}{1 + 8.7 \cdot \left(\frac{f_t}{2}\right)^{0.5} \cdot (Pr_t - 1)} \quad (1.15)$$

Valid for $Pr_t > 0.5$.
Where:

$$f_t = (1.58 \cdot lnRe_t - 3.28)^{-2} \quad (1.14)$$

Step 17. Heat transfer coefficient for the tube-side fluid (h_t):

INQUIDE
Chemical Engineering & Development
Journal of Science and Engineering
Vol. 08 / Nº 01
e – ISSN: 3028-8533
ISSN – L: 3028-8533

$$h_t = \frac{Nu_t \cdot k_t}{d_i} \quad (1.16)$$

Step 18. Net free flow area of the annulus (A_{ca}):

$$A_{ca} = \frac{\pi \cdot (D_i^2 - d_e^2)}{4} \quad (1.17)$$

Step 19. Velocity of the annulus fluid (v_a):

$$v_a = \frac{\frac{m_a}{3{,}600}}{\rho_a \cdot A_{ca}} \quad (1.18)$$

Step 20. Hydraulic diameter (D_h):

$$D_h = D_i - d_e \quad (1.19)$$

Step 21. Reynolds number of the annulus fluid (Re_a):

$$Re_a = \frac{\rho_a \cdot v_a \cdot D_h}{\mu_a} \quad (1.20)$$

Step 22. Prandtl number of the annulus fluid (Pr_a):

$$Pr_a = \frac{Cp_a \cdot \mu_a}{k_a} \quad (1.21)$$

Where Cp_a is given in J/kg.K.

Step 23. Nusselt number for the annulus fluid (Nu_a):

- Laminar flow (Re_a < 2,300)

$$Nu_a = 1.86 \cdot (Re_a \cdot Pr_a)^{0.33} \cdot \left(\frac{D_h}{L_t}\right)^{0.33} \cdot \left(\frac{\mu_a}{\mu_{aw}}\right)^{0.14} \quad (1.22)$$

Valid for smooth tubes for the following conditions:

$0.48 < Re_a \cdot Pr_a < 16{,}700$

$0.0044 < \left(\frac{\mu_a}{\mu_{aw}}\right)^{0.14} < 9.75$

$\left(Re_a \cdot Pr_a \cdot \frac{D_h}{L_t}\right)^{0.33} \left(\frac{\mu_a}{\mu_{aw}}\right)^{0.14} \geq 2$

- Turbulent flow (2,300 < Re_a < 10^4) [Gnielinski's correlation]:

$$Nu_a = \frac{\left(\frac{f_a}{2}\right) \cdot (Re_a - 1{,}000) \cdot Pr_a}{1 + 12.7 \cdot \left(\frac{f_a}{2}\right)^{0.5} \cdot (Pr_a^{2/3} - 1)} \quad (1.23)$$

Where f_a is the Fanning friction factor for the annulus fluid and is calculated using the following correlation:

$$f_a = (1.58 \cdot lnRe_a - 3.28)^{-2} \quad (1.24)$$

- Turbulent flow (10^4 < Re_a < 5 x 10^6) [Prandtl's correlation]:

$$Nu_a = \frac{\left(\frac{f_a}{2}\right) \cdot Re_a \cdot Pr_a}{1 + 8.7 \cdot \left(\frac{f_a}{2}\right)^{0.5} \cdot (Pr_a - 1)} \quad (1.25)$$

Valid for Pr_a > 0.5.

Where:

$$f_a = (1.58 \cdot lnRe_a - 3.28)^{-2} \quad (1.24)$$

Step 24. Equivalent diameter for heat transfer (D_e):

$$D_e = \frac{D_i^2 - d_e^2}{d_e} \quad (1.26)$$

Step 25. Heat transfer coefficient for the annulus fluid (h_a):

$$h_a = \frac{Nu_a \cdot k_a}{D_e} \quad (1.27)$$

Step 26. Fouled overall heat transfer coefficient based on the outside area of the inner tube (U_f):

$$U_f = \frac{1}{\frac{d_e}{d_i \cdot h_t} + \frac{d_e \cdot R_t}{d_i} + \frac{d_e \cdot ln\left(\frac{d_e}{d_i}\right)}{2 \cdot k_m} + R_a + \frac{1}{h_a}} \quad (1.28)$$

Step 27. Log-mean temperature difference (ΔTm):

- For parallel flow:

$$\Delta Tm = \frac{(T_1 - t_1) - (T_2 - t_2)}{ln\frac{(T_1 - t_1)}{(T_2 - t_2)}} \quad (1.29)$$

- For counterflow:

$$\Delta Tm = \frac{(T_1 - t_2) - (T_2 - t_1)}{ln\frac{(T_1 - t_2)}{(T_2 - t_1)}} \quad (1.30)$$

Step 28. Heat transfer surface area (A_o):

$$A_o = \frac{Q \cdot 1{,}000}{U_f \cdot \Delta Tm} \quad (1.31)$$

Where Q is given in kW.

Step 29. Heat transfer area per hairpin (A_{hp}):

$$A_{hp} = 2 \cdot \pi \cdot d_e \cdot L_t \quad (1.32)$$

Step 30. Number of hairpins (N_h):

$$N_h = \frac{A_0}{A_{hp}} \quad (1.33)$$

Step 31. Clean overall heat transfer coefficient based on the outside heat transfer area (U_c):

$$U_c = \frac{1}{\frac{d_e}{d_i \cdot h_t} + \frac{d_e \cdot ln\left(\frac{d_e}{d_i}\right)}{2 \cdot k_m} + \frac{1}{h_a}} \quad (1.34)$$

Step 32. Cleanliness factor (CF):

$$CF = \frac{U_f}{U_c} \quad (1.35)$$

INQUIDE
Chemical Engineering & Development
Journal of Science and Engineering
Vol. 08 / Nº 01
e – ISSN: 3028-8533
ISSN – L: 3028-8533

Step 33. Total fouling (R_{ft}):

$$R_{ft} = \frac{1 - CF}{U_c \cdot CF} \quad (1.36)$$

Step 34. Percent over surface (OS):

$$OS = 100 \cdot U_c \cdot R_{ft} \quad (1.37)$$

Pressure drop and pumping power

Step 35. Frictional pressure drop of the tube-side fluid (Δp_t):

$$\Delta p_t = 4 \cdot f_t \cdot \frac{2 \cdot L_t}{d_i} \cdot N_h \cdot \frac{\rho_t \cdot v_t^2}{2} \quad (1.38)$$

Where for laminar flow (Re_t < 2,300):

$$f_t = \frac{16}{Re_t} \quad (1.39)$$

Correction of the Fanning friction factor for laminar flow (f_{ct}):

$$f_{ct} = f_t \cdot \left(\frac{\mu_t}{\mu_{tw}}\right)^m \quad (1.40)$$

Where m = - 0.58 for heating and - 0.50 for cooling under laminar flow.

Step 36. Pumping power for the tube-side fluid (P_t):

$$P_t = \frac{\Delta p_t \cdot m_t}{\eta_p \cdot \rho_t} \quad (1.41)$$

Where m_t is given in kg/s and η_p is the isentropic efficiency of the pump.

Step 37. Frictional pressure drop of the annulus fluid (Δp_a):

$$\Delta p_a = 4 \cdot f_a \cdot \frac{2 \cdot L_t}{D_h} \cdot \rho_a \cdot \frac{v_a^2}{2} \cdot N_h \quad (1.42)$$

Where for laminar flow (Re_a < 2,300):

$$f_a = \frac{16}{Re_a} \quad (1.43)$$

Correction of the Fanning friction factor for laminar flow (f_{ct}):

$$f_{ca} = f_a \cdot \left(\frac{\mu_a}{\mu_{aw}}\right)^m \quad (1.44)$$

Where m = - 0.58 for heating and - 0.50 for cooling under laminar flow.

Step 38. Pumping power for the annulus fluid (P_a):

$$P_a = \frac{\Delta p_a \cdot m_a}{\eta_p \cdot \rho_a} \quad (1.45)$$

Where m_a is given in kg/s and η_p is the isentropic efficiency of the pump.

Purchased equipment cost

According to [22], the purchased equipment cost for a DPHE is calculated using the following correlation:

$$C_{DPHE}^{2007} = 1{,}600 + 2{,}100 \cdot A_o^{1.0} \quad (1.46)$$

Where:

- C_{DPHE}^{2007} - Purchased equipment cost of the DPHE referred to January 2007 (USD $).
- A_o - Heat transfer surface area of the DPHE, calculated in Step 28 (m^2).

Later on, this purchased equipment cost calculated by equation (1.46) is updated to March 2025 using the Chemical Engineering Plant Cost Index corresponding to March 2025 and by applying the following equation:

$$C_{DPHE}^{2025} = C_{DPHE}^{2007} \cdot \frac{CEPCI^{2025}}{CEPCI^{2007}} \quad (1.47)$$

Where:

- C_{DPHE}^{2025} - Purchased equipment cost of the DPHE referred to May 2025 (USD $).
- C_{DPHE}^{2007} - Purchased equipment cost of the DPHE based to January 2007 (USD $).
- $CEPCI^{2025}$ - Chemical Engineering Plant Cost Index referred to May 2025 = 806.8 [23].
- $CEPCI^{2007}$ - Chemical Engineering Plant Cost Index referred to January 2007 = 509.7 [22].

3. Analysis and Interpretation of Results.

3.1. Percent over surface.

Step 1. Definition of the initial parameters for the streams: The following table (Table 4) presents the values of the initial parameters to be defined for both streams.

Table 4. Values of the initial parameters to be defined for both streams.

Parameter	Hot fluid (Milk)		Cold fluid (Water)		Units
	Symbol	Value	Symbol	Value	
Mass flowrate	m_h	4,320	m_c	-	kg/h
Inlet temperature	T_1	60	t_1	2	ºC
Outlet temperature	T_2	10	t_2	8	ºC
Maximum allowable pressure drop	ΔP_{mh}	85,000	ΔP_{mc}	85,000	Pa

INQUIDE
Chemical Engineering & Development
Journal of Science and Engineering
Vol. 08 / Nº 01
e – ISSN: 3028-8533
ISSN – L: 3028-8533

Fouling factor	R_h	0.0001 [δ]	R_c	0.00017 [φ]	m².K/W

Source: Own elaboration.
[δ] Taken from [14].
[φ] Taken from [15].

Step 2. Definition of the geometric dimensions for the hairpins:
Table 5 shows the values of the geometric dimensions to be defined for the hairpins.

Table 5. Values of the geometric dimensions to be defined for the hairpins.

Parameter	Symbol	Value	Units
Length	L_t	3	m
Internal diameter annulus	D_i	0.05250[ϕ]	m
Internal diameter inner tube	d_i	0.02664[ϕ]	m
External diameter inner tube	d_e	0.03340[ϕ]	m
Thermal conductivity metallic material of the inner pipe	k_m	52	W/m.K

Source: Own elaboration.
[ϕ] According to [15].

Step 3. Definition of the flow arrangement inside the double-pipe heat exchanger:
The fluids will flow under counterflow arrangement inside the DPHE.

Step 4. Allocation of fluids inside the double-pipe heat exchanger.
As suggested by [14] and [22], the hot fluid (milk) will be located in the annulus, while the cold fluid (water) will be located in the inner pipe.

Step 5. Consider insulation of the double-pipe heat exchanger against heat losses.
The heat exchanger will be thermally insulated to avoid excessive heat losses.

Step 6. Average temperature of both streams:

- Hot fluid (milk) (T):

$$\bar{T} = \frac{T_1 + T_2}{2} = \frac{60 + 10}{2} = 35\ ºC \quad (1.1)$$

- Cold fluid (water) ($\bar{t}$):

$$\bar{t} = \frac{t_1 + t_2}{2} = \frac{2 + 8}{2} = 5\ ºC \quad (1.2)$$

Step 7. Physical parameters of both fluids at the average temperature:
According to [24,25,26], both the milk and the water have the physical parameters presented in Table 6 at the average temperature calculated in the previous step.

Table 6. Values of the physical parameters for the milk and the water.

Parameter	Hot fluid (Milk) Symbol	Value	Cold fluid (Water) Symbol	Value	Units
Density	ρ_h	1,013.2	ρ_c	999.97	kg/m³
Viscosity	μ_h	0.00106	μ_c	0.00152	Pa.s
Heat capacity	Cp_h	3.919	Cp_c	4.205	kJ/kg.K
Thermal conductivity	k_h	0.580	k_c	0.571	W/m.K

Source: Own elaboration.

Step 8. Heat load (Q):

- Using the data for the hot fluid (milk):

$$Q = \frac{m_h}{3{,}600} \cdot Cp_h \cdot (T_1 - T_2) \quad (1.3)$$

$$Q = \frac{4{,}320}{3{,}600} \cdot 3.919 \cdot (60 - 10) = 235.14\ kW$$

Where m_h is given in kg/h.

Step 9. Mass flowrate of one stream:

- Mass flowrate of the cold fluid (water):

$$m_c = \frac{Q}{Cp_c \cdot (t_2 - t_1)} = \frac{235.14}{4.205 \cdot (8 - 2)} = 9.32\ kg/s \quad (1.6)$$

Step 10. Tube wall temperature (T_w):

$$T_w = \frac{1}{2} \cdot (\bar{T} + \bar{t}) = \frac{1}{2} \cdot (35 + 5) = 20\ ºC \quad (1.7)$$

Step 11. Viscosity of both fluids at the tube wall temperature:
According to [25,26], both the milk and the water present the following values of the viscosity at T_w = 20 ºC.

- Hot fluid (milk) (μ_{hw}) [Pa.s] = 0.00205 Pa.s
- Cold fluid (μ_{cw}) [Pa.s] = 0.00100 Pa.s

Step 12. Net free flow area of the inner tube (A_{ct}):

$$A_{ct} = \frac{\pi \cdot d_i^2}{4} = \frac{\pi \cdot 0.02664^2}{4} = 0.00056\ m^2 \quad (1.8)$$

Because the cold fluid (water) will flow in the inner tube, and the hot fluid (milk) will flow in the annulus, the following new nomenclature presented in Table 7 will be applied for the flowrates, physical parameters and fouling factors of both streams.

Table 7. New nomenclature to be applied for both streams.

	Hot fluid (milk)	Cold fluid (water)

INQUIDE
Chemical Engineering & Development
Journal of Science and Engineering
Vol. 08 / Nº 01
e – ISSN: 3028-8533
ISSN – L: 3028-8533

Parameter	Former nomenclature	New nomenclature	Former nomenclature	New nomenclature
Flowrate	m_h	m_a	m_c	m_t
Density	ρ_h	ρ_a	ρ_c	ρ_t
Viscosity	μ_h	μ_a	μ_c	μ_t
Heat capacity	Cp_h	Cp_a	Cp_c	Cp_t
Thermal conductivity	k_h	k_a	k_c	k_t
Fouling factor	R_h	R_a	R_c	R_t

Source: Own elaboration.

Table 8 displays the values of the parameters included in steps 13-25.

Table 8. Values of the parameters included in steps 13-25.

Step	Parameter	Symbol	Value	Units
13	Velocity of the tube-side fluid (water)	v_t	16.64	m/s
14	Reynolds number of the tube-side fluid (water)	Re_t	291,629	-
15	Prandtl number of the tube-side fluid (water)	Pr_t	11.19	-
16	Fanning friction factor for the tube-side fluid (water)	f_t	0.00362	-
	Nusselt number for the tube-side fluid (water)[1]	Nu_t	1,237.84	-
17	Heat transfer coefficient for the tube-side fluid (water)	h_t	26,531.78	W/m^2.K
18	Net free flow area of the annulus	A_{ca}	0.00129	m^2
19	Velocity of the annulus fluid (milk)	v_a	0.92	m/s
20	Hydraulic diameter	D_h	0.0191	m
21	Reynolds number of the annulus fluid (milk)	Re_a	16,796	-
22	Prandtl number of the annulus fluid (milk)	Pr_a	7.16	-
23	Fanning friction factor for the annulus fluid (milk)	f_a	0.00684	-
	Nusselt number for the annulus fluid (milk)[2]	Nu_a	99.49	-
24	Equivalent diameter for heat transfer	D_e	0.0491	m
25	Heat transfer coefficient for the annulus fluid (milk)	h_a	1,175.24	W/m^2.K

Source: Own elaboration.
[1]Since $10^4 < Re_t < 5 \times 10^6$, the tube-side fluid (water) flows under turbulent regime, thus Prandtl's correlation (equation 1.15) was used to calculate the Nusselt number for this fluid. This equation is also valid to use because $Pr_t = 11.19 > 0.5$.
[2]Since $10^4 < Re_a < 5 \times 10^6$, the annulus side fluid (milk) flows under turbulent regime, thus Prandtl's correlation (equation 1.25) will be used to calculate the Nusselt number for this fluid. This equation is also valid to use because $Pr_a = 7.16 > 0.5$.

Table 9 reveals the values of the parameters included in steps 26-34.

Table 9. Values of the parameters included in steps 26.-34.

Step	Parameter	Symbol	Value	Units
26	Fouled overall heat transfer coefficient based on the outside area of the inner tube	U_f	774.31	W/m^2.K
27	Log-mean temperature difference[1]	ΔTm	23.51	ºC
28	Heat transfer surface area	A_o	12.92	m^2
29	Heat transfer area per hairpin	A_{hp}	0.629	m^2

30	Number of hairpins	N_h	21	-
31	Clean overall heat transfer coefficient based on the outside heat transfer area	U_c	1,030.11	W/m^2.K
32	Cleanliness factor	CF	0.752	-
33	Total fouling	R_{ft}	0.00032	m^2.K/W
34	Percent over surface	OS	32.96	%

Source: Own elaboration.
[1]For counterflow arrangement.

3.2. Pressure drop and pumping power.

Table 10 presents the values of the parameters included in steps 35-38.

Table 10. Values of the parameters included in steps 35-38.

Step	Parameter	Symbol	Value	Units
35	Frictional pressure drop of the tube-side fluid (water)	Δp_t	9,481,246	Pa
36	Pumping power for the tube-side fluid (water)[1]	P_t	110.5	kW
37	Frictional pressure drop of the annulus fluid (milk)	Δp_a	77,392	Pa
38	Pumping power for the annulus fluid (milk)[1]	P_a	114.58	W

Source: Own elaboration.
[1]A value of 0.80 was selected for the isentropic efficiency of the pump [15].

3.3. Purchased equipment cost

Using equation (1.46) and for a value of the heat transfer surface area of 12.92 m^2, the purchased equipment cost of the designed DPHE, based on January 2007, is:

$$C_{DPHE}^{2007} = 1{,}600 + 2{,}100 \cdot A_o^{1.0} \quad (1.46)$$
$$= USD\ \$\ 28{,}732$$
$$C_{DPHE}^{2007} \approx 28{,}800$$

Accordingly, the purchased cost of the designed DPHE, referred to May 2025, is:

$$C_{DPHE}^{2025} = C_{DPHE}^{2007} \cdot \frac{CEPCI^{2025}}{CEPCI^{2007}} = 28{,}800 \cdot \frac{806.8}{509.7} \quad (1.47)$$
$$C_{DPHE}^{2025} == USD\ \$\ 45{,}588 \approx 45{,}600$$

4. Discussion

The heat load had a relatively high value of 235.14 kW, while it is needed a mass flowrate of 9.32 kg/s for the chilled water, which can be considered high. This is because the low value required for the outlet temperature of the chilled water stream (8 ºC) which reduced the cold fluid temperature difference ($\triangle t = t_2 - t_1$ = 6 ºC), whereas the somewhat high value of the liquid milk flowrate (4,320 kg/h or 1.2 kg/s) and the relatively high temperature difference of the milk stream ($\triangle T = T_1 - T_2$ = 50 ºC) both also influence in the relatively high value of the heat load, which in turn effects on the high value obtained for the mass flowrate of chilled water, as shown by equation (1.6). In [15] the value of the heat load was 87.1 kW for a water-to-water DPHE.

The value of the velocity of the tube-side fluid (chilled water) is high (16.64 m/s), which is due to the high value obtained for the chilled water mass flowrate. This value of chilled water velocity is 18 times higher than the calculated value of the velocity (0.92 m/s) for the annulus fluid (milk), and is well above the recommended range reported by [22] for the velocity of water in tubular heat exchangers (1.5-2.5 m/s).

The Reynolds number of the tube-side fluid (chilled water) was 291,629, which is 17.4 times higher than the Reynolds number (16,796) of the annulus fluid (milk). This high value obtained for the Reynolds number of the chilled water stream occurs essentially because the high value of the velocity obtained for this fluid. This result agrees with the unfinned water-to-water DPHE designed in [15], where the value of the Reynolds number of the tube-side fluid (159,343) is higher than the Reynolds number of the annulus fluid (15,201).

In case of the Prandtl number, the value of this parameter for the chilled water (11.19) was 1.56 times higher than the Prandtl number for the milk (7.16). This is fundamentally because the highest value of the heat capacity (4,205 J/kg.K) and the viscosity (0.00152 Pa.s) obtained for the water as compared to the values of these parameters for the milk, which were 3,919 J/kg for the heat capacity and 0.00106 Pa.s for the viscosity.

In [1] the Prandtl number of the tube-side fluid (sea water) at a temperature of 25 ºC, in order to cool down a stream of engine oil in a DPHE, was 6.29, with a value for the specific heat capacity and viscosity of 4,004 J/kg.K and 0.000964 Pa.s, respectively. Likewise, in [15] the Prandtl number of

Vol. 08 / Nº 01
e – ISSN: 3028-8533
ISSN – L: 3028-8533

cold water at 27.5 ºC, in order to be heated by hot water in a DPHE, was 5.77, with a value for the specific heat capacity and viscosity of 4,179 J/kg.K and 0.000841 Pa.s, respectively.

Regarding the Nusselt number, the tube-side fluid (chilled water) had a value of 1,237.84 for this parameter, which was 12.44 times higher than the value of the Nusselt number (99.49) for the annulus fluid (milk). Considering that the same equation (Prandtl's correlation) was employed to calculate the Nusselt number for both streams, the highest value obtained of this parameter for the chilled water is due to the higher values that the chilled water stream presents for the Reynolds and Prandtl numbers, as compared to the lower values of these parameters for the milk stream. These results agree with those reported by [1], where the Nusselt number of the tube-side fluid (sea water) ranged from 422.0330 - 634.7506, which were higher than the Nusselt number (34.692) of the annulus fluid (engine oil).

Similarly, they also agree with the results reported by [15] where the Nusselt number (375.3) for the tube-side fluid (hot water) is higher than the Nusselt number (89.0) of the annulus fluid (cold fluid). It is worth to mention that all these authors also employed the Prandtl's correlation applied in our study to calculate the Nusselt number for both streams.

The heat transfer coefficient (26,531.78 W/m^2.K) for the water (tube-side fluid) was 22.57 times higher than the value of the heat transfer coefficient (1,175.24 W/m^2.K) for the milk (annulus fluid). This result is directly influenced by the higher value of the Nusselt number that the chilled water presents with respect to the value of the Nusselt number for the milk.

These findings coincide with the reported by [1], where the values of the heat transfer coefficients for the tube-side fluid (sea water) ranged between 12,885 – 19,379 W/m^2.K and were higher than the value of the heat transfer coefficient (64.549 W/m^2.K) for the annulus fluid (engine oil). In the same way, our results are similar with those reported by [15] where the heat transfer coefficient (4,911 W/m^2.K) of the tube-side fluid (hot water) is 3.65 times higher than the heat transfer coefficient for the annulus (1,345 W/m^2.K).

The value of the pressure drop of the tube side fluid (chilled water) is quite high (9,481,246 Pa), and is well above the maximum allowable limit set by the heat transfer system (85,000 Pa). This occurs fundamentally because the high value of the velocity obtained for this fluid (16.64 m/s) and the relatively high number of hairpins (21). This high value of the pressure drop for the chilled water influences on the significant value of the pumping power obtained for this fluid (110.5 kW). On the other hand, the calculated pressure drop for the annulus fluid (milk, 77,392 Pa) is below the maximum allowable set by the system, thus requiring a pumping power of 114.58 W.

As noted in [15], when a significant volume of fluid moves through the tube or the annulus of a DPHE, the pressure drop can exceed the acceptable levels due to high flow velocities, which applies to our research. In these situations, it is advisable to divide the mass flow into several parallel streams, while the lower mass flow rate side can be placed in a series configuration. Consequently, the system will be organized in a parallel-series layout.

Similarly, [14] points out that an increase in fluid velocity results in greater pressure drops, and if the heat exchanger must be integrated into an existing process, the designer should comply with the maximum permissible pressure drop for both streams. This reference also notes that if the calculated pressure drop is too high, it will be necessary to enlarge the flow area, either by increasing the diameter of the tubes or by adding more parallel branches. Conversely, if the determined pressure drop is smaller than allowable, reducing the flow area could be an option. In either scenario, the design process needs to be restarted.

This author further emphasizes that a smaller flow area for both fluids (and subsequently, a reduced tube diameter) leads to increased velocity and heat transfer coefficients, but it also causes greater pressure drops. He recommends, as an initial step, to choose the tube diameter based on fluid velocities, suggesting speeds of 1-2 m/s for liquids with low viscosity, and also proposing that upon the final length is known, the pressure drop for each fluid can be computed, which may demand adjustments to the chosen pipe diameters.

In [15] the pressure drop of the tube-side fluid is 460.1 Pa, thus requiring a pumping power of 0.84 W, while the pressure drop of the annulus fluid is 2,876.4 Pa, therefore needing a pumping power of 5.0 W. In [1], the pressure drop and the pumping power of the tube-side fluid (sea water) for the unfinned clean DPHE design type are 9,376.4 kPa and 27.468 kW, respectively, while the values of these parameters for the unfinned fouled DPHE design type are 9,597 kPa and 28.114 kW, respectively. This reference also reports that the pressure drop and pumping power for the annulus fluid (engine oil) for the unfinned clean DPHE design type are 42.237 MPa and 298.193 kW, respectively, while the values of these parameters for the unfinned fouled DPHE design type are 43.231 MPa and 305.211 kW, respectively.

Lastly, the designed DPHE will cost around USD $ 45,600 referred to May 2025.

5. Conclusions.

In this paper, an unfinned double-pipe heat exchanger was designed from the thermo-hydraulic point of view, to carry out the cooling of a liquid cow's milk stream using chilled water as coolant.

The hot fluid (milk) was located in the annulus, while the cold fluid (chilled water) was located in the inner tube.

Vol. 08 / Nº 01
e – ISSN: 3028-8533
ISSN – L: 3028-8533

Several design; geometrical and operating parameters were calculated for the DPHE such as the heat transfer surface area (12.92 m^2), total number of hairpins (21), cleanliness factor (0.752) and percent over surface (32.96%), which can be considered as acceptable and adequate. A high value of the required mass flowrate of chilled water was obtained, amounting 9.32 kg/s.

Likewise, the pressure drop of the tube-side fluid is quite high (9,481,246 Pa) and surpasses the maximum allowable pressure drop set by the heat exchange process for both streams (85,000 Pa), whereas the pressure drop of the annulus fluid (77,392 Pa) is below this maximum allowable limit. The high value obtained for the pressure drop of the tube-side fluid increases the required pumping power for this fluid to a significant value (110.5 kW), while the required value of the pumping power for the annulus fluid is 114.58 W. It's concluded that the DPHE designed in this study cannot be successfully implemented in this heat exchange system because of the high values of pressure drop and pumping power obtained for the tube-side fluid (chilled water). The designed DPHE will cost around USD $ 45,600 based on May 2025. It's recommended to increase the diameter of both pipes and redesign the unfinned DPHE to decrease the pressure drop of the tube-side fluid to a value below the minimum allowable limit set by the heat transfer system for this parameter.

6.- Author Contributions (Contributor Roles Taxonomy (CRediT))

1. Formal Conceptualization: Amaury Pérez Sánchez.
2. Data curation: Laura de la Caridad Arias Aguila, Heily Victoria González, Zamira María Sarduy Rodríguez.
3. Formal analysis: Amaury Pérez Sánchez, María Isabel La Rosa Veliz, Lizthalía Jiménez Guerra.
4. Acquisition of funds: Not applicable.
5. Research: Amaury Pérez Sánchez, Laura de la Caridad Arias Aguila, Heily Victoria González, María Isabel La Rosa Veliz
6. Methodology: Amaury Pérez Sánchez, Laura de la Caridad Arias Aguila, Lizthalía Jiménez Guerra.
7. Project management: Not applicable.
8. Resources: Not applicable.
9. Software: Not applicable.
10. Supervision: Amaury Pérez Sánchez, Laura de la Caridad Arias Aguila.
11. Validation: Amaury Pérez Sánchez, Laura de la Caridad Arias Aguila, Heily Victoria González, Zamira María Sarduy Rodríguez.
12. Display: Not applicable.
13. Wording - original draft: Heily Victoria González, María Isabel La Rosa Veliz, Zamira María Sarduy Rodríguez, Lizthalía Jiménez Guerra.
14. Writing - revision and editing: Amaury Pérez Sánchez, Laura de la Caridad Arias Aguila.

7.- References.

[1] C. Ezgi and Ö. Akyol, "Thermal Design of Double Pipe Heat Exchanger Used as an Oil Cooler in Ships: A Comparative Case Study," *Journal of Ship Production and Design,* vol. 35, no. 1, pp. 12-18, 2019. http://dx.doi.org/10.5957/JSPD.170009

[2] N. Kocyigit and H. Bulgurcu, "Modeling of overall heat transfer coefficient of a concentric double pipe heat exchanger with limited experimental data by using curve fitting and ANN combination," *Thermal Science,* vol. 23, no. 6A, pp. 3579-3590, 2019. https://doi.org/10.2298/TSCI171206111K

[3] N. Kumar and A. Bhandari, "Design and Thermal Analysis of Double Pipe Heat Exchanger by Changing Mass Flow Rate," *International Journal of Science, Engineering and Technology,* vol. 10, no. 5, pp. 1-4, 2022.

[4] S. Kotian, N. Methekar, N. Jain, and P. Naik, "Heat Transfer and Fluid Flow in a Double Pipe Heat Exchanger, Part I: Experimental Investigation," *Asian Review of Mechanical Engineering,* vol. 9, no. 2, pp. 7-15, 2020. https://doi.org/10.51983/arme-2020.9.2.2482

[5] S. Alhulaifi, "Computational Fluid Dynamics Heat Transfer Analysis of Double Pipe Heat Exchanger and Flow Characteristics Using Nanofluid TiO2 with Water " *Designs,* vol. 8, p. 39, 2024. https://doi.org/10.3390/designs8030039

[6] Rakesh, C. Nallode, M. Adhvaith, and A. H. A. Krishna, "Design and Performance Analysis of Double Pipe Heat Exchanger," *International Journal of Innovative Research in Science, Engineering and Technology,* vol. 6, no. 7, pp. 12578-12584, 2017. https://doi.org/10.15680/IJIRSET.2017.0607017

[7] Rahman, "Thermal Performance Augmentation of Double-Pipe Heat Exchanger-A Critical Review," *Journal of Heat and Mass Transfer Research,* vol. 12, no. 24, pp. 227 – 246, 2025. https://doi.org/10.22075/JHMTR.2024.34771.1581

[8] E. Ebieto, R. R. Ana, O. E. Nyong, and E. G. Saturday, "Design and Construction of a Double Pipe Heat Exchanger for Laboratory Application," *European Journal of Engineering Research and Science,* vol. 5, no. 11, pp. 1-6, 2020. http://dx.doi.org/10.24018/ejers.2020.5.11.1950

[9] S. Tazegül, M. Bitkin, A. N. Öztekin, A. Korkmaz, Ö. S. Şahin, and O. Babayiğit, "Design and Performance Optimization of Double-Pipe Type Heat Exchangers Based on CFD and Economic Analyses-A Numerical Study," *Journal of Engineering and Sciences,* vol. 2, no. 2, pp. 100-110, 2024.

[10] J. Havlik, T. Dluohy, and J. Krempasky, "Heat Transfer in Double Pipe Heat Exchangers With Small Tube Spacing," *Journal of Fluids Engineering,* vol. 147, pp. 1-10, 2025. https://doi.org/10.1115/1.4066930

[11] Peccini, J. C. Lemos, A. L. H. Costa, and M. J. Bagajewicz, "Optimal Design of Double Pipe Heat Exchanger Structures," *Industrial & Engineering Chemistry Research,* vol. 58, pp. 12080-12096, 2019. https://doi.org/10.1021/acs.iecr.9b01536

[12] P. K. Swamee, N. Aggarwal, and V. Aggarwal, "Optimum design of double pipe heat exchanger," *International Journal of Heat and Mass Transfer,* vol. 51, pp. 2260-2266, 2008. https://doi.org/10.1016/j.ijheatmasstransfer.2007.10.028

[13] L. M. Nahes, M. J. Bagajewicz, and A. L. H. Costa, "Design Optimization of Double-Pipe Heat Exchangers Using a Discretized Model," *Industrial & Engineering Chemistry Research,* vol. 60, p. 17611−17625, 2021. https://doi.org/10.1021/acs.iecr.1c02455

[14] E. Cao, *Heat transfer in process engineering*. New York, USA: McGraw-Hill, 2010.

[15] S. Kakaç, H. Liu, and A. Pramuanjaroenkij, *Heat Exchangers - Selection, Rating, and Thermal Design*, 3rd ed. Boca Raton, USA: Taylor & Francis Group, LLC, 2012. https://doi.org/10.1201/b11784

[16] M. Flynn, T. Akashige, and L. Theodore, *Kern's Process Heat Transfer*, 2nd ed. Beverly, USA: Scrivener Publishing, 2019. https://doi.org/10.1002/9781119364825

[17] N. Nwokolo, P. Mukumba, and K. Obileke, "Thermal Performance Evaluation of a Double Pipe Heat Exchanger Installed in a Biomass Gasification System," *Journal of Engineering and Sciences,* pp. 1-8, 2020. https://doi.org/10.1155/2020/6762489

[18] F. Joshua, "Design and Construction of a Concentric Tube Heat Exchanger," *AU J.T.,* vol. 13, no. 2, pp. 128-133, 2009.

[19] Venkatesh *et al.*, "Design Optimization of Counter-Flow Double-Pipe Heat Exchanger Using Hybrid Optimization Algorithm," *Processes,* vol. 11, p. 1674, 2023. https://doi.org/10.3390/pr11061674

[20] R. Gutiérrez, A. A. d. l. Rosa, L. V. Benítez, R. Serrano, and Y. Aguilera, "Determination of Thermic Parameters of a Heat Exchanger of Concentric Tubes with Organic-Steam Fluids," *Revista Ciencias Técnicas Agropecuarias,* vol. 26, no. 4, pp. 76-88, 2017.

[21] K. Silaipillayarputhur, T. A. Mughanam, A. A. Mojil, and M. A. Dhmoush, "Analytical and Numerical Design Analysis of Concentric Tube Heat Exchangers – A Review," *IOP Conf. Series: Materials Science and Engineering,* vol. 272, p. 012006, 2017. https://doi.org/10.1088/1757-899X/272/1/012006

[22] R. Sinnott and G. Towler, *Chemical Engineering Design*, 6th ed. Oxford, UK: Butterworth-Heinemann, 2020.

[23] S. Jenkins, "Economic Indicators," *Chemical Engineering,* vol. 132, no. 9, p. 56, 2025.

[24] P. Parmar *et al.*, "The Effect of Compositional Changes Due to Seasonal Variation on Milk Density and the Determination of Season-Based Density Conversion Factors for Use in the Dairy Industry," *Foods,* vol. 9, p. 1004, 2020. https://doi.org/10.3390/foods9081004

[25] P. F. Fox and P. L. H. McSweeney, *Dairy Chemistry and Biochemistry*, 1st ed. London, UK: Blackie Academic & Professional, 1998.

[26] ChemicaLogic, "Thermodynamic and Transport Properties of Water and Steam," 2.0 ed. Burlington, USA: ChemicaLogic Corporation, 2003.

Nomenclature.

A_o	Heat transfer surface area	m^2
A_{ca}	Net free flow area of the annulus	m^2
A_{ct}	Net free flow area of the inner tube	m^2
A_{hp}	Heat transfer surface area	m^2
Cp	Heat capacity	kJ/kg.K
CF	Cleanliness factor	-
d_e	External diameter inner tube	m
d_i	Internal diameter inner tube	m
D_e	Equivalent diameter for heat transfer	m
D_h	Hydraulic diameter	m
D_i	Internal diameter annulus	m
f	Fanning friction factor	-
f_c	Corrected Fanning friction factor	-
h	Heat transfer coefficient	$W/m^2.K$
k	Thermal conductivity	W/m.K
k_m	Thermal conductivity metallic material of the inner pipe	W/m.K
L_t	Tube length	m
m	Mass flowrate	kg/h
m	Factor	-
N_h	Number of hairpins	-
Nu	Nusselt number	-
OS	Percent over surface	%
P	Pumping power	kW or W
Pr	Prandtl number	-
Δp	Frictional pressure drop	Pa
ΔP_m	Maximum allowable pressure drop	Pa
Q	Heat load	kW
R	Fouling factor	$m^2.K/W$
Re	Reynolds number	-
R_{ft}	Total fouling	$m^2.K/W$
t	Temperature cold fluid	ºC
$\bar{t}$	Average temperature cold fluid	ºC
T	Temperature hot fluid	ºC
T_w	Tube wall temperature	ºC
$\bar{T}$	Average temperature hot fluid	ºC
ΔTm	Log-mean temperature difference	ºC
U_c	Clean overall heat transfer coefficient	$W/m^2.K$
U_f	Fouled overall heat transfer coefficient	$W/m^2.K$
v	Velocity	m/s

Vol. 08 / Nº 01
e – ISSN: 3028-8533
ISSN – L: 3028-8533

Greek symbols

ρ	Density	kg/m^3
μ	Viscosity	Pa.s
μ_w	Viscosity of the fluid at the tube wall temperature	Pa.s
η_p	Isentropic efficiency of the pump	-

Subscripts

1	Inlet
2	Outlet
a	Annulus fluid
c	Cold fluid
h	Hot fluid
t	Tube side fluid

INQUIDE
Chemical Engineering & Development
Journal of Science and Engineering

Vol. 08 / Nº 01
e – ISSN: 3028-8533
ISSN – L: 3028-8533

INQUIDE
Ingeniería Química y Desarrollo

Comparative evaluation of granulometric distribution in grains processed by ball and hammer Mills.

Análisis comparativo de la distribución granulométrica de granos molidos en molino de bolas y molino de martillos.

Stefanie Bonilla Bermeo [1]* ; Fernando Noblecilla Arévalo [2] ; Iván Torres Tapia[3] ; Carlos Valdiviezo Rogel[4]

Received: 10/25/2025 – Accepted: 12/05/2025 – Published: 01/01/2026

Research Articles [ ] Review Articles [ ] Essay Articles [X]

* Corresponding author.

Abstract.
The grinding of grains is fundamental in industrial processes, where the resulting particle size distribution directly impacts product quality. This study aimed to compare the granulometric distribution of corn and soybeans processed using a hammer mill, ball mill, and their combination. Samples of corn and soybeans were ground using three configurations: hammer mill, ball mill, and sequential milling with both. The resulting material was sieved to determine weight retained per mesh and calculate characteristic diameters (D10, D50, D90). Additional particle microscopy and ANOVA were performed to evaluate significant differences. The hammer mill produced coarse, heterogeneous distributions, especially for soybeans (D50 ≈ 2.9 mm). The ball mill generated a higher proportion of fine particles in corn (D50 ≈ 1.38 mm) but was ineffective for soybeans (D50 ≈ 3.53 mm). The mill combination achieved the most uniform distribution for both grains (D50 ≈ 1.05–1.25 mm). ANOVA detected no global significant differences, though morphological and distributional disparities were observed in sieve analysis. The combined milling approach optimized granulometric distribution, overcoming the limitations of each individual equipment.

Keywords.
Granulometric distribution, Hammer mill, Ball mill, Corn grinding, Soybean grinding.

Resumen.
La molienda de granos es fundamental en procesos industriales, donde la distribución granulométrica resultante incide directamente en la calidad del producto. El objetivo fue comparar la distribución granulométrica de maíz y soja procesados en molino de martillo, molino de bolas y su combinación. Se molieron muestras de maíz y soja utilizando tres configuraciones: molino de martillo, molino de bolas y la secuencia de ambos. El material obtenido se tamizó, determinándose los porcentajes retenidos por malla y calculándose los diámetros característicos (D10, D50, D90). Adicionalmente, se realizó análisis microscópico de partículas y ANOVA para evaluar diferencias significativas. El molino de martillo produjo distribuciones gruesas y heterogéneas, especialmente en soja (D50 ≈ 2.9 mm). El molino de bolas generó un mayor porcentaje de finos en maíz (D50 ≈ 1.38 mm), pero fue ineficaz para soja (D50 ≈ 3.53 mm). La combinación de molinos logró la distribución más uniforme para ambos granos (D50 ≈ 1.05-1.25 mm). El ANOVA no detectó diferencias significativas globales, aunque se observaron disparidades morfológicas y de distribución en el análisis por tamices. La combinación de molinos optimizó la distribución granulométrica, superando las limitaciones de cada equipo por separado.

Palabras clave.
Distribución granulométrica, Molino de martillo, Molino de bolas, Molienda de maíz, Molienda de soja.

1. Introduction

Particle size reduction is a process implemented in various industries, which consists of reducing the physical dimension of solid materials through the application of mechanical forces. This process is essential in operations such as mixing, drying, sintering and chemical reactions, where particle size can influence the speed and uniformity of the process. Commonly used equipment for size reduction include ball mills, hammer mills, jaw crushers, and roller mills. The choice of the right equipment depends on the properties of the material and the desired particle size, being a critical factor for the optimization of industrial processes. [1]

In addition, particle distribution plays a key role, as it directly affects the quality and properties of the final product, such as flow, compaction and dissolution. Particle size analysis is an essential technique for evaluating the particle size distribution in a pulverized material, and the sieve is one of the most widely used pieces of equipment for this purpose. Accuracy in particle classification is vital to ensure product consistency. [2]

Grinding and size reduction not only increase the specific surface area of materials, but also improve their reactivity and facilitate downstream processes such as dissolution, extraction of compounds of interest, and homogenization into mixtures. In the food industry, for example, proper control of particle size helps to optimize the texture, solubility and bioavailability of nutrients, while in the pharmaceutical industry particle size uniformity is key to ensuring the dosage and controlled release of active ingredients. [3]

In the field of construction and mining materials, the efficiency of comminution equipment, such as ball mills

[1] University of Guayaquil / stefanie.bonillab@ug.edu.ec ; https://orcid.org/0000-0002-9391-3698, Guayaquil; Ecuador.
[2] Independent Researcher / fernandoanoblex18@gmail.com; https://orcid.org/0009-0005-1898-8373, Guayaquil; Ecuador.
[3] Independent Researcher / ivanalejo17@gmail.com;https://orcid.org/0009-0008-9193-0524, Guayaquil; Ecuador.
[4] University of Guayaquil / carlos.valdiviezor@ug.edu.ec; https://orcid.org/0000-0002-6550-975, Guayaquil, Ecuador.

Vol. 08 / Nº 01
e – ISSN: 3028-8533
ISSN – L: 3028-8533

and hammer mills, has a direct impact on energy consumption and operating costs. It is estimated that up to 50% of the total energy used in a mineral processing plant corresponds to milling operations, which makes equipment selection and particle size optimization strategic factors for process sustainability. In addition, excessive particle reduction can lead to material losses due to fines formation, affecting the overall efficiency of the system.[4]

The hammer mill is one of the most widely used equipment for grain size reduction due to its simplicity of design, low cost, and high processing capacity. Its operating principle is based on the repeated impact of rotary hammers on the particles, which generates rapid fractures and produces materials with a relatively heterogeneous particle size. This type of mill is widely used in the food and feed industry, as it allows grains such as corn, wheat and soybeans to be processed efficiently, although it has the disadvantage of generating a higher content of fines and dust. [5]

On the other hand, the ball mill operates under the principle of impact and friction, where spheres of steel or other grinding material rotate inside a cylindrical drum, causing the gradual reduction of the particle size. Unlike the hammer mill, this equipment allows for a more controlled and finer distribution of particles, with less variability in size. Ball mills are widely used in the mining, ceramics, and pharmaceutical industries, as well as in the research of new materials, although they require higher energy consumption and longer operating times compared to hammer mills. [6]

Particle size analysis by sieving, laser diffraction or other modern methods is used as a quality control tool to establish the size distribution in the processed products. The sieving technique, although traditional, is still one of the most widely used due to its low cost, simplicity and reproducibility compared to more sophisticated methods. The information obtained from these analyses makes it possible to establish correlations between the distribution of particles and the behaviour of the material in subsequent processes, guaranteeing the uniformity of the final product and contributing to the optimisation of the production chain. [7]

The choice between a hammer mill and a ball mill depends largely on the material to be processed and the desired properties in the final product. For grains, the hammer mill is preferred for its speed and efficiency in large volumes, while the ball mill is more appropriate when fine, uniform grinding is required. Both pieces of equipment play a fundamental role in the optimization of industrial processes, and their comparison from the perspective of particle size distribution allows us to identify competitive advantages and areas for improvement in the reduction of particle size. In this context, it is pertinent to highlight the importance of milling in massively used grains such as corn and soybeans, whose processing not only responds to industrial purposes, but also to the optimization of the nutritional and functional quality of the derived products. [8][9]

Despite the widespread use of hammer and ball mills in different industries, there are still gaps in the comparative understanding of their efficiency in the size reduction and in the final particle size distribution of grains such as corn and soybeans. While both equipment serves similar functions, differences in their operating principle, energy consumption, and product uniformity can significantly influence the quality and utilization of processed grains. Recent studies have highlighted that grinding parameters, such as rotation speed, ball loading or screen opening, have a direct impact on the distribution of particles and the nutritional quality of the final product. Comparative research has shown that hammer mills tend to generate more irregular particles and a higher content of fines, while ball mills produce more homogeneous distributions, although with higher energy consumption and operating time. However, most of these studies have focused on individual grains or specific experimental conditions, so a more comprehensive analysis is required that relates both equipment under controlled and comparable conditions. In this way, the present research seeks to provide quantitative and updated evidence that allows to guide technical and economic decisions in the processing of corn and soybeans, strengthening the scientific basis for the selection of the most efficient milling system.[10][11]

In the case of grains such as corn and soybeans, which are widely used in the food and feed industry, milling plays a key role in improving their functional and nutritional properties. In corn, the control of particle size influences the digestibility of starch and the quality of derived products such as flour and cereals, while in soybeans it determines the availability of proteins and lipids, in addition to facilitating their incorporation into balanced formulations for animal feed. Studies have shown that the adequate reduction of the particle size in these grains not only optimizes the performance of the extraction processes and digestibility, but also impacts the [12]energy efficiency of the milling and in the final quality of the product. [13]
Previous studies have specific limitations that require attention. For example, research showed that, in corn milling, the specific energy required varies considerably according to the fraction of the material (grain, stubble, rope), which suggests that the data cannot be directly extrapolated to processed commercial grains. Another study showed that the combination of mills (hammers + rollers) improves the uniformity of particle distribution, but it does not directly compare hammer mills vs ball mills in grains such as corn or soybeans. In the field of ball milling, a study looked at how the diameter of the medium affects milling efficiency, but in mineralization, not in agricultural grains, which leaves a gap in knowledge

Vol. 08 / Nº 01
e – ISSN: 3028-8533
ISSN – L: 3028-8533

applicable to the food sector. Consequently, there is a lack of a direct comparison, under controlled conditions of food grains (corn and soybeans), between hammer mills and ball mills, which simultaneously quantifies particle size uniformity, energy consumption and their link with nutritional or procedural functionality. This gap gives relevance and urgency to the present research, aimed at ensuring a solid technical selection of the most suitable grinding system for its industrial application.[14][15][16]

Recent studies indicate that hammer milling can represent up to 50% of a power plant's total electricity consumption. On the other hand, research in biomass shows that the specific energy required for size reduction can vary between 35–65 kJ/kg**,** depending on the type of material and the grinding conditions. In addition, analyses with empirical models indicate that the energy required in ball mills can vary between [17]**~3–12** $kW \cdot h \cdot t^{-1}$ depending on the hardness and desired product size. Therefore, improper selection of the type of mill not only affects the quality of the grind and the particle size uniformity, but can also considerably increase the [18]Operating costs and the Energy consumption, impacting the viability and competitiveness of the industrial process.

Therefore, the objective of this study is to perform a comparative analysis of the particle size distribution of ground grains in ball mills and hammer mills, considering their application in the processing of raw materials such as corn and soybeans. This analysis seeks to establish relationships between the type of equipment, the grinding conditions and the uniformity of the particles obtained, in order to provide technical criteria that guide the selection of the size reduction system based on the efficiency and quality of the final product.

1.1. Grinding

Grinding is a unitary operation which is responsible for reducing the particle size to achieve a size required for a specific process, thus increasing the contact surface of the material for greater efficiency in the industrial process. This reduction is carried out by dividing or fractionating the sample by mechanical means until a required size can be reached.

For Chemical Engineering it is essential to understand the laws that govern disintegration in relation to energy consumption (time), the characteristics of the matter and the type of machines to be used, this demonstrates the study based on deductions and empirical observations. [1]

1.1.1. Types of Grinding

Different types of mills such as ball mill and hammer mill, have different mechanisms of action and efficiency, ball mills are efficient for fixed grinding and hammer mill is more for fragile materials. [19]

1.2. Sieving

The sieving method involves using a series of sieves with different openings to separate soil particles according to their size [20]

1.3. Granulometric analysis by sieving

It is the separation in size of a collection of solid particles according to a particle size scale. This separation is carried out with sieves placed in series, so that the sifting of the first sieve is the feed of the second and so on. [21]
Feeding to the sieve (F): It is the total mass that arrives at the sieve to be separated or classified.
Retained (R): It is the mass that remains on the surface of the sieve.
Sifting (C): It is the mass that passes through the openings of the sieve, that is, that passes through its surface.

1.4. Particle Size Distribution

Particle size distribution describes the proportion of different particle sizes present in a sample. It is essential to characterize the behavior of materials in various industrial processes. [22]

1.5. Granulometric curves

Particle size curves are graphical representations that show the particle size distribution in a sample. These curves are essential to understand the distribution and predictability of material behavior. [23]

2. Materials and methods.

Grinding tests were carried out with two types of grains (corn and soybeans) to evaluate the granulometry that could be obtained from grinding in the ball and hammer mills. We worked with a hammer mill model RBN rose, with 20 hammers with cast bar and 4 shafts, as well as with a tubular, discontinuous steel ball mill, single-chamber, with grate discharge. The calibration of the grinding and sieving equipment was carried out prior to the tests, verifying that all the components: chamber, grinding bodies, sieves and mesh were within their dimensional and mechanical specifications, and ensuring reproducible conditions between replicates. A set of sieves certified to standards equivalent to ASTM E11 / ISO 3310 were used for sieving, and the uniformity of the openings was checked with mesh calibration methods according to recommended procedures in the literature to ensure accuracy and minimize classification errors. The following are the case studies evaluated:

Case 1. Hammer mill grinding and sieving, fig. 1.
Case 2. Ball mill grinding and sieving, fig. 2.
Case 3. Grinding in a hammer mill, followed by the ball mill and sieving, fig. 3.

INQUIDE
Chemical Engineering & Development
Journal of Science and Engineering
Vol. 08 / Nº 01
e – ISSN: 3028-8533
ISSN – L: 3028-8533
INQUIDE
Ingeniería Química y Desarrollo

Once the three cases were carried out, a microscope (Digital Microscope USB) was used to examine the geometry obtained in each type of grinding.

The sampling protocol was established following criteria of representativeness and homogeneity recommended for granulometry studies in agricultural matrices. For each milling treatment, samples were collected immediately after unloading the equipment, employing the manual quartering method to reduce the volume and ensure that the fraction analyzed maintained the original batch distribution. This procedure is widely used in milling studies due to its effectiveness in minimizing size and density segregation biases, especially in grains such as corn and soybeans. Recent research emphasizes that correct homogenization and reduction of batch size is essential to ensure the reproducibility of the particle size distribution, since variations in the sampling protocol can generate differences of up to 15% in the percentage retained by sieve in impact or compression grinding systems. In addition, comparative studies in agricultural milling recommend using between 200 and 500 g as the minimum analytical mass to avoid losses of fine fractions and ensure sufficient representativeness, which was considered in the present work.[24]

For the representation and analysis of the collected data, granulometric distribution graphs of particle size distribution were used. These plots allow the relationship between particle size and the cumulative percentage of the sieved material to be visualized, providing a quantitative and comparative understanding of the particle size distribution.
Finally, the analysis of variance (ANOVA) of a single factor was applied using the Analysis Toolpak complement, which allowed the evaluation of significant differences between treatments.

Fig. 1. Case 1. Hammer mill grinding and sieving.

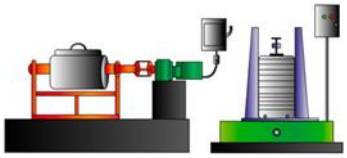

Fig. 2. Case 2. Ball mill grinding and sieving

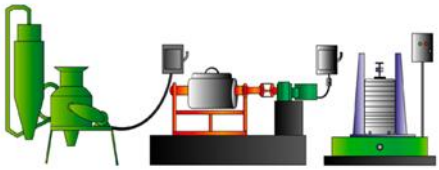

Fig. 3. Case 3. Hammer mill grinding, followed by ball mill and sieving

2.1. Raw material

4540 g of corn and soybeans were used, 2270 g of each grain. Corn with an average diameter of 0.78 mm and grain density of 0.75 g/cm3, soybeans with an average diameter of 0.57 mm and grain density of 0.85 g/cm3.
The moisture of the grain is a determining variable in the efficiency of the milling, as it modifies its hardness, its mechanical response and the resulting granulometry. To maintain experimental stability, the grains were kept in the same batch and stored in a dry environment at a controlled temperature of 22–24 °C, conditions that minimize hygroscopic variation and preserve the physical properties of the material. This approach coincides with recommendations from the literature, which highlight that the simultaneous control of temperature and environmental conditions avoids fluctuations in the internal humidity of the grain and, therefore, in its behavior during the comminution process. This ensures that the observed differences in grain size mainly reflect the performance of the grinding equipment.[25]

2.2. Ball Mill

A ball mill was used, with a ball load configured as indicated in table 1:

Table 1. Configuration of grinding bodies.

Grinding bodies	Average diameter (cm)	Total Weight (g)	% Weight
Small	2.46	5447	18.43
Medium	2.97	9286	31.43
Large	3.89	14815	50.14
Small	2.46	5447	18.43

Source: Bonilla, et al, 2024

The total weight of grinding bodies was 29548 g.
The average weight and equivalent diameter of grinding bodies were determined with the following equations:

$$Peso\ promedio = \frac{\text{peso total de cuerpos moledores}}{\text{número de cuespos moledores}} \quad [1]$$

Average weight= 126.27 g

$$Diámetro\ equivalente = \left[\left(\frac{peso\ promedio}{densidad}\right)\frac{6}{\pi}\right]^{1/3} \quad [2]$$

Equivalent diameter=. 3.12 cm

2.2.1. Parameter Calculations for Ball Mill

The ball mill was fed with 2270 g of each grain (corn and soybean) and the working parameters were determined by the following design equations:

Degree of filling (*f*):

$$f = \frac{Volumen\ de\ la\ carga}{Volumen\ del\ molino} x\ 100 \quad [3]$$

Weight of Grinding Body Load (Q):

INQUIDE
Chemical Engineering & Development
Journal of Science and Engineering
Vol. 08 / Nº 01
e – ISSN: 3028-8533
ISSN – L: 3028-8533

$$Q = \frac{\pi}{4} D^2 \, Li \, f \, Yq \quad [4]$$

Where:
D: Inner diameter of the ball mill, m.
Li: length of the mill, m.
Yq: Equivalent weight of grinding bodies, t/m3

Critical mill speed (nc):

$$nc = \frac{42.3}{\sqrt{D}} \quad [5]$$

Where:
D: Inner diameter of the ball mill, m

$$n = k \, \text{nc} \quad [6]$$

Where:
K: Percentage of Critical Speed (75%)
NC: Critical Speed, RPM

Power of the Ball Mill Motor (N):

$$N = c \, D \, Q \, n \quad [7]$$

Where:
c: power consumption factor, dimensionless
D: inner diameter of the mill, m
Q: Loading weight of ball mill, t
N: Mill Operation Speed, RPM

Specific energy consumption (CEE):

$$CEE = \frac{N}{P} \quad [8]$$

Where:
N: mill power, kW
P: Ball mill production, t

2.3. Hammer Mill

The grains were placed in the feed mouth, passed through the hammers in a period of 4 minutes and received at the unloading, for weighing and sieving.

2.4. Sieving

The sieves were placed in column in an ascending manner according to the sieve number, which means that the sieve with the highest number will receive the finest material. The column of sieves was placed in the vibrating machine for one minute and then each sieve was weighed and the weight of the retained sieve was collected.

The study process flowchart is shown below in Figure 4.

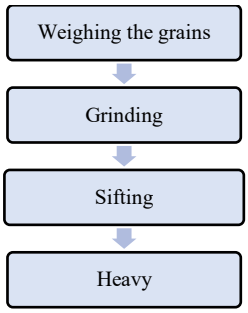

Fig.4. General flow diagram of the process.

2.5. Sieves

The column of sieves used in this study is shown in table 2 with their respective characteristics as follows:

Table 2. Sieve Classification

Mesh Number	Mesh Opening (mm)	Sieve Weight (g)
5	4,00	387
6	3,35	383
8	2,36	372
12	1,70	358
16	1,18	309
18	1,00	303
20	0,85	294
30	0,60	289
50	0,30	255
70	0,212	250
Base	-	270

Source: Bonilla, et al, 2024

3. Analysis and Interpretation of Results.

3.1. Grinding Operating Conditions

The following table 3 presents the working conditions in cases 2 and 3 with both corn and soybean grains.

Table 3. Operating conditions in milling

Parameter	Case 2		Case 3	
Grains	Corn	Soybeans	Corn	Soybeans
Temperature (°C)	27	27	27	27
f (%)	14,13	14,8	14,1	16,51
Q (t)	0,0280	0,0293	0,0279	0,0327
nc (rpm)	68,61	68,61	68,61	68,61
n (rpm) @ 75%	51	51	51	51
N (Hp)	0,194	0,203	0,194	0,203
CEE (kW h / t)	80,61	83,17	80,17	92,70

Source: Bonilla, et al, 2024

Table 3 indicates the conditions used in the ball mill in cases 2 and 3, for both grains worked at room temperature. The degree of filling (*f*) of case 2 with corn presents 14.13% and soybeans 14.8% respectively. The denser the grain, the higher the degree of filling. In case 3 with corn,

Vol. 08 / Nº 01
e – ISSN: 3028-8533
ISSN – L: 3028-8533

it presents 14.1% and soybeans 16.51%, these results depend on factors such as the volume of loading of grinding bodies, volume of raw material and volume of the mill. Therefore, corn flour, being denser, occupies less volume in the mill in contrast to soybean meal that occupies a greater volume in it, for this reason a greater load of grinding bodies was required.

It was necessary to determine the critical speed (nc) at which the mill operates in order not to exceed it since it will cause the centrifugal force to equal the force of gravity and the grinding bodies would not descend to the grinding.

The specific energy consumption (CEE) calculated in case 2 with corn had a consumption of 80.61 kW hr/t for each ton processed, in contrast soybeans increased to 83.7 kW hr/t consumed for each ton processed, this is due to the fact that they worked with a higher load of grinding bodies for this grain so the mill had to consume more energy than with corn. finally, case 3, with corn, presented a consumption of 80.17 kW hr/t for each ton produced and soybeans consumed 92.70 kW hr/t for each ton produced, the difference in specific energy consumption (CEE) between the grains in case 3 is due to the density of the soybean grain. In other words, the higher the degree of filling, the higher the specific energy consumption. [26]

3.2. Mill yields

Table 4 compares the percentage of yield of the mills in the three case studies with corn and soybeans.

Case 1. Hammer mill.
The hammer mill presented a higher yield when processing corn grain compared to soybeans, with a difference of 3.5%. This variation is mainly attributed to the difference in densities of the two
grains. Corn, being less dense, makes it easier to grind compared to soybeans.

Case 2. Ball mill.
In the ball mill, the highest yield was obtained when grinding both grains compared to the three cases analyzed, due to the ability of the ball mill to process almost all the grain fed with losses
attributable to incrustations in the shielding and the mill cover.

Case 3. Hammer mill + ball mill.
The combination of the mills presents a difference between corn and soybeans of 5.47%, in turn it presents a higher percentage of loss compared to cases 1 and 2, this is because the grain goes through two milling processes.
The hammer mill had a superior yield with corn grain compared to soybeans, due to their differences in densities. The ball mill offers a similar performance in both cases, because it does not present a major loss at the time of processing.

Table 4. Mill yields.

	Yield (%)		
	Case #1	Case #2	Case #2
Raw material	Hammer Mill	Ball Mill	Hammer Mill + Ball Mill
Corn	77,05	96,34	74,89
Soy	73,57	96,17	69,47

Source: Bonilla, et al, 2024

3.3. Comparative particle size analysis

3.3.1. Case 1. Hammer Mill with Corn

Figure 5, showing the distribution of particles, which covers a range from 2.33 to 3.7 millimeters, indicates a lack of uniformity in the reduction of size. While the median diameter (D50) is approximately 2.8-2.9 millimeters.

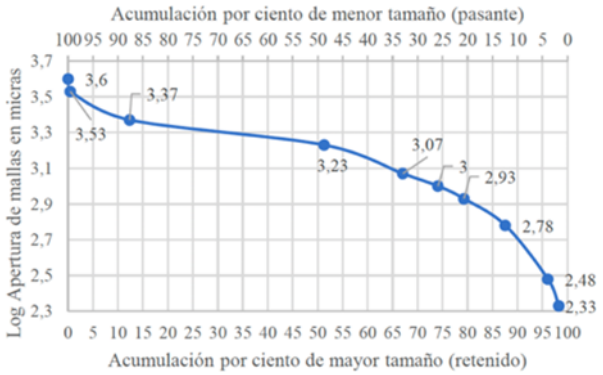

Fig.5. Particle size curve Case 1 (maize)

The data in Table 5 indicate a heterogeneous distribution with a massive concentration in the middle range. Sieve number 12 (2.03 mm/2030 microns) retains 38.94% of the total material, representing the maximum point of distribution. This indicates that the milling process predominantly generates medium-sized particles. Although the coarse fraction is adequately minimized (only 0.47% above 3.68 mm), the low proportion of fines (10.71% under 0.45 mm) suggests inefficiencies in the fracture mechanism, possibly related to rotor speed, residence time, or grain moisture.

Table 5. Experimental data % retained (maize)

Mesh Number	Average particle size (mm)	Average particle size (microns)	% Retained
5	4,00	4000	0,06
6	3,35	3680	0,41
8	2,36	2860	11,87
12	1,70	2030	38,94
16	1,18	1440	15,77
18	1,00	1090	7,04
20	0,85	930	5,18
30	0,60	730	8,32

INQUIDE
Chemical Engineering & Development
Journal of Science and Engineering
Vol. 08 / Nº 01
e – ISSN: 3028-8533
ISSN – L: 3028-8533

50	0,30	450	8,50
70	0,212	260	2,21

Source: Bonilla, et al, 2024

3.3.2. Case 1. Hammer mill (soybean)

Figure 6 shows the distribution of particles in a wide range of sizes from approximately 2.3 mm to 3.7 mm, which indicates a heterogeneous grinding with simultaneous presence of fine and coarse particles. The D50 (medium size) is located around 2.9 mm, the point where 50% of the material is thinner and 50% thicker, a value that represents the characteristic size of the final product. The gentle slope of the accumulation curve suggests an extended distribution with significant dispersion in particle sizes. It is observed that approximately 30-35% of the material has sizes greater than 3.1 mm (coarse fraction), while only about 15-20% is below 2.5 mm (fine fraction), evidencing an imbalance towards larger particles**.** The accumulation of retained material indicates that there is a proportion of particles in the medium range (2.7-3.1 mm), representing between 40-50% of the total**.** This distribution suggests that the grinding process generates an excess of intermediate-sized particles, possibly due to operating parameters such as inadequate rotor speed, insufficient residence time, hammer wear, or excessive sieve opening.

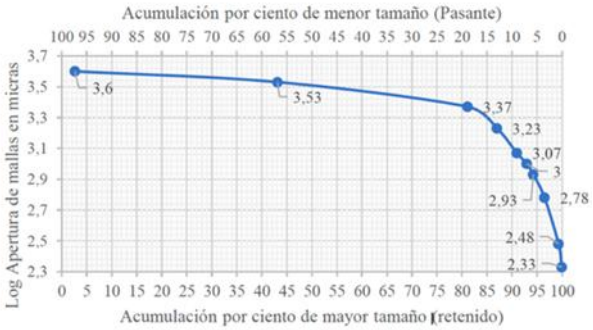

Fig.6. Particle size curve Case 1 (soybean)

The data in Table 6 indicate that the new sieves have a higher percentage of retention for particles in the range of 3680 to 2860 microns, which is associated with the presence of larger particles of soybeans. presence of larger particles of soybeans. In addition, a decrease in the retention percentage is observed for intermediate and small sizes. This trend indicates that the

Table 6. Experimental data % retained (soy)

Mesh Number	Average particle size (mm)	Average particle size (microns)	% Retained
5	4,00	4000	2,66
6	3,35	3680	40,49
8	2,36	2860	37,97
12	1,70	2030	5,87
16	1,18	1440	3,99
18	1,00	1090	1,96
20	0,85	930	1,33
30	0,60	730	2,24
50	0,30	450	2,80
70	0,212	260	0,63

Source: Bonilla, et al, 2024

3.3.3. Case 2. Ball Mill (Corn)

The particle size distribution obtained from the corn mill in the ball mill indicates a wide dispersion of particle sizes. The results in Figure 7 show that the D10 is about 0.48 mm, which means that only 10% of the material is smaller than this value, while the D50 is 1.38 mm, indicating that half of the material is below this size. The 1.96 mm D90 reveals that 90% of the material is smaller than this value. These indicators allow us to infer that the milling produces particles in a considerable range, mostly concentrated between 0.5 mm and 2 mm.

The cumulative distribution shows that the ground material has a significant proportion of coarse particles (>2 mm), approximately 8% of the total, which indicates that the ball mill does not achieve a completely fine grind for all the processed material. The dispersion of particle size is relatively high, as confirmed by the uniformity index **(**D90/D10 ≈ 4.08), indicating that there is a considerable mixture of fine and coarse particles. This characteristic is common in grinding done in ball mills.

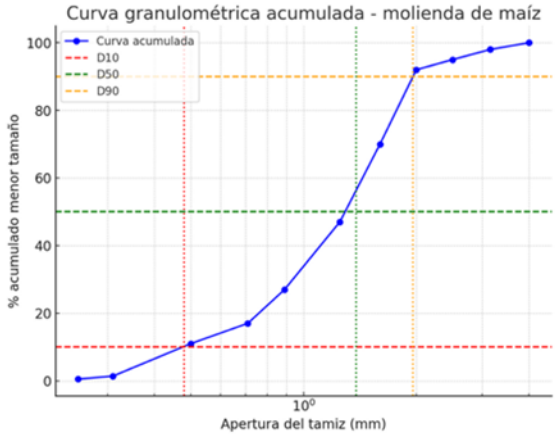

Fig.7. Cumulative particle size curve Case 2 (maize)

3.3.4. Case 2. Ball mill (soybean)

The particle size distribution of the ground soybeans in Figure 8 shows that the material is mostly coarse: the representative parameters are D10 ≈ 1.59 mm**,** D50 ≈ 3.53 mm **and** D90 ≈ 3.94 mm. This indicates that 10% of the particles are smaller than 1.59 mm, the median is 3.53 mm (half of the material is finer than this value) and that 90% is finer than 3.94 mm. These values place most of the mass in the range ~1.6–4.0 mm, with the median close to 3.5 mm. The pitch curve (the through-% in the meshes) has a steep slope in the span between approximately 2.86 mm (18.9% through) and 4.00 mm (97.34% through-screen),

INQUIDE
Chemical Engineering & Development
Journal of Science and Engineering
Vol. 08 / Nº 01
e – ISSN: 3028-8533
ISSN – L: 3028-8533

which means that a significant fraction of the material passes through large meshes and that the "cut-off zone" of the distribution is centered around 3–4 mm. The fraction of fines (<1 mm) is very small (through-% values at 0.45 mm and 0.26 mm are 0.70% and 0.07% respectively), therefore, the fines are practically insignificant in the final product. The dispersion of the distribution can be quantified with the uniformity index D90/D10 ≈ 3.94 / 1.59 ≈ 2.48, indicating a relatively narrow and fairly uniform distribution around coarse sizes (less dispersion than a very wide distribution). In other words, most of the material is clustered in a fairly compact range (mostly between ~1.6 and ~4 mm), without large tails of very fine particles or a very heterogeneous mix of sizes. From an operational and product quality point of view, this granulometry suggests that the milling process is producing a suitable product when looking for coarse or intermediate meal/particles (e.g. for certain industrial uses or animal feed). If the goal was to obtain finer fractions or increase the proportion of particles <1 mm, it would be necessary to intervene in the process (more grinding time, higher impact energy, adjust load and size of media, or use sorting and recirculation).

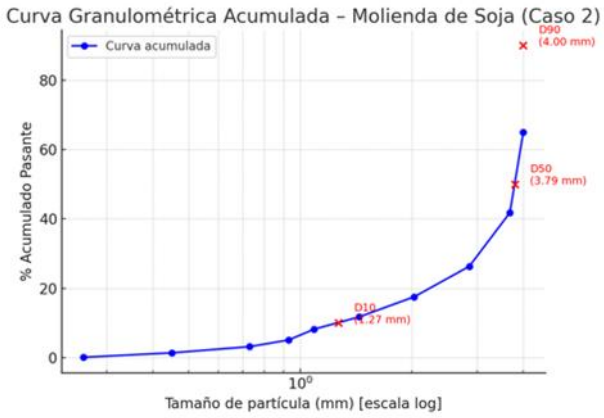

Fig.8. Cumulative particle size curve Case 2 (soybeans)

3.3.5. Case 3. Grinding Hammer Mill + Ball Mill (Corn)

Combined grinding (hammer + balls) generates an intermediate-sized product, with a D50 ≈ 1.08 mm, which means that half of the material is in the range of particles close to 1 mm. The D10 ≈ 0.60 mm indicates the finest fraction of the material, while the D90 ≈ 2.60 mm shows that 90% of the material is below this size, with a wide range of distribution.

The curve accumulated in Figure 9 shows that most of the material is concentrated between 0.6 and 2.6 mm, with a very low fraction of fines (<0.5 mm) (<1%). This indicates that the milling is efficient to produce medium granulometry, without excess powders, a favorable characteristic for uses in animal feed and processes that require an adequate flow without caking.

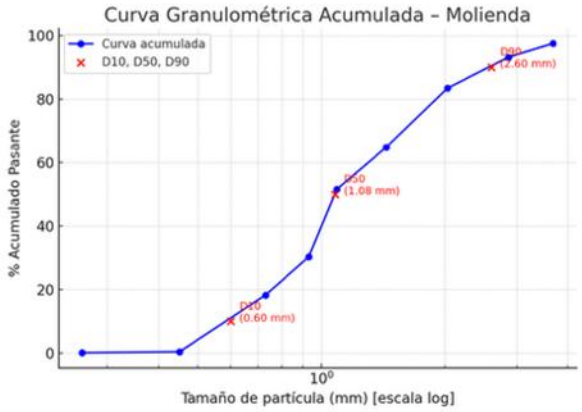

Fig.9. Cumulative particle size curve Case 3 (maize)

The uniformity index, calculated as D90/D10 ≈ 4.3, indicates a wide distribution, with coexistence of fine and coarse particles. This amplitude may be associated with the combination of grinding technologies: the hammer mill breaks more irregularly, and the ball mill refines, but maintains some dispersion.

3.3.6. Case 3. Grinding Hammer Mill + Ball Mill (soybean)

The resulting particle size distribution shows in Figure 10, a clear concentration in the range **≈0.9–1.5 mm**, with D50 ≈ 1.35 mm**,** which means that half of the mass is below that size. The sieving data indicate that the largest quantities were retained in 1.25 mm and 1.00 mm meshes (498 g and 588 g respectively), underlining that the "critical mass" of the material is around these sizes and that the process produced a product of intermediate particle size. The fraction of fines is very small: only 0.94% passes the 0.315 mm mesh and the accumulated through-that mesh is 0.94%, so particles smaller than ≈0.5 mm are practically insignificant. This means low dust generation and greater handling and transport facilities (less aerial dispersion and fewer problems of caking by fines), a positive aspect for logistics and for subsequent processes that benefit from less dusty material. The dispersion of the distribution can be quantified with the uniformity index D90/D10 ≈ 2.05 / 0.77 ≈ 2.66, a value that indicates a relatively narrow **and** homogeneous distribution around the median size. In practice this means that most of the material is grouped in a limited range (low fine tail and moderate coarse tail), which is desirable when looking for reproducibility in rheological, particle size and process properties (mixing, extrusion, pelletizing).

INQUIDE
Chemical Engineering & Development
Journal of Science and Engineering
Vol. 08 / Nº 01
e – ISSN: 3028-8533
ISSN – L: 3028-8533

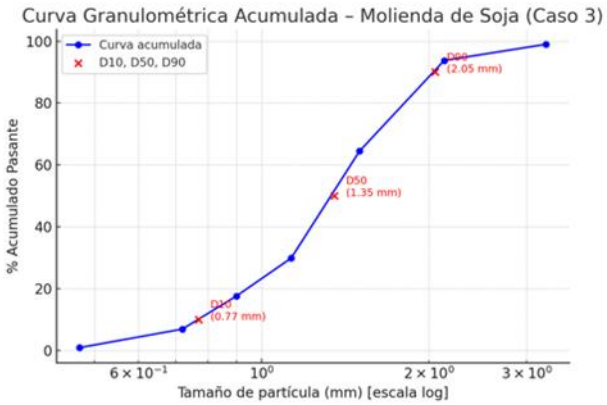

Fig.10. Cumulative particle size curve Case 3 (soybean)

From an operational point of view, these results suggest that the hammer + ball mill combination produced a sufficient reduction for applications requiring intermediate particles.

3.3.7. Comparison of the percentage of retention in each case in the sieves with the smallest and largest aperture.

Table 7 shows a comparison between the three case studies with respect to the percentage of retained obtained in the meshes with the largest aperture (4mm) and smallest aperture (0.121 mm), as well as the retention in the base (<0.212 mm).

Table 7. Comparison of the percentage of detainees.

No. Mesh	Openness (mm)	Case 1 (%)		Case 2 (%)		Case 3 (%)	
		corn	Soy	corn	Soy	corn	Soy
5	4	0,06	2,66	2,47	35,01	0,23	0,77
70	0,212	2,21	0,63	1,12	1,28	1,93	0,28
Base	< 0.212	1,69	0,07	0,04	0,09	0,12	0,14

Source: Bonilla, et al, 2024

The highest percentage of retention in soybean milling was obtained in case 2 with 35.01%, due to the density of the grain compared to corn. In case 3, a decrease in retention is observed since, having a previous grinding in the hammer mill, smaller particles could be obtained. In the three case studies, it was possible to obtain smaller particles, however, the retention percentages do not exceed 3%. The highest accumulation of retained was obtained in corn milling in all three cases, due to the lower density of the grain. The soybean milling in the three case studies did not reach 1% in those retained in the particles less than 0.212 mm. However, in the maize milling, only in case 1 could 1.69% of retained with particle size less than 0.212mm be obtained.

3.3.8. Microscopic analysis of corn and soybean meal

The microscopic analysis of corn flour shows in table 8, differences in the shape of the particles produced by the different case studies.

Case 1 (Hammer Mill): The particles have a rectangular shape, this suggests that the hammer mill's impact mechanism tends to fragment the particles into angular shapes. Case 2 (Ball Mill). The particles have an oval shape, indicating that the abrasion process in the ball mill tends to round the particles. Case 3 (Hammer Mill + Ball Mill): An intermediate shape between rectangular and oval is observed. This may be due to the combination of both grinding processes, which produces a mixture of particle forms. [27]

Table 8. Microscopic analysis of corn flour

Case 1	Case 2	Case 3
	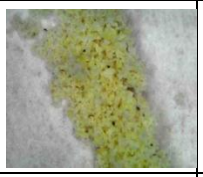	
Particle size: < 0.212 mm Particle shape: Rectangular.	Particle size: < 0.212 mm Particle shape: oval.	Particle size: < 0.212 mm Particle shape: Between rectangular and oval.

Source: Bonilla, et al, 2024

3.3.9. Microscopic analysis of soybean meal

Microscopic analysis of soybean meal shows the following observations in Table 9.

Case 1 (Hammer Mill): The particles have a rectangular shape, the direct impact of the hammer mill produces angular particles similar to those observed in corn. Case 2 (Ball Mill). Particles have an ellipsoid shape. The abrasion process of the ball mill rounds the particles, generating this shape by the mill's impact method and the characteristics of the grain. Case 3 (Hammer Mill + Ball Mill): A mixture of rectangular and ellipsoidal shapes is observed. This can be a result of process combinations, where pre-grinding in the hammer mill followed by abrasion in the ball mill produces a range of various shapes.

Table 9. Microscopic analysis of soybean meal

Case 1	Case 2	Case 3
		
Particle size: < 0.212 mm Particle shape: Rectangular.	Particle size: < 0.212 mm Particle shape: Ellipsoid	Particle size: < 0.212 mm Particle shape: Between rectangular and ellipsoid.

Source: Bonilla, et al, 2024

3.3.10. Statistical analysis

INQUIDE
Chemical Engineering & Development
Journal of Science and Engineering
Vol. 08 / Nº 01
e – ISSN: 3028-8533
ISSN – L: 3028-8533
INQUIDE
Ingeniería Química y Desarrollo

An analysis of variance was performed for a factor that allowed in each case to determine if there are significant differences between the results.

3.3.10.1. Case 1. Hammer Mill

Table 10 shows the analyzed data on the weight of the retained in the sieves of corn and soybean grains.

Null hypothesis: The granulometric analysis does not show significant differences between the sieves used. ($p>0.05$)
Alternative hypothesis: The granulometric analysis shows significant differences between the sieves used. ($p<0.05$)

Table 10. Weights of Retained in Sieves Case 1

Mesh (mm)	4	2,36	1,70	1,18	1,00	0,85	0,60	0,30	0,212
Corn (g)	2	55	472	701	296	80	96	37	2.21
Soybeans (g)	38	543	84	57	28	19	32	40	2.93
Critical Value F						4,39			
Probability						0,33			

Source: Bonilla, et al, 2024

The one-factor analysis of variance (ANOVA) applied to the particle size distributions of corn and soybeans shows that there is no statistically significant difference between both milled products, evidenced by a p-value of 0.33, much higher than the usual significance level of 0.05, which indicates that the variations observed in the retained weights in each mesh can be attributed to the randomness of the process rather than to an actual effect of the type of material. However, it may mask relevant practical differences in milling patterns, such as the marked concentration of soybeans in the 2.36 mm (543 g) mesh versus a more uniform distribution of corn, suggesting that, although globally similar, the fracture mechanisms and breakdown characteristics of each material could be influenced by factors not captured by this univariate analysis.

3.3.10.2. Case 2. Ball Mill

Table 11 shows the analyzed data on the weight of the retained in the sieves of corn and soybeans.

Null hypothesis: The granulometric analysis does not show significant differences between the sieves used. ($p>0.05$)
Alternative hypothesis: The granulometric analysis shows significant differences between the sieves used. ($p<0.05$)

Table 11. Weights of Retained in Sieves Case 2

Mesh (mm)	4	2,36	1,70	1,18	1,00	0,85	0,60	0,30	0,212
Corn (g)	55	62	482	511	447	202	153	217	1.63
Soybeans (g)	762	338	192	127	77	68	42	39	1.28
Critical Value F						4,49			
Probability						0,61			

Source: Bonilla, et al, 2024

The analysis of variance (ANOVA) of a factor applied to the particle size distribution data of corn and soybeans ground in a ball mill indicates that there is no statistically significant difference between the distributions of both grains, evidenced by a p-value of 0.612, much higher than the significance level of 0.05, and an F-value (0.267) that does not exceed the critical value (4,494). Although the means of the retained weights differ numerically (maize: 236.74 g, soybean: 183.25 g), the high variance within each group (38,378.68 for maize and 58,008.20 for soybean) suggests that the dispersion of the data in each mesh is considerable, masking possible specific differences by particle size. This could be due to the heterogeneous nature of grinding in ball mills, where factors such as hardness, humidity or residence time generate variability that the global ANOVA fails to detect, recommending an analysis by specific particle size fractions to identify practical differences in the process.

3.3.10.3. Case 3. Hammer Mill + Ball Mill

Table 12 shows the analyzed data on the weight of the retained in the sieves of corn and soybeans.

Null hypothesis: The granulometric analysis does not show significant differences between the sieves used. ($p>0.05$)
Alternative hypothesis: The granulometric analysis shows significant differences between the sieves used. ($p<0.05$)

Table 12. Weights of Retained in Sieves Case 3.

Mesh (mm)	4	2,36	1,70	1,18	1,00	0,85	0,60	0,30	0,212
Corn (g)	4	23	121	255	287	418	349	213	1.92
Soybeans (g)	11	65	139	264	189	304	170	254	0.28
Critical Value F						4,49			
Probability						0,63			

Source: Bonilla, et al, 2024

The analysis of variance (ANOVA) of one factor applied to the particle size data of case 3, where corn and soybeans were processed by a hammer mill followed by a ball mill, indicates that there is no statistically significant difference between the particle size distributions of both grains. This is supported by a p-value of 0.637, much higher than the significance level of 0.05, and an F-value of 0.231 that does not exceed the critical value of 4.494. Although the

mean retained weight differ (maize: 185.77 g, soybean: 155.14 g), the high variability within each group (variances of 24,235.87 for maize and 12,286.76 for soybeans) suggests that the observed differences may be due to the natural dispersion of the milling process and not to the type of grain. This result reflects that the grinding sequence (hammer + balls) homogenizes the distributions to the point of eliminating significant differences, possibly due to the combination of fracture mechanisms (impact and abrasion) that compensate for the individual properties of each material. However, an analysis by specific fractions could reveal differential behaviors in particular size ranges, not captured by the global ANOVA.

3.3.10.4. Diameters Comparisons in Corn

Table 13 shows the data analyzed for diameters D10, 50 and 90 for maize in its three case studies.

Null hypothesis: There are no significant differences between the values of D10, D50 and D90 in the particle size distribution of maize. ($p>0.05$)

Alternative hypothesis: At least one of the percentiles (D10, D50 or D90) differs significantly from the rest in the particle size distribution of maize. ($p<0.05$)

Table 13. Through-the-crop accumulation at D10, 50 and 90 for corn

Parameter	Case 1	Case 2	Case 3
D10 (mm)	3,39	0,48	0,60
D50 (mm)	2,80	1,38	1,08
D90 (mm)	0,30	1,96	2,60
Critical Value F	0,03		
Probability	0,97		

Source: Bonilla, et al, 2024

The analysis of variance shows that there are no significant differences between the values of D10, D50 and D90 for corn grain ($p > 0.05$). This indicates that, considering the three milling treatments, the variation between the characteristic particle size distributions (size percentiles) is statistically similar. In other words, milling generates particle sizes that, although different in numerical value, do not present sufficient variability for the differences between percentiles to be statistically detectable in corn.

3.3.10.5. Soybean Diameter Comparisons

Table 14 shows the data analyzed for diameters D10, 50 and 90 for maize in its three case studies.

Null hypothesis: There are no significant differences between the values of D10, D50 and D90 in the particle size distribution of soybeans. ($p>0.05$)
Alternate hypothesis: At least one of the percentiles (D10, D50 or D90) differs significantly from the rest in the particle size distribution of soybeans. ($p<0.05$)

Table 14 Accumulation of the through-a-basket in D10, 50 and 90 for soybeans

Parameter	Case 1	Case 2	Case 3
D10 (mm)	1.,8	1.,9	0,70
D50 (mm)	2,90	3,53	1,35
D90 (mm)	3,98	3,94	2,05
Critical Value F	4,04		
Probability	0,07		

Source: Bonilla, et al, 2024

In the case of soybeans, there is a trend towards differences between percentiles ($p = 0.773$), but these do not reach statistical significance at the conventional level of $\alpha = 0.05$. This suggests that soybeans have greater particle size variation than maize between D10, D50 and D90, probably due to their more fragile internal structure and greater heterogeneity in the fracture. However, statistical evidence is not sufficient to affirm significant differences, although it is possible that with a larger sample the results may be conclusive.

4.- Discussion

4.1.- Case 1. Hammer Mill

The particle size data reveal significant differences in the milling behavior between soybeans and corn using new sieves. Soybeans have a Extremely coarse distribution, with 81.12% of the material retained in the first three meshes (≥2.36 mm) and only 18.88% as through material in mesh 8. In contrast, corn shows a More balanced distribution, with 87.66% of through-material in mesh 8 and a progressive accumulation in intermediate meshes, reaching its inflection point (D50) around mesh 12 (1.7 mm). This difference is evident in the values of Smaller percentage accumulation size, where maize maintains significantly higher percentages across all meshes, indicating more efficient and uniform grinding. These findings are consistent with the grinding theory that states that the Physical properties of the material determine their response to the fracture. Soybeans, with a higher oil content and more flexible cell structure, have greater resistance to impact fracture, resulting in coarser particles. Maize, with vitreous endosperm and higher starch content, fractures more easily, generating a finer and more uniform distribution. The literature reports that materials with hardness greater than 45 kg/cm² (such as soybeans) require more grinding energy and produce coarser distributions, while cereals such as corn (hardness 25-35 kg/cm²) respond better to impact milling. The behavior observed in soybeans, with 81.12% of retained accumulated in mesh 8**,** It coincides with previous studies that report low milling efficiency in oilseed legumes due to their ability to absorb energy without fracturing completely. On the other hand, the distribution of maize conforms to the Gates-Gaudin-Schuhman model typical of brittle materials. In other studies, it reports 72-88% of material under 2 mm for corn, coinciding with our 87.66% through-mesh. [28] glassy nature of the endosperm**.** Just as it confirms that the

Vol. 08 / Nº 01
e – ISSN: 3028-8533
ISSN – L: 3028-8533

[29]Presence of oil in soybeans (18-22%) it acts as a shock absorber, reducing the generation of fines by 30-40% compared to dry materials. In contrast, in other research he obtains finer distributions (D50 ≈ 1.2 mm) using liquid nitrogen, suggesting that our conventional conditions limit efficiency. This shows that real-time adaptive adjustments can improve soybean uniformity by up to 60%, indicating optimization potential not explored in our study. Some studies claim that state-of-the-art mills with variable speed control can achieve narrower distributions than conventional equipment, in addition to the incorporation of current protocols recommends the humidity control implemented in the studios. These findings coincide with recent work on feed and PSD behavior in hammer milling, which shows how soybeans and corn respond differently to the same screening/screen and how moisture and composition affect fines generation and nutrient distribution by fraction. In particular, studies observed that, after hammer milling, soybeans tend to retain relatively coarse fractions and that the addition of moisture significantly modifies both the PSD and energy consumption, which supports the interpretation that grain properties (oil, structure) condition the hammer efficiency and the orientation of the particle size curve.[30][31] [32] [33] [34]

4.2.- Case 2. Ball Mill

Corn has a Significantly finer distribution than soybeans, with 91.6% of through-material in mesh 8 (2.36 mm) compared to only 26.32% in soybeans. The inflection point (D50) is located approximately at 1.3-1.4 mm for corn versus 3.0-3.2mm for soybeans, evidencing a marked difference in grinding efficiency. Soybeans show Fracture resistance, with 73.68% of retained accumulated in mesh 8, consistent with studies of *Chen et al. (2021)* on the ability of oilseed materials to absorb impact energy. Maize, with its vitreous endosperm, responds better to impact milling, generating a higher proportion of medium and fine particles. The results coincide in the higher milling efficiency of cereals versus oilseeds under similar conditions, but highlight the need to optimize specific operating parameters for each material. The interpretation of the results is based on recent scientific references, such as the study that explains the fracture resistance of soybeans due to their high oil content and flexible cell structure, which coincides with our findings of coarser particle size distributions compared to corn. Likewise [28] [35], Other studies they highlight the influence of the elastic modulus on grinding, supporting the marked difference in D50 between the two materials. When comparing our results with the literature, there are coincidences, who report finer distributions for corn under similar milling conditions, while discrepancies arise when contrasted with those who used cryogenic milling in soybeans and obtained significantly finer distributions, suggesting that our conventional operating conditions limit the efficiency of the process. Reviews and experimental work confirm that the ball mill is very effective in fractionating and reducing particles when the material is essentially friable or rich in polysaccharides, but its performance in dense oilseeds can be limited without parameter adjustments (time, media, atmosphere). This is consistent with our results: corn (endosperm) is effectively reduced, soybeans are not, except by operative changes or combined treatments.[36][28] [30] [37]

4.3.- Case 3. Hammer Mill + Ball Mill

The granulometric analysis of the Case 3 shows a noticeably finer and more uniform distribution compared to previous cases, where the corn presents a D50 ≈ 1.05 mm (near mesh 18) and the soybeans a D50 ≈ 1.25 mm (between 16-18 meshes), evidencing a more efficient grinding. This improvement is attributed to the possible use of hammer mill followed by ball mill, a combination that according to Some studies in this case It optimizes the fracture of heterogeneous materials by integrating impact and abrasion mechanisms. The results coincide with those who report distributions with D50 between 0.9-1.2 mm for corn under sequential milling, while discrepancies persist with respect to soybeans, whose studies indicate D50 >1.5 mm in conventional milling, suggesting that our sequential process partially mitigates its fracture resistance. Among the limitations, the absence of humidity control and unmonitored sieve wear may have affected reproducibility, while equipment bias underestimates the potential for cryogenic grinding. These factors highlight the need to incorporate energy-specific metrics (in future research to validate the efficiency of the sequential process. So it is evident that fragmentation methods will impact directly on the particle size as well as the shape obtained in your flour. . In recent literature, it has been shown that the use of sequential stages or multi-stage milling can decrease energy consumption per unit of reduction (depending on humidity and target sizes) and stabilize the production of intermediate/fine particles; In addition, the pre-fragmentation stage facilitates the action of subsequent fine grinding and less contact time needed to reach the target size. [30] [28] [35] [33] [38][39] [40]

Although the results obtained show clear differences between grains and treatments, there are inherent limitations to the experimental design and biophysical factors of the grain that could modulate the milling efficiency. In the Internal composition (lipid content, proteins, cell structure) and the grain moisture influence their susceptibility to fracture. For example, a recent study shows that when humidity increases, grains (corn, rice and soybeans) modify their mechanical behavior: they go from brittle to viscoelastic, changing the fracture force and the energy required. These variations can alter the fragmentation under milling, suggesting that intrinsic factors of the grain beyond the type of mill may condition the final particle size distribution.[41]

Another hypothesis to explain the lower milling efficiency in soybeans, compared to corn, is the buffering effect of oil

Vol. 08 / Nº 01
e – ISSN: 3028-8533
ISSN – L: 3028-8533

content. In soybean milling, it has been reported that higher lipid contents limit size reduction: the oil reduces brittleness and favors agglomerates or coarse particles after impact grinding. Additionally, friction grinding or fine grinding studies show that mechanical methods affect grains with a starch-rich matrix differently versus those with high lipid content, modifying the efficiency, particle shape and dispersibility. Therefore, the current results could reflect an interaction between the milling technique and the biochemical properties of the bean; This alternative hypothesis deserves to be explored in future work through characterization of oil, protein and cell structure, and rigorous humidity control.[42][28]

5.- Conclusions

The hammer mill (Case 1) showed a heterogeneous distribution, with a D50 ≈ 2.8-2.9 mm for corn and ≈2.9 mm for soybeans, evidencing an inefficient milling in soybeans, where 81.12% of the material was retained in ≥2.36 mm meshes. In contrast, the ball mill (Case 2) generated finer distributions for corn (D50 ≈ 1.38 mm), but was ineffective for soybeans (D50 ≈ 3.53 mm), confirming that soybeans, due to their higher oil content and flexible structure, resist fracture by impact and conventional abrasion.

The combination of mills (Case 3) achieved the most balanced distribution, with D50 ≈ 1.05 mm for corn and **≈1.25 mm for soybeans**, reducing the heterogeneity observed in the individual cases. This suggests that the synergy between impact (hammer) and abrasion (balls) mechanisms mitigates the limitations of each method separately, although greater dispersion persists in corn (uniformity index D90/D10 ≈ 4.3) versus soybeans (≈2.66)

The ball mill (Case 2) had the highest specific energy consumption (CEE): 92.70 kW·h/t for soybeans versus 80.17 kW·h/t for corn in Case 3, associated with the higher density and resistance of soybeans. However, this high consumption did not translate into a fine grind for soybeans, indicating energy inefficiency in oilseed processing under standard conditions.

The ANOVA applied showed $p > 0.05$ in all three cases, indicating "no significant differences" between corn and soybeans. However, the particle size data reveal critical operational disparities, such as the concentration of 40.49% of soybeans in the 3.35 mm mesh (Case 1) versus a more uniform distribution in corn. This exposes the insensitivity of univariate ANOVA to capture differences in complex distributions, underscoring the need for fraction-specific analysis.

The results of the ANOVA for maize ($F = 0.0314$; $p = 0.9692$) show a total absence of significant differences between the particle size parameters D10, D50 and D90 according to the milling method, evidencing a uniform behavior. In soybeans, although the ANOVA shows $F = 4.0430$ and $p = 0.0773$, the difference does not reach statistical significance, but suggests a tendency to variation, possibly influenced by its higher oil content and different mechanical response to fracture.

Microscopic analysis revealed that the hammer mill generates angular (rectangular) particles, while the ball mill produces rounded shapes (oval or ellipsoidal). In Case 3, a combination of morphologies was observed, which affects functional properties such as flow, compaction and reactivity. This highlights the importance of selecting the grinding technology according to the desired characteristics in the final product.

The findings of this study can be applied in the optimization of milling processes in the feed, flour and vegetable oil industry, where particle size control directly influences digestibility, mixture homogeneity and extrusion efficiency. The sequential grinding configuration (hammer + balls) is emerging as a viable alternative to reduce energy consumption and improve particle size consistency in continuous production lines. It is recommended to deepen the analysis of the specific milling energy and its relationship with the moisture and composition of the grain, as well as to evaluate the effect of particle size on the nutritional and functional quality of the final product. In addition, it would be valuable to explore the implementation of hybrid technologies (such as cryogenic or ultrasound-assisted milling) to increase the efficiency and reproducibility of the process, especially in hard-to-fracture oilseeds.

6.- Author Contributions (Contributor Roles Taxonomy (CRediT))

1. Conceptualization: Iván Torres
2. Data curation: Alejandro Noblecilla
3. Formal analysis: Alejandro Noblecilla
4. Acquisition of funds: Not applicable
5. Research: Iván Torres, Alejandro Noblecilla
6. Methodology: Iván Torres, Alejandro Noblecilla, Stefanie Bonilla, Carlos Valdiviezo.
7. Project management: Stefanie Bonilla
8. Resources: Iván Torres, Alejandro Noblecilla
9. Software: Not applicable.
10. Supervision: Stefanie Bonilla
11. Validation: Stefanie Bonilla, Carlos Valdiviezo
12. Visualization: Alejandro Noblecilla
13. Writing - original draft: Iván Torres, Alejandro Noblecilla
14. Writing - proofreading and editing: Stefanie Bonilla, Carlos Valdiviezo

7.- References.

[1] L. McCabe and J. Smith, Unit Operations in Chemical Engineering, Seventh, 2007. https://iestpcabana.edu.pe/wp-

content/uploads/2021/11/OPERACIONES-UNITARIAS-EN-LA-INGENIERIA-QUIMICA.pdf
[2] M. Roostaei, M. Soroush, V. Arian and A. Ghalambor, "Comparison of Various Particle-Size Distribution-Measurement Methods," SPE Reservoir evaluation & engineering, vol. 23, no. 04, 2020. https://doi.org/10.2118/199335-PA
[3] G. Barbosa-Cánovas, E. Ortega-Rivas and P. Juliano, Food Powders: Physical Properties, Processing, and Functionality, Boston, MA: Springer, 2005. https://doi.org/10.1007/0-387-27613-0_12
[4] A. Gupta and D. Yan, Mineral Processing Design and Operation, Western Australia: Elsevier., 2016. https://toc.library.ethz.ch/objects/pdf03/e01_978-0-444-63589-1_01.pdf
[5] V. B. L.G. Austin, "Experimental methods for grinding studies in laboratory mills," Powder Technology, vol. 5, no. 5, pp. 261-266, 2020. https://doi.org/10.1016/0032-5910(72)80029-9
[6] B. Wills and J. Finch, Wills' Mineral Processing Technology: An Introduction to the Practical Aspects of Ore Treatment and Mineral Recovery, Butterworth-Heinemann, 2016. https://shop.elsevier.com/books/wills-mineral-processing-technology/wills/978-0-08-097053-0
[7] A. International, ASTM E11-17: Standard Specification for Woven Wire Test Sieve Cloth and Test Sieves, 2017. https://standards.globalspec.com/std/3863958/astm-e11-17
[8] F. Etzler and R. Deanne, "Particle size analysis: A comparison of various methods ii," Particle & Particle system characterization, vol. 14, no. 6, pp. 278-282, 2004. https://doi.org/10.1002/ppsc.19970140604
[9] A. Freire and M. A. Lalbay Fuentes, "Implementation of a hammer mill for the wheat flour process," Technical University of Cotopaxi, La Maná, 2022. http://repositorio.utc.edu.ec/handle/27000/8473
[10] F. Lyu, A. van del Poel, W. Hendriks and M. Thomas, "Particle size distribution of hammer-milled maize and soybean meal, its nutrient composition and in vitro digestion characteristics," Animal Feed Science and Technology, vol. 281, p. 115095, 2021. https://doi.org/10.1016/j.anifeedsci.2021.115095
[11] R. Mugabi, Y. B. Byaruhanga, K. Eskridge and C. Welle, "Performance evaluation of a hammer mill during grinding of maize grains," AgricEngInt: CIGR, vol. 21, no. 2, p. 170, 2019. https://cigrjournal.org/index.php/Ejounral/article/download/5257/3011/23827?utm_source=chatgpt.com
[12] P. Pagán, R. Mollehuara-Canales, M. Sinche and J. Martínez, Mechanical Operations of Solid-Liquid Separation, Spain: Mc Graw Hill Interamericana, 2023. https://books.google.com.ec/books?hl=es&lr=&id=UYftEAAAQBAJ&oi=fnd&pg=PA2&dq=P.+Mart%C3%ADnez-Pag%C3%A1n,+Tecnolog%C3%ADa+Mineral%C3%Argica,+Cartagena:+Universidad+T%C3%A9cnica+de+Cartagena,+2011.+&ots=XT4vyqxq_5&sig=apv8WuHNxMtMiepueo-IAccQsUU&red
[13] H. G. Merkus, Production, Handling and Characterization of Particulate Materials, The Netherlands: Springer Cham, 2015. https://doi.org/10.1007/978-3-319-20949-4
[14] J. Fu, Z. Xue, Z. Chen and L. Ren, "Experimental study on specific grinding energy and particle size distribution of maize grain, stover and cob.," International Journal of Agricultural and Biological Engineering, vol. 13, no. 4, p. 135–142, 2020. https://doi.org/10.25165/j.ijabe.20201304.5327
[15] G. Niu, T. Zhang, S. Cao, X. Zhang and L. Tao, "Effect of Corn Grinding Methods and Particle Size on the Nutrient Digestibility of Chahua Chickens.," Animals, vol. 13, no. 14, p. 2364, 2023. https://doi.org/10.3390/ani13142364
[16] P. Tomach, "The Influence of the Grinding Media Diameter on Grinding Efficiency in a Vibratory Ball Mill," MDPI, vol. 17, no. 12, p. 2924, 2024. https://doi.org/10.3390/ma17122924
[17] Y. Catillo Álvarez, R. Jiménez, J. Monteagudo, B. Rodríguez and C. Patiño, "Mathematical Model to Improve Energy Efficiency in Hammer Mills and Its Use in the Feed Industry: Analysis and Validation in a Case Study in Cuba," Processes, vol. 13, no. 5, p. 1523., 2025. https://doi.org/10.3390/pr13051523
[18] T. Son, H. B. Trinh, S. Kim, B. Dugarjav and J. Lee, "Estimation of Energy Consumption for Concentrate Process of Tungsten Ore towards the Integration of Renewable Energy Sources in Mongolia," MInerals, vol. 13, no. 8, p. 1059, 2023. https://doi.org/10.3390/min13081059
[19] P. Martínez-Pagán, M. Sinche González and J. Martínez, Mechanical Operations of Solid-Liquid Separation, Cartagena: Mc Graw Hill, 2023. https://dialnet.unirioja.es/servlet/libro?codigo=990926
[20] W. Gutiérrez, "Granulometric Soil Testing Using the Sieving Method," Ciencia Latina Revista Científica Multidisciplinar, vol. 7, no. 2, pp. 6923-69-25, 2023. https://doi.org/10.37811/cl_rcm.v7i2.5834
[21] A. Roca, "Standardization of the sieving method to establish acceptance and/or rejection criteria in raw materials for an extruded line in the food industry," Universidad de Antioquia, Medellín, Colombia, 2021. https://bibliotecadigital.udea.edu.co/server/api/core/bitstreams/beaed1f9-a1d0-49d2-a007-1993bc2de107/content
[22] A. Terence, Powder Sampling and Particle Size Determination, Cartagena: Universidad Politécnica de Cartagena, 2023. https://books.google.com.ec/books?hl=es&lr=&id=5NgqTf9L63kC&oi=fnd&pg=PP1&dq=.+Terence,+Powder+Sampling+and+Particle+Size+Determination,+Cartagena:+Universidad+Polit%C3%A9cnica+de+Cartagena.+(2020).,+2023.&ots=1B0GcyOWcy&sig=QkuduBccOmwYOrSmeJxjTPD1
[23] P. Mort, "Analysis and graphical representation of particle size distributions," Powder Technology,, vol. 420, p. 118100, 2023. https://doi.org/10.1016/j.powtec.2022.118100
[24] G. Lyman, "A Statistical Theory for Sampling of Particulate Materials," Minerals, vol. 13, no. 7, p. 905, 2023. https://doi.org/10.3390/min13070905
[25] H. Jung, Y. Ju Lee and W. B. Yoon, "Effect of Moisture Content on the Grinding Process and Powder Properties in Food: A Review," Processes, vol. 6, no. 6, p. 69, 2018. https://doi.org/10.3390/pr6060069
[26] M. Warechowska, "Some physical properties of cereal grain and energy consumption of grinding," Agricultural Engineering, vol. 1, no. 149, pp. 239-2049, 2014. http://dx.medra.org/10.14654/ir.2014.149.025
[27] H. V. ,. J. Dodds, "Particle shape characterization using morphological descriptors," Particle& Particle systems characterization, vol. 14, no. 6, pp. 272-277. , 2004. https://doi.org/10.1002/ppsc.19970140603.

[28] X. Tian, X. Wang and Z. Wang, "Particle size distribution control during wheat milling: nutritional quality and functional basis of flour products—a comprehensive review," International Journal of Food Science + Technology, vol. 57, no. 12, p. 7556–7572, December 2022. https://doi.org/10.1111/ijfs.16120
[29] N. Mohamad, I. Rodriguez-Donis, A. Cavaco-Soares and P. Evon, "Bio-Refinery of Oilseeds: Oil Extraction, Secondary Metabolites Separation towards Protein Meal Valorisation—A Review," Processes, vol. 10, no. 5, p. 841, 2022. https://doi.org/10.3390/pr10050841
[30] S. Li, S. Ge, Z. Huang, Q. Wang and H. Zhao, , "Cryogenic grinding technology for traditional Chinese herbal medicine," Cryogenics, vol. 31, no. 2, pp. 136-137, 1991. https://doi.org/10.1016/0011-2275(91)90260-4
[31] N. Yancey, C. T. Wright and T. L. Westover, "Optimizing hammer mill performance through screen selection and hammer design," Biofuels, vol. 4, no. 1, pp. 85-94, 2014. https://doi.org/10.4155/bfs.12.77
[32] W. B. Rowe, "Towards High Productivity in Precision Grinding," MPDI, vol. 3, no. 2, p. 24, 2018. https://doi.org/10.3390/inventions3020024
[33] D. Wang, C. He, H. Tian, F. Liu and T. Zhang, "Parameter optimization and experimental research on the hammer mill," Imateh- Agricultural Enginerering, vol. 62, no. 3, pp. 342-349, 2020. https://doi.org/10.35633/inmateh-62-36
[34] F. Lyu, M. Thomas and W. H. Hendriks, "Particle size distribution of hammer-milled maize and soybean meal, its nutrient composition and in vitro digestion characteristics," Animal Feed Science and Technology, vol. 281, 2021. https://doi.org/10.1016/j.anifeedsci.2021.115095
[35] R. K. Gupta and S. K. Das, "Fracture resistance of sunflower seed and kernel to compressive loading," Journal of Food Engineering, vol. 46, no. 1, pp. 1-8, 2000. https://doi.org/10.1016/S0260-8774(00)00061-3
[36] Y. Haddad, F. Mabille, J. Abecassis and J. Benet, "Rheological properties of wheat endosperm with a view on grinding behaviour," Powder Technology, vol. 105, no. 1-3, pp. 89-94, 1999. https://doi.org/10.1016/S0032-5910(99)00122-9
[37] J. Ke, X. Wang, X. Gao and Y. Zhou, "Ball Milling Improves Physicochemical, Functionality, and Emulsification Characteristics of Insoluble Dietary Fiber from Polygonatum sibiricum," MDPI, vol. 13, no. 15, p. 2323, 2024. https://doi.org/10.3390/foods13152323
[38] Y. Xie, C. Zhang and S. Mei, "Optimisation decision of machining process parameters considering milling energy consumption and specific cutting energy," Alexandria Engineering Journal, vol. 128, pp. 786-795, 2025. https://doi.org/10.1016/j.aej.2025.07.034
[39] L. Feltner, E. Korte, D. F. Bahr and P. Mort, "Particle size and shape analyses for powder bed additive manufacturing," Particuology, vol. 101, pp. 33-42, 2025. https://doi.org/10.1016/j.aej.2025.07.034
[40] Y. Liu, J. Wang, J. C. Barth, K. R. Welsch, V. McIntyre and M. P. Wolcott, "Effects of multi-stage milling method on the energy consumption of comminuting forest residuals," Industrial Crops and Products, vol. 145, 2020. https://doi.org/10.1016/j.indcrop.2019.111955
[41] W. Kruszelnicka, Z. Chen and K. Ambrose, "Moisture-Dependent Physical-Mechanical Properties of Maize, Rice, and Soybeans as Related to Handling and Processing," Materials, vol. 15, no. 24, p. 8724, 2022. https://doi.org/10.3390/ma15248729
[42] R. Politiek, M. Bruins, J. Keppler and M. Schutyser, "Effect of oil content on pin-milling of soybean," Journal of Food Engineering, vol. 334, p. 111149, 2022. https://doi.org/10.1016/j.jfoodeng.2022.111149

INQUIDE
Chemical Engineering and Development
Journal of Science and Engineering

Vol. 08 / Nº 01
e – ISSN: 3028-8533
ISSN – L: 3028-8533

INQUIDE
Ingeniería Química y Desarrollo

Guidelines for publication in the journal INQUIDE – Chemical Engineering and Development

1. General Information

INQUIDE – Chemical Engineering and Development is a multidisciplinary scientific journal edited by the Faculty of Chemical Engineering of the University of Guayaquil, located in Guayaquil, Ecuador. Published since January 2015, the journal has a biannual periodicity and focuses on original contributions in the area of science and engineering.

INQUIDE is a peer-reviewed journal that uses a peer-reviewed external review system, under the double-blind review methodology, following the publication standards of the Institute of Electrical and Electronics Engineers (IEEE). This system guarantees an objective, impartial and transparent review process, which facilitates the inclusion of the journal in databases, repositories and international reference indexes.

Currently, INQUIDE is indexed in:

1.- Latindex Catalog 2.0 (Regional Online Information System for Scientific Journals of Latin America, the Caribbean, Spain and Portugal).

2.- Dialnet (Dialnet Foundation, University of La Rioja).

3.- Network of Ecuadorian Editors and Scientific Journals (RERCIE).

4.- Crossref, with DOI (Digital Object Identifier) assignment for each published article.

The journal is published in electronic format (e-ISSN: 3028-8533) and accepts manuscripts in Spanish, English and Portuguese, promoting the dissemination of high-quality research at an international level.

2. Scope and Policy

2.1. Theme

INQUIDE – Chemical Engineering and Development publishes original contributions in the area of science and engineering, with a multidisciplinary approach. Research works carried out by national and international authors are accepted, as long as they meet the required scientific quality criteria.

2.2. Types of contributions

The journal prioritizes the publication of:

- Empirical research articles that present original and significant results.
- Technology development reports describing innovations or practical applications in engineering and science.
- Proposals for innovative models and solutions that contribute to the advancement of knowledge.
- State-of-the-art reviews that synthesize and critically analyze current knowledge in a specific area.
- Essay articles that present theoretical or methodological reflections relevant to the field.

2.3. Originality requirements

INQUIDE only publishes original and unpublished works written in Spanish, English or Portuguese. Manuscripts must not have been previously published in any print or electronic media, nor be in the process of arbitration or publication in another journal.

2.4. Arbitration process

All submitted articles will be subjected to a rigorous peer-review process under the double-blind review methodology. The evaluation is based on criteria of:

- Originality: The work must present novel contributions to the field.
- Relevance: The topic must be relevant to the areas of science and engineering.
- Topicality: The study should be based on recent literature and address contemporary issues.
- Scientific rigor: The methodology and results must be solid and well-founded.
- Compliance with editorial standards: The manuscript must follow the format and style guidelines of the journal.

The receipt of a manuscript does not imply a commitment to publication. The final decision to publish will be made by the Editorial Board, based on the recommendations of the specialized reviewers.

2.5. Required Documents

Authors must submit the following documents along with their manuscript:

1. Checklist: Available for download in https://1drv.ms/w/c/7bce1d25160b4657/EdRL-JU4fBVBqSt1GD7t1N8BZVFXYapjNxM8ji3Fa9LFhA?e=Z7OqeO.
2. Presentation and assignment of rights: Available for download in https://1drv.ms/w/c/7bce1d25160b4657/EZYnPTveWCtKgV5aNNZ1icQBdaFzvOYKCLwlhD7GC76hzg?e=ldbXMf .

2.6. Submission of manuscripts

Manuscripts must be submitted through the journal's Open Journal System (OJS), available at: https://revistas.ug.edu.ec/index.php/iqd/information/authors.

Additionally, authors can send queries or complementary documents to the email: inquide@ug.edu.ec o francisco.duquea@ug.edu.ec.

3. Presentation and structure of manuscripts

All manuscripts submitted to INQUIDE must follow the format established by the journal. The rules and requirements for the presentation and structure of the articles are detailed below:

3.1. Manuscript format

- Manuscripts must be written in Microsoft Word (formato.doc or .docx).
- The official template of the magazine can be downloaded from: https://1drv.ms/w/c/7bce1d25160b4657/EXSf2GX2MuJEn-hf5qwsswUBzx4-1vYE_6qKE8ba2UF62g?e=68U2h9 .

Vol. 08 / Nº 01
e – ISSN: 3028-8533
ISSN – L: 3028-8533

- The document must be in a double column, with the following margins: Top: 3.5 cm, Bottom: 3.5 cm, Left: 1.5 cm, Right: 1.5 cm
- Use Times New Roman font, size 10, justified, with single line spacing and 0 spacing.

3.2. Manuscript structure

3.2.1. Presentation and Cover Letter

1. Título (spanish) / Title (english):
   - It should be concise but informative, with a maximum of 20 words.
   - If the article is written in Spanish, the title in English should appear on the second line, and vice versa.
2. Authors and affiliation:
   - Include the full names and surnames of all authors, in the order of preference.
   - Specify the institutional affiliation of each author, including: Dependency and institution; Institutional email; ORCID; City and country.
   - Note: A maximum of 40% of authors may be affiliated with the University of Guayaquil.
3. Abstract (Spanish) / Abstract (English):
   - Maximum length of 250 words in both languages.
   - It should include:
     1. Justification of the topic.
     2. Objectives.
     3. Methodology and sample.
     4. Main results.
     5. Main conclusions.
4. Palabras clave (español) / Keywords (inglés):
   - Provide a maximum of 7 keywords in each language, directly related to the topic of the job.
   - It is recommended to use terms from the UNESCO Thesaurus.
5. Cover Letter:
   - Include a statement certifying that the manuscript is an original contribution, not submitted or under review in another journal.
   - Confirm authorship and acceptance of formal changes according to journal standards.
   - Download the Cover Letter format from:

https://1drv.ms/w/c/7bce1d25160b4657/EdRL-JU4fBVBqSt1GD7t1N8BZVFXYapjNxM8ji3Fa9LFhA?e=Z7OqeO
https://1drv.ms/w/c/7bce1d25160b4657/EZYnPTveWCtKgV5aNNZ1icQBdaFzvOYKCLwlhD7GC76hzg?e=ldbXMf

3.2.2. Manuscript structure

1. Introduction:
   - Present the research problem, context, rationale, and objectives of the study.
   - Include a review of the most relevant and current literature, both nationally and internationally.
2. Materials and methods:
   - Describe the methodology, materials, experimental design and procedures in a clear and detailed manner.
   - If an original methodology is used, explain its rationale and possible limitations.
3. Results:
   - Present results in a clear and organized manner, using tables, graphs, and figures when necessary.
   - Avoid duplication of data between text and tables/figures.
4. Discussion:
   - Interpret the results, relating them to the objectives of the study and the existing literature.
   - Discuss the theoretical and practical implications of the findings.
5. Conclusions:
   - Summarize the most important findings of the study.
   - Highlight the contributions of the work and propose future lines of research.
6. Acknowledgements (optional):
   - Acknowledge funding sources, collaborators, or institutions that supported the research.
7. References:
   - Follow the IEEE style for citations and the reference list.
   - Use the Microsoft Word reference manager to manage citations.
   - Make sure all references are cited in the text and vice versa.

3.3. Figures, tables and equations

- Figures and tables:
  - They must be numbered consecutively (Fig. 1, Table 1, etc.) and cited in the text.
  - The figures must have a minimum resolution of 300 dpi and be in JPG, PNG format.
  - Tables should have a title above and figures a title below.
- Equations:
  - Use the Microsoft Word equation editor.
  - Number the equations consecutively, placing the number in parentheses and aligned to the left.

3.4. Submission of the manuscript

- Manuscripts must be submitted through the journal's Open Journal System (OJS): https://revistas.ug.edu.ec/index.php/iqd/information/authors.
- Be sure to load:
  - The manuscript in Word format (.doc or .docx).
  - The figures in separate files, with the appropriate resolution and format.
  - The Cover Letter and other required documents.

4. Submission Process

The submission of manuscripts to INQUIDE must be carried out following the following steps and requirements:

4.1. Shipping platform

- All manuscripts must be submitted through the journal's Open Journal System (OJS), available at: https://revistas.ug.edu.ec/index.php/iqd/information/authors.

Vol. 08 / Nº 01
e – ISSN: 3028-8533
ISSN – L: 3028-8533

- Authors must register on the OJS platform before submitting.

4.2. Required Documents

At the time of submission, authors must upload the following documents:

1. Manuscript in Word format (.doc or .docx):
   - The paper should follow the format and structure established by the journal (see section 3).
   - Include full author data and their institutional affiliation.
2. Figures and tables:
   - Figures must be sent in separate files, in JPG, PNG format, with a minimum resolution of 300 dpi.
   - Tables should be included in the manuscript, following the format indicated in section 3.
3. Cover Letter:
   - Include a statement certifying that the manuscript is an original contribution, not submitted or under review in another journal.
   - Confirm authorship and acceptance of formal changes according to journal standards.

Descargue el formato de Cover Letter desde: https://1drv.ms/w/c/7bce1d25160b4657/EZYnPTveWCtKgV5aNNZ1icQBdaFzvOYKCLwlhD7GC76hzg?e=ldbXMf

4. Checklist:

- Make sure that the manuscript meets all technical and formatting requirements.

Download the checklist from: https://1drv.ms/w/c/7bce1d25160b4657/EdRL-JU4fBVBqSt1GD7t1N8BZVFXYapjNxM8ji3Fa9LFhA?e=Z7OqeO

4.3. Correspondence Manager

- One of the authors must be designated as **the correspondence officer**.
- This author will be the primary point of contact for all manuscript-related communications.

4.4. Confirmation of receipt

- Once the manuscript has been submitted, the OJS system will automatically send a confirmation email to the corresponding author.

4.5. Inquiries and Support

- For inquiries about the submission process or technical problems, authors can contact the editorial team through the following emails:
  - inquide@ug.edu.ec
  - francisco.duquea@ug.edu.ec

5. Editorial Process

INQUIDE's editorial process is designed to guarantee the quality, originality and scientific rigor of the published manuscripts. The process is described step by step below:

5.1. Initial review

Once the manuscript is received, the editorial team performs an initial review to verify the following aspects:

1. Theme: The manuscript must be within the thematic scope of the journal (science and engineering).
2. Format and structure: The manuscript must follow the format and structure established by the journal (see section 3).
3. Citations and references: All bibliographic references must be correctly cited in the text, following the IEEE style.
4. Originality: The manuscript will be subjected to a plagiarism check using specialized software. A maximum of 15% similarity to other works is accepted.

If the manuscript does not meet any of these requirements, the author will be asked to make the necessary corrections before continuing with the evaluation process.

5.2. Peer-Review

Manuscripts that pass the initial review will be subjected to a rigorous peer review process under the double-blind review methodology. This process includes the following steps:

1. Assignment of reviewers:
   - The editor will assign at least two reviewers specialized in the subject area of the manuscript.
   - The reviewers can be national or international experts.
2. Evaluation:
   - Reviewers will evaluate the manuscript based on criteria such as originality, relevance, scientific rigor, clarity, and contribution to the field.
   - Each reviewer will issue a report with one of the following results:
     - Publishable without changes.
     - Publishable with suggested changes.
     - Publishable with mandatory changes.
     - Not publishable.
3. Editorial decision:
   - The editor will analyze the reviewers' reports and make a final decision on whether to accept or reject the manuscript.
   - If the manuscript is accepted, the author will be notified to make the suggested changes (if applicable).
   - If the manuscript is rejected, the author will be notified and the paper will be archived.

5.3. Review Time

- The peer review process lasts a minimum of 4 weeks.
- At the end of this period, the author will be notified of the outcome of the evaluation and the recommendations of the reviewers.

5.4. Corrections and final version

- If the manuscript is accepted with changes, the author must send the corrected version within the deadline established by the editor.
- The editorial team will verify that the requested corrections have been correctly incorporated before proceeding with the publication.

5.5. Publication

- Accepted manuscripts will be published in the biannual issues of the journal (January and July).

Vol. 08 / Nº 01
e – ISSN: 3028-8533
ISSN – L: 3028-8533

- Authors will receive a notification once their work is available on the journal's platform.

6. Publication

INQUIDE – Chemical Engineering and Development publishes two issues a year, on the following dates:

- First issue: January 1.
- Second issue: July 1.

6.1. Shipping times

To ensure that manuscripts are considered in the corresponding issues, authors must take into account the following deadlines:

- Manuscripts for the January issue: Must be submitted by October 31 of the previous year.
- Manuscripts for the July issue: They must be submitted by April 30 of the same year.

6.2. Availability of Articles

- Once published, the articles will be available on the journal's electronic platform, accessible through: https://revistas.ug.edu.ec/index.php/iqd.
- Each published article will include a DOI (Digital Object Identifier), which guarantees its identification and permanent access.

6.3. Open Access Policy

INQUIDE is an open access journal, which means that all articles are freely available for reading, downloading and distribution, under a Creative Commons license.

7. Information on the use of Artificial Intelligence

INQUIDE recognizes the importance of maintaining high ethical standards in scientific research, especially in the use of Artificial Intelligence (AI). Therefore, the following guidelines are established:

7.1. Use of AI in research

- If Artificial Intelligence has been used at any stage of the research presented in the manuscript, authors must explicitly state this in the Cover Letter.
- Specify the sections of the manuscript where AI has been used, describing their function and scope.

7.2. Transparency and accountability

- Authors are responsible for ensuring that the use of AI does not compromise the originality, integrity, and scientific rigor of the work.
- The editorial team will evaluate the AI usage statement and may request additional information if necessary.

7.3. Accepting Manuscripts with AI

- The final decision on the acceptance of manuscripts that have used AI is at the discretion of the Editorial Board, based on transparency and compliance with the journal's ethical standards.

INQUIDE

We explore the unknown and address the seemingly impossible.
Welcome to the frontier of knowledge, where science, engineering, and technology converge to drive transformative development.

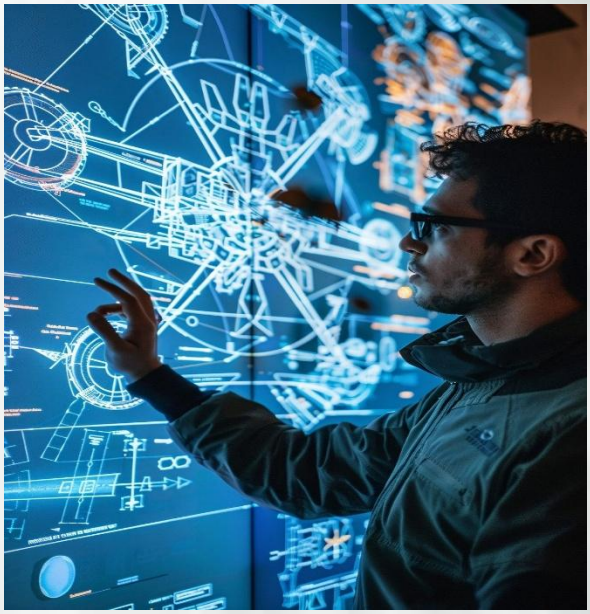

Most Viewed Articles

Title. **Search by title, author and ID.**	**Total**
Duque-Aldaz et al. Prediction of moisture content in the cocoa drying process by simple linear regression.	1375
Jiménez Sánchez et al. Obtaining bacterial cellulose from kombucha by replacing black tea with coffee husk tea.	1003
Alulema Cuesta et al. Comparative study of extraction and characterization of avocado oil, through processes of: thermobeating, enzymatic, hydraulic pressing and expeller.	851
Catarí et al. Photodegradation of microplastics.	757
Fu-López et al. Risk assessment and control measures for machinery in a food production company.	740
Bonilla Bermeo et al. Study of the bioadsorption of heavy metals (Pb and Cu) in the waters of the Puyango river, using orange and apple banana peel	711
Tigrero Zapata et al. Impact of plastic pesticide containers on agricultural soils: a cultural problem in Ecuadorian agriculture.	691
Delgado Gómez et al. Implementation of gastrodiplomacy as a strategic axis of tourism development and contribution to the cultural dissemination of Ecuador	274
España Francis et al. The cyanotoxins occurrence in water and fresh foods: human health implications.	392
Carrera Coloma et al. Theoretical study of alternatives for the control of Rupella albinella in rice cultivars (Oryza sativa)	361

Primary Contact
Francisco Javier Duque-Aldaz
University of Guayaquil
Phone: +593 98 564 1201 (WhatsApp)
Phone: +593 99 576 0762 (Telegram)
francisco.duquea@ug.edu.ec.
inquide@ug.edu.ec